Crystal and Co-Crystal Engineering of Isoniazid, 4-Aminoantipyrine, Benzophenone and their Derivatives

by

Mark Gordon Smith

Submitted in accordance with the requirements for the degree of

Doctor of Philosophy

In the subject

Chemistry

At the

UNIVERSITY OF THE WITWATERSRAND

Supervisor: Prof. A. Lemmerer

May 2018

DECLARATION

I declare that **"Crystal and Co-Crystal Engineering of Isoniazid, 4-Aminoantipyrine, Benzophenone and their Derivatives"** is my own unaided work and that all sources I have used or quoted have been indicated and acknowledged by means of complete references. It has not been submitted before for any degree or examination at any other University.

15 May 2018

Mark Gordon Smith

Date

"A crystal is like a class of children arranged for drill, but standing at ease, so that while the class as a whole has regularity both in time and space, each individual child is a little fidgety!"
~ Dame Kathleen Lonsdale in *Crystals and X-Rays* (1948). 22

All the work of the crystallographers serves only to demonstrate that there is only variety everywhere where they suppose uniformity ... that in nature there is nothing absolute, nothing perfectly regular.
~ Comte Georges-Louis Leclerc de Buffon in *Histoire Naturelle des Minéraux* (1786). **3,** 433

"One can ask: "If I crystallize a virus to obtain a crystal consisting of the molecules that make up the virus, are those molecules lifeless or not?" ... The properties of living organisms are those of aggregates of molecules. It's very difficult to draw a line between molecules that are lifeless and molecules that are not lifeless."
~ Linus Pauling in *BioScience* (1986). **36**, 738.

"I shall never forget the sight. The vessel of crystallization was three quarters full of slightly muddy water—that is, dilute water-glass—and from the sandy bottom there strove upwards a grotesque little landscape of variously colored growths: a confused vegetation of blue, green, and brown shoots which reminded one of algae, mushrooms, attached polyps, also moss, then mussels, fruit pods, little trees or twigs from trees, here, and there of limbs. It was the most remarkable sight I ever saw, and remarkable not so much for its profoundly melancholy nature. For when Father Leverkühn asked us what we thought of it and we timidly answered him that they might be plants: "No," he replied, "they are not, they only act that way. But do not think the less of them. Precisely because they do, because they try as hard as they can, they are worthy of all respect." It turned out that these growths were entirely unorganic in their origin; they existed by virtue of chemicals from the apothecary's shop."
~ Thomas Mann in "*Doktor Faustus*" (1948). 19

ABSTRACT

Isoniazid is the primary drug used for the treatment of tuberculosis. Covalent modifications to the amine group of isoniazid are currently under investigation and such modifications have been shown to render the drug effective against multiple-drug-resistant strains of *Mycobacterium tuberculosis.*

In this thesis, crystal and co-crystal engineering was applied to synthesize crystals and co-crystals of covalently modified isoniazid. Isoniazid was modified by bulky modifiers, namely benzophenone and benzophenone derivatives, and crystallized in the absence and presence of co-formers. A series of co-crystals of modified isoniazid was prepared and their supramolecular structures were studied. All co-crystals were synthesized with salicylic acid and control over the dimensionality of packing was achieved. It was found that the benzophenone modifiers sterically masked the amide functional groups from participating in any intermolecular interactions. This steric masking is predictable and consistent and provides a general method whereby an amide functional group can be sterically blocked from intermolecular interactions.

The effects of reaction and crystallization conditions on the supramolecular structure of isoniazid are also reported. Several pairs of co-crystals of modified isoniazid were synthesized under different crystallization conditions. Change in reflux time of the reagents resulted in stoichiometric variation in the resulting co-crystals. The addition of excess reagents as an additive resulted in polymorphism. Addition or absence of an acid catalyst either promoted or prevented solvate formation. The addition of either one or two methyl groups to the benzophenone aromatic rings did not substantially alter the packing patterns of the crystal structures.

As the presence of co-formers may either enhance or inhibit the bioavailability of pharmaceutical drugs, the covalent modification of isoniazid was repeated in the absence of co-formers. The covalent modification without co-formers presented several synthetic difficulties and use of new catalysts and the development of new synthetic strategies such as refluxing in high-pressure glass vials were developed. A full structural study on the covalently modified isoniazid crystals is reported.

Side reactions of benzophenone were observed during the crystallization of isoniazid derivatives. These resulted in the formation of benzophenone azine crystals. The origin and mechanism of the formation of these benzophenone azine crystals were determined to occur via a two-step photodimerization process. The benzophenone azine crystals were found to be held together through weak interactions and a structural study of the packing of these crystals was reported.

4-Aminoantipyrine is a pharmaceutical drug previously used as an antipyretic and is considered a prophylactic against oxidative stress. Two of its derivatives, aminoantipyrine and 4-(*N*,*N*-dimethyl)-aminoantipyrine, have been used as analgesic and anti-inflammatory drugs since the late 19th century. Their concurrent use with aspirin is particularly beneficial as they have been shown to prevent or attenuate the anti-platelet effects of aspirin. However, their use has been discontinued due to side effects and this discontinuation warrants further studies of methods to possibly increase the bioavailability and alter the physical properties of the drug, including via covalent modification and co-crystallization. To date, all reported attempts at co-crystallizing this drug have failed.

In this study, co-crystal design strategies were developed to synthesize the first co-crystal of 4-aminoantipyrine, and the methods leading up to the successful supramolecular synthesis of 4-aminoantipyrine with co-formers are detailed. The synthesis of two novel salts of 4-aminoantipyrine and two co-crystals of covalently modified 4-aminoantipyrine are also reported. A series of crystals of covalently modified 4-aminoantipyrine were also synthesized and a full structural study of these crystals is presented.

DEDICATION

This thesis is dedicated to my sons, Gordon and Derek,
two of the most inquisitive minds on the planet.

ACKNOWLEDGEMENTS

I would like to acknowledge the following people, who made the completion of my PhD an absolute pleasure:

My supervisor, Professor Andreas Lemmerer, the Crystal Magician, who once said to me “Just because something hasn’t been done, doesn’t mean it can’t be done.” You reminded me that nothing is impossible, which ultimately led to the success of obtaining the results reflected in this thesis. You have truly inspired me.

My mentor, Dr. Manuel Fernandes, who taught me so much about the subtleties of crystallography and motivated me when things were tough. I will always remember your kindness in taking so much time to help me and motivate me when I needed it.

Sanaz (Sehera) Khorasani, who spent many, many hours at the diffractometer with me, explaining the details of XRD collection and solving crystal structures, especially in the early years. Your friendship and constant support is appreciated more than you know.

Lee Madeley, who inspired me and challenged me with your out-of-the-box thinking. The number of new ideas that emanated from our regular Friday afternoon chats at the Postgraduate Club is immeasurable.

STRUCTURE AND OUTPUTS OF THE THESIS

There are two styles of writing in this thesis. The introductory chapter (Chapter 1), the literature review (Chapter 2), the experimental methods (Chapter 3) and the conclusion (Chapter 9) are written in a uniform style.

The central chapters consist of six publications that have either been published, submitted, or prepared for submission in well known accredited peer-reviewed crystallographic journals. In two of the papers, the reviewers' comments are being attended to at request of the editor before final resubmission to the journal. These central chapters represent the author's contribution to knowledge in the field of research and form the heart of the thesis. The advantage of presenting the six publications as chapters is that the most important findings, descriptions and conclusions from a large amount of work done during this PhD have been concisely presented. Each chapter is presented in the format required for submission by *Crystal Growth and Design* (the primary journal to which the papers have been submitted) and may vary from the format found in the introductory chapters.

Each publication presented in this thesis is preceded by a summary in which the journal name, publication status and a synopsis of the work is described.

ROLE OF AUTHORS IN PAPERS

There are six papers presented as chapters in this thesis (which have been either published, submitted or are about to be submitted). For all six papers, the original ideas and the conceptual development were my own. I did all of the experimentation, determined and refined the crystal structures, analysed the results and wrote the papers myself.

The contribution of Prof. Andreas Lemmerer was academic input and supervision.

In the published paper presented in Chapter 4.2, there is a third author, namely Dr. Roy Forbes. The reviewers of that paper requested that Pawley refinements be done for the powder diffraction patterns and this required the expertise of Dr. Forbes. This was the only contribution of Dr. Forbes to the paper. The Pawley refinements do not form part of this thesis, but are presented in **Appendix 1** for completeness.

TABLE OF CONTENTS

Table of Contents

LIST OF FIGURES

LIST OF TABLES

LIST OF ABBREVIATIONS

4AAP	**4**-**A**mino**a**nti**p**yrine
API	**A**ctive **P**harmaceutical **I**ngredients
CSD	**C**ambridge **S**tructural **D**atabase
DSC	**D**ifferential **S**canning **C**alorimetry
FDC	**F**ixed **D**ose **C**ombination
GRAS	**G**enerally **R**egarded **a**s **S**afe
INH	**I**so**n**icotinic Acid **H**ydrazide (Isoniazid)
LAG	**L**iquid **A**ssisted **G**rinding
mHBA	**M**eta-**h**ydroxy**b**enzoic **A**cid
NADH	Reduced form of **N**icotinic **A**denine **D**inucleotide
pHBA	**P**ara-**h**ydroxy**b**enzoic **A**cid
NSAID	**N**on-**S**teroidal **A**nti-**I**nflammatory **D**rug**s**
TB	Mycobacterium tuberculosis
XRD	**X**-**R**ay **D**iffraction

Chapter 1: Introduction and Aims

1.1 Overview

Crystal and co-crystal structures cannot be easily predicted from molecular structures. Small changes in crystallization conditions can have unpredictable results on the supramolecular packing and structure of a crystal or co-crystal. The field of crystal and co-crystal engineering has arisen in an attempt to understand the processes of supramolecular synthesis and to develop design strategies to elucidate predictable and exploitable mechanisms for crystallization and co-crystallization processes. These processes are particularly important to the pharmaceutical industry, as supramolecular structures such as salts and co-crystals often improve the bioavailability of active pharmaceutical ingredients (APIs). The work presented in this thesis is a contribution to the development of co-crystal design strategies and to the understanding of co-crystal and crystal structures of isoniazid, 4-aminoantipyrine, benzophenone and their derivatives.

1.2 Co-crystals, salts and solvates

For many years, the definition of a co-crystal has been debated and until recently, there has been no clear consensus. In 1985, Kitaigorodskii broadly defined a co-crystal as "a mixed crystal that contains two different molecules" (Kitaigorodskii, 1984). Desiraju expressed concern that the term "co-crystal" (also written as "cocrystal") was being used too loosely and stressed the need for consensus on several crystallographic terms for which the meaning is ambiguous. Although he supported the use of the term "co-crystal" which had gained much popularity by 2003, he warned that terms which are "scientifically suspect" such as "pseudopolymorph" should be properly debated and discarded if necessary (Desiraju, 2003).

Aakeröy later expanded the definition of co-crystals to include only reactants that are solids at room temperature, but excluded hydrates, solvates and clathrates (Aakeröy and Salmon, 2005). In contrast, Zawarotko *et al*. proposed a broader definition in the context of pharmaceutical co-crystals and defined pharmaceutical co-crystals as "*co-crystals that are formed between a molecular or ionic API and a co-former that is solid under ambient conditions"* (Almarsson and Zaworotko, 2004). This definition clearly includes several classes of supramolecular solids, including salts, hydrates, solvates and clathrates, and lessens the ambiguity of the definition.

More recently, Aitipamula *et al.* proposed a definition for co-crystals of APIs and defined co-crystals as "*solids that are crystalline single phase materials composed of two or more different molecular and/or ionic compounds generally in a stoichiometric ratio which are neither solvates nor simple salts*" (Aitipamula *et al*., 2012). In their comprehensive discussion on crystallographic nomenclature, they also provided clear definitions for classifications of several other solid forms of APIs such as polymorphs and salts. Polymorphs were defined as different crystalline forms of the same substance, including hydrates and solvates. Salts were defined as "Any of numerous compounds that result from replacement or *part or all of the acid hydrogen of an acid by a metal or a radical acting like a metal; an ionic or electrovalent crystalline solid.*" Aitipamula concluded that co-crystals should be broadly defined and should be grouped with salts, but conceded that separating salts and co-crystals into several "classes" required further thought and debate. A schematic diagram showing the several solid forms proposed by Aitipamula is shown in **Figure 1.1**.

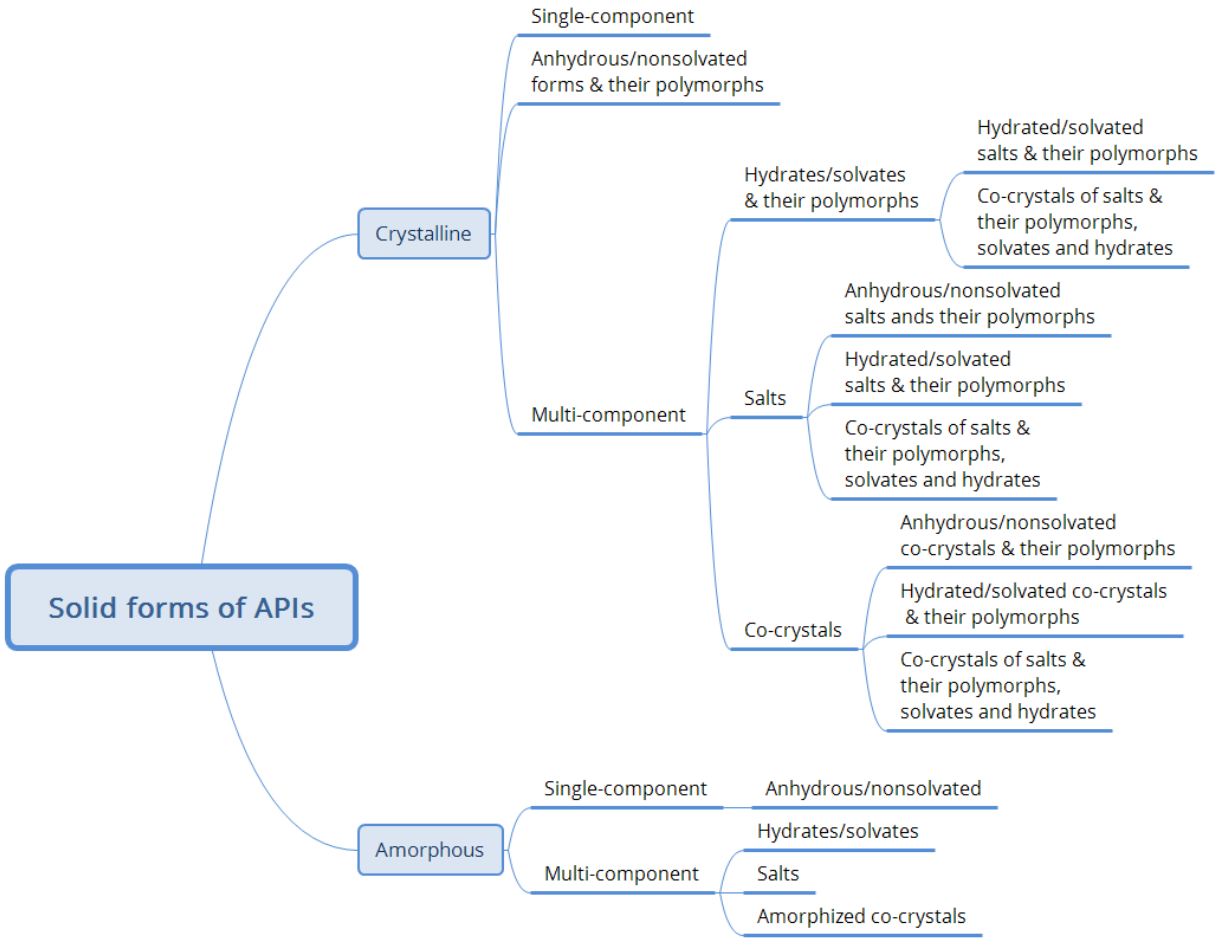

Figure 1.1: Solid forms of APIs. An adaption of a schematic diagram proposed by Aitipamula *et al.* showing the several solid forms of active pharmaceutical ingredients (APIs). Diagram adapted from *Cryst. Growth Des*. (2012). **12**, 2147−2152

Recently, in 2016, inspired by Aitipamula's comments on the need for the development of "classes" of supramolecular solids, Grothe *et al*. proposed a classification system for multicomponent crystals comprised of three classes, namely co-crystals, salts and solvates, having seven sub-classes (Grothe *et al*., 2016). According to Grothe:

1) A **co-crystal** contains only co-formers

2) A **co-crystal solvate** contains two or more co-formers and one or more solvents, but no ions. This would include hydrates, with water as a solvent.

3) A **co-crystal salt** has one or more co-formers, two or more ions, but no solvent molecules.

4) A **co-crystal salt solvate** has one or more solvents, two or more ions, and one or more conformers.

5) A **salt** contains only ions.

6) A **salt solvate** contains ions, solvent molecules, but no co-formers.

7) A **solvate** contains exactly one co-former, with one or more solvent molecules, but no ions.

A schematic diagram published by Grothe that allows for the easy visualization of his classification system is shown in **Figure 1.2**.

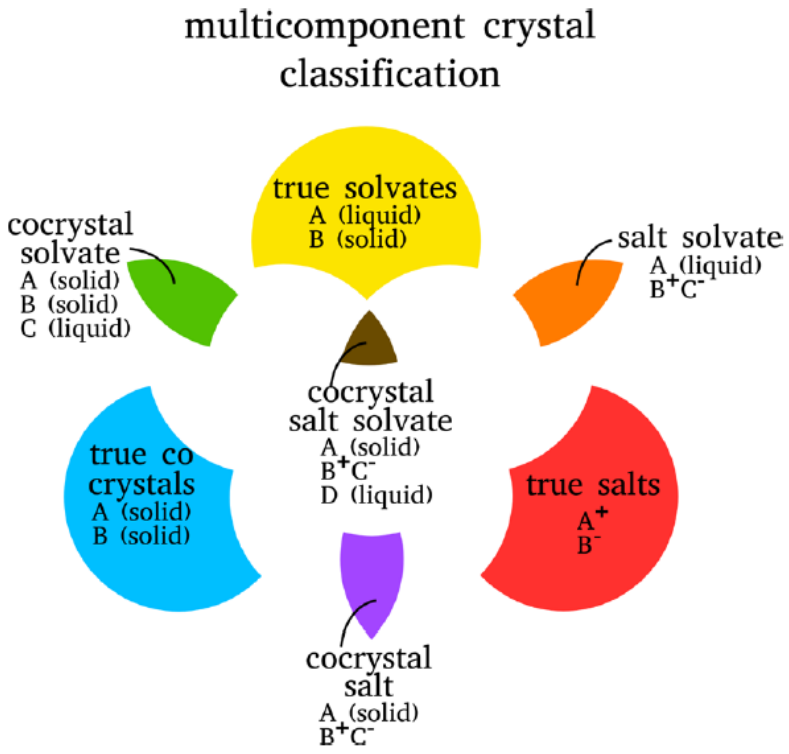

Figure 1.2: The classification system published by Grothe *et al*. showing the three classes of solids (co-crystals, salts and solvates), and their seven subclasses. Diagram taken directly from *Cryst. Growth Des*. (2016). **16**, 3237−3243.

While the differences between the sub-classes may often seem trivial, Vishweshwar points out that the differences between salts, co-crystals, solvates and hydrates can have a profound effect on the stability, physical properties and bioavailability of the APIs, and these distinctions are therefore critical to the pharmaceutical industry (Vishweshwar *et al*., 2006).

1.3 Knowledge-based co-crystal design and synthon theory

Wood *et al*. summarized the advancement of knowledge-based approaches to supramolecular synthesis in his paper "*Knowledge-based approaches to co-crystal design*" (Wood *et al*., 2014). He described the development of synthon theory from the studies of Margeret Etter to the use of modern search engines in the form of the *Cambridge Structural Database* (CSD) and *Conquest* (Groom and Allen, 2014).

Etter proposed three general rules that applied to hydrogen bonding. First, she hypothesized that all "good" proton donors and acceptors are used in hydrogen bonding. Secondly, that six-membered intramolecular hydrogen bonded rings are favoured over intermolecular interactions. And finally, she hypothesized that once all intramolecular hydrogen bonds had formed, then the remaining donors and acceptors would form intermolecular hydrogen bonds (Etter, 1990). She also described a hierarchy where particular donors, such as carboxylic acids and amides, are favoured with acceptors such as acid and amide carbonyl groups and sulfoxides. She noted that, in general, the "best donors" are usually paired with the "best acceptors". An example of a modified isoniazid co-crystal where Etter's rules are applied is shown in **Figure 1.3**.

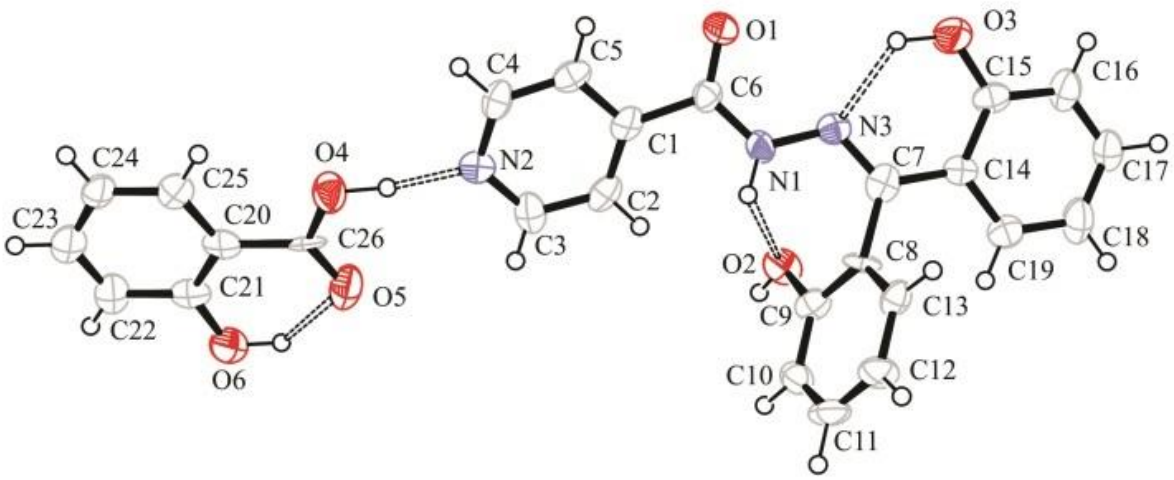

Figure 1.3: Hydrogen bonding in a modified isoniazid co-crystal. The three hydrogen bond acceptors, O2, O3 and O5, are involved in intramolecular bonding to form six membered rings rather than forming intermolecular bonds. The remaining acceptor, N2, is then involved in intermolecular bonding. O1 would generally form hydrogen bonds, but here it is sterically blocked from intermolecular interactions, as discussed in Chapter 4.2.

The term "supramolecular synthon" was first coined by Desiraju who described supramolecular synthons as structural units within supramolecular structures that can be assembled by known or conceivable intermolecular interactions and that such synthons should be robust enough to apply to different hydrogen bonding networks (Desiraju, 1995). Supramolecular synthons may involve two identical functional groups (homosynthons) or different functional groups (heterosynthons).

Zawarotko and Aakeröy later developed a usable "knowledge-based" workflow describing how synthon theory can be utilized in co-crystal design strategies (Almarsson and Zaworotko, 2004; Aakeröy and Salmon, 2005; Aakeröy *et al*., 2001, Aakeröy, 1997; Vishweshwar *et al*., 2005; Cheney *et al.*, 2011). The flowchart, published by Wood, is shown in **Figure 1.4** (Wood *et al*., 2014).

A search for robust synthons is possible on the CSD, where hydrogen bonding of various functional groups can be analyzed and the statistical data for known synthons can be determined. For example, analysis of CSD data shows that the probability of hydrogen bond formation between a carboxylic acid and a pyridyl ring is 91% (Nangia, 2009). Aakeröy *et al.* reported a study which included a search of co-crystals containing the acetaminopyridine and carboxylic

acid functional groups, and in all 28 of the compounds, the crystals were constructed via the carboxylic acid – pyridine heterosynthon. He also reported that in amide-based moieties faced with several C═O or —OH hydrogen bond acceptors, after the formation of the robust acid – pyridine synthon, the remaining N—H donor shows a preference for the amide C═O over the acid C═O (Aakeröy *et al*., 2007). This information is extremely useful in choosing a suitable co-former for the assembly of a co-crystal.

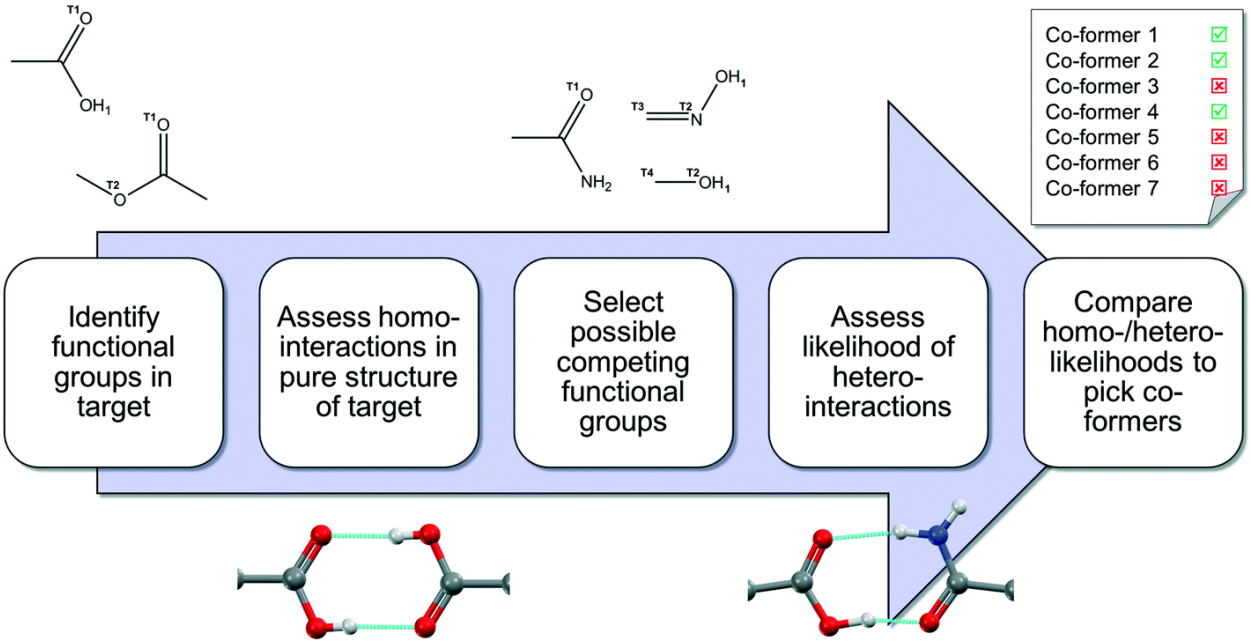

Figure 1.4: The flowchart for knowledge-based supramolecular assembly. Diagram taken directly from *CrystEngComm.* (2014). **16**, 5839-5848.

1.4 Pharmaceutical co-crystals

Co-crystals have become of great importance to the pharmaceutical industry in the last five years, and co-crystal engineering is rapidly becoming one of the most active fields of research within the industry. It is well known in the pharmaceutical industry that changing the structure and composition of an active pharmaceutical ingredient has a significant influence on the physical properties, and therefore, the bioavailability of the drug (Aakeröy and Beatty, 2001).

Poor solubility of APIs is a primary challenge facing the pharmaceutical industry (Qiao *et al*., 2011). Low solubility generally results in poor bioavailability, which may cause dosage complications, unforeseen pharmacological effects and the administration of higher doses of the affected drugs, with increased side effects. Sanphui and Nangia reported that over two thirds of all recently discovered drugs that are in the development phase experience solubility problems. They also remarked that salts and co-crystals present an immediate solution to the solubility problem due to their high solubility, stability and ease of synthesis (Sanphui and Nangia, 2014).

As with salts, co-crystals often have higher stability and solubility than their pure pharmaceutical ingredients. With regards to isoniazid, Sarcevica *et al*. observed that the solubility of isoniazid that has been co-crystallized with a dicarboxylic acid approximates the solubility of the dicarboxylic acid, although they conceded that the thermodynamic stability and crystal structure of the co-crystal also play a role in the solubility of co-crystals (Sarcevica *et al*., 2013). Sarcevica's research group has done considerable research into co-crystals of isoniazid, and have recognised that co-formers of isoniazid, for example *trans*-cinnamic acid, act synergistically with isoniazid and that co-crystallization with such co-formers may enhance multidrug resistant treatment (Sarcevica *et al*., 2013).

Shan and Zawarotko have presented several case studies that clearly demonstrate how the solubility, stability and bioavailability of API crystal forms can be enhanced through crystal engineering (Shan and Zaworotko, 2008). In addition to the improvement in bioavailability, co-crystals can be used to deliver pharmaceutical drugs that are not acidic or basic enough to form a salt, as well as other applications such as the isolation and purification of APIs, where homochiral co-crystallization can be used to separate enantiomers (Palovics *et al*., 2012).

However, crystal and co-crystal structures cannot be easily predicted from molecular structures. Very little is yet known about how or when co-crystals will form, and the synthesis of specific desired co-crystals of APIs is difficult (Lemmerer *et al*., 2011). Crystal structures are not related to molecular structures in simple ways. The way in which a molecule crystallizes depends on the nature and position of every functional group in the molecule or molecules (Desiraju, 2013). Without the systematic and modular study of functional groups, crystal and co-crystal structures must be determined empirically. For example, paracetamol, when crystallized from acetone will always form a stable monoclinic crystal structure. When crystallized from methanol, the crystals

will have a metastable orthorhombic layer structure (Boldyreva, 2003). The two polymorphs of paracetamol are shown in **Figure 1.5.**

Some recent work has been conducted using computational methods. These methods are based on searching for the most thermodynamically stable crystal structure. Although these methods do provide predictions of crystal structures, many structures may be very close in energy, providing unreliable predictions. Furthermore, there may be no routes to nucleating and growing such structures. (Price, 2014)

In summary, no tried and tested method exists to ensure successful synthesis of co-crystals. As mentioned in Section 1.3, synthon theory has been recently developed in an attempt to predict the statistical probability of hydrogen bonding, but there is a dire shortage of data regarding intermolecular forces and hydrogen bonds between different functional groups, and synthon theory is certainly far from well developed.

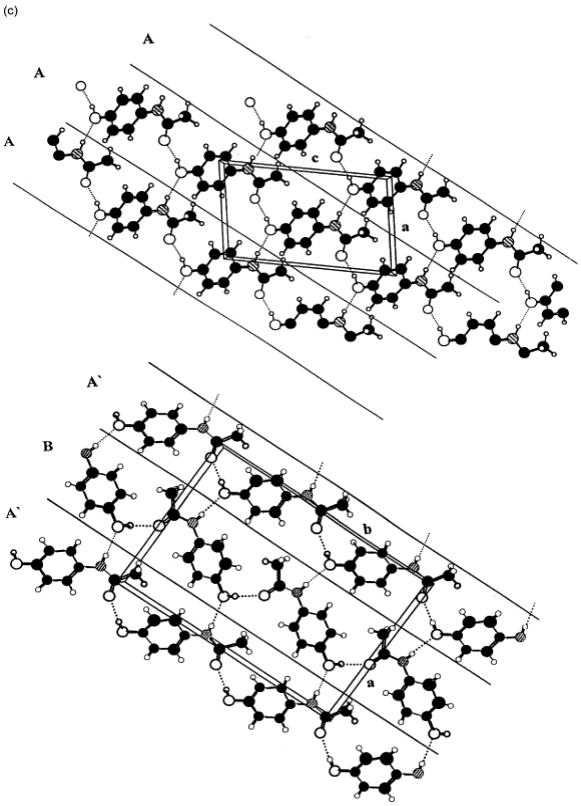

Figure 1.5: Two polymorphs of paracetamol. Diagram taken directly from *J. Mol. Struct.* (2003). **647**, 159–179.

1.5 Covalent Assisted Supramolecular Synthesis

1.5.1 Covalent assisted supramolecular synthesis and "masking" of functional groups

Covalent assisted supramolecular synthesis can be defined as the covalent modification of one part of a molecule with the purpose of gaining control over some aspect of the supramolecular synthesis of another part of the molecule, for example, the altering of the hydrogen bonding characteristics of a functional group, together with the co-crystallization of the modified molecule with a co-former (Lemmerer *et al*., 2011).

To illustrate, consider the isoniazid molecule shown in **Figure 1.6**. Isoniazid typically has five potential hydrogen bonding sites, shown by the dotted lines. The amide group, shown as **B** in the diagram, is frequently involved in intermolecular interactions. To block these intermolecular interactions, the two hydrogen atoms shown as **A** could be replaced by two more bulky ligands, for example, methyl groups or aromatic rings. This covalent modification sterically blocks any adjacent molecule from approaching **B**. The amide functional group, **B**, is then said to be sterically "masked" from any intermolecular interactions (Lemmerer *et al*., 2011). This co-crystal engineering technique of sterically modifying one part of a molecule to control the supramolecular assembly of another part of the molecule is referred to as "covalent assisted supramolecular synthesis".

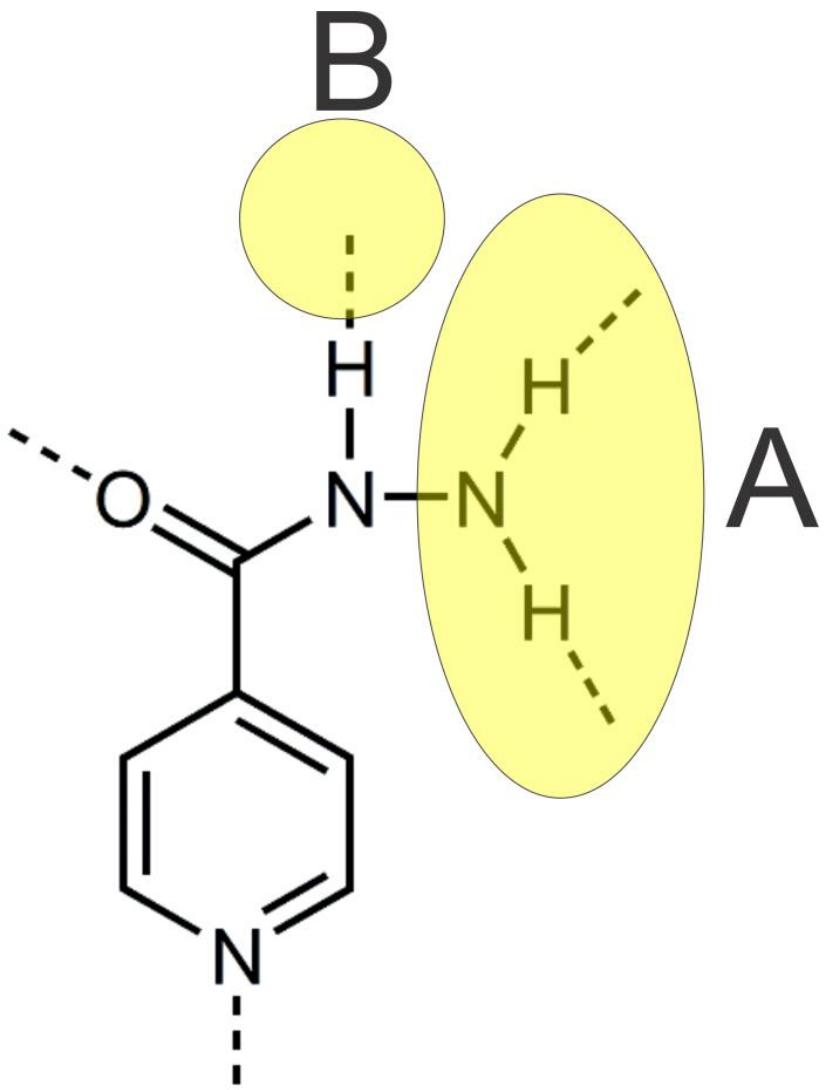

Figure 1.6: A molecule of isoniazid. Covalently modifying the terminal nitrogen atom, **A**, by replacing the two hydrogen atoms with more bulky groups has an effect on the intermolecular interactions of the amide group, **B**.

1.5.2 Benzophenone and its derivatives as covalent modifiers

While the covalent modification of isoniazid has been studied, there is no detailed or systematic study of the effect of bulky groups in particular on the supramolecular synthesis of isoniazid. The need for such data prompted an in-depth study of bulky groups and their effects in the covalent assistance of isoniazid, and a series of benzophenone and its derivatives were chosen for this study. Benzophenone and its derivatives are not pharmaceutically active, but were

chosen primarily for their steric effects when modifying isoniazid. Benzophenone and its derivatives are "Generally Regarded as Safe (GRAS)" substances and are thus suitable for use in API studies in this respect (Burdock *et al*., 1991; Elder, 1983) .

While experimenting on the covalent modification of isoniazid, a variety of crystals were often found to be formed simultaneously during crystallization. In addition to the desired modified isoniazid moiety, crystals were also harvested that were found to be benzophenone azines (**Figure 1.7**). This prompted further investigation into the behaviour of the benzophenone derivatives, and this study was thus extended to investigate the formation of crystals of side-products of benzophenone and its derivatives produced during the covalent modification of isoniazid, in order to obtain a comprehensive and complete knowledge of all processes involved during the covalent assisted supramolecular synthesis of isoniazid with these bulky groups. The eight benzophenone derivatives that were used in this study are shown in **Table 1.1**.

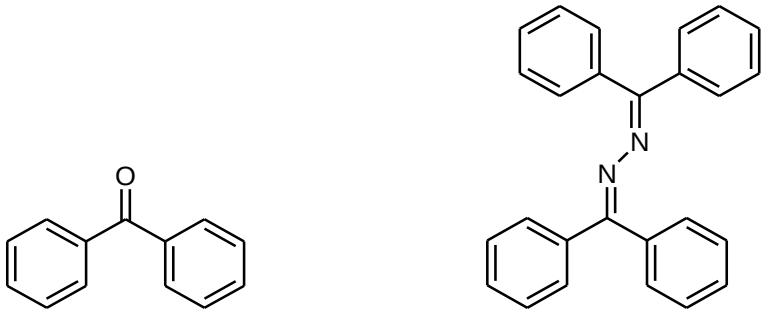

(a) (b)

Figure 1.7: (a) Benzophenone and (b) benzophenone azine.

Table 1.1: The eight benzophenone derivatives used in this study.

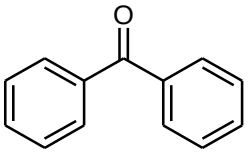 Benzophenone	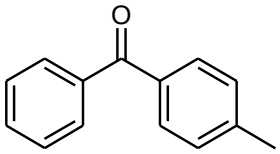 4-Methylbenzophenone
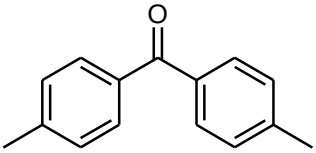 4,4'-Dimethylbenzophenone	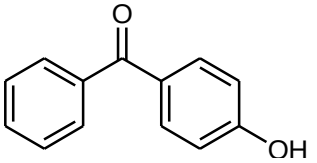 4-Hydroxybenzophenone
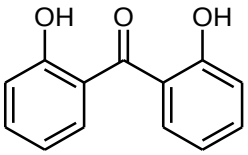 2,2'-Dihydroxybenzophenone	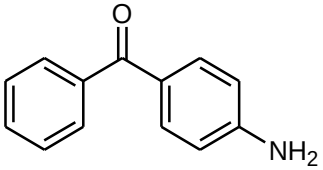 4-Aminobenzophenone
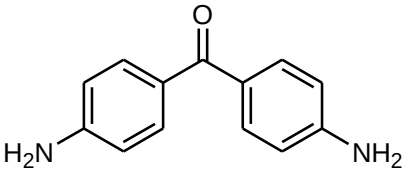 4,4'-Diaminobenzophenone	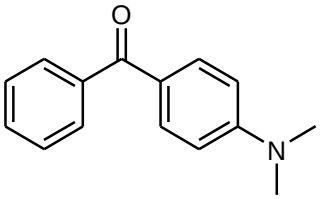 4-(Dimethylamino)benzophenone

1.6 Isoniazid and its derivatives

Isoniazid (isonicotinic acid hydrazide) is the front-line chemotherapeutic drug used in the treatment of tuberculosis in South Africa. However, *Mycobacterium tuberculosis* is becoming increasingly resistant to isoniazid, and it has become urgent that drugs which are effective against resistant strains of the bacteria are developed. It has been reported that the covalent modification of isoniazid is an effective way to enhance the efficacy of the drug against these resistant strains (Suarez *et al*., 2009; Hearn *et al*., 2009). Isoniazid is a pro-drug, and must be activated by the bacterial catalase-peroxidase enzyme called KatG in Mycobacterium tuberculosis. KatG attaches to the isonicotinic acyl group with the reduced form of nicotinic adenine dinucleotide (NADH) to form an active complex. However, N-arylaminoacetyl transferases (a different class of enzyme), rapidly acetylate the amino position of isoniazid, preventing the reaction with NADH. This decreases the efficacy of isoniazid, resulting in drug resistance (Suarez *et al*., 2009; Hearn *et al*., 2009).

However, if the isoniazid is reacted with an aldehyde or ketone group, the NH_2 functional group is replaced with an imine group (**Figure 1.8**), and the modified isoniazid becomes structurally blocked from the effects of the N-arylaminoacetyl transferases, resulting in a drug which may be effective against drug-resistant tuberculosis strains (Suarez *et al*., 2009; Hearn *et al*., 2009).

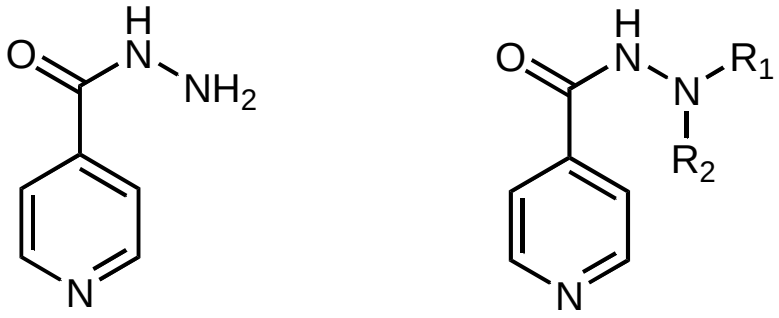

(a) (b)

Figure 1.8: (a) The structure of isoniazid and (b) covalently modified isoniazid.

In addition to such covalent modification, the bioavailability of the modified isoniazid may be further enhanced by co-crystallizing it with a co-former, as discussed in Section 1.4. From a crystal engineering point of view, the pyridine ring of isoniazid is an excellent hydrogen bond acceptor to the carboxylic acid group, as well as to other functional groups. The hydrazide group of isoniazid also has potential to hydrogen bond through its oxygen and nitrogen atoms, and has three hydrogen atoms which can act as donors. Thus, from a synthon perspective, isoniazid is an ideal choice for studies of co-crystal formation and crystal engineering (Mashhadi *et al*., 2014). In 2010, Grobelny *et al.* stated that "*Without any doubt there is a need for novel therapeutic agents and/or combinations based on drug substances already available for the treatment of TB.*" (Grobelny *et al*., 2011).

The covalent modification of isoniazid with a ketone or aldehyde occurs via an acid-catalyzed condensation reaction. The reaction starts with a nucleophilic attack on the carbonyl group by the amine nitrogen to form an unstable carbinolamine moiety, followed by acid catalyzed dehydration to form an imine (Xavier and Srividhya, 2014). This resulting imine will be referred to throughout this thesis as "modified isoniazid". The mechanism of covalent modification is shown in **Figure 1.9**.

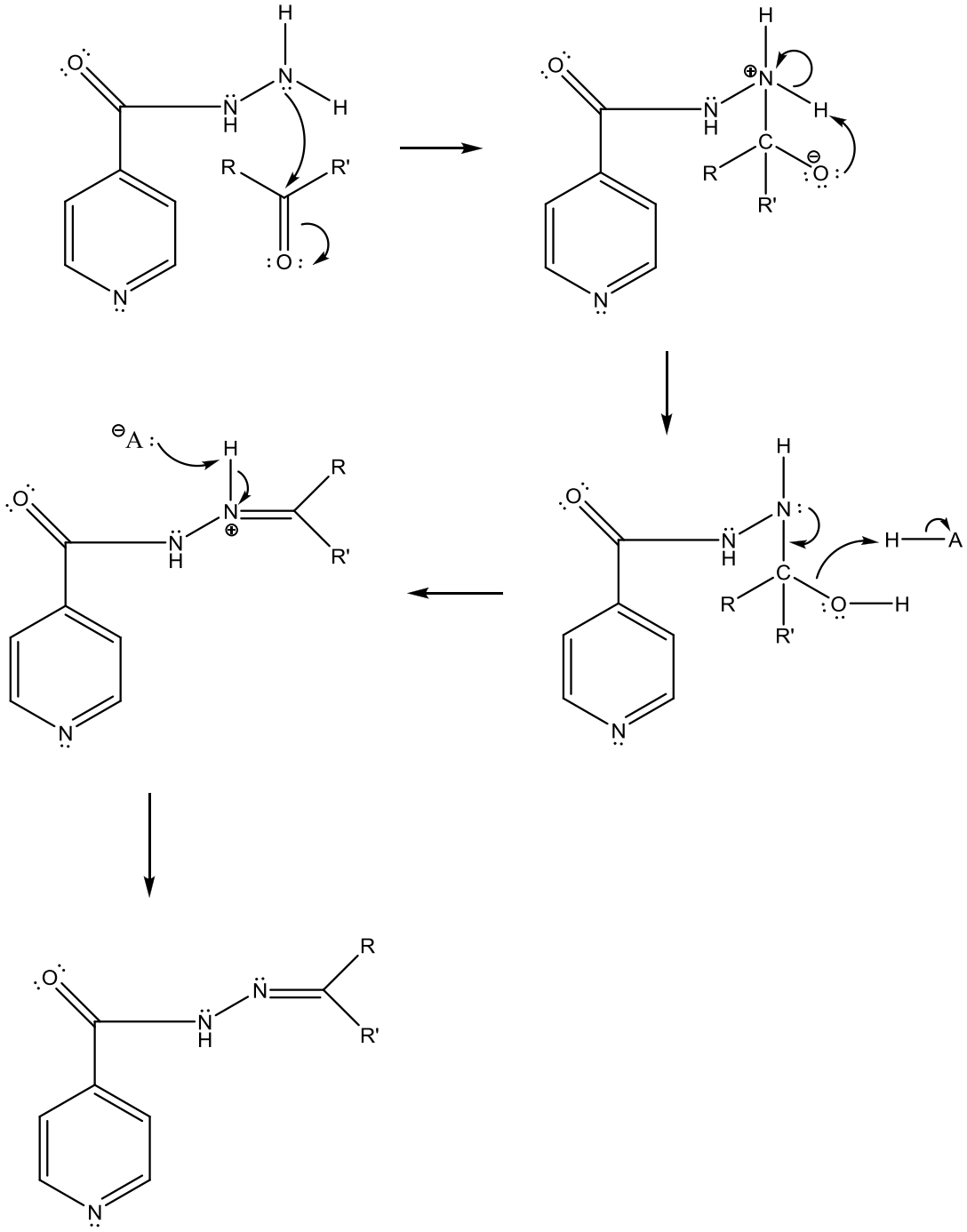

Figure 1.9: The mechanism for the acid catalyzed covalent modification of isoniazid to form an imine (modified isoniazid).

1.7 4-Aminoantipyrine and its derivatives

4-Aminoantipyrine (4AAP) is an API with powerful antipyretic (fever reducing) properties (Acheson, 1960), and is considered a prophylactic against oxidative stress (Teng *et al*., 2011a). Two of its derivatives, aminoantipyrine and 4-(*N*,*N*-dimethyl)-aminoantipyrine, have been used as analgesic and anti-inflammatory drugs since the late 19th century. Their concurrent use with aspirin is particularly beneficial as they have been shown to prevent or attenuate the anti-platelet effects of aspirin (Hohlfeld *et al*., 2008). However, despite the many documented therapeutic benefits, these pyrazolones have been associated with agranulocytosis, an acute condition involving a severe lowered white blood cell count, and their use has been largely discontinued (Teng *et al*., 2011b). This has sparked several attempts to synthesize salts and co-crystals of 4AAP (Huo, 2009), as well as a drive to produce covalently modified derivatives of 4AAP (Deshmukh *et al*., 2015). Deshmukh commented that due to the significant benefits of 4AAP derivatives, and their interactions with DNA, the precise nature and structures of these Schiff bases is of "*remarkable importance*" (Deshmukh *et al*., 2015). The desired modification of 4AAP to prepare pharmaceutically significant derivatives is by the covalent addition of adducts to the 4-amino functional group shown in **Figure 1.10**.

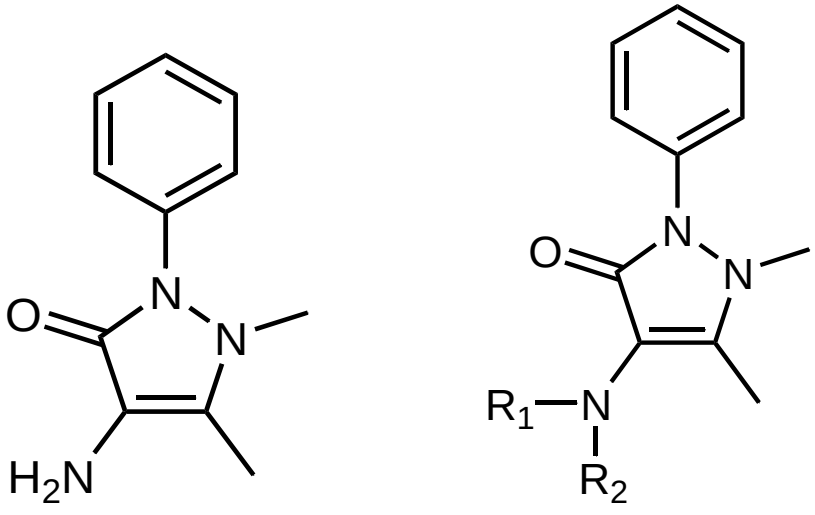

Figure 1.10: Structure of 4-aminoantipyrine (4AAP) and its derivatives. The desired modification of 4AAP is by the covalent addition of adducts (R_1 and/or R_2) to the 4-amino functional group.

In addition to its pharmaceutical interest, 4AAP is an interesting candidate for crystal engineering due to its high reactivity with ketones and aldehydes and its subsequent reluctance to form molecular salts or co-crystals. It reacts readily with ketones and aldehydes at room temperature, and its reactive properties have made it useful as a nitrogen scavenger species against hydroxyl radicals (Santos *et al.*, 2010). To date, 251 derivatives of 4AAP have been reported in the CSD (version 5.39) where the modifying adduct has attached to the amino nitrogen atom. Yet, despite the drive to synthesize salts and co-crystals of pharmaceuticals such as 4AAP, only five molecular salts of 4AAP have been reported, of which two are simple salts with halide counter-ions (**Table 1.2**). No co-crystal or complex of 4AAP in which all species are neutral has ever been reported. The scarcity of salts of 4AAP and the complete absence of any co-crystals of the species are in part due to the fact that it reacts covalently with many of its potential co-former rather than co-crystallizing on a supramolecular basis.

Therefore, it is clear that a co-crystal design strategy for the supramolecular synthesis of co-crystals (and salts) of 4AAP should be developed. There is also a need to prepare covalently modified derivatives of 4AAP, and for a study of their molecular and supramolecular structures.

Table 1.2: Reported salts of 4-aminoantipyrine

Salt	**CSD Reference Code**	**Reference**
aminoantipyrine-4-aminium chloride	HUKTIS	(Chitradevi *et al.*, 2015)
aminoantipyrine-4-aminium bromide monohydrate	PAXSOY	(Yang *et al.*, 2012)
aminoantipyrine-4-aminium thiourea chloride	EVOLIL	(Murtaza *et al.*, 2011)
aminoantipyrine-4-aminium 2,2'-dithiobenzoate	PUGHEF, PUGHEF01	(Huo *et al.*, 2009) (Fazil *et al.*, 2012)
aminoantipyrine-4-aminium salicylate	DUHYOV	(Chitradevi *et al.*, 2009)

1.8 Carboxylic acids as co-formers

The carboxylic acid – pyridine (COOH···N_{pyr}) heterosynthon is well known, and is shown in the example in **Figure 1.11.** Statistically, from analysis of CSD structures, the probability of hydrogen bond formation between a carboxylic acid and a pyridyl ring is 91% (Nangia, 2009). In particular, many successful attempts at co-crystallization of isoniazid with benzoic acids have been reported in which this heterosynthon has been used. A comprehensive list of all carboxylic acid co-formers of unmodifed isoniazid reported on the CSD (version 5.39) to date (February 2018), including their references and CSD reference codes, are listed in **Table 1.3**.

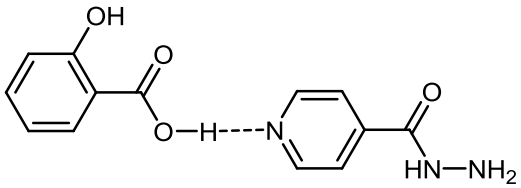

Figure 1.11: The robust COOH···N_{pyr} heterosynthon between isoniazid and 2-hydroxybenzoic acid.

Table 1.3: All reported carboxylic acid co-formers of unmodified isoniazid on the CSD (version 5.39) with their corresponding CSD reference codes and literature references.

Year	Co-former	CSD Reference Code	Reference
2008	2,2'-dithiodibenzoic acid	BIZMAZ	(Meng *et al*., 2008)
2010	malonic acid succinic acid glutaric acid adipic acid pimelic acid 4-hydroxybenzoic acid 2,4-dihydroxybenzoic acid	FADGEY FADGIC, FADGIC02 FADGOI FADGUO FADHAV FADHEZ FADHID	(Lemmerer *et al*., 2010)
2011	4-aminosalicylic acid	URUDER, URUDER01-URUDER10	(Grobelny *et al*., 2011)

2012	salicylic acid 2-chloro-4-nitrobenzoic acid	LATKUO LATLEZ	(Lemmerer, 2012)
2012	fumaric acid	LATTAD	(Cherukuvada *et al*., 2012)
2013	3-(4-hydroxyphenyl)acrylic acid	PEHFUF	(Ravikumar *et al*., 2013)
2013	4-hydroxybenzoic acid nicotinamide / succinic acid (ternary co-crystal) Nicotinamide / fumaric acid (ternary co-crystal)	BICQUB, BICQUB01, LATTAD01, LATTAD02 BICQUA BICQEL	(Aitipamula *et al*., 2013)
2013	benzoic acid sebacic acid *trans*-cinammic acid suberic acid	SETRIU SETROA SETSAN SETSAN01, SETSAN02 SETRUG	(Sarcevica *et al*., 2013)
2014	3,4,5-Trihydroxybenzoic acid	LODHOD, LODHOD01	(Kaur *et al*., 2014)
2014	2,3-dihydroxybenzoic acid 3,5-dihydroxybenzoic acid 3-hydroxybenzoic acid 3,4,5-Trihydroxybenzoic acid	BOMBOW BOMBUC BOMCAJ LODHOD02	(Mashhadi *et al*., 2014)
2014	ferulic acid vanillic acid caffeic acid	FOSFIE FOSFUQ, FOSFUQ01 FOSMIL, FOSMIL01	(Swapna *et al*., 2014)
2016	adipic acid	FADGUO01	(Sarcevica *et al*., 2016)
2016	3,4-dihydroxybenzoic acid	EJOYEV	(Mashhadi *et al*., 2016)
2017	benzene-1,2,4,5-tetracarboxylic acid	VEGHOH	(Cunha *et al*., 2017)
2018	4-cyanobenzoic acid 4-aminobenzoic acid 4-nitrobenzoic acid	ACUDAG ACUDEK, ACUDEK01 ACUDIO	(Diniz *et al*., 2018)

When considering a suitable co-former for the synthesis of 4-aminoantipyrine, it was noted that Hemamalini *et al*. successfully co-crystallized various aminobenzoic acids (in particular, 2-aminobenzoic acid) with a series of aminopyridines (excluding 4AAP). This study showed that the carboxylic acid functional group on 2-aminobenzoic acid is potentially capable of forming a robust heterosynthon with either the amine or with the carbonyl functional groups of molecules with the aminopyridine backbone (Hemamalini *et al*., 2014). Based on Hemamalini's study, 2-aminobenzoic acid may therefore be considered a potentially good choice as a possible heterosynthon for co-crystals of 4AAP. Furthermore, the molecular packing modes of carboxylic acids have been extensively studied and documented and the most important homo- and heterosynthons have been described in detail by Leiserowitz (Leiserowitz, 1976), and the use of carboxylic acids as the co-former of choice with isoniazid and 4AAP can thus be considered a knowledge based approach to co-crystal engineering.

Carboxylic acids were therefore chosen to be the co-formers for all co-crystal syntheses in this study. Benzoic acids were chosen as co-formers to co-crystallize with modified isoniazid, and a range of carboxylic acids were investigated as possible co-formers for the supramolecular synthesis of multicomponent crystals of 4AAP.

1.9 Dimensionality of packing

A crystal or co-crystal will pack as a 3-dimensional (3D) hydrogen bonded network, a 2-dimensional (2D) sheet, a 1-dimensional (1D) chain or tape (also referred to as a ribbon), or as zero-dimensional (0D) entities, depending largely on the number of hydrogen bonding sites between the co-crystallizing molecules. 3D hydrogen bonded networks are infinite three dimensional supramolecular structures which are connected by three or more hydrogen bonds, whereas 2D sheets are infinite two-dimensional structures. A 1D chain is an infinite one-dimensional structure where molecules are connected by a single hydrogen bond, whereas a 1D tape (or ribbon) refers to infinite one-dimensional structures connected by two or more hydrogen bonds, where these hydrogen bonds are essentially co-planar (Burrows, 2004). Examples of each type of packing dimensionality are shown in **Figure 1.12**.

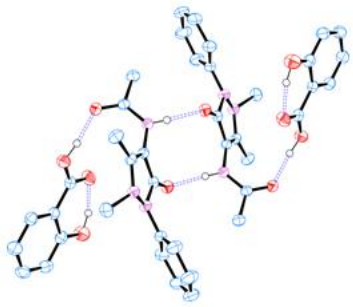

(a)

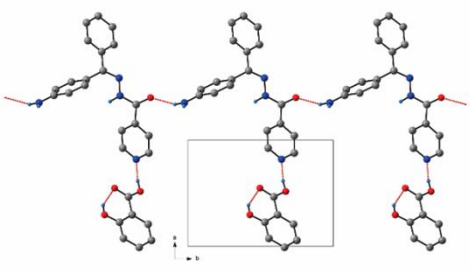

(b)

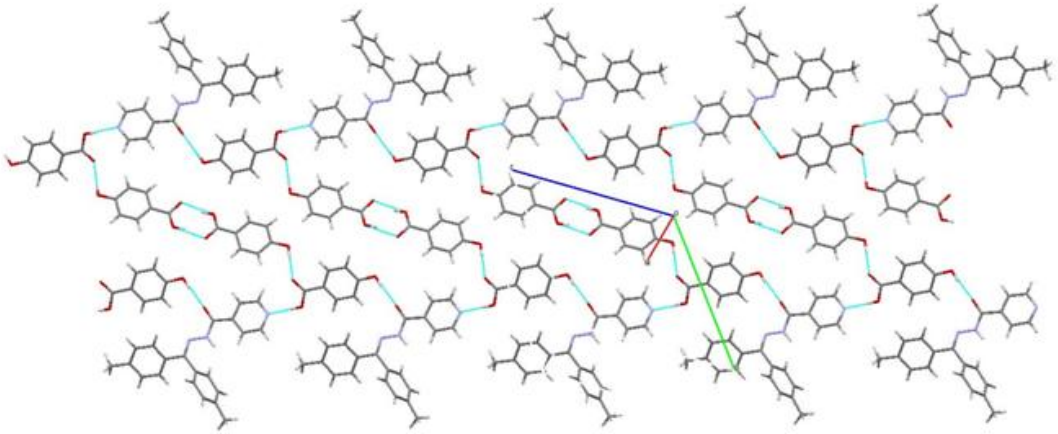

(c)

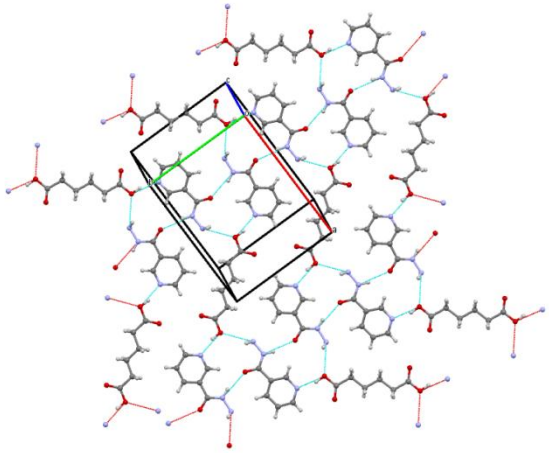

(d)

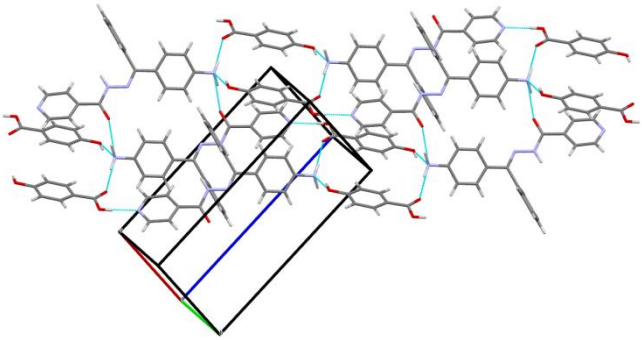

(e)

Figure 1.12: Examples of dimensionality of packing. (a) Co-crystals with 0D packing dimensionality. (b) A 1D chain. (c) A 1D tape (or ribbon). (d) A 2D sheet. (e) A 3D network.

1.11 Aims and objectives of this study

The aims of this study were to contribute to the development of crystal and co-crystal design strategies and to the understanding of crystal and co-crystal structures of isoniazid, 4-aminoantipyrine, benzophenone and their derivatives.

Crystal design involves the synthesis of crystal structures with desired properties, based on an understanding of, and use of intermolecular interactions. Co-crystal design involves a study of the processes of supramolecular synthesis and to develop design strategies to elucidate predictable and exploitable mechanisms for co-crystallization processes.

In particular, the specific objectives of this study were to:

- Prepare co-crystals of covalently modified isoniazid using bulky modifiers (namely benzophenone and derivatives of benzophenone) and examine how these bulky modifiers and crystallization conditions affect the supramolecular structure of the co-crystals.
  (Chapter 4)

- Crystallize and perform a structural study of isoniazid that has been covalently modified with benzophenone and its derivatives.
  (Chapter 5)

- Examine the formation of the crystalline benzophenone azine side-products formed during the covalent modification and co-crystallization of isoniazid.
  (Chapter 6)

- Develop a design strategy for the supramolecular synthesis of 4-aminoantipyrine.
  (Chapter 7)

- Crystallize and perform a structural study of covalently modified 4-aminoantipyrine.
  (Chapter 8)

Chapter 2: Literature

2.1 The crystal structure of isoniazid

The crystal structure of isoniazid was first published in the Journal of the American Chemical Society by H. Jensen in 1954. Crystals of isoniazid were described as well developed needles extended along the *c*-axis. The unit cell was found to be orthorhombic with dimensions a = 11.33 Å, b = 14.74 Å, c = 3.84 Å and a $P2_12_12_1$ space group (Jensen, 1954). The crystal structure of isoniazid (**Figure 2.1a**) shows four hydrogen bonding interactions of isoniazid, via the pyridine nitrogen atom (hydrogen bond acceptor), the amino hydrogen atom (donor), the amino nitrogen atom (acceptor) and the hydrazide hydrogen atom (donor). Both NH_2 hydrogens are involved in hydrogen bonding. The single crystal structure of isoniazid does not show any hydrogen bonding interactions of the carbonyl oxygen atom, but it has been demonstrated via shifts observed in a vibrational spectroscopy study that there is, in fact, hydrogen bonding of the carbonyl oxygen atom (Akalin and Akyuz, 2007). Examining the short contacts in the crystal structure suggests a weak bifurcated C—H···O interaction between the carbonyl oxygen atom and two hydrogen atoms of an adjacent pyridine ring (**Figure 2.1b**).

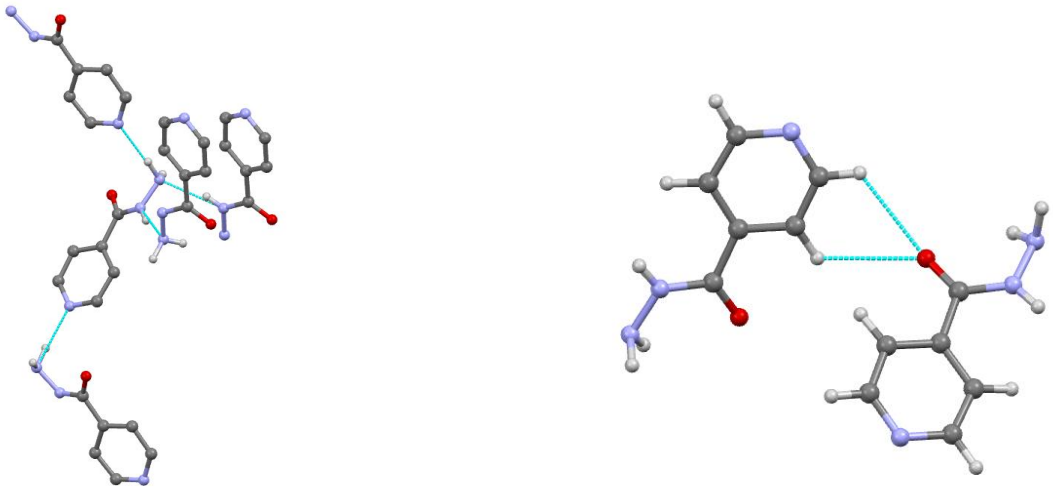

(a) (b)

Figure 2.1: The crystal structure and hydrogen bonding of isoniazid (CSD ref: INICAC1). The hydrogen bonding observed in the crystal structure is shown in (a), while (b) shows short contacts between the carbonyl oxygen atom and two hydrogen atoms of the pyridyl ring.

2.2 Co-crystal engineering of isoniazid

2.2.1 The co-crystallization of isoniazid and modified isoniazid

Since the realization that co-crystallization of APIs may lead to changes in their physicochemical properties, there has been a plethora of advances in this field. However, the investigation of co-crystals of the anti-tuberculosis drug isoniazid has only gained serious attention since 2010. In that year, Lemmerer, Bernstein and Kahlenberg made use of the "knowledge-based" approach synthon theory to synthesize seven co-crystals of isoniazid with mono and dicarboxylic acids. It was observed that the primary intermolecular interaction present in all seven co-crystals was the carboxylic acid – pyridine ($COOH\cdots N_{pyr}$) heterosynthon (Lemmerer *et al*., 2010). In the same year, Grobelny *et al.* synthesized two drug-drug co-crystals of isoniazid, having pyrazinamide and 4-aminosalicylic acid as co-formers. They confirmed that the same heterosynthon observed by Lemmerer was present in both co-crystals. They also noted that in 4-aminosalicylic acid, there are two distinct symmetry independent carboxylic acid – pyridine heterosynthons. The extent of proton transfer is dependent on the temperature, and although the first heterosynthon clearly has the characteristics of a co-crystal, the second may be more indicative of a salt, as shown in **Figure 2.2**. Inspection of the H–O lengths reveals that the H-atom is largely in the same position at different temperatures in pair I, but there is evidence for proton migration in pair II, with more salt-like character present at lower temperatures. At 100K, the $OH\cdots N_{pyr}$ bond length is 1.30Å, but this lengthens to 1.56 Å at 240K. (Grobelny *et al.*, 2011)

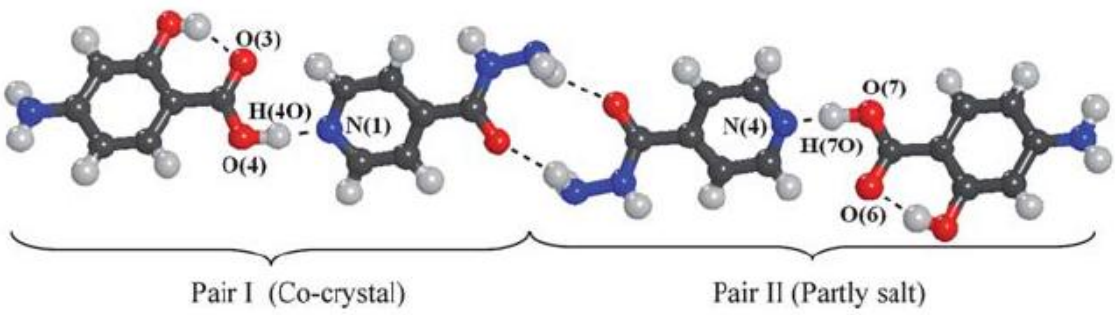

Figure 2.2: The two distinct carboxylic acid – pyridine heterosynthons observed in the supramolecular synthesis of isoniazid with 4-aminosalicylic acid. One of these heterosynthons has the characteristics of a co-crystal and the other of a salt. Diagram taken directly from *CrystEngComm*. (2011). **13**, 4358–4364.

In 2011, Sevukarajan *et al.* synthesized a co-crystal of isoniazid with L(+) tartaric acid and published an extensive study on the physical and biological properties of the co-crystal. They observed that the micrometritic properties (relating to the surface area and particle size of the drugs) was improved though co-crystallization, but that with this particular co-former, solubility decreased and the anti-tubercular activity decreased as compared with pure isoniazid. This was determined by comparing the *in vitro* antitubercular activity of pure isoniazid against *M. tuberculosis* with that of the co-crystal using a *Microplate Alamar Blue* assay. The compounds show activity up to 12.5 μg/ml for pure isoniazid and 25 μg/ml for the L(+) tartaric acid/isoniazid co-crystal. This indicates that the co-crystal has less antitubercular activity than the pure drug. (Sevukarajan *et al*., 2011).

In 2013, Aitipamula *et al*. reported the co-crystallization of isoniazid with succinic acid, fumaric acid, 4-hydroxybenzoic acid (*p*HBA) and nicotinamide. Co-crystallization of isoniazid with *p*HBA yielded two polymorphs of the hydrated co-crystal (**Figures 2.3 and 2.4**). Co-crystallization with fumaric acid likewise produced a novel polymorph. A ternary co-crystal of isoniazid, nicotinamide and succinic acid was also reported (**Figure 2.5**). Once again, all co-crystals present were hydrogen bonded through the carboxylic acid – pyridine heterosynthon. In contrast to the observation of Sevukarajan, Aitipamula reported that in the ternary co-crystal, the solubility was increased compared with pure isoniazid. However, other co-crystals displayed decreased solubility (Aitipamula *et al*., 2013). Before this publication, there had been no reported polymorphs of co-crystals of isoniazid, or of any hydrates of isoniazid co-crystals.

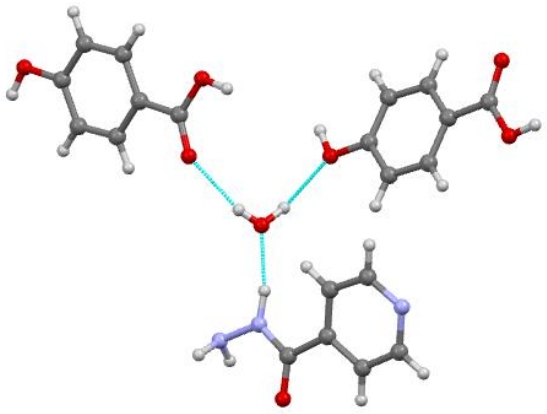

Figure 2.3: First reported hydrate of a co-crystal of Isoniazid. (CSD ref: BICQUB01)

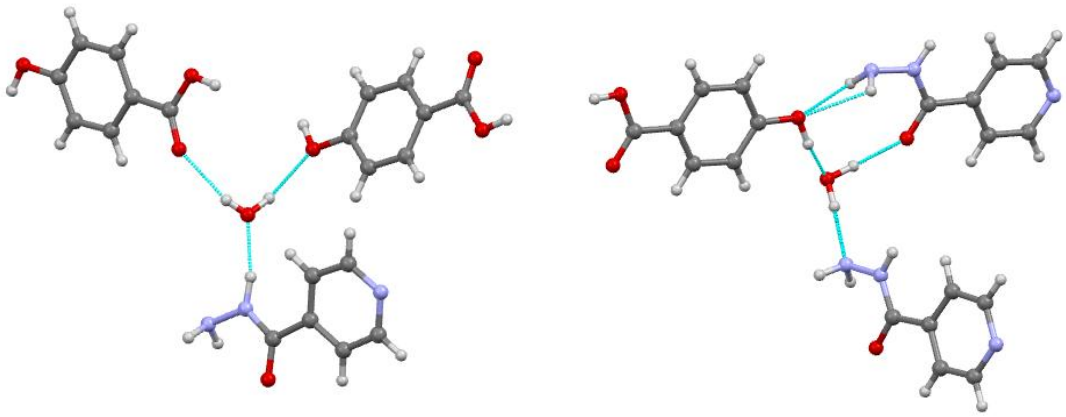

Polymorph Form I (a)

Polymorph Form II (b)

Figure 2.4: First reported polymorphs of a co-crystal of isoniazid, using 4-aminobenzoic acid as the co-former. (CSD ref: (a) BIQQUB01 and (b) BICQUB)

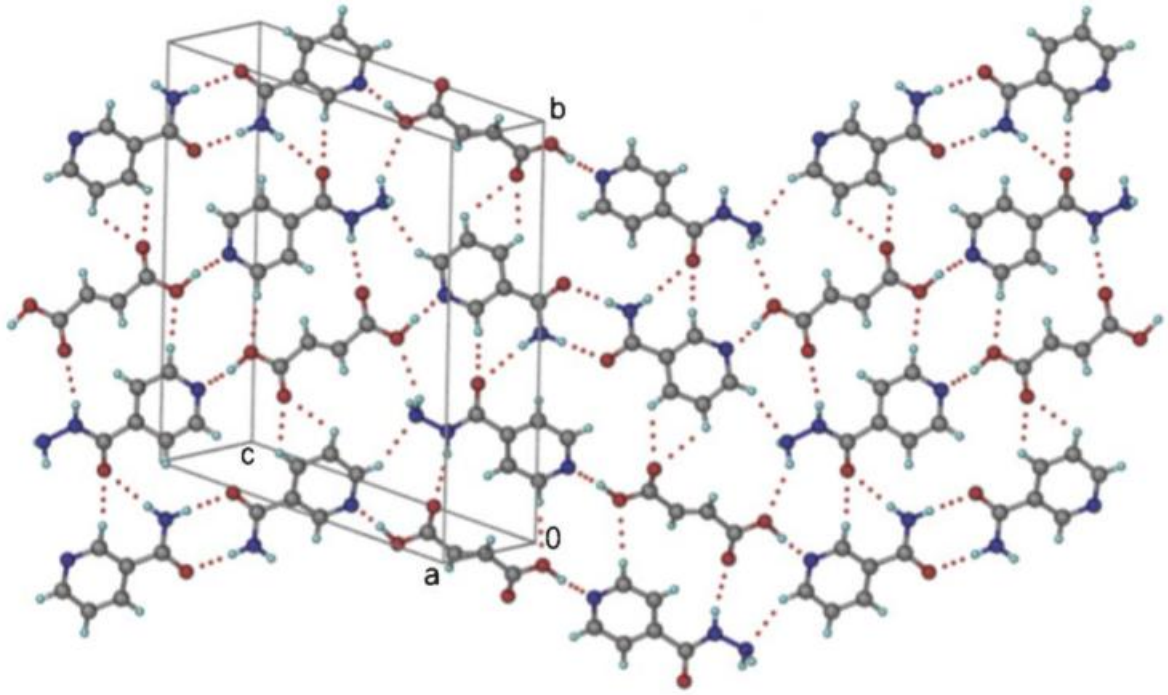

Figure 2.5: First reported ternary co-crystal of Isoniazid, using nicotinamide and fumaric acid as co-formers. Diagram taken directly from *CrystEngComm*, 2013, **15**, 5877–5887.

In the same year, Sarcevica *et al.* reported a series of isoniazid co-crystals with various carboxylic acids. However, the contribution of Sarcevica *et al.* to the understanding of the co-crystallization of isoniazid will be discussed in detail in Section 2.2.4.2 where work done on polymorphism of isoniazid co-crystals is detailed.

In 2014, Mashhadi *et al.* reported the synthesis of 1:1 co-crystals of isoniazid with four anti-oxidant hydroxybenzoic acids, namely 3-hydroxybenzoic acid, 2,3-dihydroxybenzoic acid, 3,5-dihydroxybenzoic acid and 3,4,5-trihydroxybenzoic acid (gallic acid). A notable deviation from the previously reported isoniazid co-crystals was the absence of the carboxylic acid – pyridine heterosynthon with the 3,5-dihydroxybenzoic acid co-former. While the other three co-formers displayed the usual synthon, 3,5-dihydroxybenzoic acid was hydrogen bonded to isoniazid via a phenol – pyridine heterosynthon (Mashhadi *et al*., 2014). (**Figure 2.6**)

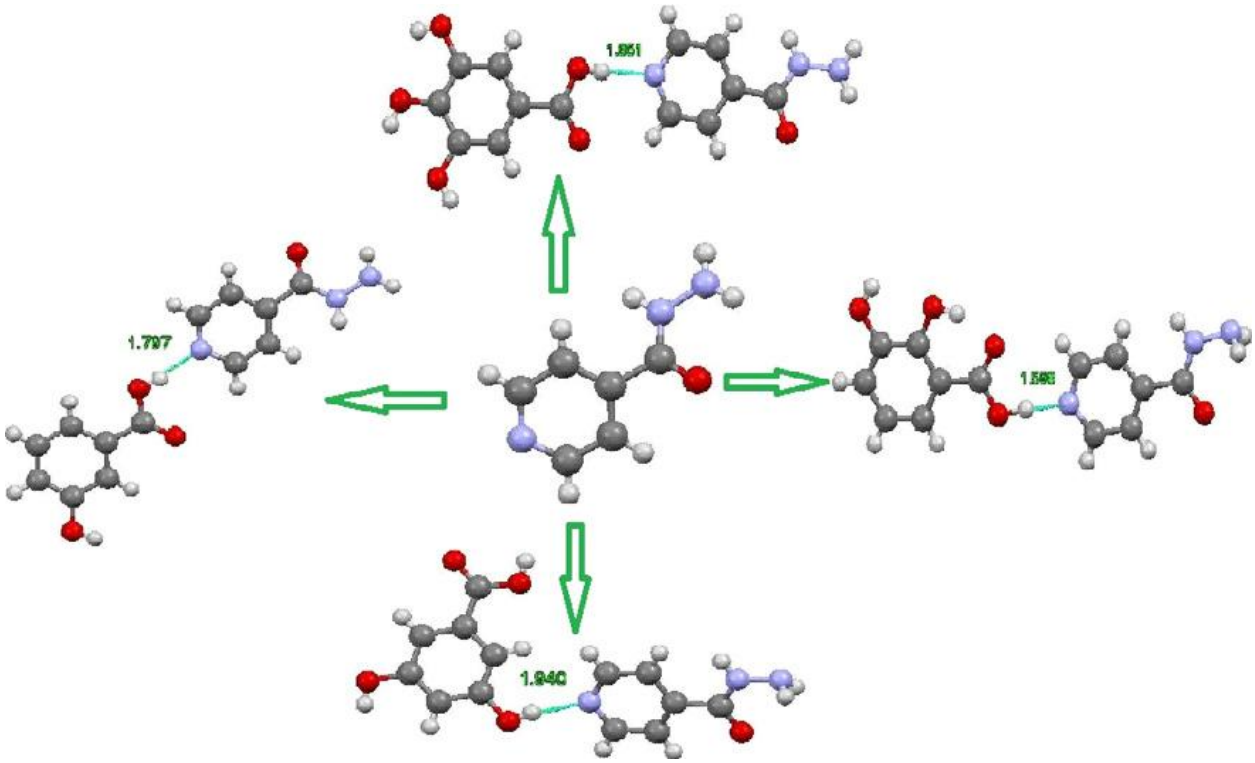

Figure 2.6: Four co-crystals of isoniazid with anti-oxidant hydroxybenzoic acids synthesized by Mashhadi *et al.* Note that the co-crystal of isoniazid with the 3,5-dihydroxybenzoic acid co-former is unusual because it forms via the phenol – pyridine synthon rather than the usual carboxylic acid – pyridine synthon . Diagram taken directly from *J. Mol. Struct.* (2014) **7**, 446-452.

Swapna *et al.* has noted that isoniazid undergoes degradation in fixed-dose combination (FDC) drugs, and has reported co-crystals of isoniazid with vanillic acid, ferulic acid, caffeic acid and resorcinol. The main goal of their work was to produce stable forms of isoniazid. Their work on solid forms of isoniazid with these co-formers was also the first report on preparing co-crystals of isoniazid using liquid-assisted grinding (LAG) (Swapna *et al*., 2014).

The synthesized co-crystals of isoniazid and vanillic acid were dimorphic. Likewise, those of isoniazid and ferulic acid were also dimorphic, and those with caffeic acid were trimorphic. The co-crystal of isoniazid and resorcinol was the only co-crystal in their report that did not exhibit polymorphism.

The co-crystals were tested for stability and were found to be stable at ambient temperature and humidity for up to one year. At the higher temperature of 40°C and 75% relative humidity, all forms except the isoniazid-resorcinol co-crystal were stable for at least six months. The isoniazid-resorcinol co-crystal started degrading after one month.

Swapna *et al.* concluded that one of the forms of each of the isoniazid-ferulic acid and isoniazid-vanillic acid co-crystals (**Figure 2.7**), as well as one of the forms of isoniazid caffeic acid co-crystal may thus be suitable co-crystals for a stable isoniazid solid form (Swapna *et al*., 2014).

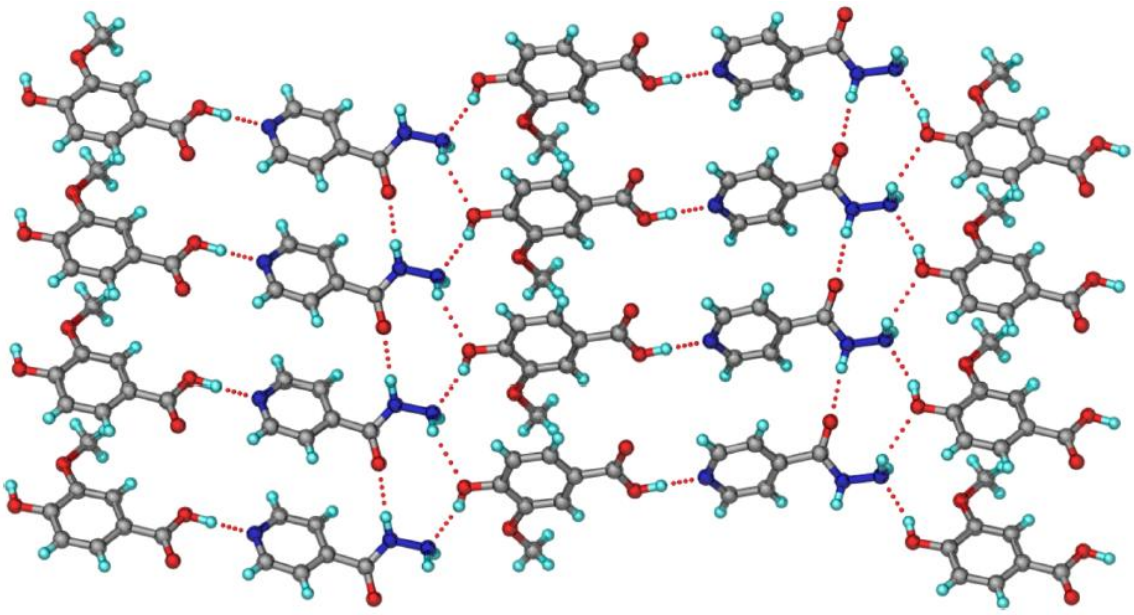

Figure 2.7: The isoniazid vanillic acid co-crystal prepared by Swapna *et al.* showing the sheet structure and the N—H···O and O—H···N heterosynthons. Diagram taken directly from *Cryst. Growth, Des.* 2014, **14**, 5991–6005.

Of further interest in their study, Swapna *et al.* reported a screening study of all heterosynthons found in co-crystals of isoniazid to date. As expected, the carboxylic acid – pyridine heterosynthon was the predominant synthon in co-crystals of isoniazid, but seven other homo- and heterosynthons have been reported in isoniazid co-crystal structures and are shown in **Figure 2.8** (Swapna *et al.*, 2014).

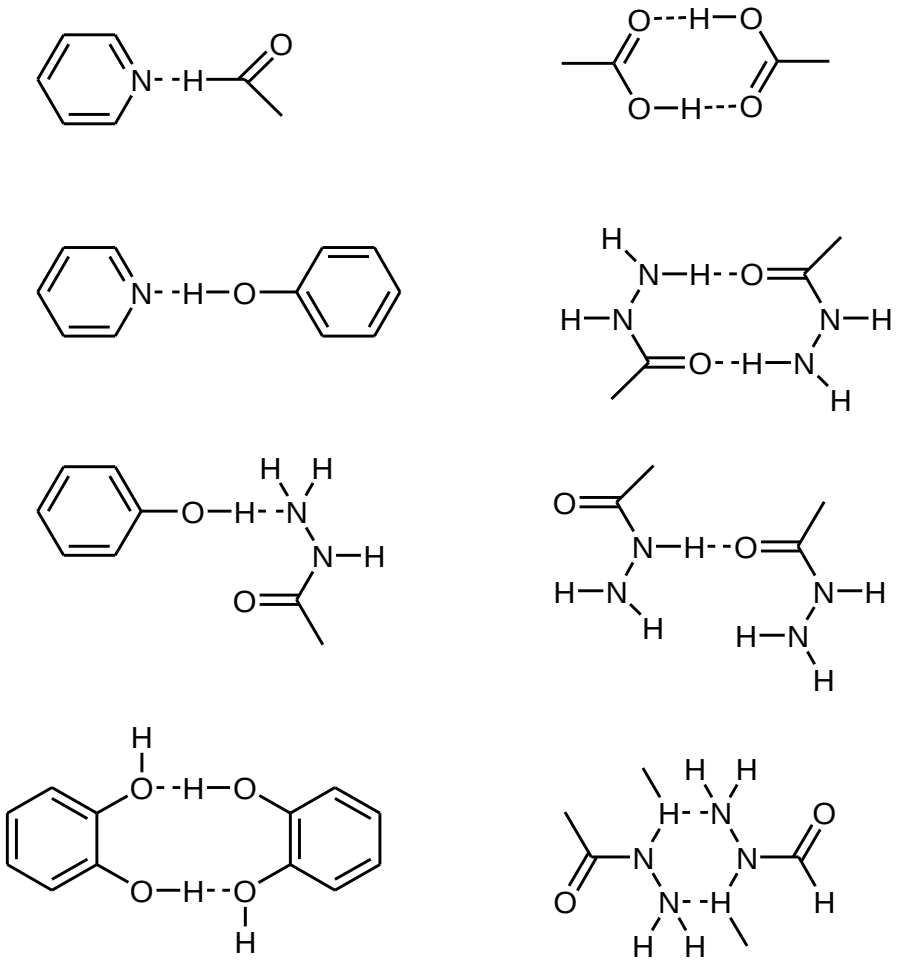

Figure 2.8: The eight hetero- and homosynthons found in isoniazid co-crystals.

In 2016, co-crystals of two Schiff bases of isoniazid modified with acetone were reported by Oruganti *et al.*, having 2,5-dihydroxybenzoic acid and 3-aminobenzoic acid as the co-formers. They also report that attempts to synthesize co-crystals of the same modified Schiff base with

2,6-dihydroxybenzoic acid and with phthalic acid failed and suggest that the failure of these to co-crystallize could be due to the steric effects of the hydroxy and carboxylic acid groups in the 2-position being too close to the carboxylic acid in the 1-position. (**Figure 2.9**) Oruganti suggests that the steric hindrance blocks the formation of the robust carboxylic acid – pyridine heterosynthon typically observed in co-crystals of isoniazid *(Oruganti et al*., 2016). It should be noted, however, that they did succeed in preparing salts of unmodified isoniazid with 2,6-dihydroxybenzoate and with *o*-phthalate.

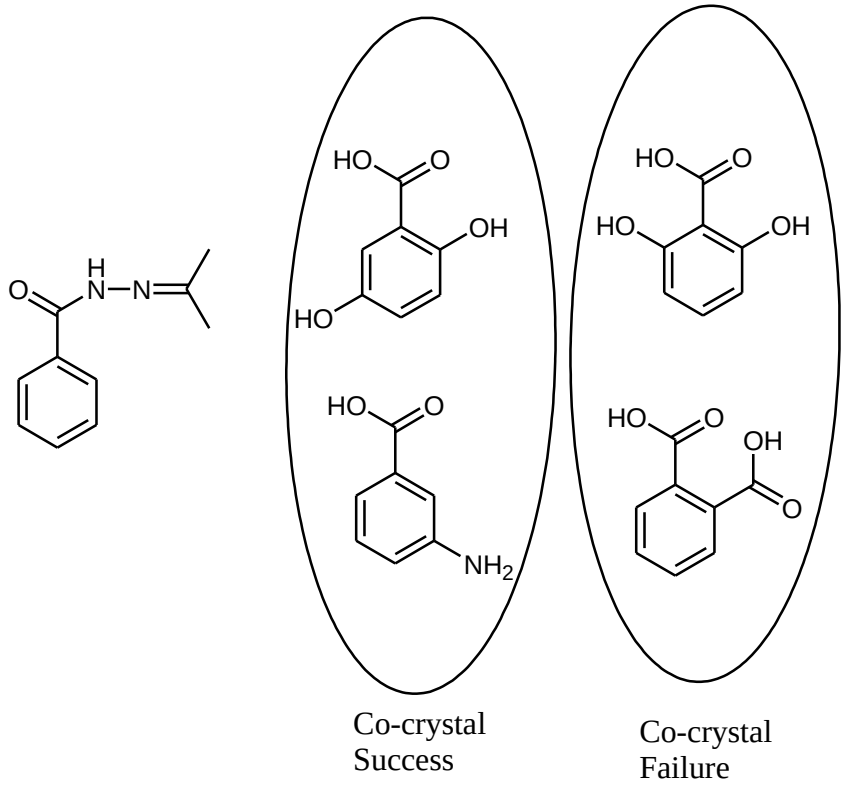

Figure 2.9: A summary of the attempted synthesis of co-crystals by Oruganti *et al.* Success was achieved with the modified isoniazid molecule shown on the left and the two co-formers indicated, whereas failure was reported for the two co-crystals with substituents on the 2- and 6-positions, which Oruganti attributed to steric effects.

2.2.2 Covalent assisted supramolecular synthesis

A series of papers have been written on covalent assisted supramolecular synthesis. Covalent assisted supramolecular synthesis can be defined as the covalent modification of a molecule with the purpose of gaining control over some aspect of the supramolecular synthesis, for example, the altering the hydrogen bonding characteristics of a functional group or control over dimensionality of the packing, together with the co-crystallization of the modified molecule with a co-former.

In Lemmerer *et al.* (2010) isoniazid was co-crystallized with 4-hydroxybenzoic acid and 2,4-dihydroxybenzoic acid, and with several dicarboxylic acids, including malonic, glutaric, succinic, and pimelic acids. It was then demonstrated that the covalent modification of isoniazid with acetone and 2-butanone did not affect the supramolecular synthesis of isoniazid co-crystals, as the essential functional groups, pyridine and carboxylic acid, were not affected by the modification. In their experiment, acetone was added to the crystallizing solution, and the two amino hydrogen atoms were replaced by the acetone in a Schiff base reaction to form an imine. (**Figure 2.10**)

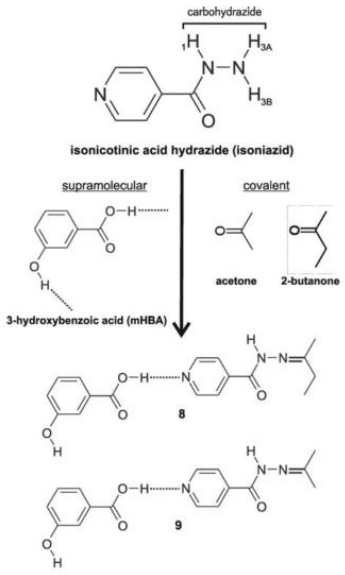

Figure 2.10: A schematic diagram showing the one-pot covalent assisted supramolecular synthesis of the modification of isoniazid with acetone and 2-butanone and simultaneous co-crystallization with 3-hydroxybenzoic acid. Diagram taken directly from *CrystEngComm*, 2010, **12**, 2856-2864.

Lemmerer, Bernstein and Kahlenberg subsequently carried out a series of covalently assisted supramolecular reactions where nine modified co-crystals were prepared (Lemmerer *et al*., 2011). An interesting aspect of this paper was that both the covalent modification and supramolecular synthesis were done in a one-pot reaction. Lemmerer points out that this one-pot technique is unusual, and that most examples of crystals where an API has been modified and co-crystallized require two distinct steps – first, the modification of the API, and then the supramolecular synthesis in an additional step. Specifically, Lemmerer demonstrated that the hydrogen bonding functionality can be carried out *in situ* by simply adding ketones to the crystallizing solution. Lemmerer also demonstrated that, as isoniazid will invariably hydrogen bond through the carboxylic acid – pyridine heterosynthon, the same heterosynthon is involved in the intermolecular hydrogen bonding of covalently modified isoniazid (Lemmerer *et al*., 2011).

A further series of covalently assisted co-crystallizations have also been reported (Lemmerer, 2012) showing the potential medical importance of covalent assisted molecular synthesis and showed how the physical properties of co-crystals could be manipulated through this technique, which could potentially allow for the biological activity of APIs to be improved and modified. Lemmerer provides a detailed explanation of how the structures and hydrogen bonding patterns changed due to the modification of the hydrogen bonding functionality and by the use of different crystal co-formers.

2.2.3 "Masking" of functional groups / masked synthons

Recently, there has been interest in the controlled "masking" of functional groups. This is a concept in which hydrogen bonding sites can be blocked from their regular intermolecular interactions by predictable means. The concept of "masked" synthons in co-crystal engineering was developed concurrently by MacGillivray *et al.* (Sander *et al*., 2013) where interjected water molecules were used to inhibit hydrogen bonding between the co-crystal components, and by Lemmerer (Lemmerer *et al*., 2011), who found that it was possible to block hydrogen bonding functionality by sterically blocking the site via covalent modification of an adjacent site.

2.2.3.1 Masking of functional groups by interjected water molecules

In 2009, Bhatt *et al*. demonstrated that control over robust heterosynthons can be achieved by interjecting solvent molecules between the API and co-former (Bhatt *et al*., 2009). They classified their modification as a "moderate synthon success." In cases where interjected solvent molecules (for example, water) completely blocked the formation of synthons, this was classified as "masked synthons". This is illustrated in **Figure 2.11**, which has been adapted from MacGillivray's paper on *'Masked synthons' in crystal engineering* (Sander *et al*., 2013). In the example shown in the figure, the regular $COOH\cdots N_{pyr}$ / $COOH\cdots OH_{phenol}$ synthon is shown, and is classified as "synthon success." When one part of the synthon is masked by the interjection of a water molecule, it was classified as "moderate synthon success". Finally, complete modification of the synthon by the interjection of two water molecules was called a "masked synthon" (Sander *et al*., 2013). MacGillivray *et al.* confirmed the proof of concept by preparing hydrated co-crystals of acetaminophen and trans-1,2-bis(4-pyridyl)ethylene where water molecules were interjected between the synthons. The result was a complete lack of hydrogen bonding between the molecules. Instead, the molecules were connected to each other by water bridges, consisting of one or two water molecules. They demonstrated that depending on the stoichiometry, either moderate synthon success or complete masking could be achieved by the interjection of water molecules.

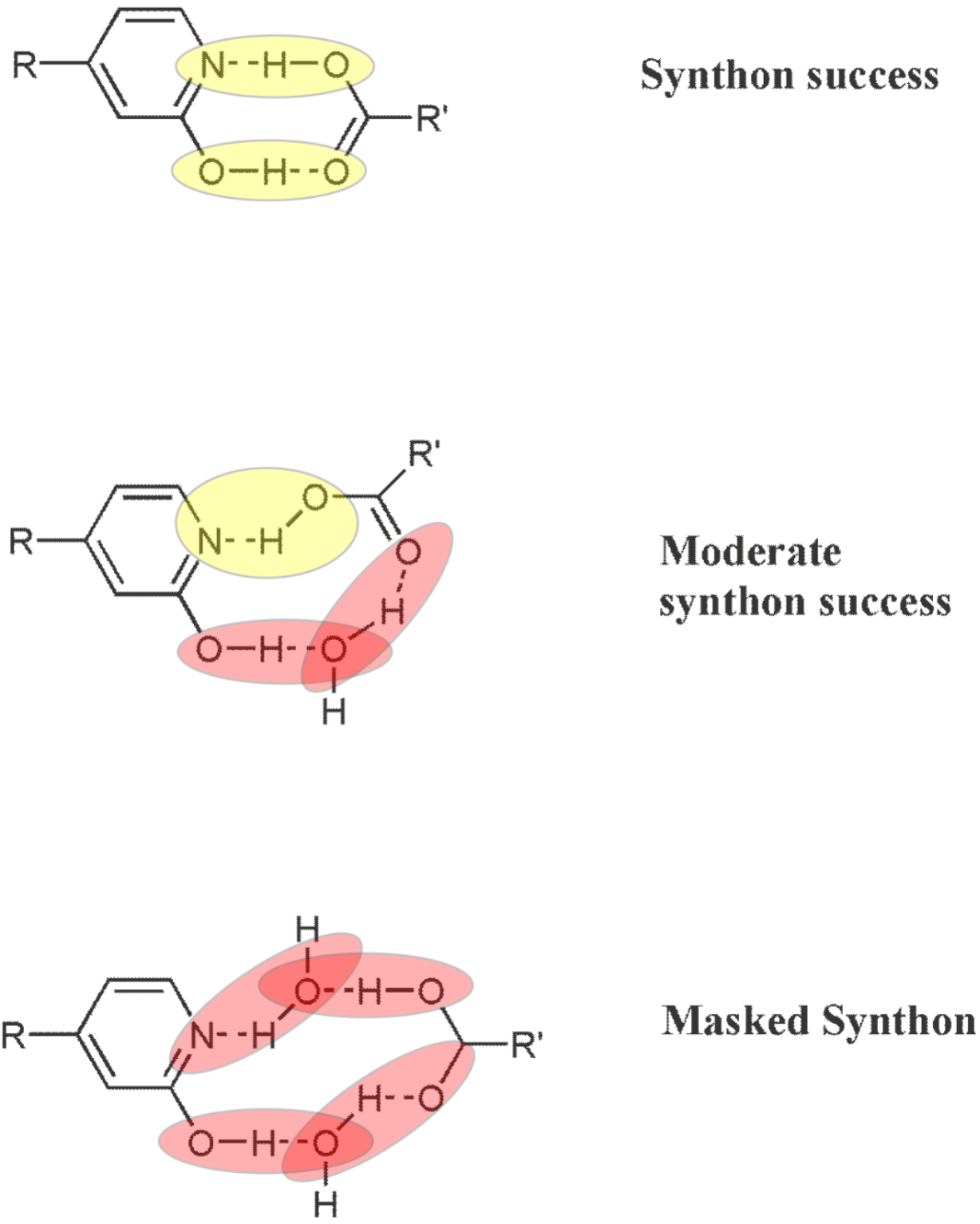

Figure 2.11: MacGillivray's "masking" of synthons by interjected water molecules. Adapted from *CrystEngComm*. 2013, **15**, 4816-4822.

2.2.3.2 Masking of functional groups through covalent modification of adjacent groups

Lemmerer's approach to masking was somewhat different in that he observed that masking of hydrogen bonding functionality could be achieved by the steric interference obtained by the covalent modification of a different functional group to that where masking is required. He demonstrated that the covalent modification of isoniazid with acetone and 2-butanone did not affect the supramolecular synthesis of isoniazid co-crystals, as the essential functional groups, pyridine and carboxylic acid, were not affected by the modification (Lemmerer *et al*., 2010). Lemmerer also demonstrated that the modifiers bonded to the isoniazid could give a measure of control of the outcome of the supramolecular synthesis depending on the identity and steric size of the modifier used. It was shown that the steric size itself can be used to shield or to ''mask'' the remaining hydrogen bonding functionality of isoniazid in such a way that common hydrogen bonds and intermolecular interactions are prevented from taking place as shown in **Figure 2.12** (Lemmerer *et al*., 2011).

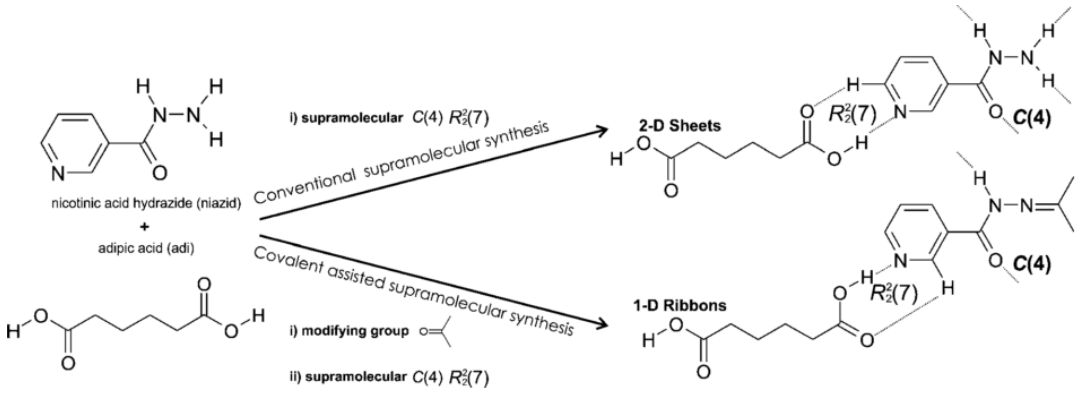

Figure 2.12: Diagram adapted from *CrystEngComm*. (2011). **13**, 5692–5708. Lemmerer shows that by masking two of the hydrogen bonding sites by covalent modification with acetone, the dimensionality of packing can be altered, from 2D sheets to 1D ribbons, for example.

As an example of steric control over intermolecular interactions, when the NH_2 functional group on the hydrazide moiety of isoniazid was covalently modified by the addition of a benzophenone modifier to form a Schiff base, the amide hydrogen donor and nitrogen acceptor atoms of isoniazid are completely inaccessible to intermolecular interactions with neighbouring isoniazid

or 3-hydroxybenzoic acids co-formers due to the steric effects of the bulky benzophenone modifier (Lemmerer *et al*., 2011). (**Figure 2.13**)

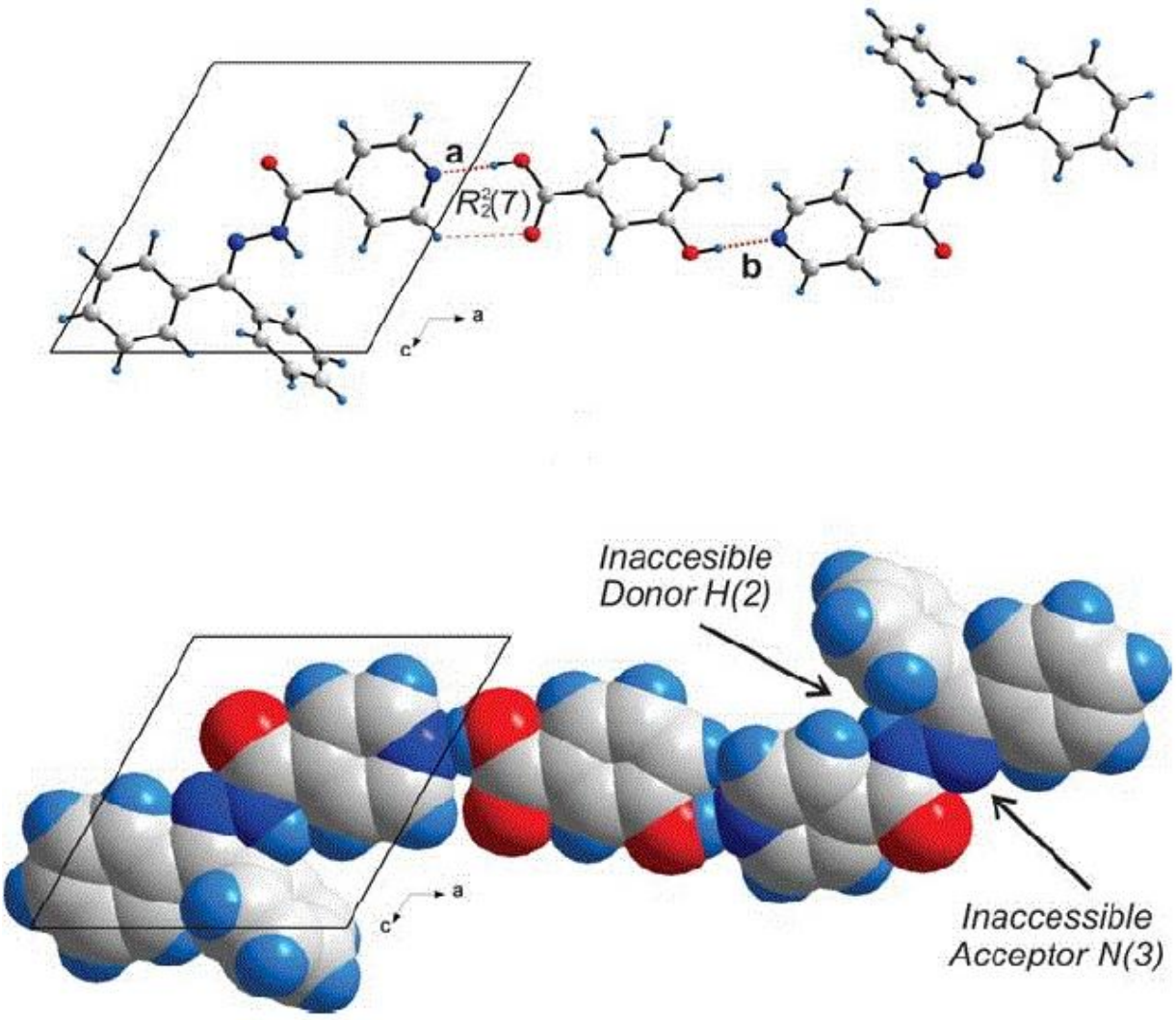

Figure 2.13: Diagram adapted from *CrystEngComm*. (2011). **13**, 5692–5708. Lemmerer demonstrated that when isoniazid is covalently modified with benzophenone, the amide hydrogen donor and nitrogen acceptor atoms are completely inaccessible to intermolecular interactions with neighbouring isoniazid or 3-hydroxybenzoic acids co-formers due to the steric effects of the bulky benzophenone modifier.

2.2.4 Effect of crystallization conditions on supramolecular synthesis

Changing crystallization and reaction conditions often has a profound effect on the resulting supramolecular structure of salts and co-crystals. However, to date, there are no tried and tested rules to dictate what products will be formed by changing variables such as the solvent, temperature, or ratio of products during synthesis, amongst others. Much of the available data in this regard is empirical, and there is still a great need for more data. Statistical analysis of hydrogen bonding synthons and other variables can be extracted from the CSD, and the more data that is available, the more robust the information gained from statistical analysis becomes.

A recent example of empirical work looking at the influence of crystallization conditions on the synthesis of 4-aminosalicylic acid and of various forms of multicomponent crystals has been very recently published (André *et al*., 2017). Andre' *et al.* highlighted how making changes such as changing of evaporating conditions, grinding of reagents (LAG) rather than the use of solvents, and choice of synthon results in different forms of the supramolecular products (André *et al*., 2017).

2.2.4.1 Stoichiometric variation

Stoichiometric variation in co-crystals can be influenced by the different synthons available to the molecules to be co-crystallized. In isoniazid, which has five potential hydrogen bonding sites, changing crystallization or reaction conditions is known to result in stoichiometric variation, as isoniazid hydrogen bonds readily through its pyridine and its hydrazide functional groups. Chiya *et al.* showed that it was possible to create stoichiometric variation in salts of isoniazid with 2-butynoic acid by varying the stoichiometric ratio of isoniazid to 2-butynoic acid during the synthesis process (Chiya and Lemmerer, 2012). A 1:1 ratio of isoniazid to this co-former resulted in a 1:1 salt of these two molecules (**Figure 2.14a**), the salt having been formed by proton transfer from 2-butynoic acid to the pyridine nitrogen atom of isoniazid. However, a 1:4 ratio of isoniazid to the 2-butynoic acid co-former resulted in a 1:2 salt of these two molecules (**Figure 2.14b**).

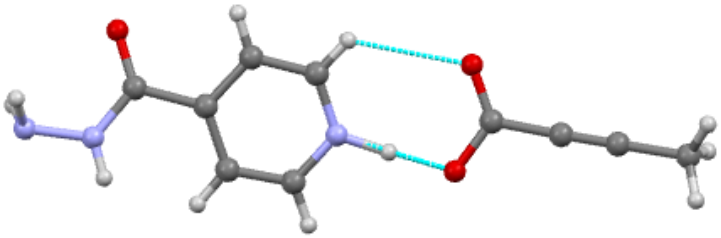

(a)

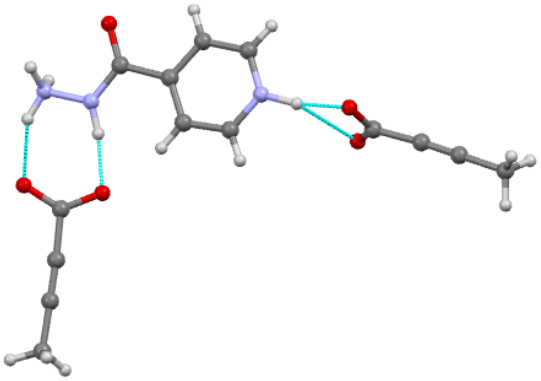

(b)

Figure 2.14: Salts of isoniazid and 2-butynoic acid.
(a) The 1:1 salt (4-(hydrazinylcarbonyl)pyridinium)·(but-2-yn-1-olate) (CSD ref: VAXROD)
(b) The 1:2 salt (4-(hydrazinylcarbonyl)pyridinium)·(but-2-yn-1-olate)$_2$ (CSD ref: VAXRUJ)

2.2.4.2 Polymorphism

Just as changing the ratio of supramolecular reagents in isoniazid co-crystals and salts can result in stoichiometric variation, so it has also been reported that the use of different solvents may result in polymorphism. Sarcevica *et al.* have done considerable research in the field of isoniazid co-crystals. Sarcevica has recognised that co-formers of isoniazid, for example *trans*-cinnamic acid, act synergistically with isoniazid and that co-crystallization with such co-formers may enhance multidrug resistant treatment (Sarcevica *et al.*, 2013). They have reported three co-

crystals of isoniazid with cinnamic acid, as well as polymorphism in isoniazid/suberic acid, where the experimental method was changed to make use of a different solvent. A 1:1 ratio of isoniazid : cinnamic acid, crystallized from a 2:1 mixture of ethanol : acetonitrile afforded two polymorphs (Sarcevica *et al*., 2013). However, a 1:1 ratio of isoniazid : cinamic acid, crystallized from a 1:1 mixture of ethyl acetate : acetonitrile resulted in a third polymorph (Sarcevica *et al*., 2014). All three polymorphs exhibit the same hydrogen bonding patterns in their asymmetric units, but differ in their packing arrangements. The hydrogen bonding in the asymmetric units is via the COOH···N_{pyr} and COOH···NH_{amide} heterosynthons. Details of these polymorphs and their unit cell dimensions can be found in **Table 2.1**. The asymmetric unit and three packing arrangements are shown in **Figure 2.15**.

Table 2.1. The three polymorphs of isoniazid with cinammic acid.

Polymorph	**CSD Refererence Code**	**Unit Cell Dimensions**	**Space Group**
Form I	SETSAN	a = 7.4573Å α = 96.904° b = 9.5154Å β = 103.264° V = 676.699Å^3 c = 10.1737Å γ = 101.946°	$P\bar{1}$
Form II	SETSAN01	a = 14.9124Å α = 90° b = 3.7468Å β = 90° V =1348.18Å^3 c = 24.3089Å γ = 90°	$P2_1/c$
Form III	SETSAN02	a = 6.4872Å α = 95.1691° b = 8.1478Å β = 101.111° V = 690.082Å^3 c = 13.5603Å γ = 98.6376°	$P\bar{1}$

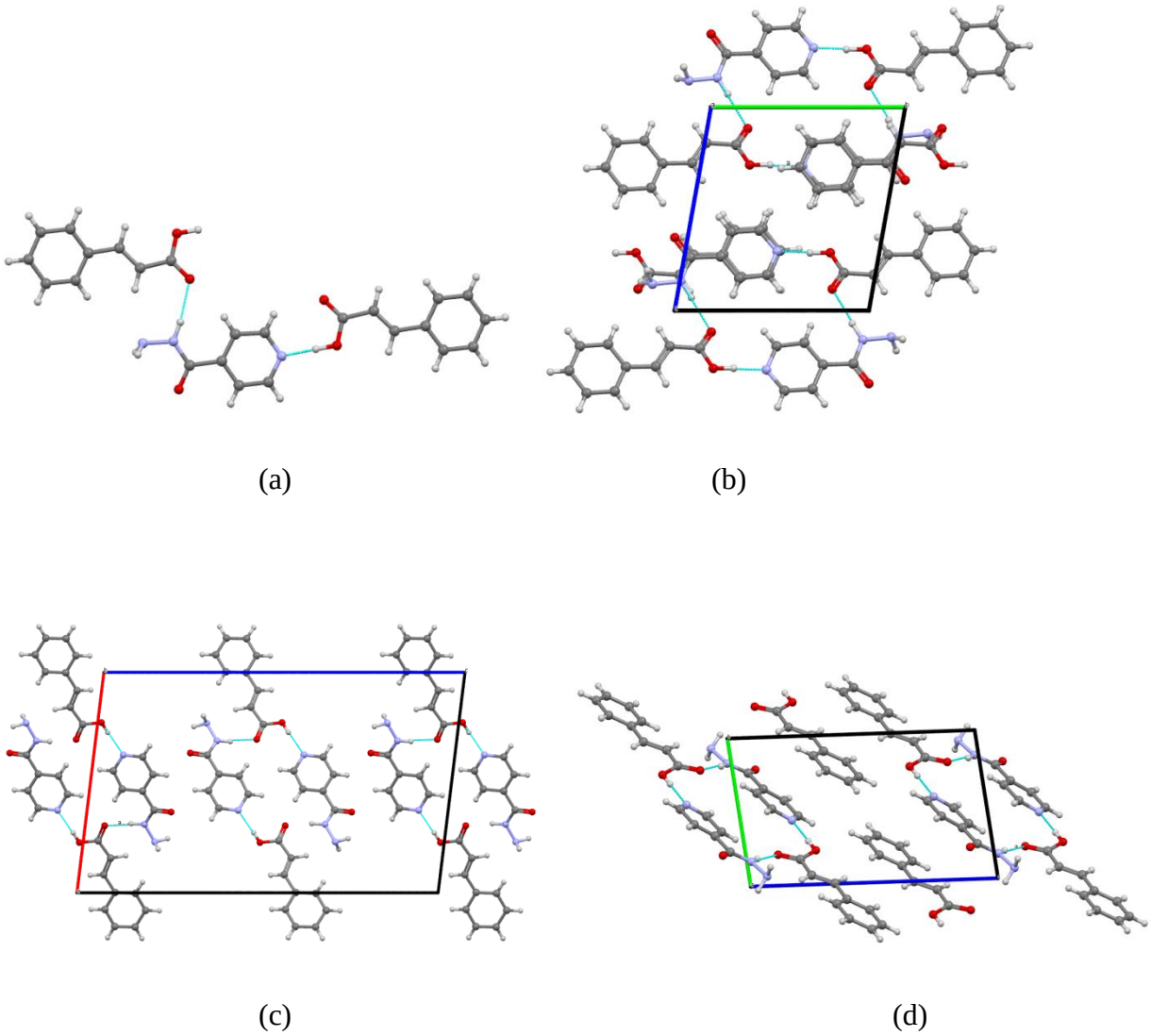

Figure 2.15: Polymorphs of isoniazid and cinnamic acid
(a) The asymmetric unit of all three polymorphs exhibit the same hydrogen bonding pattern.
(b) Packing arrangement of Form I (CSD ref: SETSAN)
(c) Packing arrangement of Form II (CSD ref: SETSAN01)
(d) Packing arrangement of Form III (CSD ref: SETSAN02)

Sarcevica *et al.* similarly showed that polymorphs of isoniazid and suberic acid could be prepared from a 1:1 ratio of isoniazid and suberic acid, and crystallized from a 2:1 mixture of ethanol : acetonitrile, and from a 1:1 mixture of acetonitrile : methyl *tert*-butyl ether respectively. (Sarcevica *et al.*, 2013). The first polymorph (CSD Ref: SETRUG) was synthesized using the

slow evaporation method. The second polymorph was synthesized using liquid assisted grinding (LAG) on a Retsch mill using 0.2 mL of the solvent. Single crystals were obtained with seed addition (seed crystals were obtained from LAG experiments). However, the second polymorph could only be identified from powder diffraction patterns as the poor quality of the crystals did not allow crystal structure determination.

2.2.4.3 Impurities and additives

It is well known that the presence of even tiny amounts of impurities in a crystallization solution may affect the nucleation, growth and dissolution properties of a crystal (Weissbuch *et al*., 2001). In fact, it has been reported that the presence of additives during a crystallization process will *invariably* affect the morphology and crystal structure during crystallization (Meir and Leslie, 2015; Addadi *et al*., 1981). In certain instances, it may be desirable to add impurities or additives to a crystallization solution in order to induce changes in supramolecular structure, for example, stoichiometric variation or polymorphism. An example of the addition of "tailor-made" additives has been reported where control over the optical activity of crystallization was achieved by the induced preferential crystallization through the use of additives (Addadi *et al*., 1981). Typically, a crystallizing solution contains a 1:1 stoichiometry of the API and co-former, and varying this ratio may result in changes in supramolecular structure and the formation of new co-crystals (Chiya and Lemmerer, 2012). These changes may be understood if one considers an excess of one or the supramolecular agents to be an additive. In other words, it may be useful in certain specific situations or experiments to consider anything other than a 1:1 ratio of supramolecular reagents as additives in order to induce changes in the desired products.

2.3 Crystal engineering of isoniazid

2.3.1 Covalent modification of isoniazid

As described in Section 1.6, the covalent modification of isoniazid by the replacement of NH_2 hydrogen atoms with modifiers is the primary focus in the synthesis of medicines that target

drug-resistant strains of tuberculosis, as this covalent modification prevents the enzymes of the TB bacteria from rendering the drug ineffective (Hearn *et al*., 2009). Hearn *et al.* prepared a series of Schiff bases of isoniazid and compared the biological activity of isoniazid and modified isoniazid on mice. Hearn demonstrated that the NH_2 functional group of isoniazid is subject to deactivating acetylation by a class of enzymes known as N-arylaminoacetyl transferases (NATs). He explained that this deactivation is the reason for the resistance of the tuberculosis bacteria against isoniazid. However, if the isoniazid drug is modified by the covalent modification of the amine group to form Schiff bases (before entering the body) (**Figure 2.16b**), the enzymatic deactivation process no longer works to deactivate the drug and the resulting modified isoniazid can be effective for the treatment of multi-drug resistant strains of the bacteria. Hearn *et al*. prepared 43 Schiff bases of isoniazid and found that all of them exhibited at least some activity against M. Tuberculosis *in vitro*. Four of the modified isoniazid derivatives, compounds 3, 36, 38 and 46 in **Figure 2.17**, were tested *in vivo* in mice and displayed considerable activity against multidrug-resistant strains of *M. Tuberculosis*. A complete list of the modifiers used by Hearn as well as the experimental results of his primary in vitro screening of his compounds are detailed in **Figure 2.17**. Where the Schiff bases were crystallized, the drugs were reported to be pure. In his conclusion Hearn noted that "*Schiff bases [of isoniazid (INH)] may serve as discovery tools in probing INH-based treatment modalities, particularly for those patients chronically underdosed in conventional INH therapy*." (Hearn *et al*., 2009).

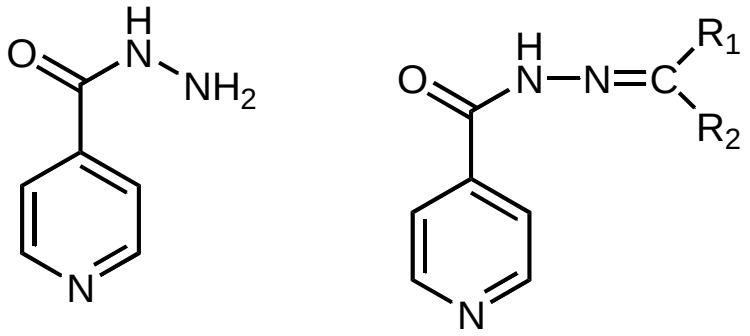

(a) (b)

Figure 2.16: (a) Isoniazid. (b) The general structure of the Schiff bases prepared and tested by Hearn *et al*.

Entry	Compound	R_1	R_2	% Yield	mp, °C	C log P[a]	MIC, μg/mL[b]
1.	**3**	H	2-($OCH_2C_6H_5$)C_6H_4	90	185	4.57	0.06[c]
2.	**4**	$(CH_2)_4CH_3$	C_6H_5	64	116–117	4.49	0.39
3.	**5**	H	4-BrC_6H_4	91	218–219	3.84	3.13
4.	**6**	H	2-ClC_6H_4	66	218–221	3.56	0.78
5.	**7**	H	3,4-$F_2C_6H_3$	86	195–196	3.32	1.56
6.	**8**	H	4-IC_6H_4	92	243	4.30	0.20
7.	**9**	H	3-I-4,5-$(OCH_3)_2C_6H_2$	90	234	3.80	0.20
8.	**10**	H	3-I-4-OH-5-$OCH_3C_6H_2$	87	221	3.76	0.39
9.	**11**	H	4-ClC_6H_5	94	215–216	3.56	0.20
10.	**12**	H	3,4-$Cl_2C_6H_3$	88	241–244	4.08	0.20
11.	**13**	H	2,6-$F_2C_6H_3$	100	239	3.32	0.10
12.	**14**	H	2,3-$Cl_2C_6H_3$	98	227	4.08	0.78
13.	**15**	H	2,6-$Cl_2C_6H_3$	97	Semisolid	4.08	<6.25
14.	**16**	H	2-$NO_2C_6H_4$	97	230	1.06	0.39
15.	**17**	H	4-Cl-3-$NO_2C_6H_3$	100	231	1.58	0.39
16.	**18**	CH_3	C_6H_5	92	169–170	2.68	<6.25
17.	**19**	H	4-$CH_3(CH_2)_5OC_6H_4$	87	135–138	5.49	0.39
18.	**20**	H	3-$NO_2C_6H_4$	85	225	1.06	0.125[c]
19.	**21**	H	C_6H_5	98	197	3.04	0.05
20.	**22**	H	4-$CH_3(CH_2)_3OC_6H_4$	91	148–149	4.00	0.10
21.	**23**	H	*t*-CH=$CHCH_2CH_3$	54	161–164	2.24	0.05
22.	**24**	H	*t*-CH=$CHCH_3$	73	198–201	1.85	<6.25
23.	**25**	H	*t*-CH=$CHCH_2CH_2CH_3$	93	152–154	2.64	<6.25
24.	**26**	H	*t*-CH=$CH(CH_2)_3CH_3$	84	152–154	3.03	<6.25
25.	**27**	H	C=$CCH_3CH_2CH_2CH=CH_2$	59	124–125	2.97	0.10
26.	**28**	H	$CH_2CHCH_3CH_2CH_2CH=C(CH_3)_2$	29	78–80	3.58	0.20
27.	**29**	CH_3	CH_3	48	161–162	1.70	0.10
28.	**30**	CH_2Ph	$CH_2CO_2CH_2CH_3$	90	104	3.78	0.10
29.	**31**	R_1R_2=$CCH_2CH(CH_3)CH_2C(CH_3)_2CH_2$		76	149–151	3.94	<0.025
30.	**32**	H	CH=$C(C_6H_5)_2$	86	223	4.43	0.10
31.	**33**	H	*t*-CH=CH-4-$OCH_3C_6H_4$	89	218	2.73	0.20
32.	**34**	H	*t*-CH=CH-2-$NO_2C_6H_4$	94	204	1.08	0.25[c]
33.	**35**	H	C(*n*-C_3H_7)=$CH(CH_2)_3CH_3$	84	121	4.10	0.50
34.	**36**	H	C(*i*-C_3H_7)=$CHCH_2CH(CH_3)_2$	99	129	3.97	0.06[c]
35.	**37**	H	*t*-CH=CH-2-$OCH_3C_6H_4$	92	206	2.81	0.10
36.	**38**	H	*t*-CCH_3=CHC_6H_5	90	200	3.34	0.50
37.	**39**	H	CH=$NNHCOC_5H_4N$	90	>300 (d)[d]	1.58	0.10
38.	**40**	$CH_2CH_2CH_3$	$CH_2CO_2CH_2CH_3$	98	89–90	2.96	0.39
39.	**41**	CH_3	$CH_2CO_2CH_2CH_3$	85	99	1.93	0.20
40.	**42**	H	4-(CH=$NNHCOC_5H_4N$)C_6H_4	90	>300 (d)[d]	4.04	0.05
41.	**43**	$CH_2CH_2C_6H_5$	$CO_2CH_2CH_3$	90	104	4.24	0.10
42.	**44**	H	$CH_3(CH_2)_{11}CH_2$	73	89–91	5.73	0.20
43.	**45**	H	$CH_3(CH_2)_{10}CH_2$	73	92–93	5.33	0.20
44.	**46**	R_1R_2=$C(CH_2CH_2)_2CH_2$		81	167–168	2.85	0.03

[a] Calculated using HyperChem Pro, Version 7.5. For INH, C log P is 0.49.
[b] MIC_{90} against *M. tuberculosis* strain $H_{37}Rv$, unless otherwise noted. MIC INH control 0.03–0.06 μg/mL.
[c] MIC_{90} against *M. tuberculosis* strain Erdman. MIC INH control 0.03–0.06 μg/mL. MIC PAS control 0.03–0.06 μg/mL.
[d] Decomposed without melting.

Figure 2.17. The R-groups used for the covalent modification of isoniazid and the experimental results reported by Hearn *et al.* in his study of the effects of the covalent modification of isonazid on antitubercular activity. Figure taken directly from *Eur. J. Med. Chem.* (2009). **44**, 4169-4178.

Other early work on the covalent modification of isoniazid was by the covalent modification of isoniazid with two halogenated aromatic modifiers (Silva *et al*., 2006). (**Figure 2.18**)

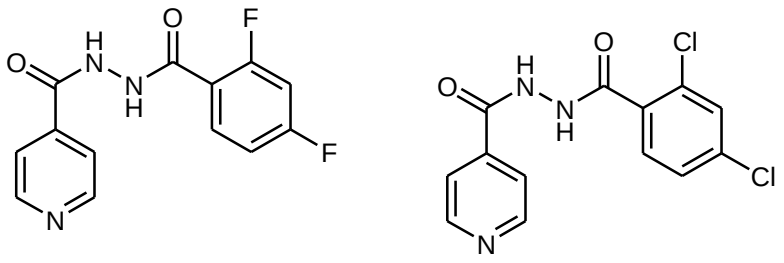

Figure 2.18: The two modified isoniazid molecules prepared by Silva et al. using halogenated aromatics as modifiers.

In 2012, Coelho *et al.* prepared a series of 23 *N*-acylhydrazones derived from isoniazid and determined the biological activity of those modified isoniazid derivatives. Thirteen of the modified isoniazid products showed a more than 10-fold higher biological activity against *katG*-resistant strains of *M. tuberculosis* (Coelho *et al*., 2012).

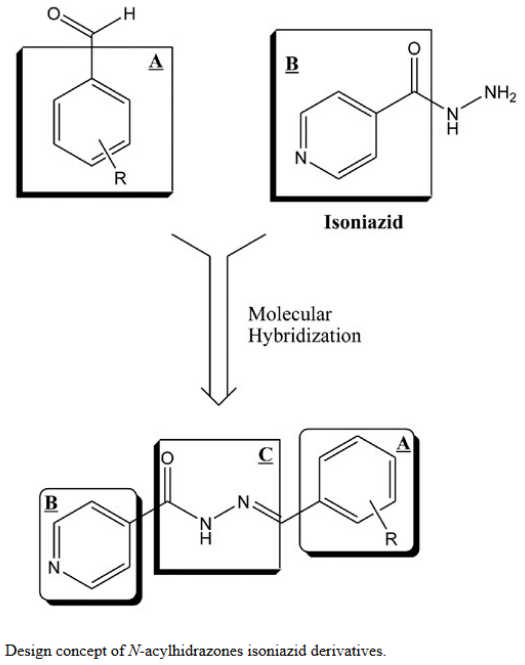

Figure 2.19: Taken directly from *Infect. Dis. Rep.*, 2012, **4(1)**:e13. The figure shows the design concept of the acylhydrazones prepared by Coelho *et al*.

Very recently, Ferraresci-Curotto *et al.* reported a series where isoniazid was modified to produce isoniazid hydrazones using four halogenated aldehydes, namely vanillin, 5-bromovanillin, 5-chlorosalicylaldehyde and 5-bromosalicylaldehyde (**Figure 2.20**). The four modified isoniazid products were found to be isomorphic. The molecules in the packing of the hydrazones were bonded to each other via OH···N_{pyr} hydrogen bonds, resulting in 2-dimensional planar polymeric structures (Ferraresi-Curotto *et al*., 2017).

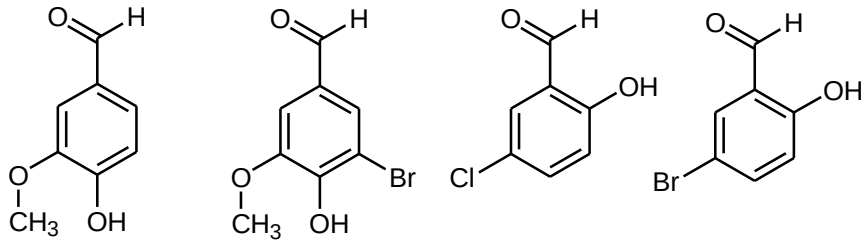

(a)

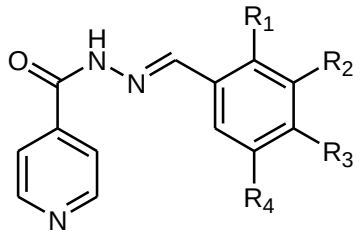

(b)

Figure 2.20: Part (a) shows the four modifiers used by Ferraresi-Curotto *et al.* to prepare a series of isoniazid hydrazones, and (b) is the general structure of the series.

2.4 Photodimerization of benzophenones

2.4.1 Previous synthetic methods for benzophenone azines

While experimenting on the covalent modification of isoniazid, benzophenone azine was found to occasionally crystallize together with the modified isoniazid crystals and co-crystals. The formation of the benzophenone azine that occurred was studied and will be described in Chapter 6. The study also resulted in the development of a new method of synthesizing benzophenone azines. The literature described in this section therefore details the previously reported methods of benzophenone azine synthesis.

Ketone azides are frequently used in synthetic chemistry as starting materials for the synthesis of basic aromatic rings (Kost and Grandberg, 1959; Carty, 1972; Wuts and Greene, 2006), as well as for ligands in metal complex catalysis (Verner and Potacek, 2006). The synthesis of benzophenone azine was first proposed by Lauer and Dyer in 1942 (Lauer and Dyer, 1942). (**Figure 2.21**) They reported benzophenone azine as one of several products of the oxidation of benzophenone oxime. The method of synthesis required inert conditions and several synthetic

steps, as well as oxidation with the highly toxic potassium ferricyanide. During the synthesis, a mixture of benzophenone, benzophenone azine and the benzophenone oxime ester $(C_6H_5)_2C{=}N{-}O{-}N{=}C(C_6H_5)_2$ were formed, and manual separation was required. In addition to benzophenone azine, a mix of the product from the other reaction was observed. The presence of benzophenone azine was supported by molecular weight determinations (Lauer and Dyer, 1942).

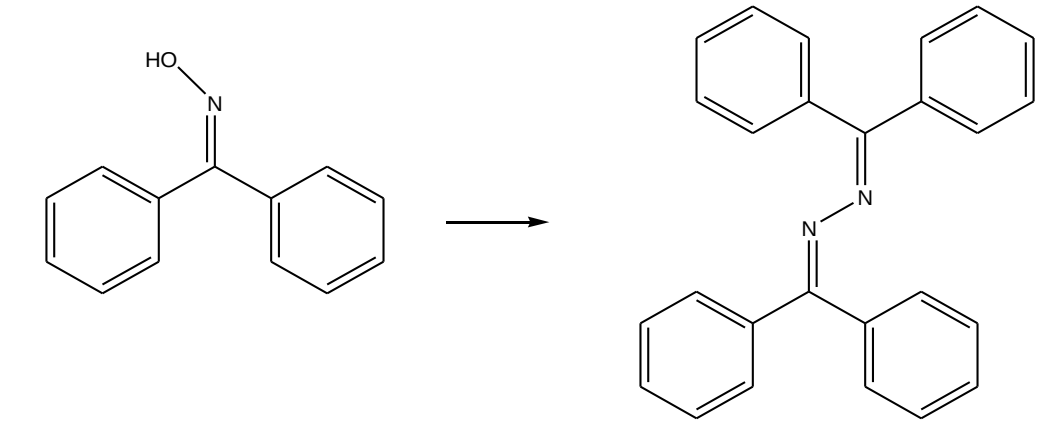

Benzophenone oxime — Benzophenone azine

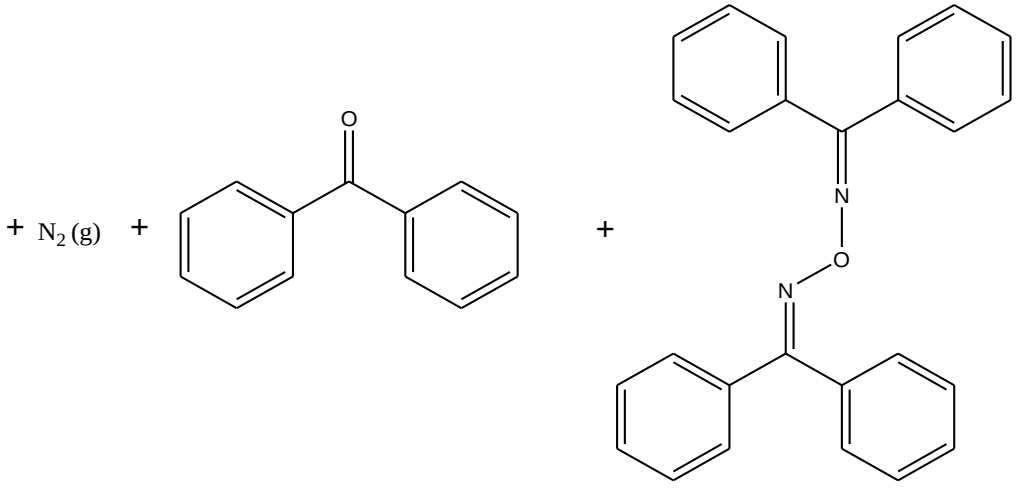

Nitrogen gas — Benzophenone — Benzophenone *o*-diphenylmethyleneamino oxime

Figure 2.21: Lauer and Dyer's method of synthesis of benzophenone azine from benzophenone oxime showing also the many side products produced from their method of synthesis

In 1995, Saha *et al*. (Saha *et al*., 1995) synthesized benzophenone azine via the reaction of the iron-containing Lewis acid complex $[\eta^5\text{-}(C_5H_5)Fe(CO)_2(THF)]^+[BF_4]^-$ and provided evidence of an iron carbine intermediate. Inert conditions were required for the synthesis and benzophenone azine was found to be one of two components in a product mixture, along with tetraphenylethylene, with benzophenone having a 39% yield after separation. The crystal and molecular structure was determined and was used to confirm that the azine, rather than the azitine product was afforded. In their paper, the first crystal structure of benzophenone azine was reported (CSD ref: ZOSLUO) and the monoclinic unit cell dimensions were determined to be a = 16.303(3) Å, b = 5.4864(2) Å, c = 21.973(5) Å, β = 85.52(2)°, V = 1959.4(8) Å^3. It was reported that the asymmetric unit contained two half a molecules of benzophenone azine, but they determined that despite the high crystallographic symmetry, the two halves of the molecule were not related by symmetry. Rather, the molecule possesses a C_2 symmetry, with the molecular C_2 axis coincident with the crystallographic twofold axis (Saha *et al*., 1995).

2.4.2 Weak hydrogen bonds in benzophenone azines: C−H···O and C−H···π

A particularly interesting feature of the crystals that will be described in Chapter 6, relating to a new method of synthesis of benzophenone azines, is the abundance of the weak C−H···O and C−H···π hydrogen bonding patterns in their packing. Desiraju has described C−H···π interactions as being "supportive" interactions and mentions that although C−H···π interactions are fairly ubiquitous, they are "*very weak and merely exist in a structure that is wholly determined by other interactions*" (Desiraju, 2005). He also asks the question of whether it is possible to engineer crystal structures consisting of only weak interactions. Desiraju mentions that historically, these weak hydrogen bonds were dismissed as having little impact on crystal structure, but stresses that today, an understanding of these interactions is considered crucial with regards to the elucidation of crystal structures, as well as for knowledge-based crystal design processes. Kuduva *et al.* remarks that there is a distinct awareness between weak and strong hydrogen bonds, but that the differences between the weak and strong types of bonds are more a matter of degree rather than a fundamental difference in the types of reaction (Kuduva *et al*., 2001).

2.4.3 Stereochemistry of benzophenone azines

Structural isomerism exists in benzophenone azines and the spectroscopic resolution of their configurations are not trivial. Benzophenone azines that have two non-equivalent substituents can exist as three stereoisomers, namely *EE*, *EZ* or *ZZ* (**Figure 2.22).** Afonin *et al.* has, however reported that the ^{13}C NMR shielding constant of the C_{ipso} atom is stereospecific. Should it be necessary for the stereochemistry of benzophenones to be known unambiguously, a complete configurational assignment has been published by Afonin which can be used as a reference (Afonin *et al*., 2012).

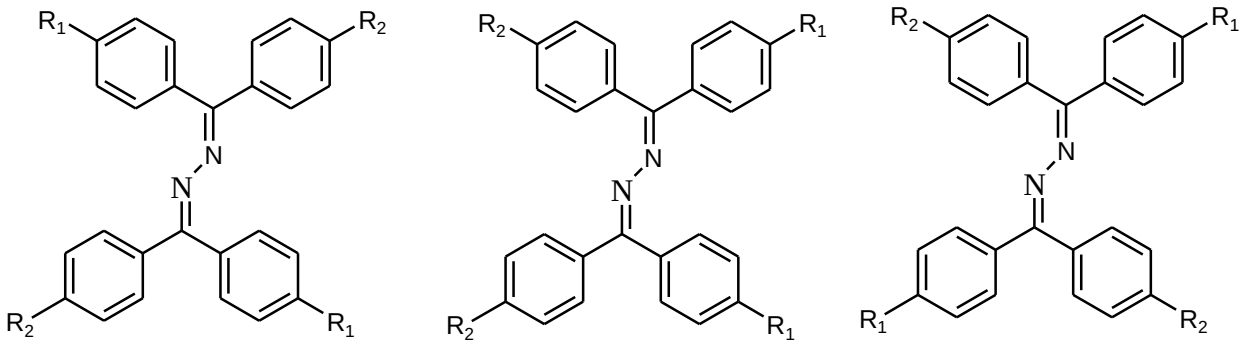

Figure 2.22: The three stereoisomers of benzophenone azines. This E/Z stereochemistry applies if R_1 has a lower priority than R_2.

2.5 The crystal structure of 4-aminoantipyrine

The crystal structure of 4-aminoantipyrine has been reported by Li *et al.* (Li *et al*., 2013) and by Mnguni *et al.* (Mnguni and Lemmerer, 2015). (**Figure 2.23**) The unit cell was found to be hexagonal with dimensions a = 7.4519 Å, b = 7.4519 Å, c = 31.8705 Å (V =1532.69 Å^3) and a $P6_1$ space group. The crystal structure has an intermolecular N−H···O heterosynthon involving the amino group hydrogen atom donor and the carbonyl oxygen atom hydrogen bond acceptor. This forms an infinite chain with graph set notation $C(5)$ (Etter *et al.*, 1990). There is a sixfold

screw axis that defines the chain, and a symmetrically pleasing helical form results down the crystallographic *c*-axis (**Figure 2.23d**). There are also two C−H···π interactions involving the methyl group hydrogen atoms and the phenyl ring. The dimensionality of the packing is a three-dimensional (3D) network (Li *et al*., 2013).

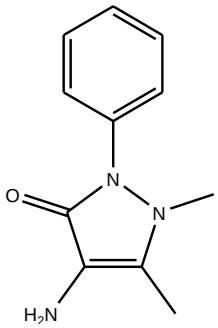

(a)

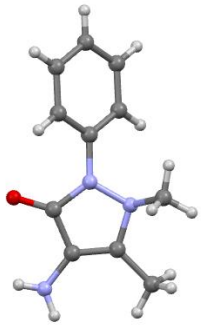

(b)

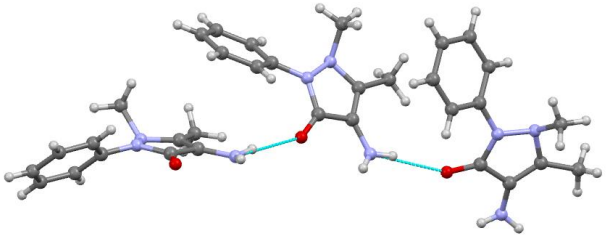

(c)

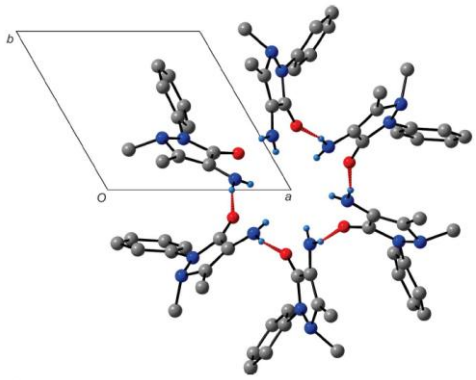

(d)

Figure 2.23: (a) Structure diagram, (b) asymmetric unit and (c) hydrogen bonding of 4-aminoantipyrine. (CSD ref: LOYXEE) and (d) the helical packing of the 4AAP. Part (d) of Figure 2.23 is taken directly from *Acta Cryst.* (2015). *C***71**, 103–109

2.6 Co-Crystal and crystal engineering of 4-aminoantipyrine

2.6.1 Salts of 4-aminoantipyrine

To date, 251 derivatives of 4-aminoantipyrine have been reported in the CSD (version 5.39), where the modifying adduct has attached to the amino nitrogen atom. However, there are no reported co-crystals of 4AAP. Only five molecular salts of 4AAP have been reported in literature, summarized in **Figure 2.24** and **Figure 2.25**, with CSD reference codes and literature references shown in **Table 2.2**. Two of these are simple salts with halide counter-ions. The exocyclic nitrogen atom of 4AAP is readily protonated and forms a chloride salt in the presence of hydrochloric acid and a bromide salt when refluxed in an aqueous dibromomethane solution (**Figure 2.24b and 2.24c**).

Table 2.2: Reported salts of 4-aminoantipyrine

Salt	**CSD Reference Code**	**Reference**
aminoantipyrine-4-aminium chloride	HUKTIS	(Chitradevi *et al.*, 2015)
aminoantipyrine-4-aminium bromide monohydrate	PAXSOY	(Yang *et al.*, 2012)
aminoantipyrine-4-aminium thiourea chloride	EVOLIL	(Murtaza *et al.*, 2011)
aminoantipyrine-4-aminium 2,2'-dithiobenzoate	PUGHEF, PUGHEF01	(Huo *et al.*, 2009) (Fazil *et al.*, 2012)
aminoantipyrine-4-aminium salicylate	DUHYOV	(Chitradevi *et al.*, 2009)

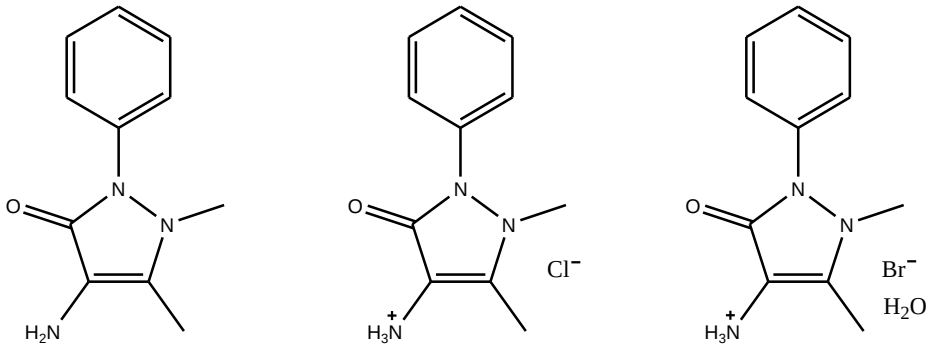

(a) (b) (c)

Figure 2.24: The structure of 4AAP and its reported simple salts with their CSD reference codes:
(a) 4-aminoantipyrine (SIKBAR), (LOYXEE)
(b) aminoantipyrine-4-aminium chloride (HUKTIS)
(c) aminoantipyrine-4-aminium bromide monohydrate (PAXSOY)

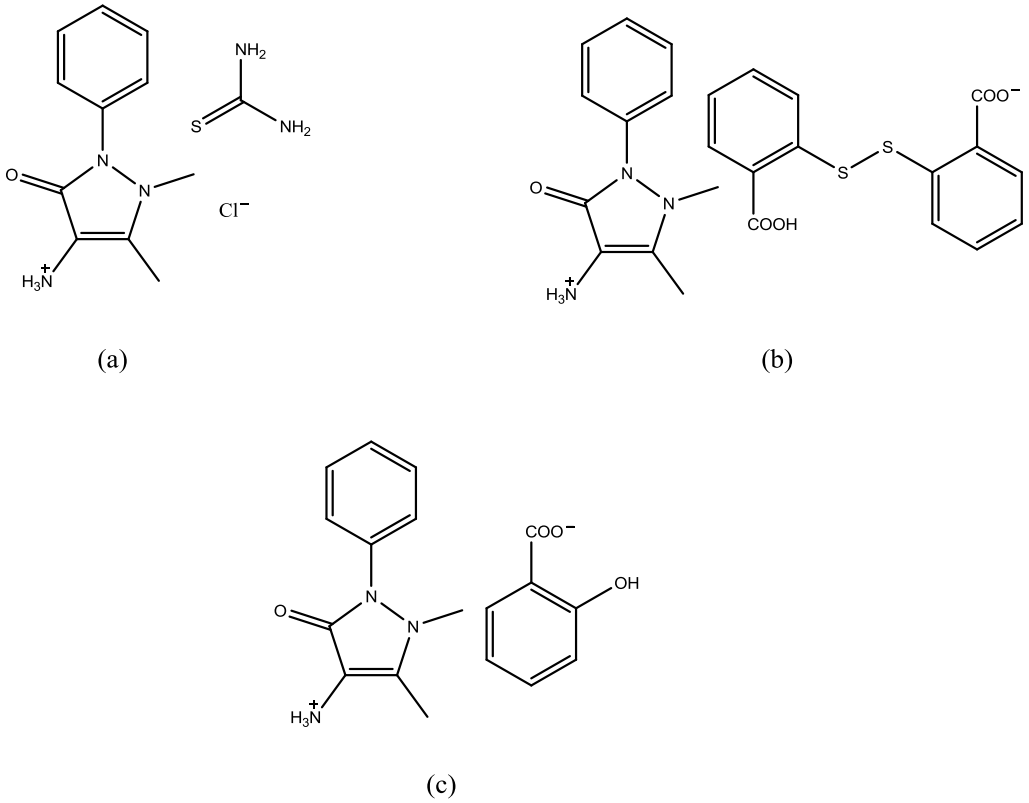

(a) (b) (c)

Figure 2.25: Molecular salts of 4AAP reported in literature with their CSD reference codes:
(a) aminoantipyrine-4-aminium thiourea chloride (EVOLIL)
(b) aminoantipyrine-4-aminium 2,2'-dithiodibenzoate (PUGHEF), (PUGHEF01)
(c) aminoantipyrine-4-aminium salicylate (DUHYOV)

The chloride salt of 4AAP reported by Chitradevi forms the same hydrogen bonding as does pure 4AAP described in Section 2.5 but has an additional N−H···Cl hydrogen bond to a halogen. This forms a dimeric $R_2^2(10)$ ring around the inversion center of the unit cell (Chitradevi *et al*., 2015). (**Figure 2.26**) As expected, the bromide salt hydrogen bonds through the same synthons as the chloride salt with the additional water molecule being hydrogen bonded to the methyl group and the bromine ion (Yang *et al*., 2012). (**Figure 2.27**)

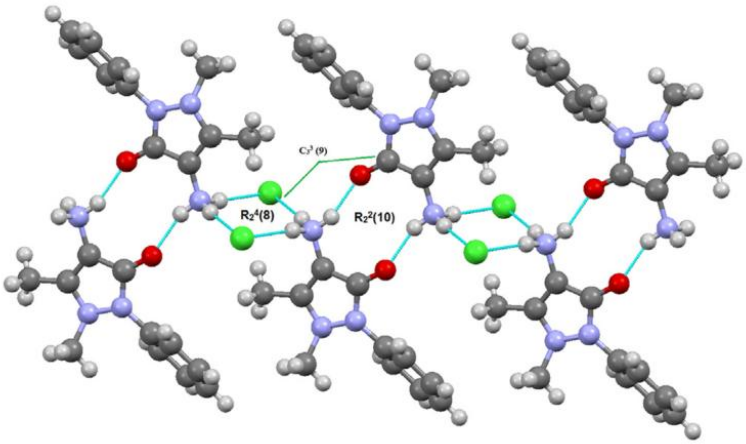

Figure 2.26: The crystal structure of the 4-aminiumantipyrine chloride salt reported by Chitradevi. Diagram taken directly from *J. Mol. Struct*., 2015, **1099**, 58-67.

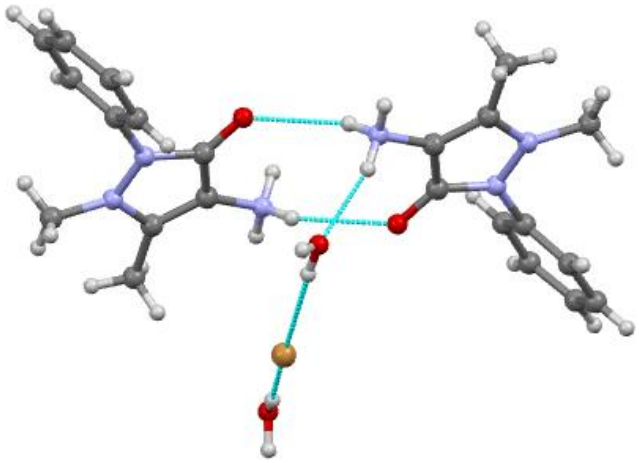

Figure 2.27: Hydrogen bonding of the bromide salt of 4-aminiumantipyrine reported by Yang *et al*.. (CSD ref: PAXSOY)

Murtaza *et al*. prepared a three-component salt (**Figure 2.25(a)**) by acidifying the 4AAP with an aqueous solution of hydrochloric acid, and then refluxing with ethanol (Murtaza et al., 2011). It was reported that the three components form a two-dimensional structure parallel to (001) via a network of N−H···Cl, N−H···S, N−H···O, and C−H···S hydrogen bonds (**Figure 2.28**).

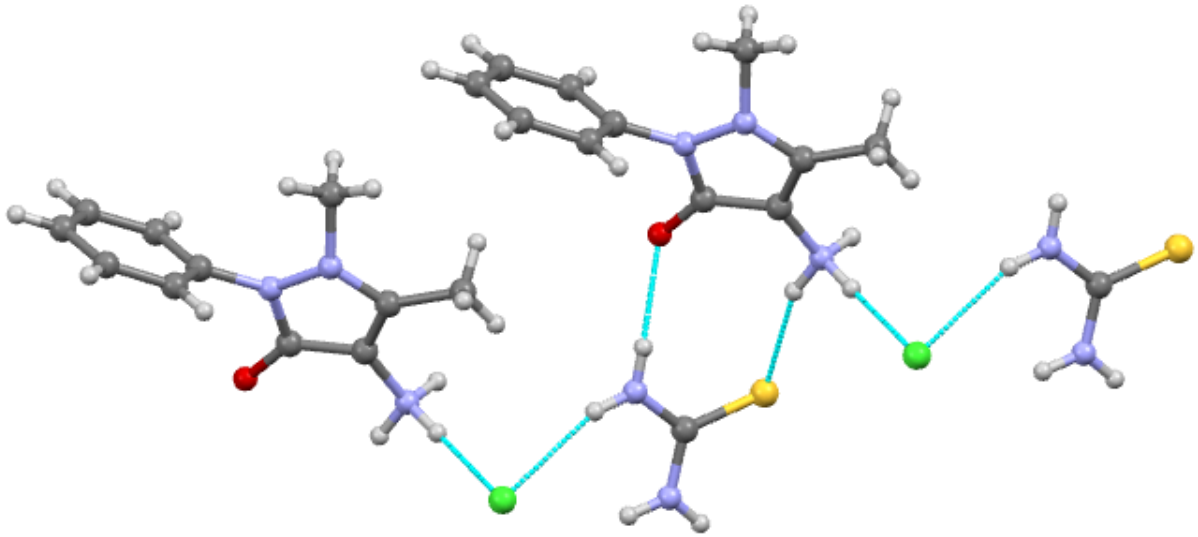

Figure 2.28: Hydrogen bonding of the bromide salt of 4-aminiumantipyrine reported by Murtaza *et al.* (CSD ref: EVOLIL)

A molecular salt of 4AAP and 2,2'-dithiobenzoic acid was synthesized first by Huo and then Fazil *et al* (Huo, 2009, Fazil et al., 2012). and was crystallized from ethanol and from a 50% ethanol/water mixture respectively (**Figure 2.25(b)**). Huo commented that the components were selected as building blocks for creating a co-crystal, but proton transfer was observed in the ethanol medium. In the molecular salt, a carboxylic acid group is deprotonated and the exocyclic amino atom is protonated. N−H···O and O−H···O intermolecular hydrogen bonds connect the ions into 1D chains along the *b*-axis (**Figure 2.29**).

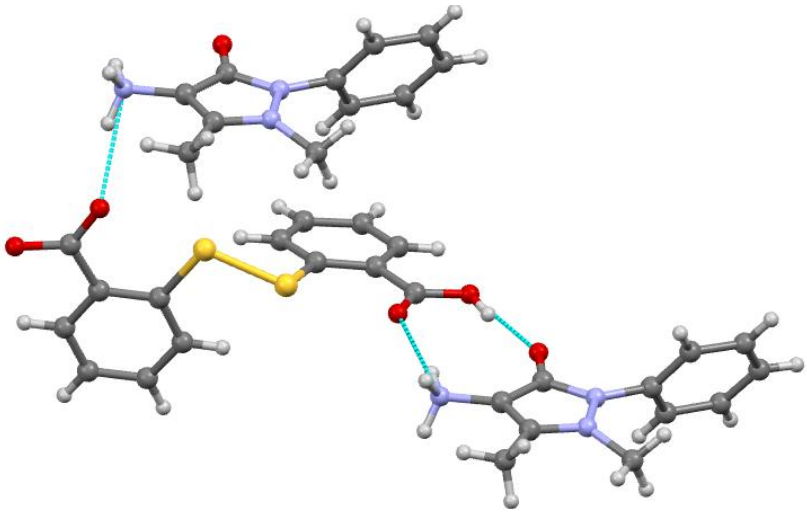

Figure 2.29: Hydrogen bonding of the molecular salt of 4AAP and 2,2'-dithiobenzoic acid reported by Huo and by Fazil *et al.* (CSD ref: PUGHEF01)

Finally, a salt of 4AAP with salicylic acid was prepared in aqueous solution by Chitradevi *et al*. Chitradevi et al., 2009). Ionic interaction exists between the carboxylate anion and the aminium cation, forming a $R_2^2(10)$ ring motif. As expected by Etter's rules, an $S(6)$ intramolecular O−H···O hydrogen bond was also found in the crystal structure **(Figure 2.30).**

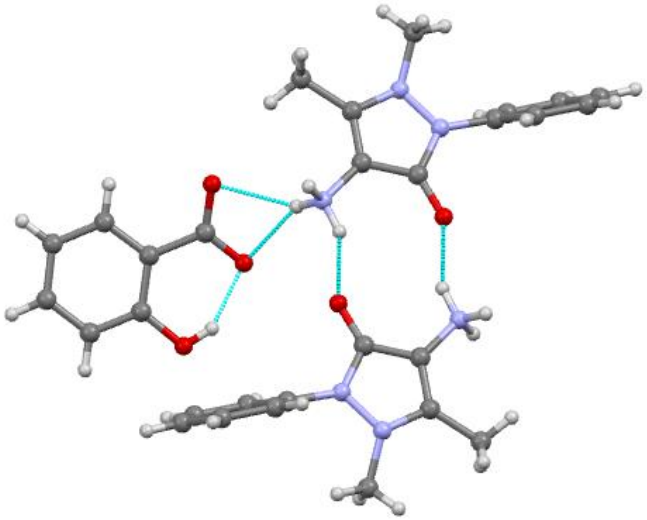

Figure 2.30: Hydrogen bonding of the molecular salt of 4AAP and salicylic acid reported by Chitradevi *et al.* (CSD ref: DUHYOV)

2.6.2 Salt or co-crystal? The effect of pK_a

The effect of pK_a on co-crystal formation has recently come into the spotlight. Childs *et al*. states that the absolute separation of the pK_a values of a molecule and its potential co-former plays a critical role in determining whether the supramolecular synthesis of two such molecules will result in a salt or in a co-crystal (Childs et al., 2007). It is generally accepted that in supramolecular synthesis two molecules will form a salt if the pK_a separation (where ΔpK_a = pK_a(protonated base) – pK_a(acid)) of the acid and base is greater than 2 or 3, a phenomenon known as the "pK_a rule" (Guillory, 2003). A larger pK_a separation is expected to result in salt formation. Bhogala *et al*. commented that in pyridine / carboxylic acid complexes, a negative pK_a difference between the acid / base pairs will invariably result in co-crystal formation (Bhogala et al., 2005).

Cruz-Cabeza conducted a statistical study of the pK_a separations of 6465 salts and co-crystals. The statistical analysis validated the pK_a rule and it was confirmed that salts were observed exclusively where $\Delta pK_a > 4$ and co-crystals were observed exclusively when $\Delta pK_a < -1$. For ΔpK_a separations between –1 and 4, the probability of salt formation was found to have a linear relationship to the ΔpK_a value (Cruz-Cabeza, 2012).

More recently, Lemmerer *et al*. presented empirical evidence to suggest that in pyridine / carboxylic acid complexes, an absolute ΔpK_a separation of less than 3 will greatly enhance the formation of a co-crystal rather than a salt (the "Rule of Three") (Lemmerer *et al*., 2015). A series of carboxylic acid complexes with nine pyridines, and 109 literature examples containing pyridine and carboxylic functional groups were used for this study. The results obtained by Lemmerer show that a salt can be formed if $\Delta pK_a < 3$, but that the likelihood of salt formation increases as the ΔpK_a increases from 0. Likewise, co-crystal formation is extremely unlikely at $\Delta pK_a > 3$. This can be shown in the plot of ΔpK_a vs salt/co-crystal distribution shown in **Figure 2.31** (Lemmerer *et al.*, 2015)

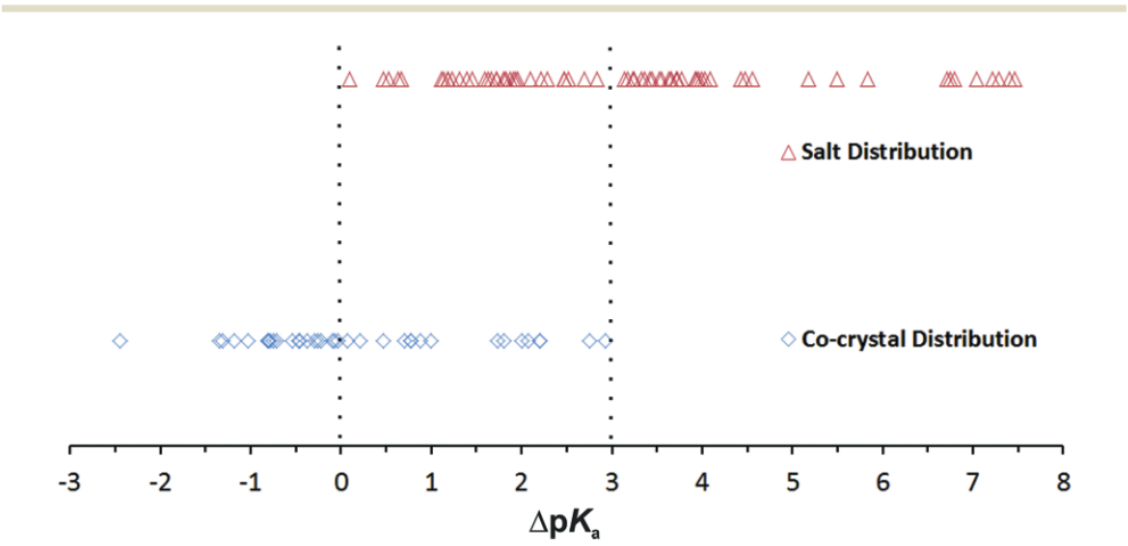

Figure 2.31. A plot of 109 complexes found in the CSD that have a carboxylic acid group and a pyridine group, respectively, on separate molecules, plotted as a function of ΔpK_a and the observed co-crystal or salt complex. Diagram taken directly from *CrystEngComm*. (2015). **17**, 3591-3595.

Stilnović *et al*. prepared a series of 22 co-crystals and salts of various pyridines with gentisic acid and analysed the proton transfer in the formation of these complexes. Proton transfer was found to be absent where ΔpK_a was less than 2, and always occurred when ΔpK_a was greater than 2 (Stilinović and Kaitner, 2012). Stilnović reported that the carboxylic acid – pyridine synthon existed in all but one of the structures and made the interesting observation that this bond was shorter and stronger in the co-crystals than in the salts.

2.6.3 The covalent modification of 4-aminoantipyrine

In a recent study of Schiff base derivatives of 4-aminoantipyrine, Mnguni and Lemmerer reported that in 4AAP that has been covalently modified to form Schiff bases to form enamines, six-membered intermolecular N−H···O hydrogen bonding is favoured, with imines having C−H···O bonds. It was noted that of 146 structures of modified isoniazid that crystallize with an imine backbone, all 136 non-solvated or hydrated structures have an intramolecular C−H···O bond. All five structures having an enamine backbone contain intramolecular N−H···O hydrogen bonding (Mnguni and Lemmerer, 2015).

Chapter 3: Experimental

3.1 Covalent modification and supramolecular synthesis

The covalent modification of isoniazid with benzophenone and its derivatives generally requires heating, increased pressure and extended refluxing over several days, as isoniazid does not readily react with benzophenone and its derivatives at ambient conditions. As many crystals were often synthesized simultaneously, and since small volumes of solvent (typically 3 mL) were used, the setup of reflux apparatus was not practical. Hence, a novel method of creating the required conditions was developed, using high-pressure glass screw-top rubber-lined dram vials (**Figure 3.1a**).

Glass screw-top rubber-lined dram vials were purchased, which were airtight when screwed closed. The reagents were added to the vials and roughly 3mL of solvent was added to each vial so that the vial was no more than half full. A magnetic stirrer bar was added and the top was tightly closed and the vial placed on a heater-stirrer and heated to up to 120°C. This resulted in considerable convection currents within the vial which mimicked a reflux setup on a small scale (**Figure 3.1b**). The reflux could be carried out for several days in these vials at up to 120°C without any noticeable loss of solvent. This method also allowed reflux to be carried out at higher temperatures than the boiling points of the solvents. However, heating the vial to above 150°C or filling the vial more than half full caused too high pressure and resulted in the vial bursting, and this method should therefore only be used noting these limitations. For safety reasons, an inverted beaker was placed over the sealed vials while heating at all times. Should this method be used, care should be taken to prevent injury in the case of the vial bursting.

Figure 3.1: (a) The glass screw-top rubber-lined dram vials used for refluxing. The vials have a rubberized seal and can boil without significant loss of solvent. (b) When refluxing in the closed vial, solvent evaporates and flows back down the side of the vial.

In general, the slow evaporation method was used for growing crystals. After the reagents are completely reacted and dissolved in solution, the solution is added to a poly-top vial. The top is loosely placed on the vial, which is left open to the atmosphere for several days. In cases where the resulting crystals were small, the solution was re-dissolved, and the vial was covered with a plastic film to slow evaporation, and small holes punched in the film.

Detailed information on the synthetic methods and crystallization techniques can be found in the chapters that follow.

3.2 Crystal data and X-ray structure analysis

Single crystal data was collected on a Bruker APEX II CCD area detector diffractometer fitted with an Oxford CRYOSTREAM 700. All temperature collections were carried out at 173K. Data reduction was carried out using *SAINT+* version 6.02.6 software and *SADABS* was used to make empirical absorption corrections (Bruker, 2004).

3.3 Powder X-ray diffraction

In certain cases of polymorphism (Chapter 4.2), powder diffraction patterns were required to confirm that the single crystal structures were representative of the bulk material. Where powder diffraction patterns were required, these were collected on a Bruker D2 Phaser using Co $K_{\alpha 1/2}$ radiation ($K_{\alpha 1}$ =1.788960 Å and $K_{\alpha 2}$ = 1.789879 Å) and a Lynxeye PSD detector. Pawley refinements were carried out using Bruker AXS *TOPAS* version 4.2. Powder X-ray diffraction patterns for the polymorphs synthesized in Chapter 4.2 are presented in **Appendix 1**.

3.4 Melting points and differential scanning calorimetry (DSC)

Melting points were collected on a Mettler Toledo MP50 melting point system.

Where polymorphism was present (Chapter 4.2), DSC and powder diffraction measurements were done to characterize the purity and stability of the materials. Differential scanning calorimetry traces were collected using a using a Mettler Toledo 822^e with aluminium pans under air purge. *STAR SW 9.20* was used for instrument control and data analysis. Exothermic events were shown as peaks. Various heating and cooling protocols were performed as quantitative analysis of certain polymorphs in Chapter 4.2. The temperature and energy calibrations were performed using pure indium (purity 99.99%, m.p 156.6 °C, heat of fusion 28.45J.g^{-1}). DSC thermograms for the polymorphs synthesized in Chapter 4.2 are presented in **Appendix 1**.

3.5 Software used

All crystal structures were solved using direct methods on *SHELXS-97*. All non-hydrogen atoms were first refined isotropically, followed by anisotropic refinement by full matrix least-squares calculations based on F^2 using *SHELXS-97* (Sheldrick, 2015). All structures which had not yet been published by the time of release of the later *SHELXL-2017* (Sheldrick, 2015) version were refined further using this latest version of the software.

Publication material and diagrams of crystals structures were generated using *WinGX* (Farrugia, 2012), *ORTEP-3* (Farrugia, 2012), *PLATON* (Spek, 2009), and *MERCURY-3* (Macrae *et al.*, 2008). In general, diagrams of asymmetric units were generated using *ORTEP-3* and packing diagrams were generated using *MERCURY*.

Chapter 4: Co-crystal engineering of isoniazid: covalent assisted supramolecular synthesis

4.1 Introduction

This chapter contains two papers on co-crystal engineering.

In the first paper, covalent assisted supramolecular synthesis of co-crystals is reported and details how co-crystal engineering was used to mask functional groups in co-crystal structures and control the dimensionality of packing.

The second paper examines the effect of changing experimental and crystallization conditions to induce stoichiometric variation, polymorphism, and the formation of solvates by changing crystallization conditions.

Details of the publication status of each paper precede the relevant paper.

4.2 Covalent assisted supramolecular synthesis: Masking of amides in co-crystal synthesis using benzophenone derivatives

Title of paper:	Covalent Assisted Supramolecular Synthesis: Masking of Amides in Co-Crystal Synthesis using Benzophenone Derivatives
Journal:	*Crystal Growth and Design*
Reference:	*Cryst. Growth Des.* 2015, 15, 3813−3821
Status:	Published
Date Received:	April 2015
Date Revised:	09 June 2015
Date Published:	11 June 2015

Synopsis of Paper

In this paper, eight co-crystals of salicylic acid with covalently modified isoniazid were prepared. Co-crystal engineering was used to control the dimensionality of the supramolecular structures. Bulky modifiers (benzophenone derivatives) were used to mask the hydrogen bonding functionality of the amide group on the isoniazid. No hydrogen bonding or short intermolecular contacts were present between the amide nitrogen atoms in isoniazid and any neighboring isoniazid or salicylic acid atoms.

The paper was published in the *Crystal Growth & Design* Mikhail Antipin Memorial virtual special issue.

Table 4.1: List of compounds reported in chapter 4.2

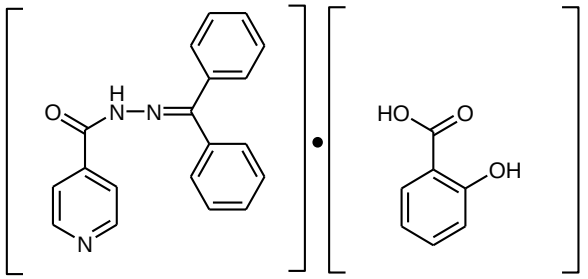	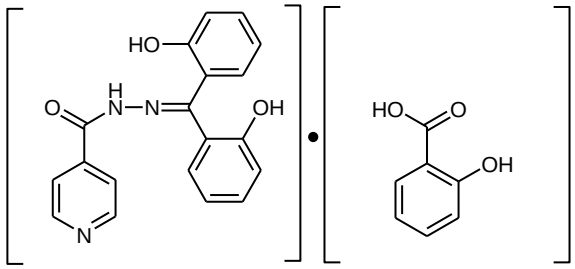
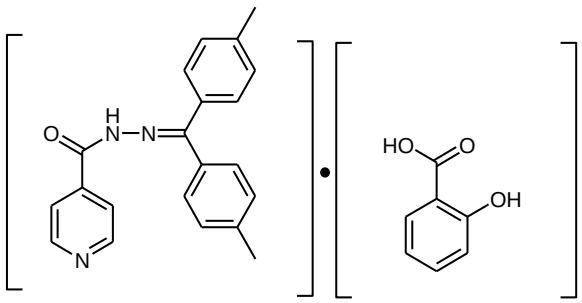 Polymorph Form I	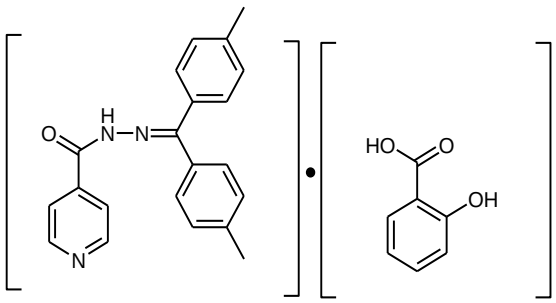 Polymorph Form II
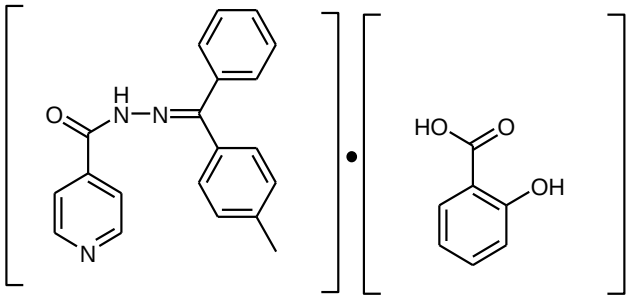	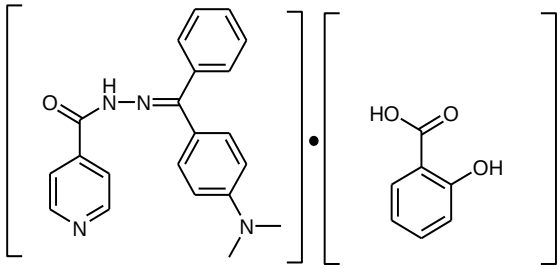
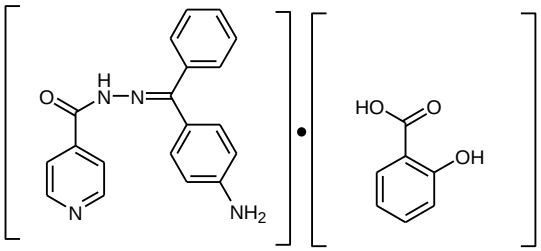 Polymorph Form I	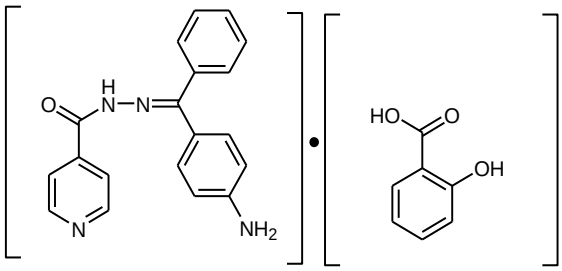 Polymorph Form II

Covalent Assisted Supramolecular Synthesis: Masking of Amides in Co-Crystal Synthesis using Benzophenone Derivatives

Mark G. Smith,[†] Roy P. Forbes[‡] and Andreas Lemmerer*[‡]

†*Department of Chemistry, University of South Africa, Unisa Science Campus, Florida, 1709, Johannesburg, South Africa, and* [‡]*Molecular Sciences Institute, School of Chemistry, University of the Witwatersrand, 2050, Johannesburg, South Africa*

RECEIVED DATE (to be automatically inserted after your manuscript is accepted if required according to the journal that you are submitting your paper to.)

To whom correspondence should be addressed:

Dr. Andreas Lemmerer, Molecular Sciences Institute, School of Chemistry, University of the Witwatersrand, Private Bag 3, 2050, Johannesburg, South Africa.
E-mail: andreas.lemmerer@wits.ac.za. Fax: +27-11-717-6749. Tel: +27-11-717-6711.

ABSTRACT:

Control over hydrogen bonding patterns and the dimensionality of supramolecular structures is possible through covalent assisted supramolecular synthesis. Consistent and predictable 'masking' of the amide functionality has been achieved through the covalent modification of isoniazid with benzophenone and benzophenone derivatives while co-crystallizing with salicylic acid. A series of co-crystals using benzophenones as masking agents was prepared using one-pot synthetic methods. No short intermolecular contacts were present between the amide nitrogen atoms in isoniazid and neighbouring isoniazid or salicylic acid atoms.

KEYWORDS:

Masking, Amides, Co-crystals, Supramolecular synthesis, Crystal engineering, Robust heterosynthons, Benzophenone

Introduction

In crystal engineering, 'robust heterosynthons' are molecules containing functional groups which have predictable and reliable hydrogen bonding functionality.[1] A prime example of such functionality can be found in the carboxylic acid···pyridine hydrogen bond. The robustness of the functionality has been illustrated by the consistent hydrogen bonding pattern that occurs between the COOH···N bond of carboxylic acid groups and the pyridine nitrogen atom of isonicotinic acid hydrazide (isoniazid).[2] A rapidly growing field of research in co-crystal engineering is that of exercising control over the dimensionality of such supramolecular assemblies. A recent review by Burrows highlights the progress that has been made to date in the synthesis of one-, two-, and three-dimensional hydrogen-bonded networks.[3] A co-crystal will pack as a 3-dimensional network, a 2-dimensional sheet, or a 1-dimensional ribbon or chain, depending largely on the number of hydrogen bonding sites between the co-crystallizing molecules. Masking of specific hydrogen bond functionalities has recently been achieved through the covalent modification of supramolecular reagents.[4] By reacting isoniazid with molecules containing ketone or aldehyde functional groups, the NH_2 group of the hydrazide moiety undergoes a condensation reaction and replaces the two H atoms with alkyl groups. This process is called 'modifying' isoniazid's hydrogen bonding functionality.[4a] Subsequently, depending on the steric size of the now added R groups, the amide H donor and/or the imine lone pair can be 'masked' by making access to them impossible for any hydrogen bonding donors or acceptors. For example, the crystal structure of the unmodified co-crystal (isoniazid)·(2-hydroxybenzoic acid) has been determined, and the packing diagrams show that isoniazid and 2-hydroxybenzoic acid (salicylic acid) molecules are connected through hydrogen bonding between the pyridine nitrogen atom and the nitrogen and oxygen atoms on the carbohydrazide functional group on isoniazid to form a 2-dimensional sheet along the *bc* plane (Fig. 1a); whereas the crystal packing where isoniazid is modified with an isopropyl group (by reacting with acetone), a 1-dimensional chain is formed by the isoniazid, with the salicylic acid carboxylic acid group still hydrogen bonding to the pyridine nitrogen atom (Fig. 1b).[4c]

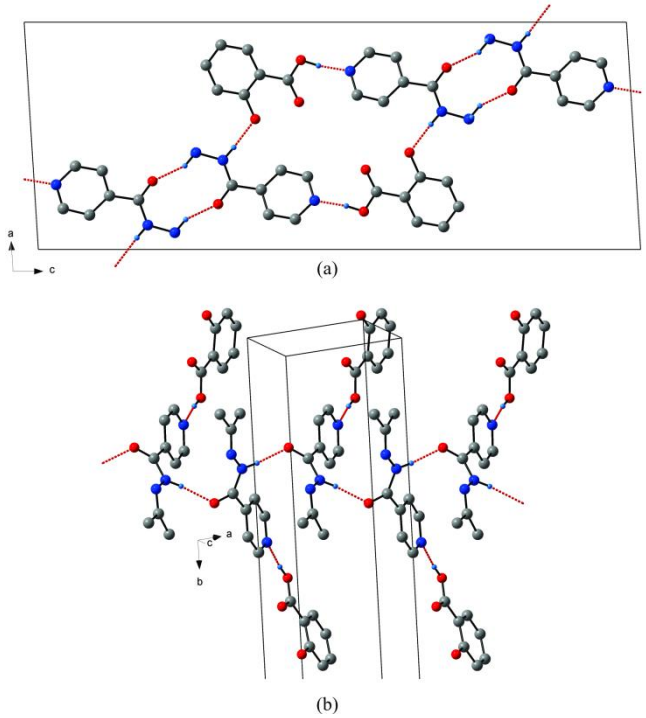

Figure 1: The hydrogen boding functionality of isoniazid and the carboxylic acid···pyridine heterosynthon with salicylic acid (a), compared with the reduced hydrogen functionality of a modified isoniazid with acetone (b). Hydrogen atoms not involved in hydrogen bonding are omitted for clarity. (Adapted from ref. 4c)

Through *in situ* modification of the carbohydrazide functional group on isoniazid, where isoniazid was reacted with numerous covalent modifiers, the dimensionality of supramolecular structures formed between the co-crystallization of modified isoniazid and carboxylic acids was reduced to 1-dimensional ribbons, due to the NH_2 group being replaced with a ketone group, and the N-H···O hydrogen bonds no longer being able to form.[c] Lemmerer *et al*. also demonstrated that when diphenylmethylene (benzophenone) was used as a covalent modifier in the supramolecular synthesis of (*N*'-(diphenylmethylene)isonicotinohydrazide)·(3-hydroxybenzoic acid), the steric effects from the bulky benzophenone moiety rendered the lone pair on the amide N atom completely inaccessible to the 3-hydroxybenzoic acid phenol as an acceptor group, as well as masking the amide H atom from hydrogen bonding with adjacent amide groups.[4a]

We wished to investigate the robustness of bulky groups similar to benzophenone in their ability to mask the amide nitrogen atom in isoniazid, and we report here the synthesis of eight co-crystal structures where isoniazid has been covalently modified by benzophenone and benzophenone

derivatives and co-crystallized with salicylic acid (Fig. 2). Due to the position of the phenolic group on salicylic acid, it was expected that the molecule should be stabilized via intramolecular hydrogen bonding and the salicylic acid molecule therefore only bond to the modified supramolecular reagent via the carboxylic acid group's hydrogen atom. In addition, we demonstrate that benzophenone and its derivatives as amide masking agents can be prepared in a three component one-pot synthesis through the condensation reaction of these modifiers with isoniazid, while co-crystallizing at the same time with salicylic acid. A further reason to investigate isoniazid being reacted with benzophenone derivatives is that the isoniazid molecule is a pro-drug, and must be activated by a bacterial catalase-peroxidase enzyme that in *Mycobacterium tuberculosis* is called KatG.[5a] KatG couples the isonicotinic acyl with the reduced form of nicotinamide adenine dinucleotide (NADH) to form a isonicotinic acyl-NADH complex which then becomes the active molecule. However, the isoniazid efficacy can be reduced by a class of enzymes known as *N*-arylaminoacetyl transferases (NAT), which rapidly acetylate the NH_2 position preventing the reaction with NADH. A way to overcome this problem is to react the NH_2 group with aldehyde or ketone groups that then structurally block isoniazid from the effects of NAT.[5b]

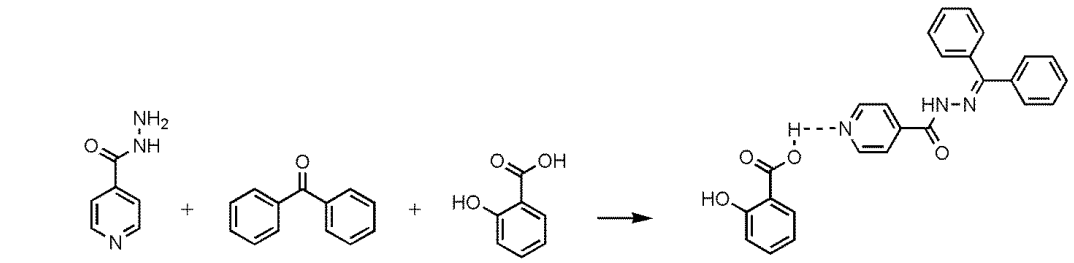

(a)

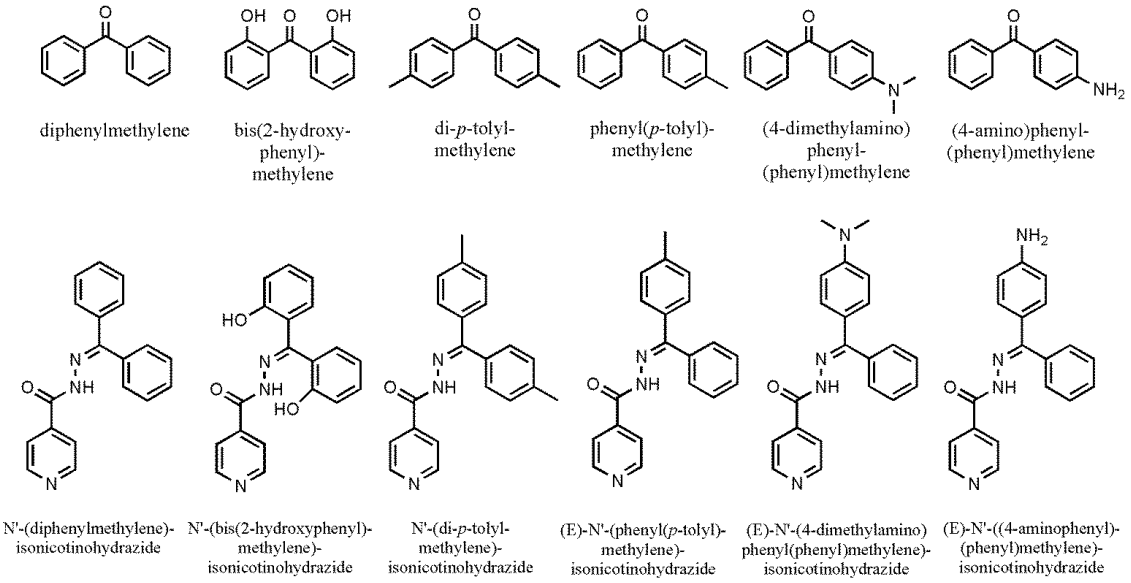

(b)

1: (N'-(diphenylmethylene)isonicotinohydrazide)·(salicylic acid)
2: (N'-(bis(2-hydroxyphenyl)methylene)isonicotinohydrazide)·(salicylic acid)
3a: (N'-(di-*p*-tolylmethylene)isonicotinohydrazide)·(salicylic acid) Form I
3b: (N'-(di-*p*-tolylmethylene)isonicotinohydrazide)·(salicylic acid) Form II
4: ((E)-N'-(phenyl(*p*-tolyl)methylene)isonicotinohydrazide)·(salicylic acid)
5: ((E)-N'-((4-(dimethylamino)phenyl)(phenyl)methylene)isonicotinohydrazide)·(salicylic acid)
6a: ((E)-N'-((4-aminophenyl)(phenyl)methylene)isonicotinohydrazide)·(salicylic acid) Form I
6b: ((E)-N'-((4-aminophenyl)(phenyl)methylene)isonicotinohydrazide)·(salicylic acid) Form II

(c)

Figure 2: Summary of reagents and products in the covalent assisted supramolecular synthesis. Part (a) summarizes the general one-pot reaction scheme, where isoniazid reacts with a benzophenone modifier to form a modified hydrazide, which co-crystallizes with salicylic acid. The various benzophenone modifiers and their corresponding isonicotinohydrazide products (modified isoniazid) are shown in (b). Supramolecular synthesis resulting from the co-crystallization of the modified isoniazid molecules in (b) with salicylic acid resulted in eight co-crystal structures (c), with co-crystals **3a** and **3b**, as well as **6a** and **6b**, having dimorphic structures.

Experimental Methods

Synthesis:

The general method for the one-pot synthesis of co-crystals **1-6** follows the method described for co-crystal **1** below. Compounds **2 - 6** were synthesized in a similar manner. The masses of reagents, modifiers, solvents and catalysts used, as well as reflux and crystallization conditions are described in Table 1.

Method of synthesis of co-crystal 1, *N*'-(diphenylmethylene)isonicotinohydrazide)·(salicylic acid):

0.1165 g of isonicotinic acid hydrazide (0.8495 mmol), 0.1562 g of benzophenone (0.8572 mmol) and 0.1160 g of salicylic acid (0.8398 mmol) were added into a sample vial. The solids were dissolved in AP-grade methanol (10 mL), refluxed in a closed vial for 72 hours at 110°C, and were left to stand at room temperature open to the atmosphere. Colourless needles were afforded after 3 days.

Table 1 Reagents and conditions for synthesis of co-crystals 1-6

Co-Crystal	Mass of Isoniazid	Mass of Modifier	Mass of Salicylic Acid	Catalyst	Solvent	Reflux Conditions	Crystallization
1	0.1165g (0.8495mmol)	0.1562g benzophenone (0.8572mmol)	0.1160g (0.8398mmol)	None	10mL methanol	Closed vial, 72 hours at 110°C.	Slow evaporation at room temperature. Colourless needles afforded after 3 days
2	0.1003g (0.7314mmol)	0.1595g 2,2'-dihydroxybenzophenone (0.7446mmol)	0.1136g (0.8225mmol)	0.0106g nickel nitrate (0.0364mmol)	10mL acetonitrile	Closed vial, 4 days at 70°C.	Slow evaporation at room temperature. Clear plates afforded after 5 days.
3a	0.1175g (0.8567mmol)	0.1803g 4,4'-dimethylbenzophenone (0.8574mmol)	0.1175g (1.2851mmol)	None	10mL methanol	Closed vial, 72 hours at room temperature.	Slow evaporation at room temperature. Yellow cubes afforded after 3 days.
3b	0.0988g (0.720mmol)	0.1514g 4,4'-dimethylbenzophenone (0.7200mmol)	0.1994g (1.4437mmol)	None	10mL methanol	Closed vial, 24 hours at 90°C.	Slow evaporation at room temperature. Yellow plates afforded after 3 days.
4	0.1100g (0.8021mmol)	0.1571g 4-methylbenzophenone (0.8005mmol)	0.1107g (0.8015mmol)	None	10mL methanol	Closed vial, 24 hours at 70°C.	Slow evaporation at room temperature. Colourless needles afforded after 3 days
5	0.1037g (0.7561mmol)	0.1707g 4-(dimethylamino)-benzophenone (0.7577mmol)	0.1045g (0.7565mmol)	None	10mL methanol	Closed vial, 24 hours at 90°C.	Slow evaporation at room temperature. Red Needles afforded after 3 days.
6a	0.1015g (0.7401mmol)	0.1484g 4-aminobenzophenone (0.7446mmol)	0.1014g (0.7341mmol)	0.0094g nickel nitrate (0.0323mmol)	10mL methanol	Closed vial, 18 hours at 50°C.	Slow evaporation at room temperature. Clear plates afforded after 7 days.
6b	0.1005g (0.7328mmol)	0.1467g 4-aminobenzophenone (0.7438mmol)	0.2240g (1.6218mmol)	0.0097g nickel nitrate (0.0334mmol)	10mL methanol	Closed vial, 18 hours at 50°C.	Slow evaporation at room temperature. Clear plates afforded after 5 days.

Crystal Data and X-ray Structure Analysis. The intensity data for the eight co-crystals were collected on a Bruker APEX II CCD area detector diffractometer with graphite monochromated Mo-K_α radiation (50 kV, 30 mA) at 173K. The collection method involved ω-scans having a width of 0.5°. Data reduction was carried out using *SAINT+* version 6.02.6 software and SADABS was used to make empirical absorption corrections.[6] The crystal structures were solved through direct methods using *SHELXS-97*.[7] Non-hydrogen atoms were first refined isotropically followed by anisotropic refinement by full matrix least-squares calculations based on F^2 using *SHELXL-97*.[7] C-bound H atoms were first located in the difference electron density map, then positioned geometrically and allowed to ride on their respective parent atoms, with thermal displacement parameters 1.2 times that of the parent C atom. Where possible, the coordinates and isotropic displacement parameters of the N-bound and O-bound H atoms involved in hydrogen bonding interactions were allowed to refine freely, except for co-crystals **2** and **5** due to poor refinement stability. The diffraction data and refinement statistics of co-crystal **2** were poor even after numerous attempts at recrystallization. Diagrams and publication material were generated using *WinGX*,[8] *ORTEP-3*,[9] *PLATON*[10] and *DIAMOND*.[11] The crystallographic data of each co-crystal is summarized in Table 2.

Powder X-ray Diffraction. Experimental diffraction patterns of Co-crystals **1** – **6b** were collected on a Bruker D2 Phaser using Co $K\alpha_{1/2}$ radiation ($K\alpha_1$ =1.788960 and $K\alpha_2$ = 1.789879 Å) and a Lynxeye PSD detector. Pawley refinements were carried out on all data using Bruker AXS TOPAS version 4.2. Powder X-ray diffraction confirmed that the single crystal structures were representative of the bulk material except for **5**, which shows some impurity phases (See ESI).

Melting Points. Melting points of all compounds except the dimorphs **3** and **6** were collected on a Mettler Toledo MP50 melting point system. The melting points of dimorphic structures **3a** and **3b** and for **6a** and **6b**, were done using DSC (below). Melting points of all compounds can be found in the ESI and Table 2.

Differential Scanning Calorimetry (DSC). Differential scanning calorimetry traces were collected using a using a Mettler Toledo 822^e with aluminium pans under air purge." STAR SW 9.20 was used for instrument control and data analysis. Exothermic events were shown as peaks.

Various heating and cooling protocols were performed as quantitative analysis of the polymorphs. The temperature and energy calibrations were performed using pure indium (purity 99.99%, m.p 156.6 °C, heat of fusion 28.45 J g-1). DSC traces are given in the supporting information.

Table 2 Crystallographic data for all co-crystals.

	1	**2**	**3a**	**3b**
Formula	$(C_{19}H_{15}N_3O)\cdot(C_7H_6O_3)$	$(C_{19}H_{15}N_3O_3)\cdot(C_7H_6O_3)$	$(C_{21}H_{19}N_3O)\cdot(C_7H_6O_3)$	$(C_{21}H_{19}N_3O)\cdot(C_7H_6O_3)$
M_r	439.46	471.46	467.51	467.51
Melting point (°C)	146	128	134	152
Temperature/K	173(2)	173(2)	173(2)	173(2)
Wavelength/Å	0.71073	0.71073	0.71073	0.71073
Crystal size/mm^3	0.54×0.41×0.25	0.47×0.40×0.10	0.90×0.28×0.21	0.40×0.39×0.26
Crystal system	Monoclinic	Monoclinic	Triclinic	Triclinic
Space group	$P2_1/c$	$P2_1/c$	$P\bar{1}$	$P\bar{1}$
a/Å	25.8071(6)	25.010(2)	9.9062(2)	8.2520(3)
b/Å	6.9240(2)	6.9708(7)	12.0906(3)	11.2852(4)
c/Å	12.2426(3)	12.4779(11)	12.4633(3)	12.9411(5)
α/°	90	90	113.5360(10)	77.516(2)
β/°	103.5010(10)	90.949(6)	113.0770(10)	85.880(2)
γ/°	90	90	96.2970(10)	82.910(2)
V/Å^3	2127.16(9)	2175.1(4)	1194.70(5)	1166.39(7)
Z	4	4	2	2
ρ (calcd)/Mg m^{-3}	1.372	1.440	1.300	1.331
μ/mm^{-1}	0.094	0.104	0.088	0.090
F(000)	920	984	492	492
Θ Range for data/° collection/°	1.62 to 28.00	0.81 to 22.99	1.94 to 28.00	1.61 to 28.00
Reflections collected	14559	13760	18654	20720
No. of unique data [R(int)]	4952 [0.0371]	3030 [0.0799]	5748 [0.0427]	5618 [0.0440]
No. data with $I \geq 2\sigma(I)$	3895	2548	4586	4409
Final R(I > 2σ(I))	0.0417	0.1378	0.0460	0.0428
Final wR_2 (all data)	0.1178	0.4083	0.1373	0.1219
CCDC deposition number	998017	998011	998014	998015

	4	**5**	**6a**	**6b**
Formula	$(C_{20}H_{17}N_3O)\cdot(C_7H_6O_3)$	$(C_{21}H_{20}N_4O)\cdot(C_7H_6O_3)$	$(C_{19}H_{16}N_4O)\cdot(C_7H_6O_3)$	$(C_{19}H_{16}N_4O)\cdot(C_7H_6O_3)$
M_r	453.48	482.53	454.48	454.48
Melting point (°C)	128	205	137	163
Temperature/K	173(2)	173(2)	173(2)	173(2)
Wavelength/Å	0.71073	0.71073	0.71073	0.71073
Crystal size/mm^3	0.45×0.15×0.10	0.42×0.17×0.11	0.48×0.24×0.12	0.41×0.20×0.16
Crystal system	Triclinic	Triclinic	Triclinic	Monoclinic
Space group	$P\bar{1}$	$P\bar{1}$	$P\bar{1}$	$P2_1$
a/Å	6.6193(2)	7.0057(4)	9.2815(3)	7.8452(3)
b/Å	12.3234(3)	11.5495(7)	11.7198(3)	10.7034(4)
c/Å	14.4180(3)	15.6046(9)	12.2187(3)	13.1775(5)
α/°	98.727(2)	87.598(4)	94.4050(10)	90
β/°	98.596(2)	82.792(4)	110.971(2)	93.234(3)
γ/°	100.665(2)	72.850(3)	113.076(2)	90
V/Å^3	1123.17(5)	1196.91(12)	1104.72(5)	1104.76(7)
Z	2	2	2	2
ρ (calcd)/Mg m^{-3}	1.341	1.339	1.366	1.366
μ/mm^{-1}	0.091	0.091	0.091	0.091
F(000)	476	508	476	476
Θ Range for data/° collection/°	1.45 to 28.00	1.32 to 28.00	1.84 to 28.00	1.55 to 27.99
Reflections collected	19872	17076	18697	9610
No. of unique data [R(int)]	5411 [0.0321]	5783 [0.1444]	5336 [0.0397]	2801 [0.0538]
No. data with $I \geq 2\sigma(I)$	3823	2927	3894	1952
Final R($I > 2\sigma(I)$)	0.0469	0.0572	0.0483	0.0713
Final wR_2 (all data)	0.1338	0.1511	0.1403	0.2280
CCDC deposition number	998013	998016	1056771	1056772

Results and discussion

Eight co-crystals were synthesized using one-pot synthetic methods. Six benzophenone derivatives were used to modify isoniazid to form eight modified hydrazide molecules, including two sets of dimorphic structures (Fig. 2). Each of these modified hydrazide molecules were co-crystallized with salicylic acid to form eight co-crystals (Fig. 2), numbered **1**-**6**, with the dimorphic structures being labelled **3a** and **3b**, and **6a** and **6b** respectively. The asymmetric units and atomic numbering schemes for each co-crystal are shown in Figure 3. Hydrogen bonding details of co-crystals **1**-**6** are given in Table 3; and comparative structural and packing features are summarized in Table 4.

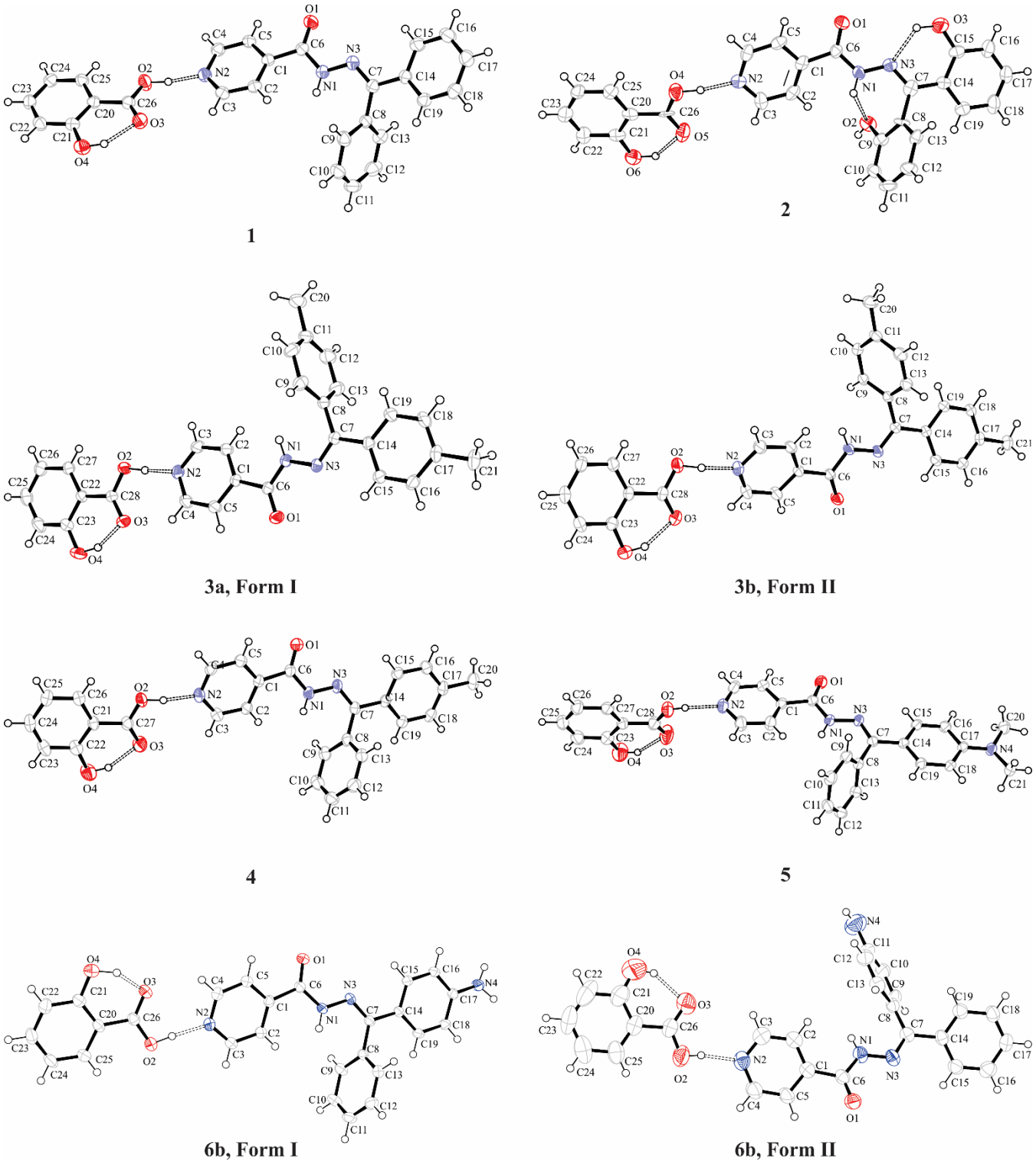

Figure 3: Asymmetric units of co-crystals **1-6**, showing the atomic numbering scheme for each co-crystal. Note the repeated intermolecular COOH···N and intramolecular O-H···O hydrogen bonds.

Compound **1** crystallizes in the $P2_1/c$ space group, and the asymmetric unit contains one molecule of (*N*'-(diphenylmethylene)isonicotinohydrazide) and one molecule of salicylic acid**.** As is expected from co-crystals reported in the literature,[12] the robust carboxylic acid···pyridine heterosynthon is present, O2─H2···N2 (Table 3). The phenol group on the salicylic molecules forms the expected intramolecular *S*(6) hydrogen bond.[13] However, the N─H hydrogen bonding is markedly absent, as the bulky benzophenone group has masked the H1 donor and the :N3 acceptor, by making the amide and hydrazide group inaccessible to any donors and acceptors, such as for example the two lone pairs on the amide carbonyl O1. Hence, all the strong hydrogen bonding interactions occur within the asymmetric unit to form 0-dimensional hydrogen bonded heteromolecular entities (Fig. 3), and there are no further intermolecular hydrogen bonds to *any* neighbouring entities. The pyridine ring is essentially coplanar with the salicylic acid molecule, with a 2.7° angle between the planes. The relative orientation of the two moieties is such that the salicylic carbonyl C26=O2 lies on the same side of the pyridine/salicylic acid plane as the isoniazid carbonyl C6=O1. The packing of the salicylic molecules is such that they are enfolded by the diphenylmethylene rings of the modified isoniazid on neighbouring entities, and stabilized by π-stacking along the *b*-axis (Figure 4a).

Compound **2** crystallizes in the $P2_1/c$ space group, and has similar unit cell axis lengths to **1** (Fig. 4b), but has a significantly different packing to co-crystals **3-6a** as will be described below. In this compound, the amide N1-H1 donor and :N3 lone pair are masked from the other donor and acceptor hydrogen bond functionalities not only by the steric effect of the benzophenone derivative groups, but by intramolecular hydrogen bonding between the phenol donor groups in the 2-position of the 2-hydroxyphenyl rings, O2 and O3, and the N1 and N3 atoms to form N1-H1···O2 and O3-H3···N3 hydrogen bonds (Table 3). However, one of the phenol groups, O3, has its hydrogen atom free to hydrogen bond further, and in fact forms a O2─H2···O1 heterosynthon to the amide O1 to form 1-dimensional ribbons not observed in the other structures except for **6b** (Fig. 5)**.** It is significant, however, that the amide group in compound **2** is still masked by the bulky dihydroxybenzophenone moiety, and the lone pair on :N3 remains inaccessible to the phenol donor of salicylic acid.

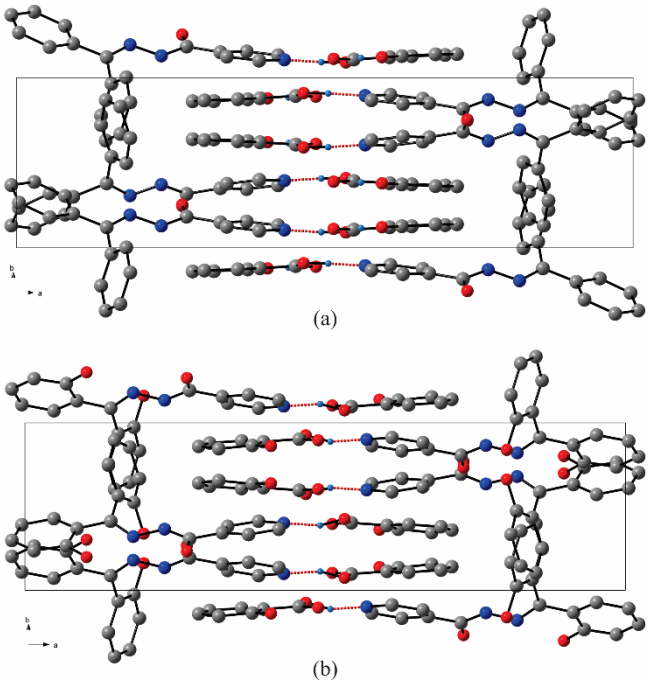

Figure 4: (a) Packing of the salicylic and *N*'-(diphenylmethylene)isonicotinohydrazide in co-crystal **1**. Note the interdigitation of the co-crystal former and supramolecular reagent. (b) The isostructural crystal packing of salicylic acid and the related modified *N*'-bis(2-hydroxyphenyl)methylene)isonicotinohydrazide in co-crystal **2**. All C-bound H atoms are omitted for clarity.

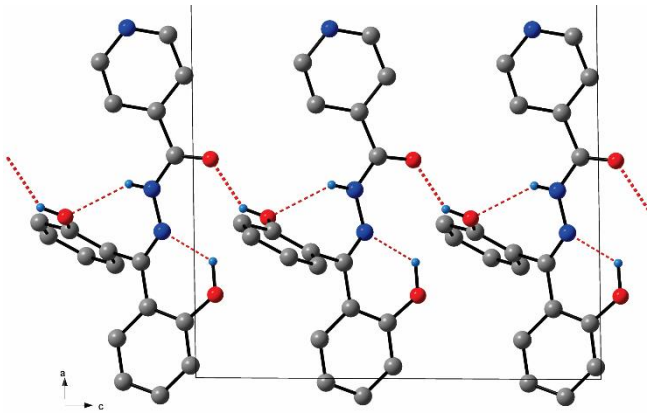

Figure 5: The 1-D hydrogen bonded chain formed by hydrogen bonds between one of the phenol groups on the 2-hydroxyphenyl rings and the carbonyl O of the amide in **2**. Shown are also the intramolecular hydrogen bonds of the amide and the phenol groups. All C-bound H atoms are omitted for clarity.

Compounds **3, 4** and **5** crystallize in the $P\bar{1}$ space group forming similar isolated hydrogen bonding entities as **1**. These compounds follow the same hydrogen bonding pattern as **1**, with only the intermolecular carboxylic acid···pyridine heterosynthon present (Table 3). The packing of **4** and **5** has the salicylic molecules and modified isoniazid molecules packing in distinct layers (Fig. 6a and b). Structures **3a** and **3b** are dimorphs, and only differ in their molecular conformations and packing arrangements. Structure **3a** has a layered packing, where each layer is made of both salicylic and modified isoniazid molecules, and adjacent layers stabilized by □-stacking of the di-*p*-tolylmethylene rings (Fig. 7a). Structure **3b** has similar □-stacking between the salicylic and *N*'-(di-*p*-tolylmethylene)isonicotinohydrazide as seen in **1** and **2** (Fig. 7b). The DSC traces of **3a** and **3b** show phase transition endotherms at approx. 117°C. **3a** then melts at 134.3°C and **3b** at 151.7°C showing possible extra phases in this system.

The C9-C8-C7-N3 torsion angle of **3b** is -61.6°, and is comparable to that of the other five co-crystals, whereas the two benzophenone rings in **3a** have an angle of +82.5°, with one benzophenone ring being almost perpendicular to the other. The pyridine ring in all co-crystals except for **5** is co-planar with the salicylic acid molecule, but **5** is notably different from the other co-crystals in that salicylic acid lies perpendicular to the plane of the pyridine ring, with an angle of -86.1° between the planes. The orientation of the salicylic acid molecule in **3a** and **3b** is different to that of **1** and **2** in that the salicylic carbonyl C28=O2 lies on the opposite side of the pyridine/salicylic acid plane as the isoniazid carbonyl C6=O1.

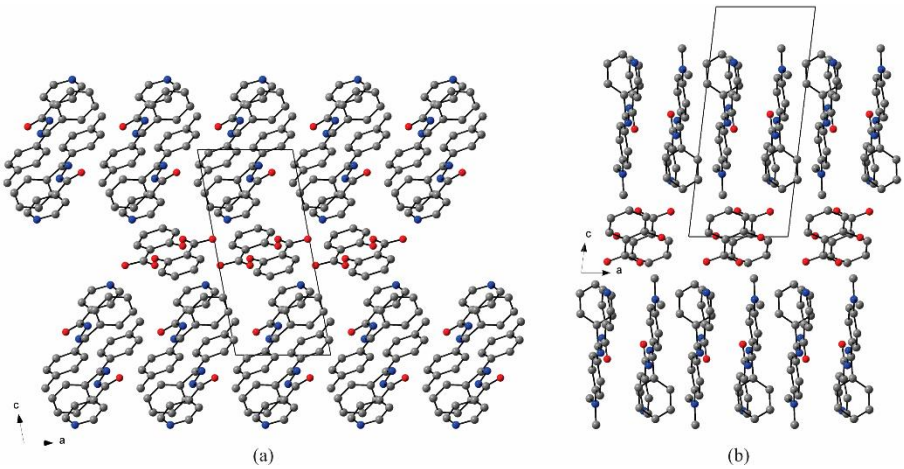

Figure 6: Similar layer packing of the salicylic and (*E*)-*N*'-(phenyl(*p*-tolyl)methylene)-isonicotinohydrazide (a) and ((*E*)-*N*'-((4-(dimethylamino)phenyl)(phenyl)methylene)-isonicotinohydrazide (b) molecules in co-crystals **4** and **5** respectively. Note especially the similar *anti*-parallel orientations of neighbouring salicylic and modified isoniazid molecules. All H atoms are omitted for clarity.

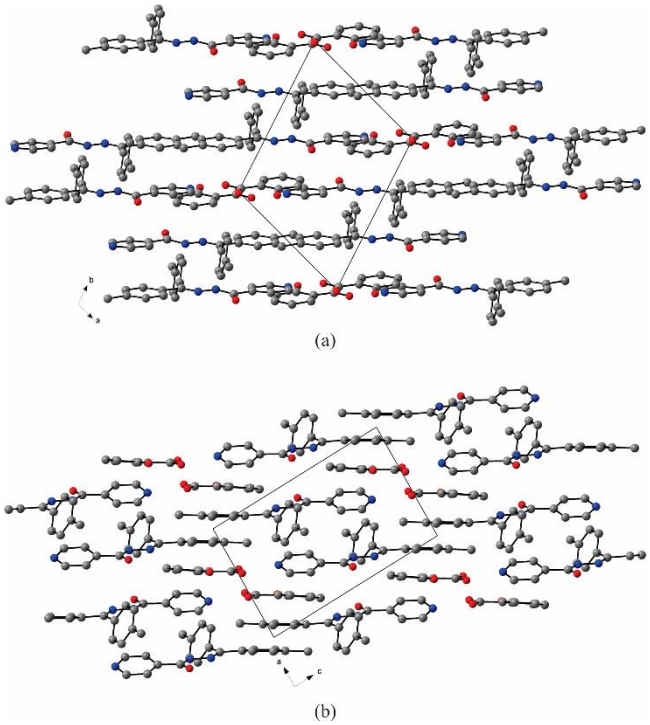

Figure 7: The different packing of (*N*'-(di-p-tolylmethylene)isonicotinohydrazide)·(salicylic acid) units in polymorphs **3a** and **3b**. All H atoms are omitted for clarity.

Compounds **6a** and **6b** are dimorphs, but differ significantly from each other in their molecular conformations, dimensionality and packing arrangements. Compound **6a** crystallizes in the $P\bar{1}$ space group, and **6b** in the $P2_1$ space group. In both compounds, the amino groups of the 4-aminobenzophenone moiety are involved in intermolecular bonding. In addition to the intermolecular carboxylic acid···pyridine heterosynthon, each modified isoniazid molecule in **6a** is hydrogen bonded to a second modified isoniazid molecule through two N4─H4A···O1 hydrogen bonds to form dimers with 0-dimensional packing dimensionality (Fig. 8a). In **6b**, each modified isoniazid molecule hydrogen bonds through its N4─H4A to one adjacent molecule, forming 1-dimensional ribbons instead (Fig. 8b). In both **6a** and **6b**, the salicylic acid molecule is co-planar with the pyridine ring of isoniazid. However, the orientation of the salicylic carboxylic acid C=O bond for **6a** is *syn* with respect to the amide C6=O1 of the modified isoniazid, whereas for **6b**, the orientation is *anti*. There is no hydrogen bonding between the second amide N4─H4B with any neighbouring entities. The DSC trace of **6a** shows a melting point at 136.6 °C, followed by a recrystallization exotherm for a new phase which then melts at 160.0 °C. Instead, **6b** show no phase transition endotherms and melts at 163.2°C.

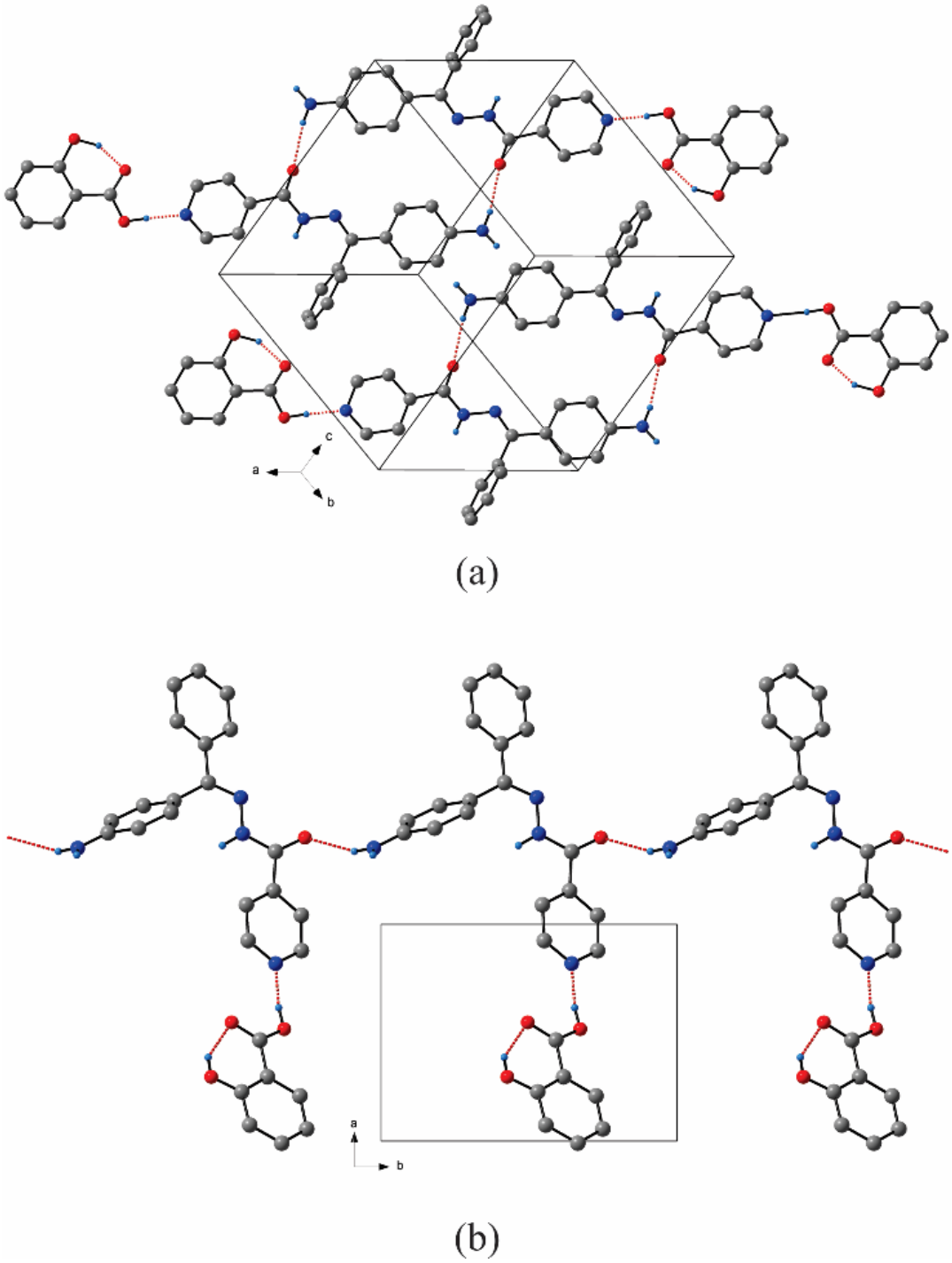

Figure 8: Packing of dimorphic structures **6a** (a) and **6b** (b), showing their differing supramolecular dimensionality. **6a** has a zero-dimensional supramolecular structure, whereas **6b** forms a one-dimensional ribbon. The orientation of the salicylic carboxylic acid C=O bond for **6a** is *syn* with respect to the amide C6=O1, whereas for **6b**, the orientation is *anti*. All C-bound H atoms are omitted for clarity.

Table 3 Hydrogen bonding details of co-crystals **1-6**

	d(D─H)/Å	*d*(H···A)/Å	*d*(D···A)/Å	∠(D─H···A)
1				
O2─H2···N2	1.01(2)	1.58(2)	2.5904(13)	171(2)
O4─H4···O3	0.91(2)	1.79(2)	2.6195(13)	149(2)
2				
N1─H1···O2	0.88	2.31	2.812	116
O2─H2···O1	0.84	1.84	2.5737(13)	145[i]
O3─H3···N3	1.05	1.92	2.685(8)	127
O4─H4···N2	1.05	1.66	2.633(7)	152
O6─H6···O5	0.96	1.83	2.603(11)	136
3a Form I				
O2─H2···N2	0.99(2)	1.65(2)	2.6381(13)	175(2)
O4─H4···O3	0.95(3)	1.67(3)	2.5651(14)	154(2)
3b Form II				
O2─H2···N2	1.05(2)	1.59(3)	2.6383(14)	175(2)
O4─H4···O3	0.91(2)	1.77(2)	2.6031(14)	152(2)
4				
O2─H2···N2	0.97(3)	1.61(3)	2.5704(16)	171(3)
O4─H4···O3	0.90(3)	1.77(3)	2.6073(19)	154(3)
5				
O2─H2···N2	0.84	1.78	2.615(2)	172
O4─H4···O3	0.84	1.82	2.548(3)	144
6a Form I				
N4─H4A···O1	0.87(2)	2.16(2)	2.989(2)	160(2)[ii]
O2─H2···N2	0.96(2)	1.71(2)	2.6720(18)	177(2)
O4─H4···O3	1.08(3)	1.56(3)	2.5681(18)	153(2)
6b Form II				
N4─H4A···O1	0.88	2.23	3.068(8)	159[iii]
O2─H2···N2	0.84	1.73	2.563(6)	170
O4─H4···O3	0.84	1.87	2.599(8)	145

(i): x, -y+1/2, z-1/2

(ii): -x+1, -y, -z+1

(iii): x, y-1, z

Table 4 Comparison of planar orientations and torsion angles in co-crystals **1-6**

	1	**2**	**3a**	**3b**	**4**	**5**	**6a**	**6b**
Orientation of plane of salicylic acid ring wrt plane of pyridine ring	Co-planar	Co-planar	Co-planar	Co-planar	Co-planar	Perpendicular	Co-planar	Co-planar
Angle between plane of salicylic acid ring and plane of pyridine ring	2.7°	5.9°	-6.9°	-28.6°	1.4°	-86.1°	-4.0°	4.1°
Orientation of salicylic carboxylic acid C28/C26=O2 wrt amide C6=O1	*anti*	*anti*	*syn*	*syn*	*Anti*	Perpendicular	*syn*	*anti*
Hydrogen bonding dimensionality	0D	1D	0D	0D	0D	0D	0D	1D
Packing dimensionality	0D	1D chains	0D	0D	0D	0D	0D	1D chains
Torsion angles:								
C13-C8-C14-C19	-80.7°	68.1°	65.9°	-63.4°	74.0°	-63.2°	69.0°	72.9°
N3-N1-C6-C7	7.6°	-12.1°	-3.9°	2.50°	-9.5°	2.0°	2.1°	4.4°
C9-C8-C7-N3	-73.9°	65.2°	82.5°	-61.6°	63.5°	-67.9°	71.4°	62.8°

Conclusion

In this paper, we have described eight co-crystals formed between isoniazid, which has been covalently modified with a series of benzophenone derivatives, and then co-crystallized with salicylic acid. Each co-crystal was synthesized in a one-pot synthesis, with covalent modification occurring *in situ*. In all eight co-crystals, the benzophenone derivative effectively masked the amide nitrogen on the carbohydrazide group of isoniazid. The only intermolecular hydrogen bonding observed in co-crystals **1**, **3-6a** was the carboxylic acid···pyridine N2 hydrogen bonding to form isolated hydrogen bonded entities; and in **2**, additional hydrogen bonding between the carbonyl oxygen of isoniazid and the phenol donor group of the 2-hydroxybenzophenone ring was observed to form 1-dimensional chains. Structures **3a** and **3b** are dimorphs, and only differ in their molecular conformation and packing arrangement. Dimorphs **6a** and **6b** differ in the dimensionality of their supramolecular structure. **6a** packs in a zero-dimensional arrangement, whereas **6b** forms one-dimensional ribbons. In all cases, the amide nitrogen was completely

inaccessible to either the phenol donor group of salicylic acid or the amide carbonyl group. In conclusion, benzophenone and its derivatives are reliable and predictable in their ability to mask the amide group in the carbohydrazide moiety. Co-crystals **2** and **6b** shows further that if additional hydrogen bonding functionalities exist on the phenyl rings of the benzophenone modifiers, they can replace the amide moiety to form 1-dimensional chains in a similar way to the amide group if it were not masked.

Acknowledgement

The University of the Witwatersrand and the Molecular Sciences Institute are thanked for providing the infrastructure and financial support to do this work. A Lemmerer thanks the Wits Friedel Sellschop award for funding and M Smith thanks the Chemistry department of the University of South Africa for their financial support.

Supporting Information Available

PXRD patterns, DSC traces and melting points for all compounds. Crystallographic data were deposited at the Cambridge Crystallographic Data Center with reference numbers CCDC 998011, CCDC 998013-998017, and CCDC 1056771-1056772 which can be requested from The Cambridge Crystallographic Data Centre (http://www.ccdc.cam.ac.uk/data_request/cif). This information is available free of charge via the Internet at http://pubs.acs.org/.

References

(1) McMahon, J. A.; Bis, J. A.; Vishweshar, P.; Shattock, T. R.; McLaughlin, O. L.; Zaworotko, M. J. *Z. Kristallogr.* **2005**, *220*, 340-350.

(2) (a) Lemmerer, A.; Bernstein, J.; Kahlenberg, V. *CrystEngComm*. **2010**, *12*, 2856-2864; (b) Aitipamula, S.; Wong, A. B. H.; Chow, P. S.; Tan, R. G. B. C*rystEngComm.* **2013**, *15*, 5877-5887.

(3) Burrows, AD. *Crystal engineering using multiple hydrogen bonds*. Struct Bonding (Berlin), **2004**, *108*, 55-96.

(4) (a) Lemmerer, A.; Bernstein, J.; Kahlenberg, V. *CrystEngComm*. **2011**, *13*, 5692-5708. (b) Sander, J. R. G.; Bucar, D.; Henry, R. F.; Giangiorgi, B. N.; Zhang, G. G. Z.; MacGillivray, L. R. *CrystEngComm.* **2013**, *15*, 48164822; (c) Lemmerer, A. *CrystEngComm.* **2012**, *14*, 2465-2478.

(5) (a) Suarez J; Ranguelova K; Jarzecki A. A.; Manzerova, J.; Krymov, V.; Zhao, X.; Yu, S.; Metlitsky, L.; Gerfen, G. J.; Magliozzo, S. *J. Biol. Chem.* **2009**, *284*, 7017–7029; (b) Hearn, M. J.; Cynamon, M. H.; Chen, M. F.; Coppins, R.; Davis, J.; Kang, H. J.-O.; Noble, A.; T-Sekine, B.; Terrot, M. S.; Trombino, D.; Thai, M.; Webster, E. R.; Wilson, R. *Eur. J. Med. Chem.* **2009**, *44*, 4169-4178.

(6) SAINT+, Version 6.02 (Includes XPREP and SADABS); Bruker AXS Inc.: Madison, Wisconsin, USA, **2004**.

(7) Sheldrick, G. M. *Acta Crystallogr., Sect. A.* **2008**, *64*, 112-122.

(8) Farrugia, L. J. *J. Appl. Crystallogr*. **1999**, *32*, 837-838.

(9) Farrugia, L. J. *J. Appl. Crystallogr*. **1997**, *30*, 565.

(10) Spek, A. L. *J. Appl. Crystallogr*. **2003**, *36*, 7-13.

(11) Brandenburg, K.; Diamond, Version 2.1e, **1996-2001**, Crystal Impact GbR, Bonn, Germany.

(12) Aakeröy, C. B.; Hussain, I.; Forbes, S.; Desper, J. *CrystEngComm*. **2007**, *9*, 46-54.

(13) Bernstein, J.; Davis, R. E.; Shimoni, L.; Chang, N.-L. *Angew. Chem. Int. Ed. Engl.* **1995**, *34*, 1555-1573.

4.3 Covalent assisted supramolecular synthesis: The influence of crystallization conditions on co-crystals of "masked" isoniazid derivatives

Title of paper:	Covalent Assisted Supramolecular synthesis: The Influence of Crystallization Conditions on Co-Crystals of "Masked" Isoniazid Derivatives
Journal:	*Crystal Growth and Design*
Reference:	Pending
Status:	Submitted. Has been reviewed and currently attending to reviewers' comments as per editor's request.
Date Received:	December 2017
Date Revised:	February 2018
Date Published:	

Synopsis of Paper

In this paper, eight co-crystals of salicylic acid with covalently modified isoniazid were prepared. The effect of crystallization conditions on co-crystals of "masked" isoniazid derivatives was studied and reported. Co-crystal engineering was applied to induce stoichiometric variation, polymorphism and solvate formation via changes in reflux time, stoichiometry of reagents (additives), addition of catalysts and addition of substituents to the aromatic rings.

Table 4.2: List of compounds reported in chapter 4.3

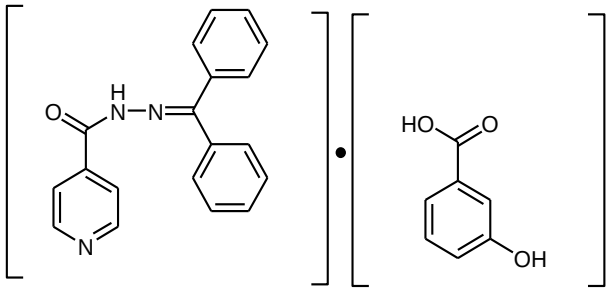 1:1 Stoichiometric ratio in asymmetric unit	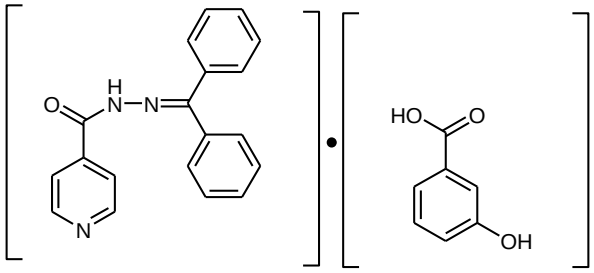 2:1 Stoichiometric ratio in asymmetric unit
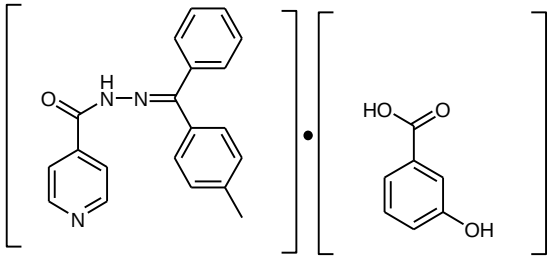 Polymorph Form I	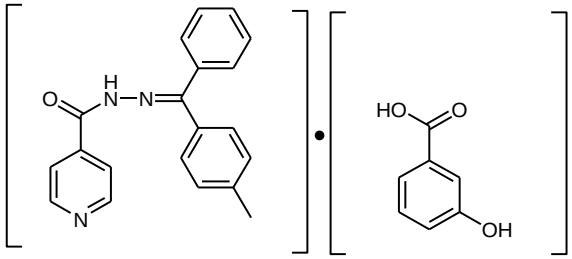 Polymorph Form II
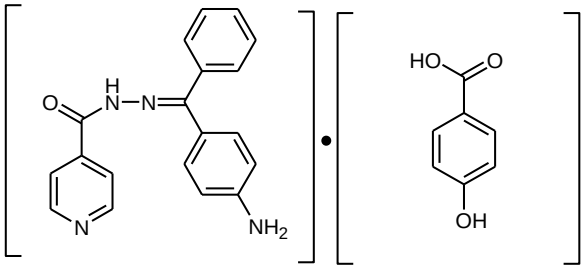	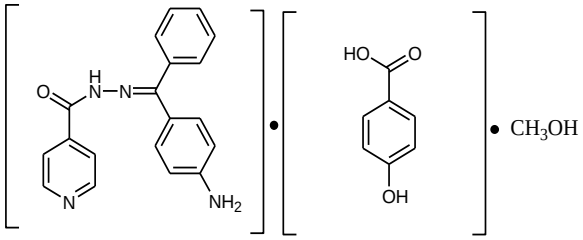
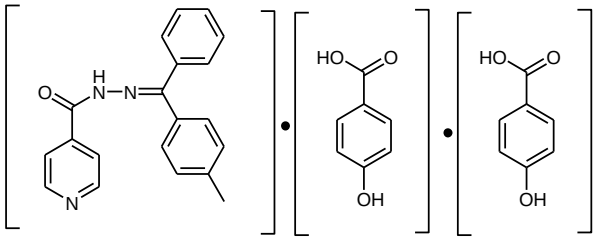	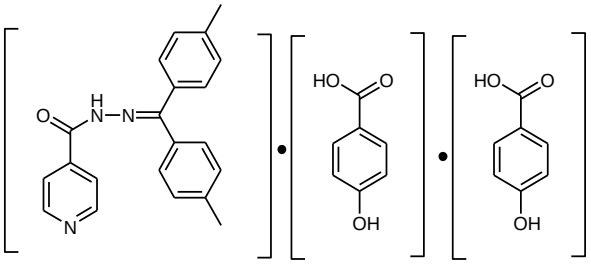

Covalent Assisted Supramolecular Synthesis: The Influence of Crystallization Conditions on Co-Crystals of "Masked" Isoniazid Derivatives

Mark G. Smith[†] and Andreas Lemmerer*[‡]

†*Department of Chemistry, University of South Africa, Unisa Science Campus, Florida, 1709, Johannesburg, South Africa, and* [‡]*Molecular Sciences Institute, School of Chemistry, University of the Witwatersrand, 2050, Johannesburg, South Africa*

RECEIVED DATE (to be automatically inserted after your manuscript is accepted if required according to the journal that you are submitting your paper to)

To whom correspondence should be addressed:

Dr. Andreas Lemmerer, Molecular Sciences Institute, School of Chemistry, University of the Witwatersrand, Private Bag 3, 2050, Johannesburg, South Africa.
E-mail: andreas.lemmerer@wits.ac.za. Fax: +27-11-717-6749. Tel: +27-11-717-6711.

ABSTRACT:

Eight co-crystals of covalently modified isoniazid were synthesized, using either 3- or 4-hydroxybenzoic acid as the co-former. It was demonstrated that for the co-crystallization of "masked" isoniazid by benzophenone derivatives, a small change in reaction or crystallization conditions played a large role in the outcome of the resulting supramolecular structure, whereas the addition of either one or two methyl substituents to the benzophenone rings did not affect the supramolecular structure of the resulting co-crystals. Changing the reflux time for the supramolecular synthesis resulted in stoichiometric variation. Adding larger quantities of one of the starting supramolecular reagents as "additives" resulted in polymorphism. Using a catalyst for the covalent modification of isoniazid during one-pot supramolecular synthesis prevented the formation of a solvate.

KEYWORDS:

Isoniazid, Co-crystals, Supramolecular synthesis, Crystal engineering, Robust heterosynthons, Crystallization Conditions

Introduction

The influence of crystallization conditions on the synthesis of 4-aminosalicylic acid and of various forms of multicomponent crystals has been very recently published.[1] Andre' *et al.* highlighted how making changes such as changing of evaporating conditions, grinding of reagents (LAG) rather than the use of solvents, and choice of synthon results in different forms of the supramolecular products.[1]

A series of papers have been written on covalent assisted supramolecular synthesis.[2-5] Covalent assisted supramolecular synthesis can be defined as the covalent modification of a molecule with the purpose of gaining control over some aspect of the supramolecular synthesis (for example, the altering the hydrogen bonding characteristics of a functional group[3] or control over dimensionality of the packing),[5] together with the co-crystallization of the modified molecule with a co-former.

In Lemmerer *et al.*[2], it was demonstrated that the covalent modification of isoniazid with acetone and 2-butanone did not affect the supramolecular synthesis of isoniazid co-crystals, as the essential functional groups, pyridine and carboxylic acid, were not affected by the modification.

A series of covalently assisted co-crystallizations have been reported[4] showing the potential medical importance of covalent assisted molecular synthesis and showed how the physical properties of co-crystals could be manipulated through this technique, which could potentially allow for the biological activity of Active Pharmaceutical Ingredients (APIs) to be improved and modified.

Lemmerer *et al.*[3] then demonstrated that the modifiers bonded to the isoniazid could give a measure of control of the outcome of the supramolecular synthesis depending on the identity and steric size of the modifier used. It was shown that the steric size itself can be used to shield or to ''mask'' the remaining hydrogen bonding functionality of isoniazid in such a way that common hydrogen bonds and intermolecular interactions are prevented from taking place. The concept of "masked" synthons in co-crystal engineering was developed concurrently by MacGillivray *et al.*[6] where interjected water molecules were used to inhibit hydrogen bonding between the co-crystal components.

In Smith et al.,[5] isoniazid was modified with a series of benzophenone derivatives and co-crystallized with 2-hydroxybenzoic acid. The predictable "masking" of the amide functionality was achieved, and it was shown that the bulky benzophenone modifiers rendered the amide nitrogen atom inaccessible for hydrogen bonding and no short intermolecular contacts were present between the amide nitrogen atoms in "masked" isoniazid derivatives and any neighbouring isoniazid or 2-hydroxybenzoic acid atoms.

Grobelny *et al.* has synthesized two drug-drug co-crystals of isoniazid, having pyrazinamide and 4-aminosalicylic acid as co-formers. In 4-aminosalicylic acid, there are two distinct symmetry independent carboxylic acid – pyridine heterosynthons. The extent of proton transfer is dependent on the temperature, and although the first heterosynthon clearly has the characteristics of a co-crystal, the second may be more indicative of a salt.[7]

Aitipamula *et al.* reported the co-crystallization of isoniazid with succinic acid, fumaric acid, 4-hydroxybenzoic acid (*p*HBA) and nicotinamide. Co-crystallization of isoniazid with *p*HBA yielded two polymorphs of the hydrated co-crystal. Co-crystallization with fumaric acid likewise produced a novel polymorph. A ternary co-crystal of isoniazid, nicotinamide and succinic acid was also reported.[8]

Sarcevica *et al.* has reported that the use of different solvents may result in polymorphism. They have reported three co-crystals of isoniazid with cinnamic acid, as well as polymorphism in isoniazid/suberic acid, where the experimental method was changed to make use of a different solvent. A 1:1 ratio of isoniazid : cinamic acid, crystallized from a 2:1 mixture of ethanol : acetonitrile afforded two polymorphs.[9] However, a 1:1 ratio of isoniazid : cinamic acid, crystallized from a 1:1 mixture of ethyl acetate : acetonitrile resulted in a third polymorph.[10]

Mashhadi *et al.* reported the synthesis of 1:1 co-crystals of isoniazid with 3-hydroxybenzoic acid, 2,3-dihydroxybenzoic acid, 3,5-dihydroxybenzoic acid and 3,4,5-trihydroxybenzoic acid. A notable deviation from previously reported isoniazid co-crystals was the absence of the carboxylic acid – pyridine heterosynthon with the 3,5-dihydroxybenzoic acid co-former.[11]

Swapna *et al.* has noted that isoniazid undergoes degradation in fixed-dose combination drugs, and has reported co-crystals of isoniazid with vanillic acid, ferulic acid, caffeic acid and resorcinol. The synthesized co-crystals of isoniazid and vanillic acid were dimorphic. Likewise,

those of isoniazid and ferulic acid were also dimorphic, and those with caffeic acid were trimorphic. The co-crystal of isoniazid and resorcinol was the only co-crystal in their report that did not exhibit polymorphism.[12]

In this report, we have continued the systematic study of the covalent modification of isoniazid with bulky benzophenone modifiers, and have replaced the 2-hydroxybenzoic acid co-former with 3-hydroxybenzoic acid (meta-hydroxybenzoic acid or *m*HBA) and 4-hydroxybenzoic acid (para-hydroxybenzoic acid, or *p*HBA), with four co-crystal structures reported for each of these co-formers. The effect of the reaction and crystallization conditions on the resulting co-crystals of "masked" isoniazid derivatives is described. A general reaction scheme and summary of reagents used in the covalent assisted supramolecular synthesis is shown in Scheme 1.

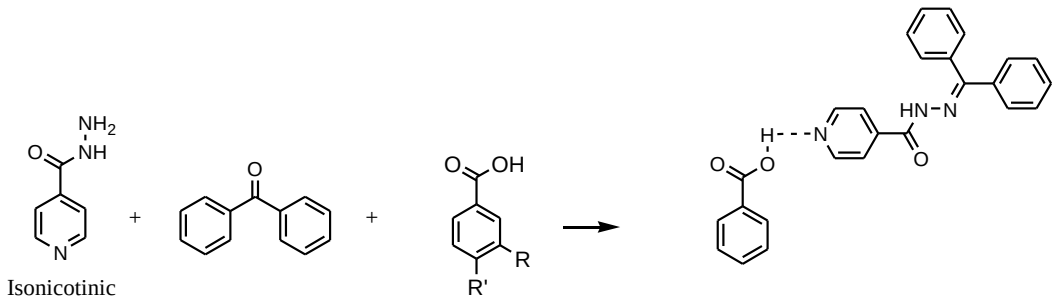

(a)

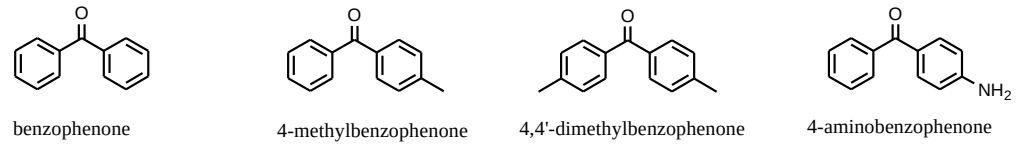

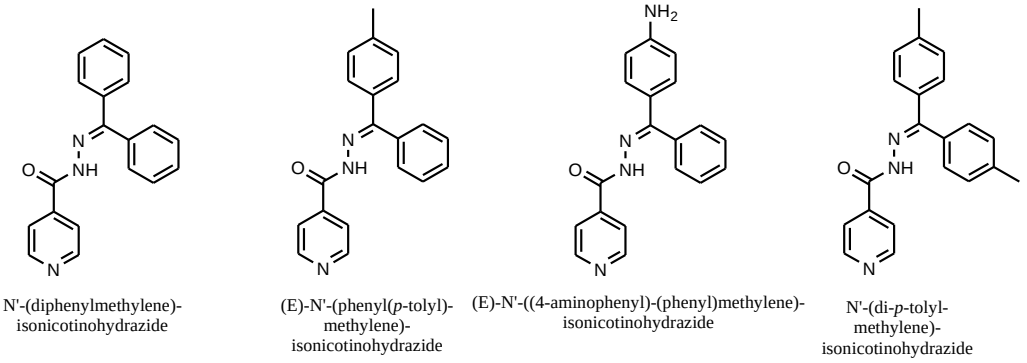

(b)

I: (N'-(diphenylmethylene)isonicotinohydrazide)$_2$·(3-hydroxybenzoic acid)*
II: (N'-(diphenylmethylene)isonicotinohydrazide)·(3-hydroxybenzoic acid)
IIIa: ((E)-N'-(phenyl(p-tolyl)methylene)isonicotinohydrazide)·(3-hydroxybenzoic acid) Form I
IIIb: ((E)-N'-(phenyl(p-tolyl)methylene)isonicotinohydrazide)·(3-hydroxybenzoic acid) Form II
IV: ((E)-N'-((4-aminophenyl)(phenyl)methylene)isonicotinohydrazide)·(4-hydroxybenzoic acid)
V: ((E)-N'-((4-aminophenyl)(phenyl)methylene)isonicotinohydrazide)·(4-hydroxybenzoic acid)·(methanol)
VI: ((E)-N'-(phenyl(p-tolyl)methylene)isonicotinohydrazide)·(4-hydroxybenzoic acid)$_2$
VII: (N'-(di-p-tolylmethylene)isonicotinohydrazide)·(4-hydroxybenzoic acid)$_2$

(c)

Scheme 1: General reaction scheme and summary of reagents used in the covalent assisted supramolecular synthesis. Part (a) shows the general reaction scheme of isoniazid with a benzophenone modifier, which results in a modified hydrazide, and co-crystallizes with a benzoic acid derivative. Part (b) shows the different benzophenone modifiers and their corresponding isonicotinohydrazide products. Part (c) is a summary of the co-crystals that were synthesized, presented here for easy reference. **IIIa** and **IIIb** are dimorphic structures. *Stucture **I** has been published in *CrystEngComm*, 2011, **13**, 5692

Experimental Methods

The covalent modification of isoniazid generally required significant heating, increased pressure and extended refluxing over several days, as isoniazid does not readily react with benzophenone and its derivatives at ambient conditions. Hearn *et al.* observed that stereo-electronic effects often make the covalent modification of isoniazid more difficult with bulky modifiers and explained that "*with alkyl modifiers larger than methyl in the ketone component of the transition state, the conformational preference for the lone pair on* N^2 *renders this nitrogen poorly poised for nucleophilic attack.*" (Hearn *et al.*, 2009). Since small volumes of solvent were typically used, the setup of a traditional reflux apparatus was not practical. As a practical alternative, glass screw-top, airtight rubber-lined dram vials were used for refluxing. The reagents and solvent were added to the vial, a magnetic stirrer bar was added and the top was tightly closed and the vial placed on a heater-stirrer. This mimicked a reflux setup on a small scale (Figure 1). It also allowed for heating to above the boiling point of the solvent, which was occasionally necessary in order for the condensation reaction to occur. The reflux could be carried out for several days in these vials at up to 120°C without any noticeable loss of solvent. Note, for safety reasons, that heating the vial to above 150°C or filling the vial more than half full caused too high a pressure and resulted in the vial bursting, and this method should therefore only be used noting these limitations. For safety reasons, an inverted beaker was placed over the sealed vials while heating at all times. Should this method be used, care should be taken to prevent injury in the case of the vial bursting.

Figure 1: (a) The glass screw-top rubber-lined dram vials used for refluxing. The vials have a rubberized seal and can boil without significant loss of solvent. (b) When refluxing in the closed vial, solvent evaporates and flows back down the side of the vial.

Synthesis:

I: (*N'*-(diphenylmethylene)isonicotinohydrazide)$_2$·(3-hydroxybenzoic acid),

The method for the synthesis of this compound is published in *CrystEngComm.* (2011). **13**, 5692 and is reproduced here: "0.200 g of isonicotinic acid hydrazide (1.46 mmol), 0.213 g of 3-hydroxybenzoic acid (1.54 mmol) and 0.266 g of benzophenone (1.46 mmol) were added into a sample vial. The solids were dissolved in AP-grade hot methanol (5 ml), refluxed for 3 hours at in a closed vial, and left to stand at room temperature open to the atmosphere. Colourless plates were afforded after 7 days.

II: (*N'*-(diphenylmethylene)isonicotinohydrazide)·(3-hydroxybenzoic acid),

0.1057 g of isonicotinic acid hydrazide (0.7709 mmol), 0.1420 g of benzophenone (0.7793 mmol) and 0.1076 g of 3-hydroxybenzoic acid (0.7790 mmol) were added into a sample vial. The solids were dissolved in AP-grade methanol (3 mL), refluxed in a closed vial for 72 hours at

70°C, and were left to stand at room temperature open to the atmosphere. Colourless blocks were afforded after 7 days.

IIIa: ((*E*)-*N*'-(phenyl(*p*-tolyl)methylene)isonicotinohydrazide)·(3-hydroxybenzoic acid) Form I,

0.1050 g of isonicotinic acid hydrazide (0.7658 mmol), 0.1598 g of 4-methylbenzophenone (0.8143 mmol) and 0.1059 g of 3-hydroxybenzoic acid (0.7666 mmol) were added into a sample vial. The solids were dissolved in AP-grade methanol (10 mL), refluxed in a closed vial for 24 hours at 70°C, and were left to stand at room temperature open to the atmosphere. Colourless plates were afforded after 7 days.

IIIb: ((*E*)-*N*'-(phenyl(*p*-tolyl)methylene)isonicotinohydrazide)·(3-hydroxybenzoic acid) Form II 0.0937 g of isonicotinic acid hydrazide (0.683 mmol), 0.1352 g of 4-methylbenzophenone (0.6889 mmol) and 0.1539 g of 3-hydroxybenzoic acid (1.1142 mmol) were added into a sample vial. The solids were dissolved in AP-grade methanol (10 mL), refluxed in a closed vial for 24 hours at 70°C, and were left to stand at room temperature open to the atmosphere. Colourless plates were afforded after 7 days.

IV: ((*E*)-*N'*-((4-aminophenyl)(phenyl)methylene)isonicotinohydrazide)·(4-hydroxybenzoic acid)

0.1008 g of isonicotinic acid hydrazide (0.7351 mmol), 0.1370 g of 4-aminobenzophenone (0.6946 mmol) and 0.1020 g of 4-hydroxybenzoic acid (0.7384 mmol) were added into a sample vial. 1 drop of concentrated HCl was added to catalyze the condensation reaction of isonicotinic acid hydrazide and 4-aminobenzophenone. The solids were dissolved in AP-grade methanol (10 mL), refluxed in a closed vial for 72 hours at 110°C, followed by work-up with sodium bicarbonate: the solution was saturated with sodium bicarbonate, stirred for 5 minutes and then filtered. The filtered solution was then left to stand at room temperature open to the atmosphere. Clear plates were afforded after 7 days.

V: ((*E*)-*N'*-((4-aminophenyl)(phenyl)methylene)isonicotinohydrazide)·(4-hydroxybenzoic acid)· (methanol)

0.0967 g of isonicotinic acid hydrazide (0.705 mmol), 0.0974 g of 4-aminobenzophenone (0.705 mmol) and 0.0973 g of 4-hydroxybenzoic acid (0.704 mmol) were added into a sample vial. The solids were dissolved in AP-grade methanol (10 mL), refluxed in a closed vial for 24 hours at 110°C, and were left to stand at room temperature open to the atmosphere. Yellow plates were afforded after 7 days.

VI: ((*E*)-*N'*-(phenyl(*p*-tolyl)methylene)isonicotinohydrazide)·(4-hydroxybenzoic acid)$_2$

0.0866 g of isonicotinic acid hydrazide (0.632 mmol), 0.1239 g of 4-methylbenzophenone (0.6313 mmol) and 0.1740 g of 4-hydroxybenzoic acid (1.260 mmol) were added into a sample vial. The solids were dissolved in AP-grade methanol (10 mL), refluxed in a closed vial for 5 days at 110°C, and were left to stand at room temperature open to the atmosphere. Colourless blocks were afforded after 7 days.

VII: (N'-(di-*p*-tolylmethylene)isonicotinohydrazide)·(4-hydroxybenzoic acid)$_2$

0.0989 g of isonicotinic acid hydrazide (0.721 mmol), 0.1520 g of 4,4'-dimethylbenzophenone (0.7228 mmol) and 0.2038 g of 4-hydroxybenzoic acid (1.4755 mmol) were added into a sample vial. The solids were dissolved in AP-grade methanol (10 mL), refluxed in a closed vial for 24 hours at 110°C, and were left to stand at room temperature open to the atmosphere. Colourless blocks were afforded after 7 days.

Crystal Data and X-ray Structure Analysis.

The intensity data for the new crystal structures reported here (**II – VII**) were collected on a Bruker APEX II CCD area detector diffractometer with graphite monochromated Mo-K_α radiation (50 kV, 30 mA) at -100°C. The collection method involved ω-scans with a 0.5° width. *SAINT+* version 6.02.6 software was used for data reduction and *SADABS* was used to make empirical absorption corrections.[13] The crystal structures were solved using direct methods on *SHELXS-97*.[14] Non-hydrogen atoms were first refined isotropically, followed by anisotropic refinement by full matrix least-squares calculations based on F^2 using *SHELXL-2017*.[14] C-bound H atoms were located in the difference electron density map, then positioned geometrically and were allowed to ride on their respective parent atoms, with thermal displacement parameters 1.2 times that of the parent C atom. Where possible, the coordinates and isotropic displacement parameters of the N-bound and O-bound H atoms involved in hydrogen bonding interactions were allowed to refine freely, except for co-crystal **IIIb** to poor refinement stability. The diffraction data and refinement statistics of co-crystal **IIIb** was poor even after numerous attempts at recrystallization. Diagrams and publication material were generated using *WinGX*,[15] *ORTEP-3*,[15] *PLATON*[16] and *MERCURY*[17]. The crystallographic data of each co-crystal is summarized in Table 1.

Table 1 Crystallographic data for compounds **I-VII**

	I*	**II**	**IIIa**	**IIIb**
Formula	$(C_{19}H_{15}N_3O)_2\cdot$ $(C_7H_6O_3)$	$(C_{19}H_{15}N_3O)\cdot$ $(C_7H_6O_3)$	$(C_{20}H_{17}N_3O)\cdot$ $(C_7H_6O_3)$	$(C_{20}H_{17}N_3O)\cdot$ $(C_7H_6O_3)$
M_r	740.80	439.46	453.48	453.48
Temperature/K	173(2)	173(2)	173(2)	173(2)
Wavelength/Å	1.5418	0.71073	0.71073	0.71073
Crystal size/mm^3	0.42×0.33×0.20	0.09×0.32×0.34	0.07×0.15×0.59	0.08×0.15×0.26
Crystal system	Triclinic	Triclinic	Triclinic	Triclinic
Space group	$P\bar{1}$	$P\bar{1}$	$P\bar{1}$	$P\bar{1}$
a/Å	9.8338(9)	6.8909(2)	7.0137(3)	7.2172(10)
b/Å	10.2475(9)	10.5354(3)	10.5797(6)	11.5224(16)
c/Å	10.8863(10)	15.3153(4)	15.5605(8)	15.070(2)
α/°	104.295(8)	89.916(2)	90.635(3)	110.481(7)
β/°	112.784(8)	83.7670(10)	94.052(3)	97.188(7)
γ/°	103.370(8)	85.9270(10)	93.174(3)	95.826(7)
V/Å^3	912.17(14)	1102.48(5)	1149.85(10)	1150.4(3)
Z	1	2	2	2
ρ (calcd)/Mg m^{-3}	1.350	1.324	1.310	1.309
μ/mm^{-1}	0.727	0.091	0.089	0.089
F(000)	389	460	476	476
Θ Range for data collection/°	4.75 to 62.65	1.938 to 28.000	2.316 to 25.498	1.464 to 25.499
Reflections collected	4365	20075	11166	10843
No. of unique data [R(int)]	2793 [0.0202]	5320 [0.0588]	4189 [0.0606]	4199 [0.0944]
No. data with $I \geq 2\sigma(I)$	2516	4244	2771	1678
Final R($I > 2\sigma(I)$)	0.0568	0.0418	0.0652	0.1041
Final wR_2 (all data)	0.1618	0.1121	0.1785	0.1739
CCDC deposition number	SAYPEP	1810898	1810897	1810899

*_CrystEngComm_, 2011, **13**, 5692

	IV	**V**	**VI**	**VII**
Formula	$(C_{19}H_{16}N_4O)\cdot(C_7H_6O_3)$	$(C_{19}H_{16}N_4O)\cdot(C_7H_6O_3)\cdot(CH_4O)$	$(C_{20}H_{17}N_3O)\cdot(C_7H_6O_3)_2$	$(C_{21}H_{19}N_3O)\cdot(C_7H_6O_3)_2$
M_r	454.47	486.52	591.60	605.63
Temperature/K	173(2)	173(2)	173(2)	173(2)
Wavelength/Å	0.71073	0.71073	0.71073	0.71073
Crystal size/mm^3	0.10×0.22×0.24	0.11×0.19×0.56	0.06×0.15×0.20	0.12×0.15×0.25
Crystal system	Triclinic	Triclinic	Triclinic	Triclinic
Space group	$P\bar{1}$	$P\bar{1}$	$P\bar{1}$	$P\bar{1}$
a/Å	8.3764(5)	8.8944(2)	8.8777(3)	9.0790(3)
b/Å	8.8620(6)	10.8401(3)	13.2137(5)	13.2861(5)
c/Å	16.1081(10)	13.3606(3)	13.9693(4)	14.0354(5)
α/°	75.315(3)	70.5460(10)	112.474(2)	114.298(2)
β/°	76.160(3)	81.4800(10)	102.586(2)	103.514(2)
γ/°	73.677(3)	79.6840(10)	91.773(2)	90.060(2)
V/Å^3	1091.73(12)	1189.55(5)	1465.95(9)	1491.27(9)
Z	2	2	2	2
ρ (calcd)/Mg m^{-3}	1.383	1.358	1.340	1.349
μ/mm^{-1}	0.095	0.093	0.095	0.095
F(000)	476	512	620	636
Θ Range for data collection/°	1.329 to 25.498	1.624 to 27.998	1.681 to 25.496	1.647 to 25.498
Reflections collected	12420	24184	19566	23071
No. of unique data [R(int)]	4063 [0.0805]	5753 [0.0410]	5452 [0.0762]	5530 [0.0597]
No. data with $I \geq 2\sigma(I)$	2366	4483	2364	3183
Final R($I > 2\sigma(I)$)	0.0519	0.0414	0.0598	0.0647
Final wR_2 (all data)	0.1434	0.1113	0.1820	0.1937
CCDC deposition number	1810900	1810901	1810902	1810903

Table 2 A summary of the angles between the planes of three rings of modified isoniazid and the co-former. A general scheme of the ring numbering is shown in the diagram included in the table.

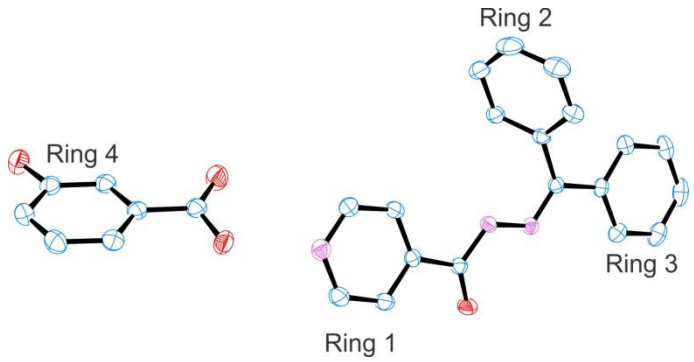

Angle between Rings (°)	Rings 1,2	Rings 1,3	Rings 1,4	Rings 2,3	Rings 2,4	Rings 3,4
I	72.7	13.3	0.9	82.94	71.9	14.2
II	70.28	1.55	61.63	69.5	83.52	63.15
IIIa	70.90	0.37	62.14	70.69	82.41	62.49
IIIb	76.35	14.24	85.41	73.79	29.33	86.32
IV	71.79	44.40	23.55	71.41	54.31	58.84
V	84.18	7.53	6.64	88.30	78.69	9.94
VI*	56.8	42.06	37.5	80.0	76.6	4.63
VII*	64.24	34.27	32.1	82.39	80.36	2.40

- The angles for the second *p*HBA molecule in **VI** and **VII** is not shown on the table. For **VI**, the angle between the plane of the two *p*HBA molecules is 46.79°, and for **VII**, 48.55°.

Table 3 Hydrogen bonding details of compounds **I - VII**

	d(D─H)/Å	*d*(H···A)/Å	*d*(D···A)/Å	∠(D─H···A)/°
I				
O1-H1···N1	0.85(3)	1.89(3)	2.745(3)	178(3)
C10A-H10A···O2	0.95	2.84	3.498(12)	127
II				
O2-H2···N2	1.01(3)	1.59(3)	2.6008(13)	176(2)
O4-H4···O3[a]	0.87(2)	1.88(2)	2.7517(15)	171(2)
IIIa				
O2-H2···N2	0.84	1.78	2.613(3)	173
O4-H4···O3[b]	0.84	1.94	2.775(3)	178
IIIb				
N1-H1···O3[c]	0.88	2.08	2.840(4)	145
O2-H2···O1[d]	0.84	1.86	2.665(3)	159
O4-H4···N2	0.84	1.92	2.758(4)	179
IV				
O2-H2···N2	0.98(3)	1.74(3)	2.722(3)	178(3)
O4-H4···N4[e]	0.96(3)	1.87(3)	2.786(3)	160(3)
N4-H4A···O3[f]	0.97(3)	1.97(3)	2.926(3)	172(3)
N4-H4B···O1[g]	0.98(3)	1.98(3)	2.929(3)	164(2)
V				
N4-H4A···O1[h]	0.92(2)	2.12(2)	3.0060(16)	163(2)
N4-H4B···O4[i]	0.901(18)	2.407(18)	3.2621(17)	159(2)
O2-H2···N2	1.01(2)	1.63(2)	2.6352(14)	178(2)
O4-H4···O5	0.93(2)	1.76(2)	2.6665(17)	163(2)
O5-H5···O3[j]	0.88(2)	1.93(2)	2.8082(16)	174(2)
VI				
O2-H2···N2	0.82	1.82	2.640(4)	174
O4-H4···O1[k]	0.77(4)	1.98(4)	2.751(4)	177(5)
O5-H5···O6[l]	1.00(5)	1.63(5)	2.628(3)	173(5)
O7-H7···O3	0.77(3)	1.92(3)	2.669(4)	163(4)
VII				
O2-H2···N2	0.84	1.80	2.639(3)	173
O4-H4···O1[m]	0.90(5)	1.89(5)	2.757(4)	161(5)
O5-H5···O6[n]	0.84	1.81	2.652(3)	177
O7-H7···O3	0.90(4)	1.79(4)	2.674(4)	170(4)

[a]-x, -y + 1, -z + 1. [b]-x - 1, -y, -z + 2, [c]x + 1, -y + 1, -z. [d]x, y, z - 1. [e]x + 2, y + 1, z + 1. [f] –x + 2, -y + 1, -z + 1. [g]-x + 3, -y, -z + 1. [h]-x - 1, -y, -z + 2. [i]x - 2, y-1, z. [j]-x + 2, -y + 1, -z + 1. [k]x - 1, y, z - 1. [l]-x + 1, -y, -z + 1. [m]x - 1, y, z - 1. [n] –x + 1, -y, -z + 1.

Results

The steps of a supramolecular synthetic process are discreet and the crystallization process is independent of the assembly of the supramolecular structure in situ.[18] In this study eight co-crystals were synthesized using one-pot synthetic methods (Figure 2). In all eight co-crystals reported, the same solvent (methanol) was used throughout and the method of crystallization was kept identical (slow evaporation method at room temperature over a seven day period). We here describe how simply changing only the synthetic method resulted in polymorphism, stoichiometric variation, a solvate vs non-solvate, change in dimensionality of packing, and bonding through differing heterosynthons in "masked" isoniazid derivatives. Four modified isoniazids were co-crystallized with 3-hydroxybenzoic acid and four with 4-hydroxybenzoic acid. As we were interested in the effect of changes in the synthetic method on the results of co-crystallization, the eight co-crystals were divided in to pairs, where the synthetic method for each pair was kept the same, except for one substantial change in the synthetic method having been applied to each pair. For the first pair of co-crystals (**I** and **II**), the refluxing time of the reagents was changed. For the second pair (**IIIa** and **IIIb**), the stoichiometric ratio of the reagents was changed. For the third pair (**IV** and **V**), the reaction was carried out in the presence and absence of a catalyst respectively, and for the fourth pair (**VI** and **VII)** a methyl group was added to one of the aromatic rings.

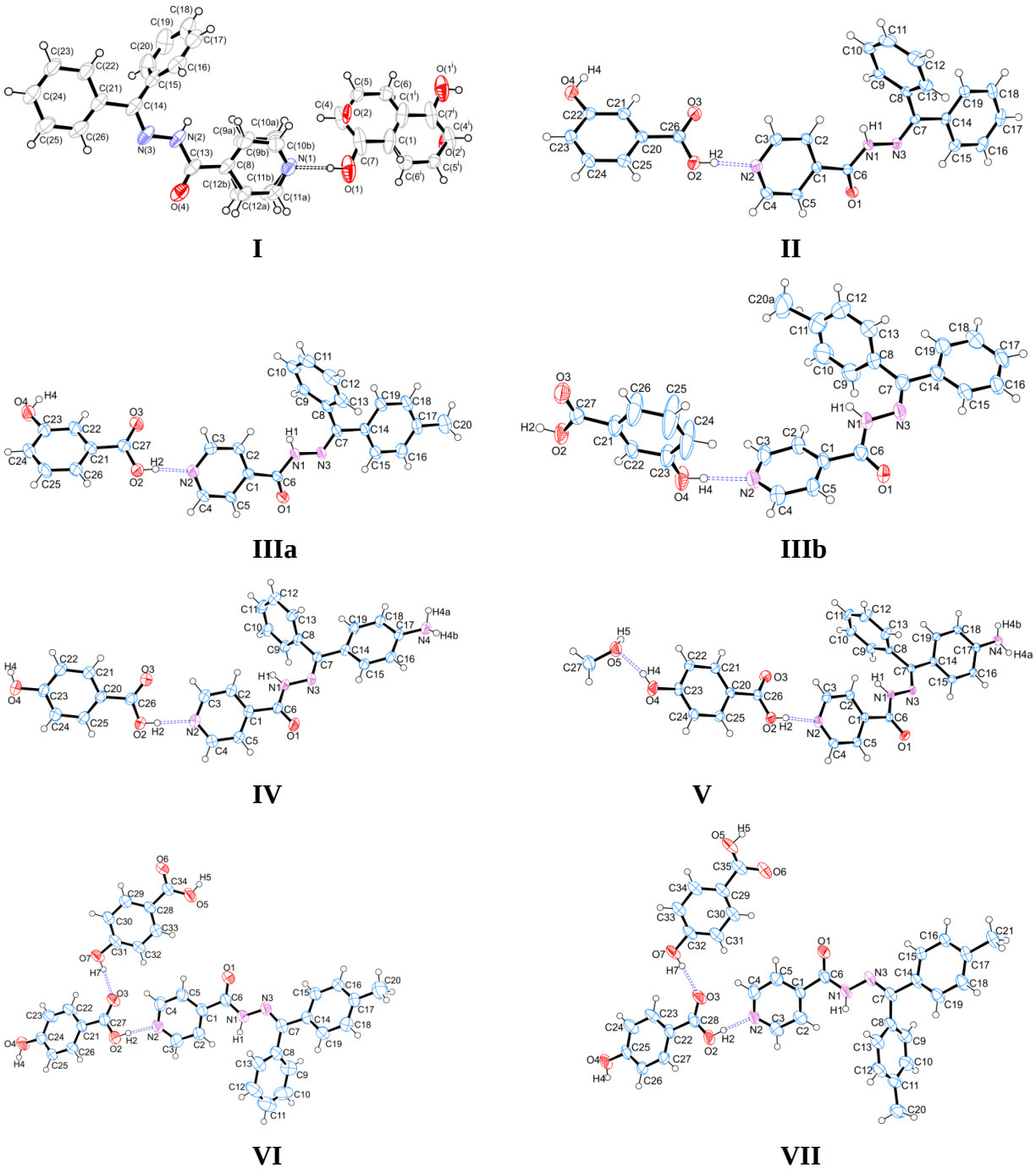

Figure 2: Asymmetric units of co-crystals **I** - **VII**, showing the atomic numbering scheme for each co-crystal. *Stucture I was previously published in *CrystEngComm.* (2011). **13**, 5692

Change in reflux time of one-pot synthesis

In co-crystals **I** and **II,** isoniazid has been modified with benzophenone and co-crystallized with *m*HBA. For both **I** and **II**, a 1:1:1 ratio of isoniazid : benzophenone : *m*HBA were dissolved in methanol. The reagents for **I** were reluxed for 3 hours and for **II** were refluxed for 72 hours. Both were then allowed to crystallize out for 7 days by slow evaporation. Therefore, the only substantial change to the synthetic method was the change in reflux time. The result was the formation of two co-crystals, **I** and **II**, having different stoichiometric ratios.

The structure of **I** has been described in *CrystEngComm.* (2011). **13**, 5692. A summary of the results is reported here for comparison purposes. Compound **I** crystallizes in the $P\bar{1}$ space group. The asymmetric unit of **I** contains one modified isoniazid molecule and one half *m*HBA acid molecule (**Figure 2**). The *m*HBA acid molecule crystallizes with static disorder around a centre of inversion (**Figure 3**). The carboxylic acid group and four carbon atoms of the aromatic ring of *m*HBA are found in the asymetric unit. The carboxylic acid functions as both the alcohol group as well as the carboxylic acid group. The two missing C atoms of the aromatic ring are generated by the O2 atom and the C7 atom of the carboxylic acid functional group. The *m*HBA molecule therefore exists in two different arrangements in between the modified isoniazid molecules, shown in Figure 3a and 3b.

Compound **II** crystallizes in the $P\bar{1}$ space group and the asymmetric unit contains one modified isoniazid molecule and one *m*HBA molecule (Figure 2). The hydrogen bonding in the asymmetric unit is via the typical expected robust COOH···N_{pyr} heterosynthon reported in literature, namely via O2—H2···N2.[19] Also, as expected from literature, the amide group is rendered inaccessible to any hydrogen bond acceptors of neighbouring isoniazid or *m*HBA molecules by the steric effects of the bulky benzophenone group.[5] Each modified isoniazid molecule is hydrogen bonded by a single O2—H2···N2 hydrogen bond to a *m*HBA molecule. Each *m*HBA is also hydrogen bonded via its phenol O—H donor to the carbonyl oxygen acceptor of the COOH functional group of an adjacent *m*HBA molecule, thus forming an $R_2^2(14)$ ring in graph-set notation.[20] (Figure 4a). All the hydrogen bonding interactions in **II** occur within the asymmetric unit to form zero-dimensional (0D) hydrogen bonded heteromolecular entities.

The pyridine ring of the modified isoniazid is essentially coplanar with one ring of the benzophenone, with an angle between the planes of 1.55°, and the packing is thus stabilized by π-stacking along the *a*-axis (Figure 4b).

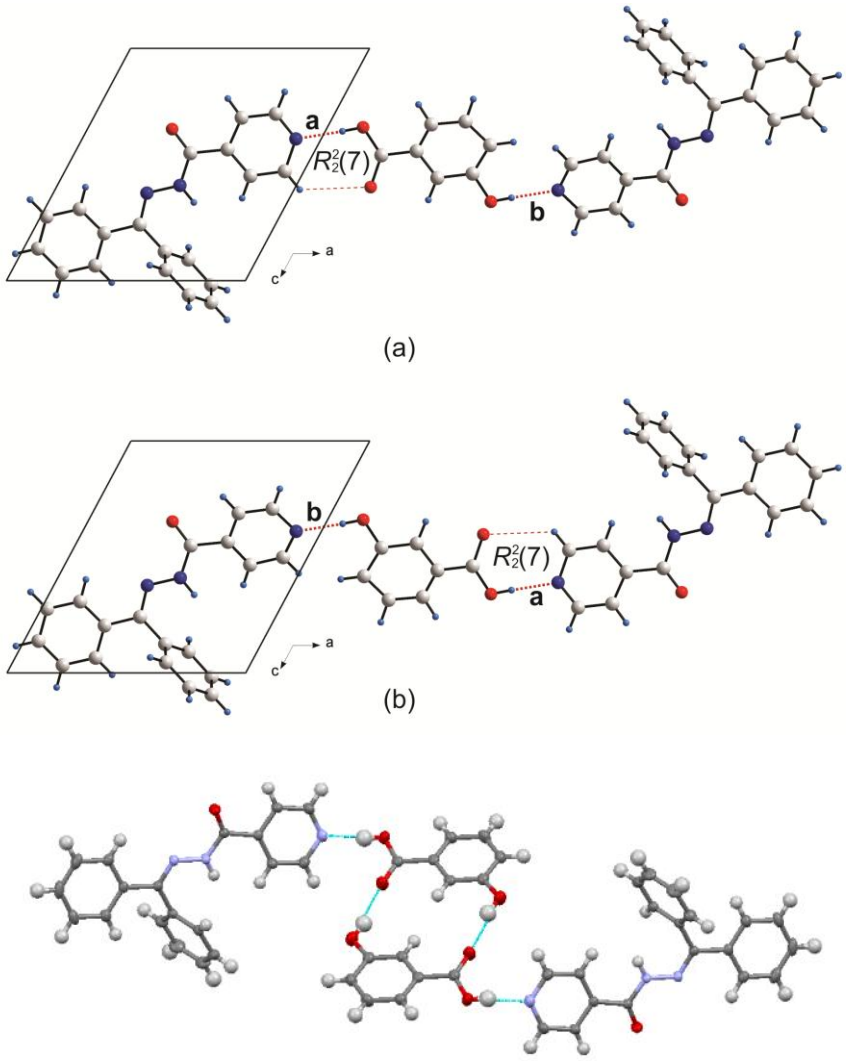

Figure 3: Disordered hydrogen bonding of **I,** and hydrogen bonding of **II.**

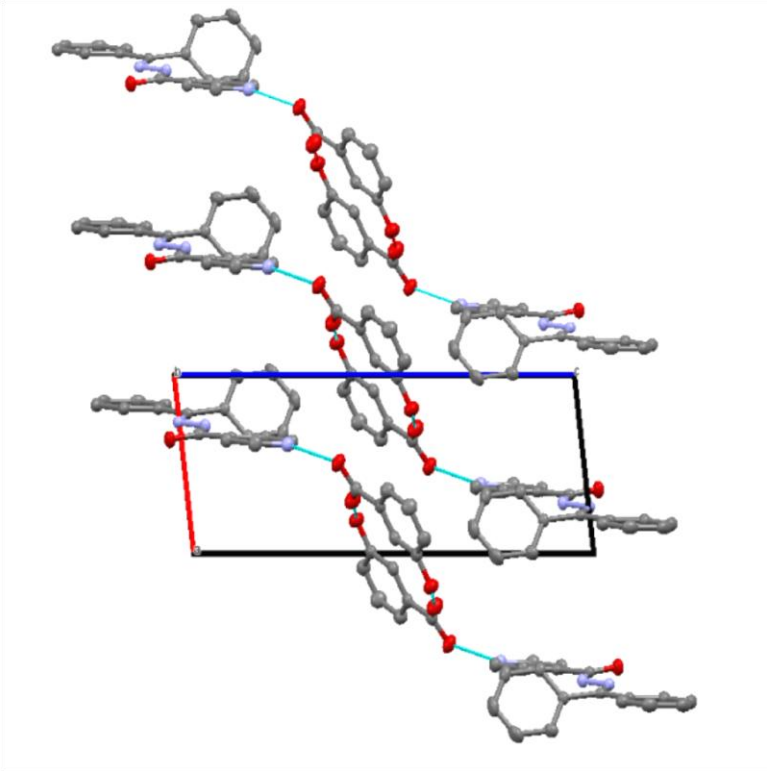

(a)

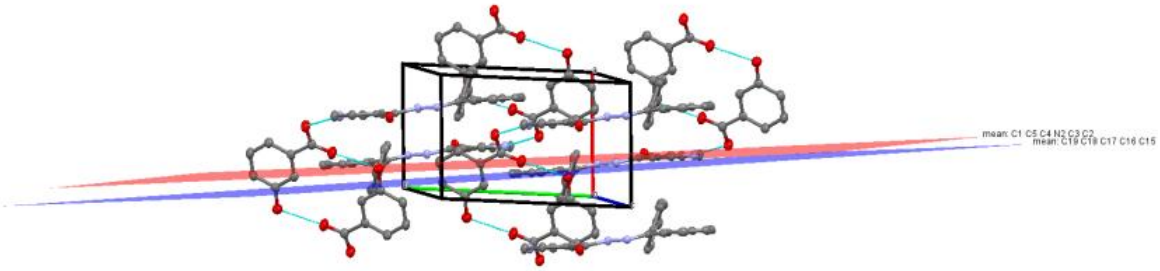

(b)

Figure 4: Part (a) shows the packing of **II.** (b) shows the planes of the pyridine ring and one of the benzophenone rings, which are essentially parallel and therefore suitable for π-stacking interactions along the *a*-axis.

Change in stoichiometry of reagents

In co-crystals **IIIa** and **IIIb,** isoniazid was modified with 4-methylbenzophenone and co-crystallized with *m*HBA. For **IIIa**, the ratio of isoniazid : 4-methylbenzophenone : *m*HBA used in the one-pot synthesis was 1:1:1, but for **IIIb**, a 1:1:1.6 ratio was used, with all other reaction and crystallizing conditions remaining the same. The result was the formation of two polymorphs, **IIIa** and **IIIb**, having very different hydrogen bonding and packing arrangements from each other.

Compound **IIIa** crystallizes in the $P\bar{1}$ space group and contains one isoniazid molecule modified with 4-methylbenzophenone and one *m*HBA molecule. The hydrogen bonding in the asymmetric unit is via the COOH···N_{pyr} heterosynthon (Figure 2). The methyl group on the benzophenone moiety is directed away from the sites of any intermolecular interactions and does not therefore interfere with the π-stacking interactions along the *a*-axis found in **II**, and therefore, the hydrogen bonding and packing arrangement in **IIIa** remains essentially isostructural to co-crystal **II,** despite the presence of the extra methyl group (Figure 5). A comparison of the angles between the four rings (Table 2) confirms the isostructural packing as the difference in all angles is negligible. The hydrogen bonding interactions within the packing form zero-dimensional (0D) hydrogen bonded heteromolecular entities. The pyridine ring is coplanar with the methylated ring of the 4-methylbenzophenone, with the acute angle between the planes in **III**a being 0.37°, and the packing is thus stabilized by π-stacking of the pyridine and 4-methylated ring of the modified isoniazid along the *a*-axis.

Compound **IIIb** crystallizes in the $P\bar{1}$ space group and the asymmetric unit contains one isoniazid molecule modified with 4-methylbenzophenone and one *m*HBA molecule (Figure 2). The hydrogen bonding arrangement is unusual as the *m*HBA hydrogen bonds to the pyridine ring via its phenol hydrogen (H4) rather than through the expected COOH···N_{pyr} heterosynthon. The 4-methylbenzophenone moiety is disordered, with the methyl group being found on either aromatic ring of the 4-methylbenzophenone. **IIIb** packs in one dimensional (1D) tubes along the *c*-axis (Figure 6a). The geometrical shape of the tubes are almost square, with the "walls" of the tube being formed by two modified isoniazid molecules and two *m*HBA molecules. with the

plane of the pyridine ring of the modified isoniazid being almost normal to the plane of the mBA with an acute angle of 85.41° between the planes. These "walls" are held together by an $R_4^4(16)$ ring, where the *m*HBA carboxylic acid group acts as the hydrogen bond donor (H2) to the modified isoniazid carbonyl acceptor (O1). The amide hydrogen of the modified isoniazid provides the other hydrogen bond donor (H1A) with the carbonyl carbon of the *m*HBA carboxylic acid group being the acceptor. This is highly unusual as the amide hydrogen is usually masked from intermolecular interactions by the steric effects of the benzophenone modifier. To date, this is the only reported structure of isoniazid which has been modified with a benzophenone modifier where the amide hydrogen is not masked. This unusual interaction occurs because the small size and planar geometry of the *m*HBA allows the *m*HBA to align itself in a plane which is fairly well aligned to the plane of the strerically blocking benzophenone ring with an acute angle of 29.33° between the two planes. This allows the *m*HBA to "sneak in" between the pyridine ring and the benzophenone ring and hydrogen bond to the amide hydrogen atom (Figure 6b).

In co-crystal **IIIb**, there is therefore a marked deviation in the hydrogen bonding and packing arrangements of the co-crystal from the patterns expected from literature. It has been demonstrated that the presence of additives during a crystallization process will invariably affect the morphology and crystal structure during crystallization.[21,22] The frequent variation found in crystal morphology and structure as a result of changes in stoichiometry of the reagents during crystallization may be understood if one considers an excess of one of the reagents as an additive. In this sense, the change of ratio of isoniazid : 4-methylbenzophenone : *m*HBA from 1:1:1 in **IIIa** to 1:1:1.6 in **IIIb** should be seen as the addition of a mole ratio of 0.6 *m*HBA as an additive, and if one considers the profound impact of additives on crystal structure as decribed by Lahav[21,22] then the large variation in crystal structure between **IIIa** and **IIIb** is therefore not unexpected. Changing the reagent stoichimetry during co-crystallization could thus be a rich source of polymorphs and certainly warrants further investigation.

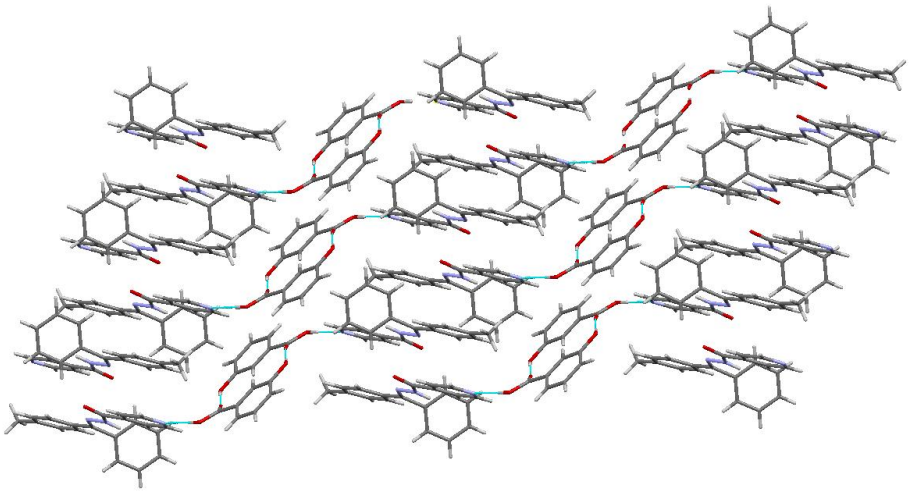

Figure 5: Packing diagram of **IIIa**, which is isostructural to the packing of **II**.

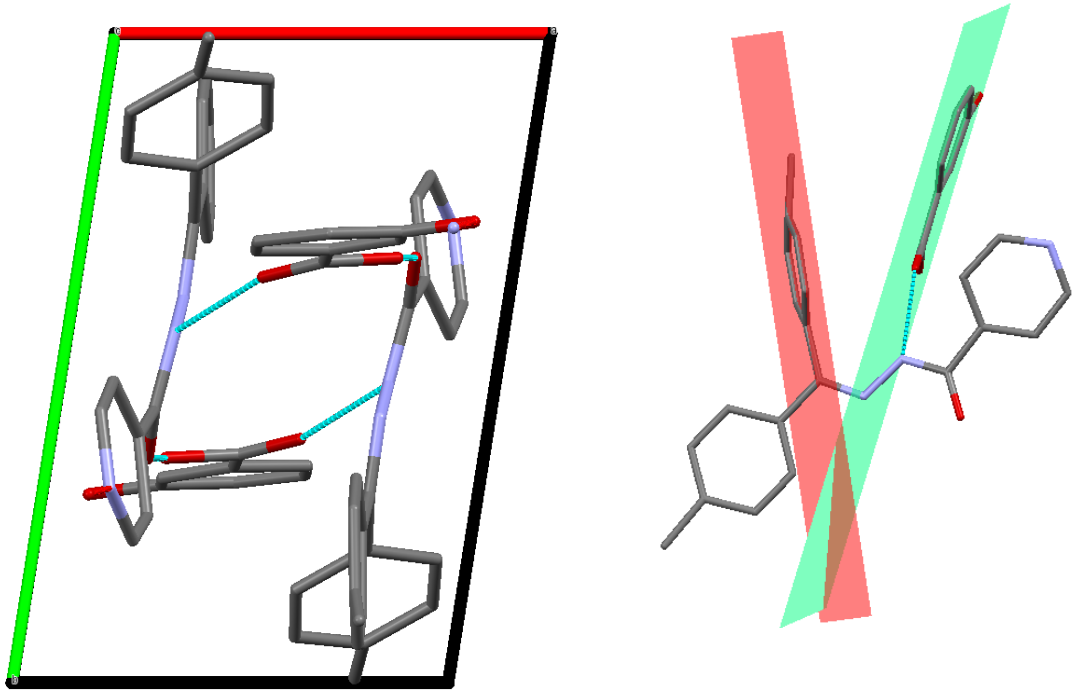

(a) (b)

Figure 6: Packing of **IIIb**. Part (a) shows the almost square tube formed along the *c*-axis with an angle of 85.41° between the plane of the modified isoniazid pyridine ring and the *m*HBA plane. Part (b) shows the orientation of the *m*HBA molecule relative to the sterically hindering benzophenone ring, allowing the *m*HBA molecule to "sneak in" between the pyridine ring and benzophenone ring to hydrogen bond to the amide hydrogen atom.

Presence or absence of a catalyst in the covalent modification of Isoniazid during one-pot synthesis

In co-crystals **IV** and **V,** isoniazid was modified with 4-aminobenzophenone, and co-crystallized with *p*HBA. The ratio of isoniazid : 4-aminobenzophenone : *p*HBA used in the one-pot synthesis was 1:1:1. A drop of concentrated HCl was added to the reaction solution of **IV** to catalyze the condensation reaction of isonicotinic acid hydrazide and 4-aminobenzophenone followed by work-up with sodium bicarbonate and filtration. **V** was allowed to react without the catalyst. All other reaction and crystallizing conditions remaining the same. Therefore, the only substantial change to the synthetic method of the two co-crystals was the use of a catalyst in **IV**, and the absence thereof in **V**. The presence of the catalyst in **IV** prevented the formation of a solvate, whereas in co-crystal **V**, the solvate was formed.

Compound **IV** crystallizes in the $P\bar{1}$ space group. The asymmetric unit contains one modified isoniazid molecule and one *p*HBA molecule. In the asymmetric unit, the modified isoniazid is hydrogen bonded to the *p*HBA molecule via an COOH···N_{pyr} heterosynthon. Co-crystal **IV** packs in a three dimensional (3D) network with extensive hydrogen bonding. Apart from the amide funcional group of the modified isoniazid, which is effectively masked by the steric effects of the benzophenone modifier, every potential hydrogen bonding atom on the modified isoniazid, as well as every potential hydrogen bonding atom on the *p*HBA is involved in hydrogen bonding. Each modified isoniazid molecule is hydrogen bonded to five different molecules. Three of its atoms act as hydrogen bond acceptors: 1) the pyridine nitrogen (N1) is hydrogen bonded to the carboxylic acid group donor (H2) of a *p*HBA molecule via the robust COOH···N_{pyr} heterosynthon. 2) its amine nitrogen to the phenol hydrogen (H4) of *p*HBA. 3) its carbonyl oxygen (O1) to one of the amine hydrogens (H4B) of an adjacent modified isoniazid molecule. Both amine hydrogens act as hydrogen bond donors: 1) H4A hydrogen bonds to the carbonyl oxygen of the carboxylic acid group of a pHBA molecule. 2) H4B to the carbonyl of a modified isoniazid (Figure 7). Each pHBA is hydrogen bonded to three modified isoniazid molecules via O3, H2 and H4 in the synthons described in the hydrogen bonding description of the modified isoniazid above.

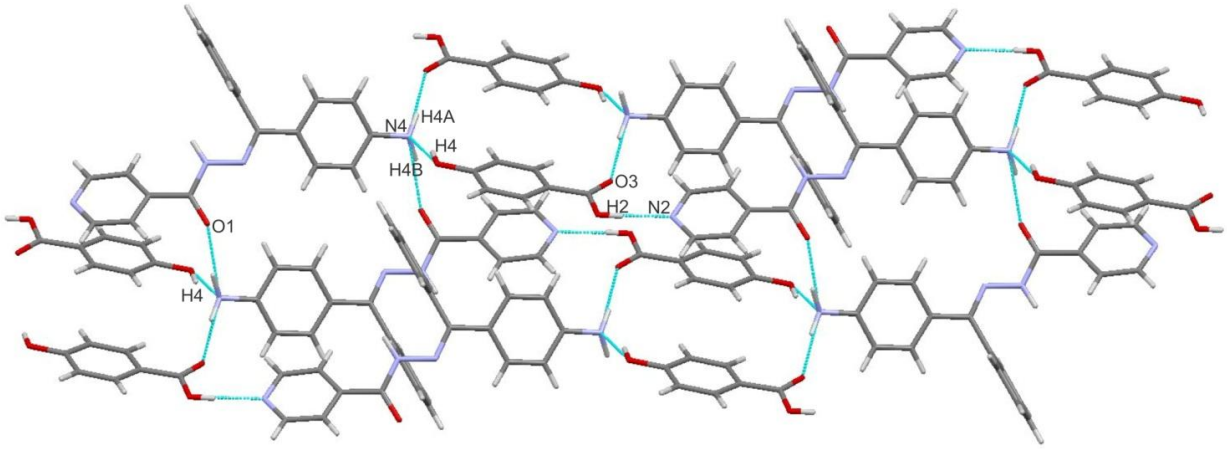

Figure 7: Packing diagram of **IV** showing the extensive hydrogen bonded 3D network. Apart from the amide functional group, which is masked by the benzophenone ring, every potential hydrogen bonding atom in the modified isoniazid, as well as in *p*HBA, is involved in hydrogen bonding.

Compound **V** crystallizes in the $P\bar{1}$ space group. The asymmetric unit contains one modified isoniazid molecule, one *p*HBA molecule and one methanol molecule (a solvate of **IV**). The modified isoniazid is hydrogen bonded to the *p*HBA molecule via an COOH$\cdots$N$_{pyr}$ heterosynthon. The *p*HBA phenol hydrogen donor atom (H4) is hydrogen bonded to the methanol oxygen atom (O5). Co-crystal **V** packs in a one dimensional (1D) ribbon. Each modified isoniazid forms a dimer with another modified isoniazid molecule where the carbonyl of one molecule is hydrogen bonded to an amine hydrogen of another, forming an an $R_2^2(22)$ ring. Unlike co-crystal **IV**, only one of the amine hydrogens is involved in hydrogen bonding. There is a centre of inversion about the centre of the ring. A tetramer, consisting of two *p*HBA and two methanol molecules is also formed, with *p*HBA and methanol alternating. The methanol hydroxyl hydrogen is hydrogen bonded to the carbonyl oxygen of the carboxylic acid group of *p*HBA and the methanol oxygen is hydrogen bonded to the phenol hydrogen of another *p*HBA molecule to form an $R_4^4(20)$ ring with a centre of inversion in the centre of the ring. Each modified isoniazid dimer is connected to a *p*HBA tetramer through an COOH$\cdots$N$_{pyr}$ heterosynthon (Figure 8).

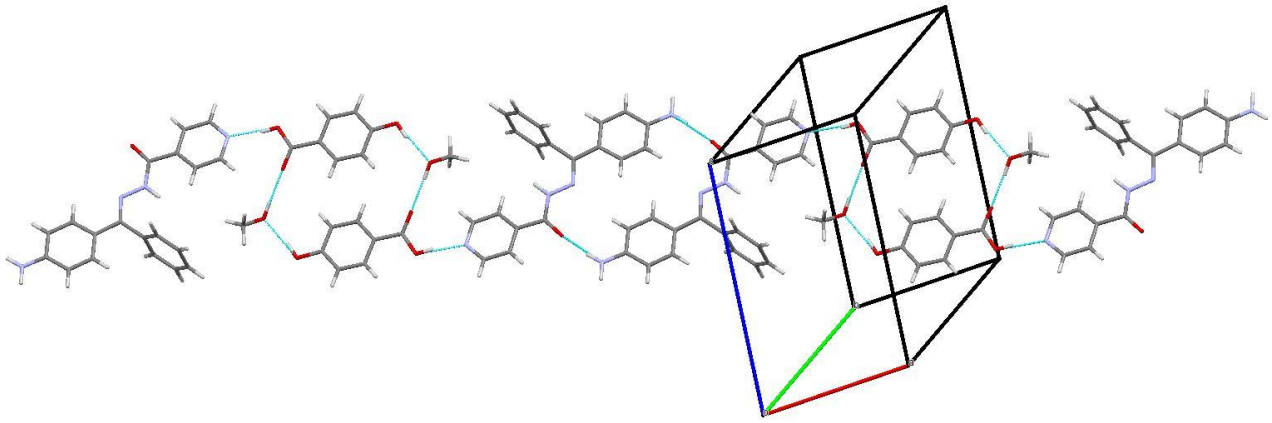

Figure 8: Packing diagram of **V** showing the 1D ribbon. Apart from the amide functional group, which is masked by the benzophenone ring, every potential hydrogen bonding atom in the modified isoniazid, as well as in *p*HBA, is involved in hydrogen bonding.

Addition of substituent to benzophenone ring

In co-crystals **VI** and **VII,** isoniazid was modified with 4-methylbenzophenone and 4,4'-dimethylbenzophenone respectively, and co-crystallized with *p*HBA. For **VI** and **VII**, the ratio of isoniazid : 4-methylbenzophenone / 4,4'-dimethylbenzophenone : *p*HBA used in the one-pot synthesis was 1:1:2. All reaction and crystallizing conditions remaining the same. Therefore, the only substantial change to the synthetic method of the two co-crystals was the addition of a methyl group on one of the benzophenone rings.

Co-crystal **VI** and **VII** are isostructural (Figure 9(a) and (b)). Both crystallize in the $P\bar{1}$ space group and each asymmetric unit contains one modified isoniazid molecule and two *p*HBA molecules. In the asymmetric unit, the modified isoniazid is hydrogen bonded to one of the *p*HBA molecules via the expected COOH$\cdots$N$_{pyr}$ heterosynthon. This *p*HBA is also hydrogen bonded to the second *p*HBA molecule through the carbonyl oxygen (O3) of its carboxylic acid group to the phenol hydrogen donor atom (H7) of the second *p*HBA molecule (Figure 2). **VI** and **VII** pack into a thick one dimensional (1D) tape with all of the modified isoniazid molecules on the edge of the tape and all the *p*HBA molecules forming a four molecule thick arrangement of *p*HBA molecules in the centre of the tape. Thus, the modified isoniazid and *p*HBA molecules (which have a 1:2 ratio in the asymmetric unit) form a six-molecule thick tape with the

arrangement I-*p*-*p*-*p*-*p*-I (where I denotes modified isoniazid and *p* denotes *p*HBA) (Figure 9(c)). Each modified isoniazid molecule is hydrogen bonded to two *p*HBA molecules, one in which its carbonyl oxygen (O1) acts as the acceptor to the phenol hydrogen bond donor atom (H5) of a *p*HBA molecule, and secondly, in which its pyridine nitrogen atom accepts hydrogen bonding from the carboxylic acid group hydrogen of another *p*HBA molecule. Each of these *p*HBA molecules is the first *p*HBA molecule in a chain of four *p*HBA molecules which form the centre of the tape. The first *p*HBA molecule hydrogen bonds to the second via its carboxylic acid group carbonyl oxygen (O3). The two centre *p*HBA molecules are hydrogen bonded to each other through a robust COOH···COOH homosynthon, forming a $R_2^2(8)$ ring. The other half of the tape is the symmetrical inverse of the half which has been described, with the centre of symmetry about the centre of the $R_2^2(8)$ ring.

The crystal structures of **II** and **IIIa** have already been discussed. However, it should be mentioned here that in co-crystals **II** and **IIIa**, their method of synthesis was kept constant except that a methyl group to one of the benzophenone rings in **IIIa**. As with co-crystals **VI** and **VII**, the addition of an additional methyl group to the benzophenone modifier did not affect the supramolecular synthesis. To summarize the addition of benzophenone rings, in **II**, benzophenone was used as a modifier and in **IIIa**, 4-methylbenzophenone was used, and the resulting co-crystals were isostructural. In **VI**, 4-methylbenzophenone was used as the modifier, and in **VII**, 4,4-dimethylbenzophenone was used, and the resulting co-crystals **VI** and **VII** were also isostructural. Therefore, the addition of a methyl substituent to the benzophnone modifiers has no effect on the supramolecular outcome.

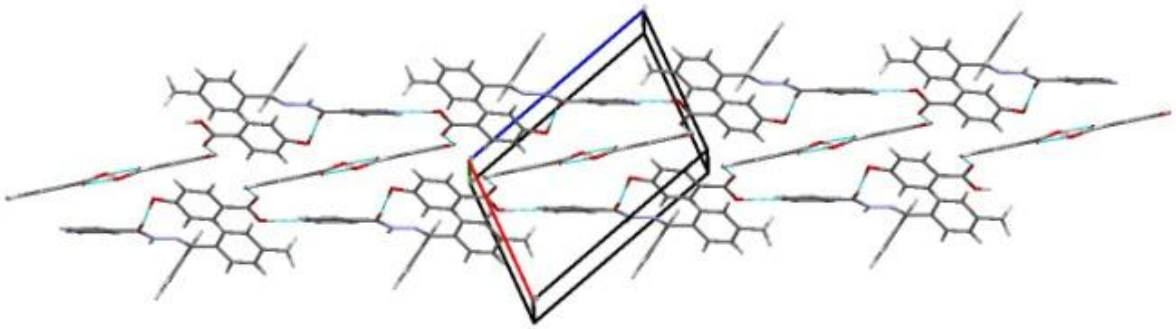

(a)

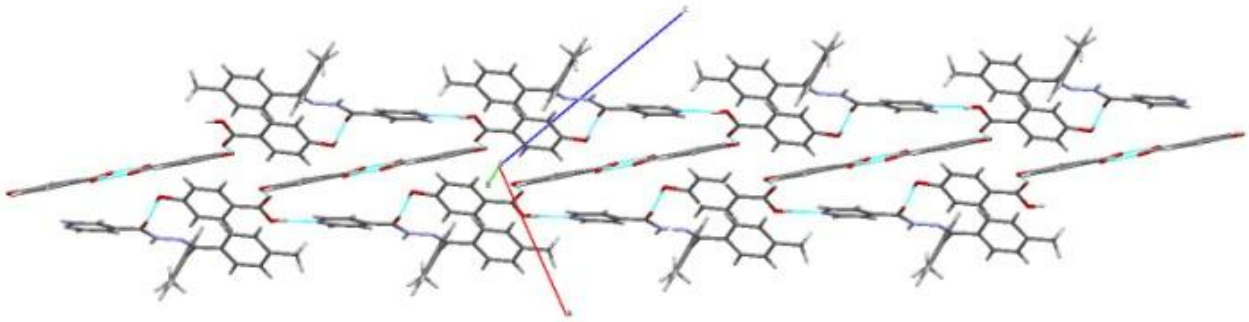

(b)

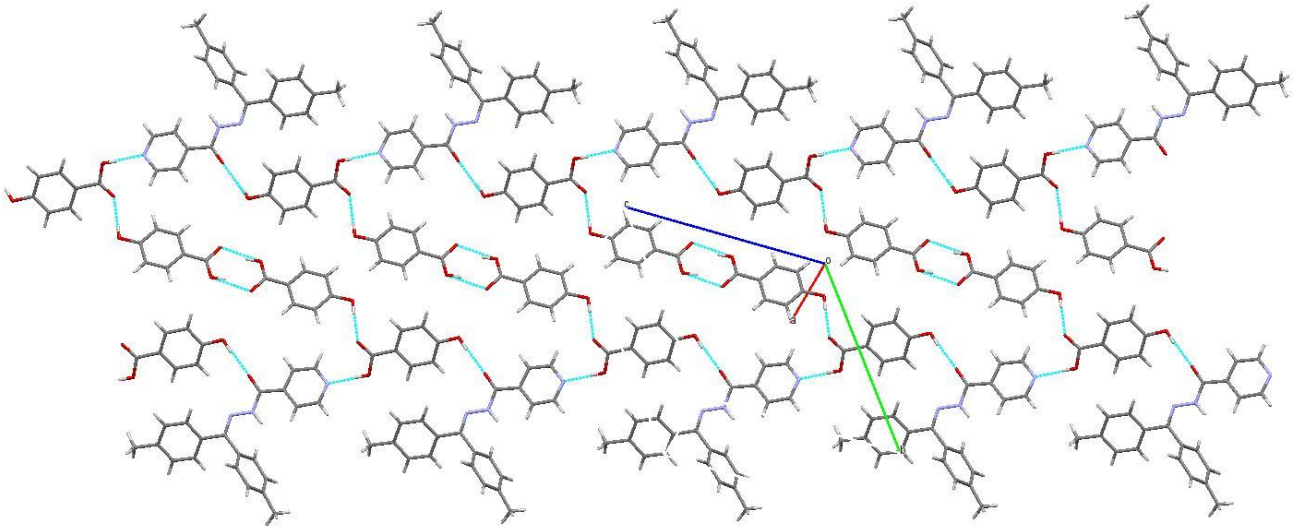

(c)

Figure 9: Parts (a) and (b) show the isostructural packing of **VI** and **VII** respectively. Part (c) shows how the molecules of the co-crystal pack into a tape with all the modified isoniazid molecules on the edge of the tape and all the *p*HBA molecules in the centre of the tape.

In summary, therefore, in this study, any small change in the reaction and crystallization conditions had a big effect on the outcome of crystallization, whereas changing a substituent on a molecule did not. For masked isoniazid molecules, it would thus appear that small changes in the crystallization and reaction conditons play a bigger role in the resulting supramolecular structure than the addition of small substituents or making small changes to the molecules themselves.

Conclusion

Eight co-crystals of isoniazid which have modified by benzophenone or a derivative thereof, were co-crystallized with either 3- or 4-hydroxybenzoic acid. The co-crystals were divided into pairs and all crystallization conditions were kept constant except for one substantial change in crystallization conditions being made per pair. Pairs of co-crystals were then compared and the results are tabulated in Table 4.

Table 4 A summary of the changes made to the crystallization conditions and the effect of the change of the outcome of supramolecular synthesis.

Co-crystals compared	**Change made to reaction or crystallization conditions**	**Effects of change on outcome of supramolecular synthesis**
I and **II**	Reflux time in one-pot synthesis was changed	Stoichiometric variation of the products resulted
IIIa and **IIIb**	The stoichiometry of reagents was changed to create an “additive”	Polymorphs were formed
IV and **V**	A acid catalyst was added to the one-pot synthesis	A solvate was formed in one structure and prevented in the other
VI and **VII**	A second methyl group was added to the benzophenone rings (one methyl group on each ring)	No effect on supramolecular structure
II and **IIIa**	An extra methyl group was added to a benzophenone ring	No effect on supramolecular structure

Where a small change was made to the reaction conditions, a large change in the hydrogen bonding and packing arrangements resulted. A change in reflux time of the one-pot synthesis resulted in stoichiometric variation of the products. The addition of extra co-former reagent as an "additive" resulted in polymorphism, where hydrogen bonding through different heterosynthons was observed, as well as a change in dimensionality of the packing. Adding an acid catalyst to catalyze the modification of isoniazid prevented the formation of a solvate, whereas in the absence of the catalyst, the solvate was formed. On the other hand, adding either one or two methyl groups to the benzophenone had no effect on the supramolecular structure, and both pairs where the number of methyl groups were varied were isostructural. Thus, in this study, the changes in reaction and crystallization conditions had a bigger effect on the supramolecular structure than changing small substituents on the reagents.

Acknowledgement

The University of the Witwatersrand and the Molecular Sciences Institute are thanked for providing the infrastructure and financial support to do this work. Andreas Lemmerer thanks the Wits Friedel Sellschop award for funding and Mark Smith thanks the Chemistry department of the University of South Africa for the financial support.

Supporting Information Available

Crystallographic data were deposited at the Cambridge Crystallographic Data Center with reference numbers CCDC 1810897-1810903, These data can be obtained free of charge via https://www.ccdc.cam.ac.uk/structures (or from the Cambridge Crystallographic Data Centre, 12, Union Road, Cambridge CB2 1EZ, UK; fax: +44 1223 336033). This information is also available free of charge via the internet at http://pubs.acs.org.

References

(1) André, V.; Shemchuk, O.; Grepioni, F.; Braga, D.; Duarte, M. T., *Cryst. Growth Des.* **2017**. (Accepted)

(2) Lemmerer, A.; Bernstein, J.; Kahlenberg, V., *CrystEngComm.* **2010,** *12* (10), 2856-2864.

(3) Lemmerer, A.; Bernstein, J.; Kahlenberg, V., *CrystEngComm.* **2011,** *13* (19), 5692-5708.

(4) Lemmerer, A., *CrystEngComm.* **2012,** *14* (7), 2465-2478.

(5) Smith, M. G.; Forbes, R. P.; Lemmerer, A., *Cryst. Growth Des.* **2015,** *15* (8), 3813-3821.

(6) Sander, J. R. G.; Bucar, D.-K.; Henry, R. F.; Giangiorgi, B. N.; Zhang, G. G. Z.; MacGillivray, L. R., *CrystEngComm.* **2013,** *15* (24), 4816-4822.

(7) Grobelny, P.; Mukherjee, A.; Desiraju, G. R., *CrystEngComm.* **2011**, *13*, 4358-4364.

(8) Aitipamula, S.; Wong, A. B. H.; Chow, P. S.; Tan, R. B. H., *CrystEngComm.* **2013**, *15***,** 5877-5887.

(9) Sarcevica, I.; Orola, L.; Veidis, M. V.; Podjava, A.; Belyakov, S., *Cryst. Growth Des.* **2013**, *13***,** 1082-1090.

(10) Sarcevica, I.; Orola, L.; Veidis, M. V.; Belyakov, S., *Acta Crystallogr., Sect. C.* **2014**, *70***,** 392-395.

(11) Mashhadi, S. M. A.; Yunus, U.; Bhatti, M. H.; Tahir, M. N., *J. Mol. Struct.* **2014**, *1076***,** 446-452.

(12) Swapna, B.; Maddileti, D.; Nangia, A., *Cryst. Growth Des.*, **2014**, *14***,** 5991-6005.

(13) *SAINT+*, , Version 6.02 (Includes XPREP and SADABS); Bruker AXS Inc: Madison, Wisconsin, USA, 2004.

(14) Sheldrick, G. M., *Acta Crystallogr., Sect. C.* **2015,** *71* (Pt 1), 3-8.

(15) Farrugia, L., *J. Appl. Crystallogr.* **2012,** *45* (4), 849-854.

(16) Spek, A., *Acta Crystallogr., Sect. D.* **2009,** *65* (2), 148-155.

(17) Macrae, C. F., Bruno, I. J., Chisholm, J. A., Edgington, P. R., McCabe, P., Pidcock, E., Rodriguez-Mange, L., Taylor, R., van de Streek, J., & Wood, P. A. (2008). *J. Appl. Cryst.* **41**, 466-470.

(18) Desiraju, G. R., *J. Am. Chem. Soc.* **2013,** (135), 9952-9967.

(19) Aakeröy, C. B.; Hussain, I.; Forbes, S.; Desper, J., *CrystEngComm.* **2007,** *9* (1), 46-54.

(20) Bernstein, J.; Davis, R. E.; Shimoni, L.; Chang, N.-L., *Angew. Chem. Int. Ed.* **1995,** *34* (15), 1555-1573.

(21) Meir, L.; Leslie, L., *Phys. Scr.* **2015,** *90* (11), 118003.

(22) Addadi, L.; van Mil, J.; Gati, E.; Lahav, M., *Origins of life.* **1981,** *11* (1-2), 107-18.

Chapter 5: Crystal engineering of isoniazid

5.1 Introduction

Isoniazid was covalently modified with bulky benzophenone and benzophenone derivative modifiers in the absence of co-formers. This chapter details the synthesis of the crystals and a structural study of crystalline covalently modified isoniazid molecules is reported.

Details of the publication status of the paper precede the paper.

5.2 Synthesis and structural study of crystalline isoniazid derivatives with benzophenone modifiers

Title of paper:	Synthesis and structural study of crystalline isoniazid derivatives with benzophenone modifiers
Journal:	Will be submitted to *Acta Crystallographica B: Structural Science, Crystal Engineering and Materials*
Reference:	
Status:	Submission Pending. To be submitted by end March 2018.
Date Received:	
Date Revised:	
Date Published:	

Synopsis of Paper

In this paper, ten crystalline derivatives of isonicotinic acid hydrazide (isoniazid) that have been covalently modified with bulky benzophenone and benzophenone derivative modifiers have been synthesized and structurally characterized.

Table 5.1: List of compounds reported in chapter 5.2

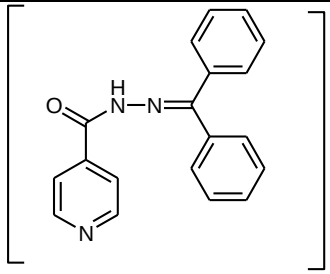	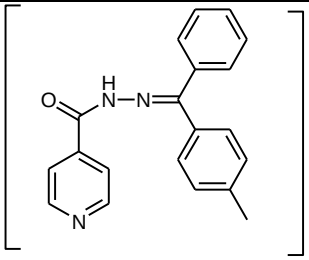
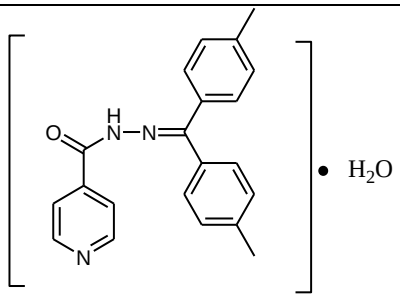	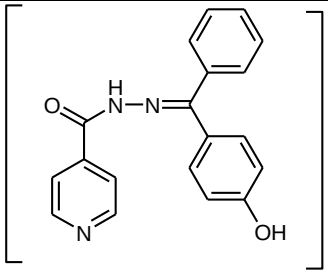
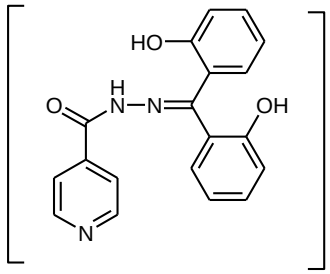	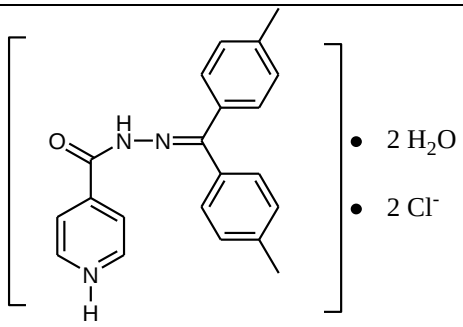
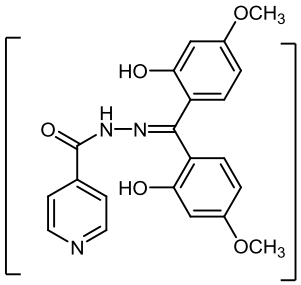	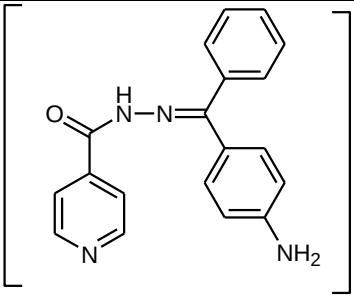
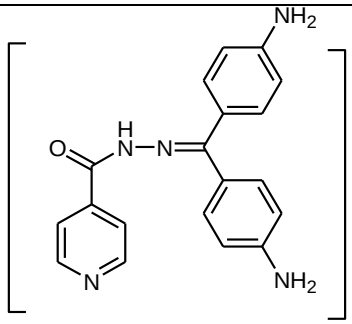	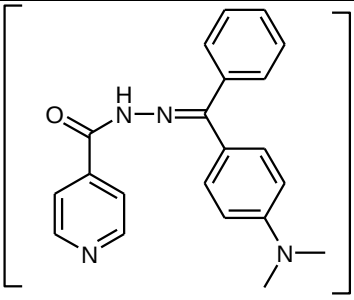

Synthesis and structural study of crystalline isoniazid derivatives with benzophenone modifiers

Mark G. Smith[†] and Andreas Lemmerer*[‡]

†*Department of Chemistry, University of South Africa, Unisa Science Campus, Florida, 1709, Johannesburg, South Africa, and* [‡]*Molecular Sciences Institute, School of Chemistry, University of the Witwatersrand, 2050, Johannesburg, South Africa*

RECEIVED DATE (to be automatically inserted after your manuscript is accepted if required according to the journal that you are submitting your paper to)

To whom correspondence should be addressed:

Professor Andreas Lemmerer, Molecular Sciences Institute, School of Chemistry, University of the Witwatersrand, Private Bag 3, 2050, Johannesburg, South Africa.
E-mail: andreas.lemmerer@wits.ac.za. Fax: +27-11-717-6749. Tel: +27-11-717-6711.

ABSTRACT:

Isonicotinic acid hydrazide (isoniazid) has been covalently modified with bulky benzophenone and benzophenone derivatives to yield a series of potentially pharmaceutically active Schiff bases. The acid-catalyzed condensation reaction between isoniazid and the modifiers yielded ten crystalline isoniazid derivatives, including one salt solvate, namely:

N'-(diphenylmethylene)isonicotinohydrazide, $C_{19}H_{15}N_3O$, (**I**),
(*E*)-*N*'-(phenyl(*p*-tolyl)methylene)isonicotinohydrazide), $C_{20}H_{17}N_3O$, (**II**),
N'-(di-*p*-tolylmethylene)isonicotinohydrazide monohydrate, $C_{21}H_{19}N_3O{\cdot}H_2O$, (**III**),
(*E*)-*N*'-(phenyl(*p*-hydroxy)methylene)isonicotinohydrazide), $C_{19}H_{15}N_3O_2$, (**IV**),
N'-(bis(2-hydroxyphenyl)methylene)isonicotinohydrazide, $C_{19}H_{15}N_3O_3$, (**V**),
N'-(di-*p*-tolylmethylene)isonicotinohydrazide chloride salt dihydrate, $C_{19}H_{15}N_3O_3^{+}{\cdot}H_2O{\cdot}Cl^{-}$, (**VI**),
N'-(bis(2-hydroxy-4-methoxyphenyl)methylene)isonicotinohydrazide, $C_{21}H_{19}N_3O_5$, (**VII**),
(*E*)-*N*'-(4-aminophenyl(phenyl)methylene)isonicotinohydrazide), $C_{19}H_{16}N_4O$, (**VIII**),
N'-(bis(4-aminophenyl)methylene)isonicotinohydrazide), $C_{19}H_{17}N_5O$, (**IX**), and
(*E*)-*N*'-((4-(dimethylamino)phenyl)(phenyl)methylene)isonicotinohydrazide), $C_{20}H_{20}N_4O_2$, (**X**).

The choice of acid catalyst for the synthesis was dependent on the nature of the substituents on the benzophenone rings. The synthesis of these Schiff bases is described and a full structural study of these isoniazid derivatives is reported.

KEYWORDS:

Isoniazid, Crystal engineering, Benzophenone, Mycobacterium Tuberculosis drugs

Introduction

The covalent modification of isonicotinic acid hydrazide (isoniazid) via the replacement of the NH_2 hydrogen atoms with ketone modifiers is the primary focus in the synthesis of medicines that target drug-resistant strains of tuberculosis. This covalent modification prevents the enzymes of the *Mycobacterium tuberculosis* bacteria (TB) from rendering the drug ineffective (Hearn *et al.*, 2009). Hearn *et al.* prepared a series of Schiff bases of isoniazid and compared the biological activity of pure isoniazid with that of covalently modified isoniazid on mice. Hearn demonstrated that the NH_2 functional group of isoniazid is subject to deactivating acetylation by a class of enzymes known as N-arylaminoacetyl transferases (NATs). He explained that this deactivation is the reason for the resistance of the tuberculosis bacteria against isoniazid. However, if the isoniazid drug is modified by the covalent modification of the isoniazid to form Schiff bases (**Figure 1**), the enzymatic deactivation process no longer works to deactivate the drug and the resulting modified isoniazid can be effective for the treatment of multi-drug resistant strains of the bacteria. Hearn *et al*. prepared 46 Schiff bases of isoniazid and found that in nearly all of them, the biological activity of the drug was effective against multidrug-resistant strains of TB. When the Schiff bases were crystallized, the drugs were reported to be pure. In his conclusion Hearn noted that "*Schiff bases [of isoniazid (INH)] may serve as discovery tools in probing INH-based treatment modalities, particularly for those patients chronically underdosed in conventional INH therapy.*" (Hearn *et al*., 2009).

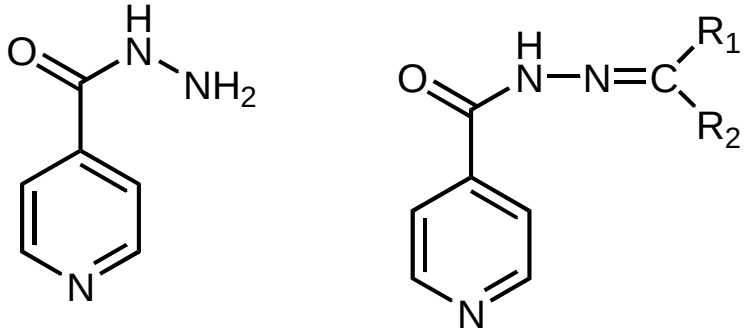

(a) (b)

Figure 1: (a) Isoniazid. (b) The general structure of the Schiff bases prepared and tested by Hearn *et al*. (Hearn *et al*., 2009)

Coelho *et al.* prepared a series of 23 N-acylhydrazones derived from isoniazid and determined the biological activity of those modified isoniazid derivatives. Thirteen of the modified isoniazid products showed a more than 10-fold higher biological activity against *katG*-resistant strains of *M. tuberculosis* (Coelho *et al*., 2012).

In Smith *et al.* (Smith *et al*., 2015), isoniazid was modified with a series of benzophenone derivatives and co-crystallized with 2-hydroxybenzoic acid. The predictable "masking" of the amide functionality was achieved, and it was shown that the bulky benzophenone modifiers rendered the amide nitrogen atom inaccessible for hydrogen bonding and no short intermolecular contacts were present between the amide nitrogen atoms in "masked" isoniazid derivatives and any neighbouring isoniazid or 2-hydroxybenzoic acid atoms. Sevukarajan *et al.* synthesized a co-crystal of isoniazid with L(+) tartaric acid and observed that with this particular co-former, solubility decreased and the anti-tubercular activity decreased as compared with pure isoniazid (Sevukarajan *et al*., 2011). In contrast, Aitipamula *et al*. synthesized a ternary co-crystallization of isoniazid with nicotinamide and succinic acid and reported that the in co-crystal, the solubility was increased compared with pure isoniazid (Aitipamula *et al*., 2013). It is clear that the solubility and activity of isoniazid and modified isoniazid against tuberculosis may either increase or decrease with a co-former in its supramolecular structure, but may be more effective in the absence of a co-former.

This report contains a structural study of isoniazid that has been modified with bulky benzophenone and benzophenone derivatives to form Schiff bases in the absence of any co-formers.

Experimental Methods

N'-(diphenylmethylene)isonicotinohydrazide, I

0.0920 g of isonicotinic acid hydrazide (0.671 mmol) and 0.1202 g of benzophenone (0.6596 mmol) were added into a sample vial. 0.0111 g of *p*-toluenesulphonic acid monohydrate (0.0584 mmol) was added to catalyze the reaction. The solids were dissolved in 3 mL of a 1:1 mixture of AP-grade 1,2-dichloroethane and 1,1,1-trichloroethane and refluxed in a closed sealed screw-top

vial for 72 hours at 50°C, and were left to stand at room temperature very slightly opened to the atmosphere. Colourless needles were afforded after 3 days.

(*E*)-*N*'-(phenyl(*p*-tolyl)methylene)isonicotinohydrazide), II

0.0964 g of isonicotinic acid hydrazide (0.703 mmol) and 0.1386 g of 4-methylbenzophenone (0.7062 mmol) were added into a sample vial. 0.0124 g of *p*-toluenesulphonic acid monohydrate (0.0652 mmol) was added to catalyze the reaction. The solids were dissolved in 3 mL of a 2:1 mixture of AP-grade ethanol and acetonitrile and refluxed in a closed sealed screw-top vial for 5 days at 110°C, and were left to stand at room temperature very slightly opened to the atmosphere. Colourless needles were afforded after 3 days.

N'-(di-*p*-tolylmethylene)isonicotinohydrazide monohydrate, III

0.1197 g of isonicotinic acid hydrazide (0.8728 mmol) and 0.1841 g of 4,4-dimethylbenzophenone (0.8755 mmol) were added into a sample vial. 1 drop of 5M hydrochloric acid was added to catalyze the reaction. The solids were dissolved in 3 mL of methanol and refluxed in a closed sealed screw-top vial for 3 days at room temperature, followed by work-up with sodium bicarbonate: the solution was saturated with sodium bicarbonate, stirred for 5 minutes and then filtered. The filtered solution was then left to stand at room temperature very slightly opened to the atmosphere. Yellow plates were afforded after 3 days.

(*E*)-*N*'-(phenyl(*p*-hydroxy)methylene)isonicotinohydrazide), IV

0.0975 g of isonicotinic acid hydrazide (0.711 mmol) and 0.1410 g of 4-hydroxybenzophenone (0.7113 mmol) were added into a sample vial. 0.0981 g of *p*-hydroxybenzoic acid (0.0981 mmol) was added to catalyze the reaction. The solids were dissolved in 3 mL of AP-grade methanol and refluxed in a closed sealed screw-top vial for 24 hours at 67°C, and were left to stand at room temperature very slightly opened to the atmosphere. Colourless needles were afforded after 3 days.

***N*'-(bis(2-hydroxyphenyl)methylene)isonicotinohydrazide, V**

0.0857 g of isonicotinic acid hydrazide (0.625 mmol) and 0.1340 g of 2,2'-dihydroxybenzophenone (0.6255 mmol) were added into a sample vial. 0.0864 g of *p*-

hydroxybenzoic acid (0.626 mmol) was added to catalyze the reaction. The solids were dissolved in 3 mL of AP-grade methanol and refluxed in a closed sealed screw-top vial for 24 hours at 67°C, and were left to stand at room temperature very slightly opened to the atmosphere. Yellow plates were afforded after 3 days.

N'-(di-*p*-tolylmethylene)isonicotinohydrazide, chloride salt dihydrate, VI

0.1094 g of isonicotinic acid hydrazide (0.7977 mmol) and 0.1737 g of 2,2'-dihydroxybenzophenone (0.8108 mmol) were added into a sample vial. 0.1202 g of salicylic acid (0.8702 mmol) was added to catalyze the reaction. The solids were dissolved in 3 mL of a 1:1 mixture of 1,2-dichloroethane and AP-grade methanol and refluxed in a closed sealed screw-top vial for 6 hours at 70°C, and were left to stand at room temperature very slightly opened to the atmosphere. Yellow plates were afforded after 3 days.

N'-(bis(2-hydroxy-4-methoxyphenyl)methylene)isonicotinohydrazide, VII

0.0710 g of isonicotinic acid hydrazide (0.518 mmol) and 0.1425 g of 2,2'-dihydroxy-4,4'-dimethoxybenzophenone (0.5196 mmol) were added into a sample vial. 0.0728 g of salicylic acid (0.527 mmol) and 0.0195 g *p*-toluenesulphonic acid monohydrate (0.103 mmol) were added to catalyze the reaction. The solids were dissolved in 10 mL of a ethanol and refluxed in a closed sealed screw-top vial for 48 hours at 90°C, and were left to stand at room temperature very slightly opened to the atmosphere. Yellow needles were afforded after 5 days.

(*E*)-*N*'-(4-aminophenyl(phenyl)methylene)isonicotinohydrazide), VIII

0.0995 g of isonicotinic acid hydrazide (0.726 mmol) and 0.1441 g of 4-aminobenzophenone (0.7306 mmol) were added into a sample vial. 0.0159 g of *p*-toluenesulphonic acid monohydrate (0.0836 mmol) was added to catalyze the reaction. The solids were dissolved in 3 mL of AP-grade methanol and refluxed in a closed sealed screw-top vial for 72 hours at 125°C, and were left to stand at room temperature very slightly opened to the atmosphere. Colourless blocks were afforded after 3 days.

***N*'-(bis(4-aminophenyl)methylene)isonicotinohydrazide), IX**

0.0540 g of isonicotinic acid hydrazide (0.394 mmol) and 0.0749 g of 4,4'-diaminobenzophenone (0.353 mmol) were added into a sample vial. 0.0176 g of *p*-toluenesulphonic acid monohydrate (0.0925 mmol) was added to catalyze the reaction. The solids were dissolved in 3 mL of AP-grade methanol and refluxed in a closed sealed screw-top vial for 72 hours at 100°C, and were left to stand at room temperature very slightly opened to the atmosphere. Red blocks were afforded after 3 days.

(*E*)-*N*'-((4-(dimethylamino)phenyl)(phenyl)methylene)isonicotinohydrazide), X

0.1043 g of isonicotinic acid hydrazide (0.7605 mmol) and 0.1732 g of 4-(dimethylamino)benzophenone (0.7688 mmol) were added into a sample vial. 0.0232 g of *p*-toluenesulphonic acid monohydrate (0.122 mmol) was added to catalyze the reaction. The solids were dissolved in 3 mL of a methanol and refluxed in a closed sealed screw-top vial for 72 hours at 100°C, and were left to stand at room temperature very slightly opened to the atmosphere. Yellow blocks were afforded after 3 days.

Crystal Data and X-ray Structure Analysis.

Intensity data for the ten crystal structures were collected on a Bruker APEX II CCD area detector diffractometer with graphite monochromated Mo-K_α radiation (50 kV, 30 mA) at 173K. The collection method involved ω-scans with a 0.5° width. *SAINT+* version 6.02.6 software was used for data reduction and *SADABS* was used to make empirical absorption corrections (Bruker, 2004). The crystal structures were solved using direct methods on *SHELXS-97* (Sheldrick, 2015). Non-hydrogen atoms were first refined isotropically, followed by anisotropic refinement by full matrix least-squares calculations based on F^2 using *SHELXL-2017* (Sheldrick, 2015). C-bound H atoms were located in the difference electron density map, then positioned geometrically and were allowed to ride on their respective parent atoms, with thermal displacement parameters 1.2 times that of the parent C atom. The diffraction data and refinement statistics of crystal **X** was poor even after numerous attempts at recrystallization. Diagrams and publication material were generated using *WinGX* (Farrugia, 2012), *ORTEP-3* (Farrugia, 2012), *PLATON* (Spek, 2009) and *MERCURY (*Macrae, C. F. e*t al.*, 2008). The crystallographic data of each crystal is summarized in Table 1 and the hydrogen bonding geometries in Table 2.

Table 1 Crystallographic data for compounds **I-X**

	I	**II**	**III**	**IV**	**V**
Formula	$C_{19}H_{15}N_3O$	$C_{20}H_{17}N_3O$	$C_{21}H_{19}N_3O{\cdot}H_2O$	$C_{19}H_{15}N_3O_2$	$C_{19}H_{15}N_3O_3$
M_r	301.34	315.36	347.41	317.34	333.34
Temperature/K	173(2)	173(2)	173(2)	173(2)	173(2)
Wavelength/Å	0.71073	0.71073	0.71073	0.71073	0.71073
Crystal size/mm^3	0.226×0.324×0.522	0.066×0.091×0.325	0.084×0.169×0.384	0.072×0.103×0.395	0.242×0.419×0.521
Crystal system	Orthorhombic	Triclinic	Monoclinic	Orthorhombic	Monoclinic
Space group	$P2_12_12_1$	$P\bar{1}$	$P2_1/c$	$P2_12_12_1$	$C2/c$
a/Å	9.7738(4)	7.1641(7)	21.3512(13)	9.8650(5)	20.6917(6)
b/Å	9.9605(5)	10.7669(10)	5.9227(4)	9.9131(5)	10.1392(3)
c/Å	15.8005(7)	12.0237(10)	14.8729(11)	15.8923(7)	16.9544(5)
α/°	90	64.009(4)	90	90	90
β/°	90	82.346(5)	106.040(6)	90	115.7390
γ/°	90	82.885(5)	90	90	90
V/Å^3	1538.21(12)	823.99(13)	1807.6(2)	1554.15(13)	3204.07(16)
Z	4	2	4	4	8
ρ (calcd)/Mg m^{-3}	1.301	1.271	1.277	1.356	1.382
μ/mm^{-1}	0.083	0.081	0.084	0.091	0.096
F(000)	632	332	736	664	1392
Θ Range for data	2.417 to 27.989	1.892 to 25.495	1.985 to 25.491	2.421 to 27.992	2.185 to 27.995
Reflections collected	27237	9199	10908	8892	23999
No. of unique data	3710 [0.0421]	3066 [0.0755]	3256 [0.1805]	3455 [0.0400]	3872 [0.0371]
No. data with $I \geq 2\sigma(I)$	3496	1430	1139	2913	3340
Final R($I \geq 2\sigma(I)$)	0.0309	0.0627	0.0521	0.0410	0.0375
Final wR_2 (all data)	0.0816	0.1525	0.1103	0.0970	0.1054
CCDC deposition					

	VI	**VII**	**VIII**	**IX**	**X**
Formula	$C_{19}H_{15}N_3O_3^+$ ·H_2O·Cl^-	$C_{21}H_{19}N_3O_5$	$C_{19}H_{16}N_4O$	$C_{19}H_{17}N_5O$	$C_{20}H_{20}N_4O_2$
M_r	387.81	393.39	316.36	331.38	348.40
Temperature/K	173(2)	173(2)	173(2)	173(2)	173(2)
Wavelength/Å	0.71073	0.71073	0.71073	0.71073	0.71073
Crystal size/mm^3	0.082×0.160×0.393	0.063×0.125×0.821	0.211×0.322×0.689	0.118×0.242×0.306	0.093×0.196×0.256
Crystal system	Orthorhombic	Monoclininc	Monoclinic	Monoclinic	Monoclinic
Space group	$Pca2_1$	$P2_1/c$	$P2_1/c$	$P2_1/c$	Cc
a/Å	8.0689(2)	17.1398(12)	9.2605(3)	9.3882(2)	13.200(2)
b/Å	10.7998(2)	14.5323(10)	15.4712(5)	15.8901(4)	13.698(2)
c/Å	42.4741(10)	7.9026(6)	12.0003(4)	11.7784(3)	39.908(7)
α/°	90	90	90	90	90
β/°	90	91.731(4)	111.6250(10)	111.6510(10)	97.004(5)
γ/°	90	90	90	90	90
V/$Å^3$	3701.30(14)	1967.5(2)	1598.28(9)	1633.13(7)	7162(2)
Z	8	4	4	4	16
ρ (calcd)/Mg m^{-3}	1.392	1.328	1.315	1.348	1.292
μ/mm^{-1}	0.237	0.096	0.085	0.088	0.086
F(000)	1616	824	664	696	2944
Θ Range for data	1.886 to 27.998	1.838 to 27.997	2.251 to 27.996	2.259 to 27.990	2.76 to 26.36
Reflections collected	23895	18049	23604	22908	17910
No. of unique data	8160 [0.0792]	4753 [0.0908]	3841 [0.0541]	3936 [0.0592]	10563 [0.0512]
No. data with $I \geq 2\sigma(I)$	6067	2587	3221	3329	7867
Final R($I \geq 2\sigma(I)$)	0.0543	0.0567	0.0602	0.0423	0.1265
Final wR_2 (all data)	0.1437	0.1549	0.1438	0.1159	0.4207
CCDC deposition					

Table 2 Hydrogen bonding details of compounds **I-X**

	d(D─H)/Å	*d*(H···A)/Å	*d*(D···A)/Å	∠(D─H···A)/°
I				
N1-H1···N2[a]	0.85(2)	2.32(2)	3.0568(19)	146(2)
N1-H1···N2[a]	0.85(2)	2.32(2)	3.0568(19)	146(2)
III				
N1-H1···O1W	0.95(3)	2.00(4)	2.935(4)	166(3)
O1W-H1W···N2[b]	0.85	1.98	2.799(4)	163
O1W-H2W···O1[c]	0.85	2.55	3.034(4)	117
IV				
C3-H3···O2B[d]	0.95	2.41	3.261(19)	149
O2B-H2B···O1[e]	0.84	1.93	2.773(19)	176
C12-H12···O2A[f]	0.95	2.59	3.405(3)	144
O2A-H2A···O1[d]	0.84	1.87	2.703(3)	169
C18-H18···O2B[g]	0.95	2.50	3.351(16)	150
N1-H1···N2[h]	0.88	2.35	2.990(3)	130
V				
N1-H1···O2[i]	0.88	2.22	2.8802(12)	132
O2-H2···N2[j]	0.84	1.83	2.6526(13)	165
O3-H3···N3	0.84	1.85	2.5807(12)	145
VI				
C4-H4A···Cl2[k]	0.95	2.77	3.485(6)	133
C4-H4A···Cl2[l]	0.95	2.69	3.343(5)	127
N1-H1···O1[l]	0.88	1.99	2.808(5)	155
N2-H2···Cl1[l]	0.88	2.29	3.083(4)	151
O2-H2A···Cl2	0.84	2.22	3.050(3)	171
O3-H3···N3	0.84	1.89	2.609(5)	144
C22-H22···Cl2[m]	0.95	2.68	3.386(5)	132
N4-H4···O4[n]	0.88	2.02	2.845(5)	156
N5-H5···O2W[o]	0.88	1.81	2.684(5)	173
O5-H5A···O1W[m]	0.84	1.88	2.714(5)	176
O6-H6···N6	0.84	1.91	2.617(5)	141
O1W-H1W···Cl1[l]	0.859(14)	2.31(2)	3.150(4)	166(7)
O1W-H2W···Cl1	0.856(14)	2.284(15)	3.140(4)	178(7)

O2W-H3W···Cl1	0.848(14)	2.408(17)	3.239(4)	166(5)
O2W-H4W···Cl2[n]	0.848(13)	2.52(3)	3.271(4)	149(5)
VII				
C10-H10···N2[p]	0.95	2.68	3.354(3)	128
C16-H16···O5[q]	0.95	2.62	3.511(3)	157
O2-H2···N2[p]	0.84	1.89	2.730(2)	176
O4-H4···N3	0.84	1.81	2.535(2)	144
VIII				
C12-H12···N3[r]	0.95	2.68	3.596(3)	162
N1-H1···N4B[s]	0.88	2.58	3.356(4)	148
N4A-H4A···O1[r]	0.95(5)	2.22(5)	3.157(4)	168(4)
N4A-H4B···N2[t]	1.00(5)	2.14(5)	3.093(4)	159(4)
N4B-H4D···O1[u]	0.95(6)	1.86(6)	2.800(5)	168(5)
IX				
N(1)-H(1)···N(5)[v]	0.88	2.41	3.2167(15)	153
N(4)-H(4A)···O(1)[w]	0.882(19)	2.221(19)	3.0644(16)	160(16)
N(4)-H(4B)···N(2)[x]	0.89(2)	2.26(2)	3.0794(16)	153(17)
N(5)-H(5B)···O(1)[y]	0.907(18)	2.024(18)	2.9242(15)	172(16)
X				
N(1)-H(1)...N(5)[z]	0.88	2.41	3.2167(15)	152.7
N(4)-H(4A)...O(1)[aa]	0.882(19)	2.221(19)	3.0644(16)	160.1(16)
N(4)-H(4B)...N(2)[ab]	0.89(2)	2.26(2)	3.0794(16)	153.4(17)
N(5)-H(5B)...O(1)[ac]	0.907(18)	2.024(18)	2.9242(15)	171.8(16)

[a] x+1/2,-y+1/2,-z+2. [b] -x+1,y+1/2,-z+1/2. [c] x,-y+3/2,z-1/2. [d] -x+3/2,-y+2,z-1/2. [e] x,y+1,z. [f] -x+1,y+1/2,-z+1/2. [g] -x+3/2,-y+3,z-1/2. [h] -x+2,y+1/2,-z+1/2. [i] -x,y,-z+1/2. [j] x+1/2,-y+3/2,z+1/2. [k] x,y-1,z. [l] x+1/2,-y,z. [m] -x+1/2,y,z-1/2. [n] x+1/2,-y+1,z. [o] -x+1,-y+1,z-1/2. [p] -x,y-1/2,-z+1/2. [q] -x+1,-y+1,-z+2. [r] x,-y+1/2,z-1/2. [s] x+1,y,z. [t] -x+2,y+1/2,-z+3/2. [u] -x,-y,-z+1. [v] x-1,y,z. [w] x,-y+1/2,z+1/2. [x] -x-1,y-1/2,-z+1/2. [y] -x+1,-y+1,-z+1. [z] x-1,y,z. [aa] x,-y+1/2,-z+1/2. [ab] –x-1,y-1/2,-z+1/2. [ac] -x+1,-y+1,-z+1.

Results

The covalent modification of isoniazid with a ketone occurs via an acid-catalyzed condensation reaction. The reaction involves the nucleophilic attack on the carbonyl group by the amine nitrogen to form an unstable carbinolamine moiety, followed by acid catalyzed dehydration to form an imine. This resulting imine is referred to as "modified isoniazid." However, isoniazid does not readily undergo condensation reactions with benzophenone or its derivatives and requires harsh reaction conditions and the use of acid catalysts for a successful reaction. Hearn *et al.* observed that stereo-electronic effects often make the covalent modification more difficult with bulky modifiers and explained that "*with alkyl modifiers larger than methyl in the ketone component of the transition state, the conformational preference for the lone pair on N renders this nitrogen poorly poised for nucleophilic attack.*" (Hearn *et al.*, 2009). The conditions required for the reaction generally required significant heating, increased pressure and extended refluxing over several days. Glass screw-top, airtight rubber-lined dram vials were used for refluxing. The reagents and solvent were added to the vial, a magnetic stirrer bar was added and the top was tightly closed and the vial placed on a heater-stirrer. This mimicked a reflux setup on a small scale. It also allowed for heating to a temperature considerably higher than that of the boiling point of methanol.

The choice of acid catalyst was also important. In order to avoid salt formation, weak acids were chosen, but where these failed, stronger acids were applied. Originally, the covalent modification of isoniazid was attempted with the GRAS acids, salicylic acid or *p*-hydroxybenzoic acid, which proved successful only for structures **IV** and **VI**. The apparent ease of reaction of isoniazid with these two modifiers (4-hydroxybenzophenone and 2,2'-dihydroxybenzophenone) is due to the electron withdrawing hydroxyl groups on these molecules rendering the electrophilic carbon atom more positive. For all but one of the remaining reactions, *p*-toluenesulfonic acid proved a successful catalyst. As the electron donating nature of the benzophenone substituents increased, the required reaction conditions became increasingly harsh. With 4-methylbenzophenone as a modifier, reflux at 110°C for 5 days was required with the *p*-toluenesulfonic acid catalyst. With the 4,4'-dimethylbenzophenone modifier, having two electron donating substituents, the reaction failed completely and concentrated hydrochloric acid was required for the reaction to occur.

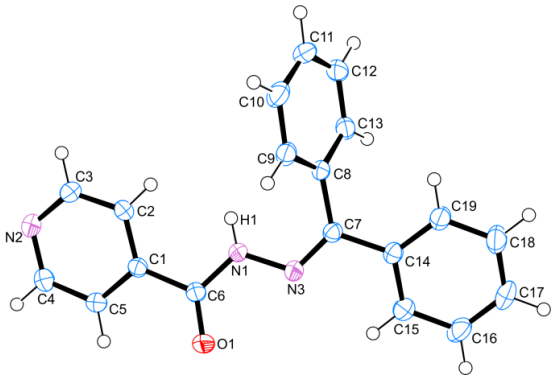

I

(a)

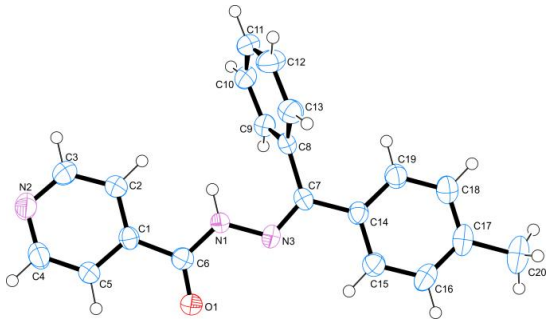

II

(b)

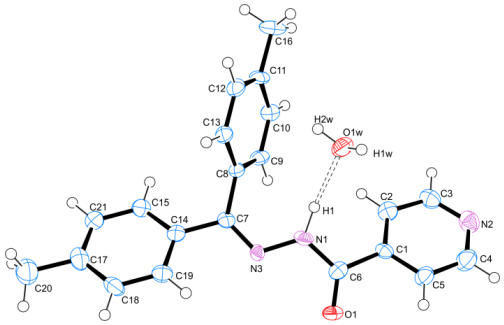

III

(c)

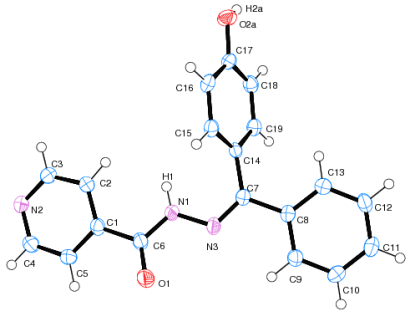

IV

(d)

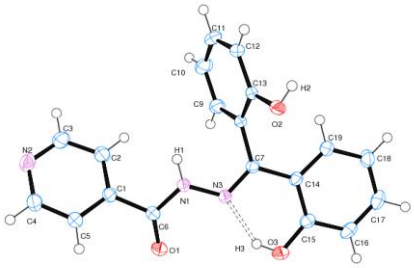

V

(e)

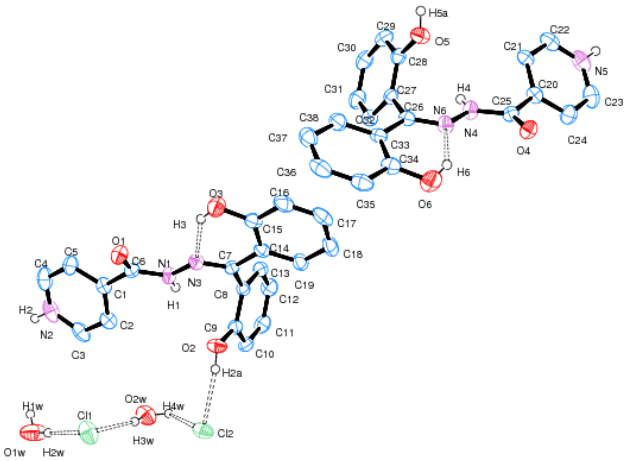

VI

(f)

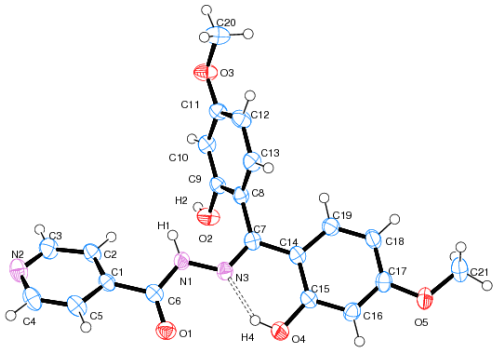

VII

(g)

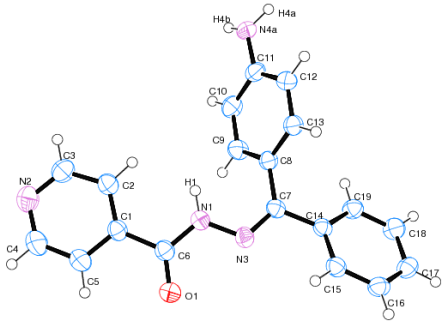

VIII

(h)

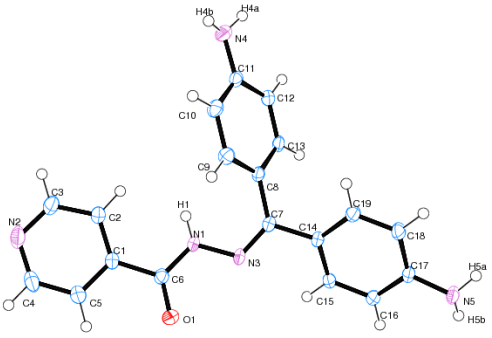

IX

(i)

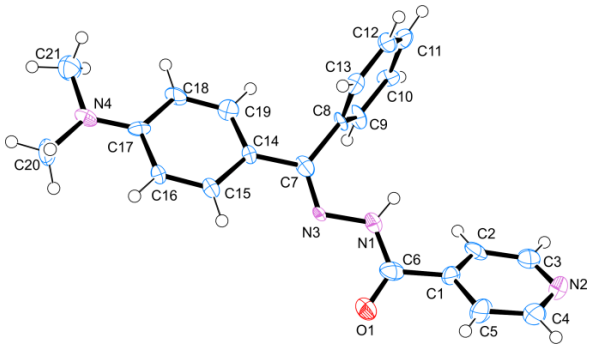

X

(j)

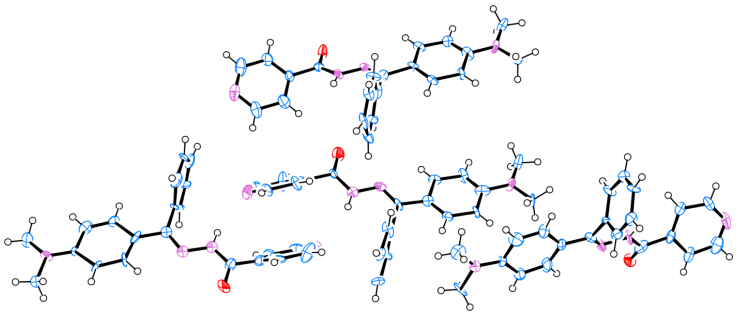

X

(k)

Figure 2: Asymmetric units (a)-(i) of crystals **I-IX**, showing the numbering schemes. Part (j) shows the numbering scheme of a quarter of the asymmetric unit of crystal **X** (which has four molecules in the asymmetric unit). The complete asymmetric unit of **X** is shown in (k) without atom labels.

Compound **I** crystallizes in the $P2_12_12_1$ space group and the asymmetric unit contains one molecule of *N*'-(diphenylmethylene)isonicotinohydrazide, the product of the covalent modification of isoniazid with benzophenone. The modified isoniazid molecules in **I** hydrogen bond to each other via the $NH_{amide}\cdots N_{pyridine}$ heterosynthon (**Figure 3**) and form one-dimensional (1D) ribbons along the *a*-axis with translational symmetry via a twofold screw axis along the crystallographic *a*-axis, stabilized by π-stacking. The ribbons are formed via chains of seven atoms between hydrogen bonds, with graph-set notation $C_1^1(7)$ (Bernstein *et al.*, 1995).

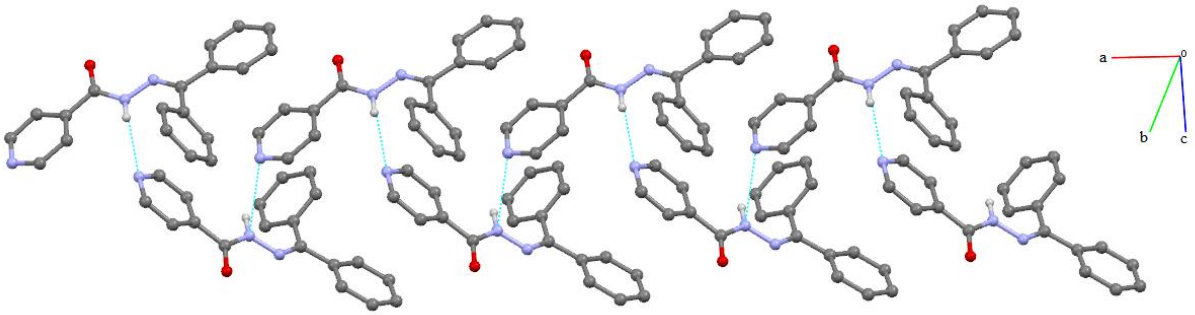

Figure 3: Packing diagram of **I**. One dimensional ribbons extend along the *a*-axis.

Compound **II** crystallizes in the $P\bar{1}$ space group and the asymmetric unit contains one molecule of (E)-*N*'-(phenyl(*p*-tolyl)methylene)isonicotinohydrazide). The molecules are aligned in parallel planes, and held together via multiple weak C−H···O and C−H···N interactions and further stabilized via π···π stacking. Each molecule interacts with an adjacent molecule on one side of its plane by a carbonyl oxygen atom (O1) that is hydrogen bonded via a weak C−H···O interaction to a C−H hydrogen atom (H13) of the non-substituted benzophenone ring on an adjacent molecule to form a $R_2^2(16)$ ring. The pyridyl nitrogen atom (N2) also interacts with a hydrogen atom of the methyl group substituent of the other benzophenone ring of the adjacent molecule (H20C) via a weak C−H···N hydrogen bond. On the opposite side of each plane, the hydrazide nitrogen (N3) of each molecule is similarly involved in C−H···N hydrogen bonding, but to a C−H hydrogen atom on the non-substituted benzophenone ring of the adjacent molecule to form a $R_2^2(10)$ ring. The packing is further stabilized by π···π stacking to form 1D ribbons along the *a*-axis (**Figure 4**).

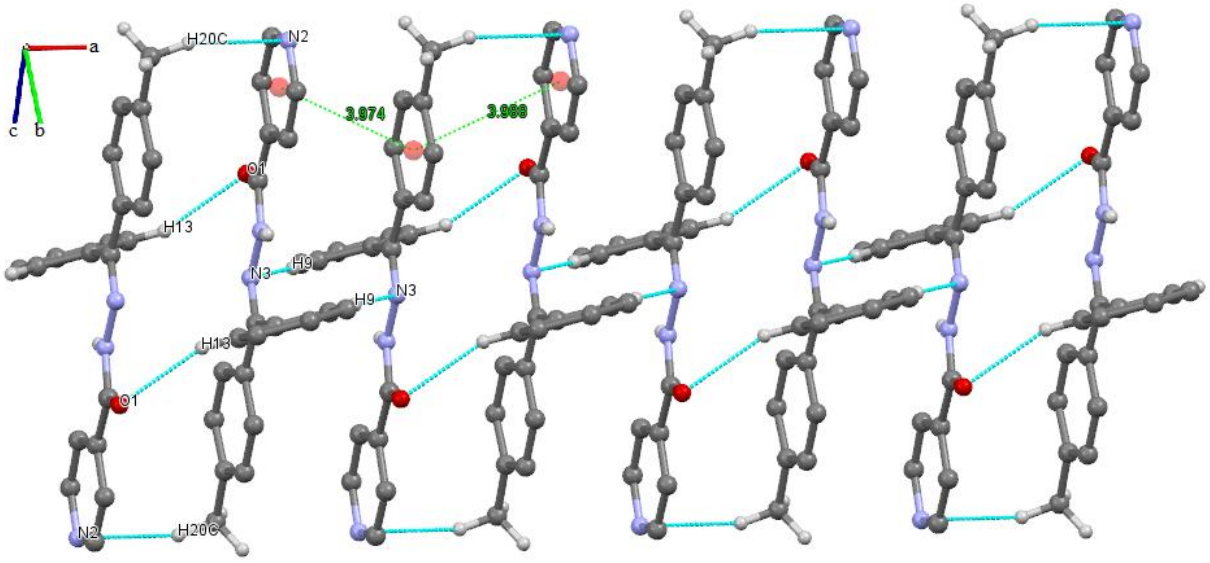

Figure 4: Packing diagram of **II**.

Compound **III** crystallizes in the monoclinic $P2_1/c$ space group and the asymmetric unit contains one molecule of *N*'-(di-*p*-tolylmethylene)isonicotinohydrazide and one water molecule. The hydrate version of isoniazid molecules that have been covalently modified via reaction with ketones are common, as the water molecule is a byproduct of the acid-catalyzed condensation reaction. This reaction occurs via nucleophilic attack on the carbonyl group by the amine nitrogen to form an unstable carbinolamine moiety, followed by acid catalyzed dehydration to form an imine (Xavier and Srividhya, 2014). In the asymmetric unit the hydrogen bond occurs between the amide nitrogen atom (H1) and the water oxygen atom (O1W). The packing of **III** is a three-dimensional (3D) network with all molecules being hydrogen bonded to water. Each water molecule has three hydrogen bonds and an O−H···π interaction. The bonding of the carbonyl oxygen atom acceptor of the modified isoniazid molecule is bifurcated and hydrogen bonds to both water hydrogen donors. One of the water hydrogen atoms is also hydrogen bonded to the isoniazid pyridine nitrogen acceptor atom (**Figure 5a**). The other water hydrogen atom forms an O−H···π interaction with one of the benzophenone rings on an adjacent modified isoniazid molecule (**Figure 5b**). The oxygen atom of this water molecule acts as a hydrogen bond acceptor to the amide N−H donor atom. The packing is further stabilized by π···π stacking of the pyridyl rings along the *c*-axis.

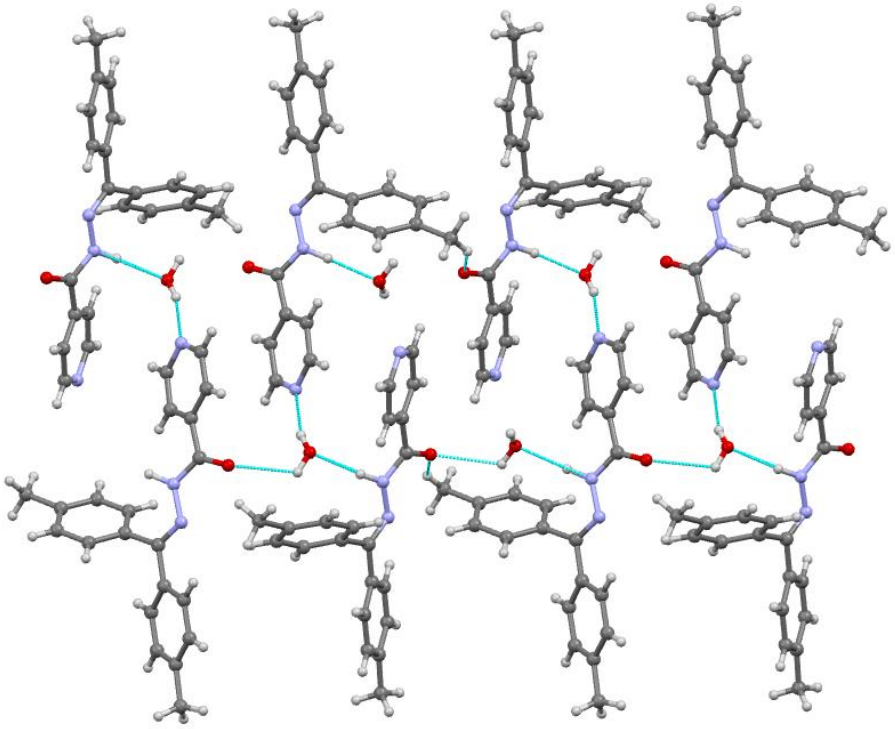

(a)

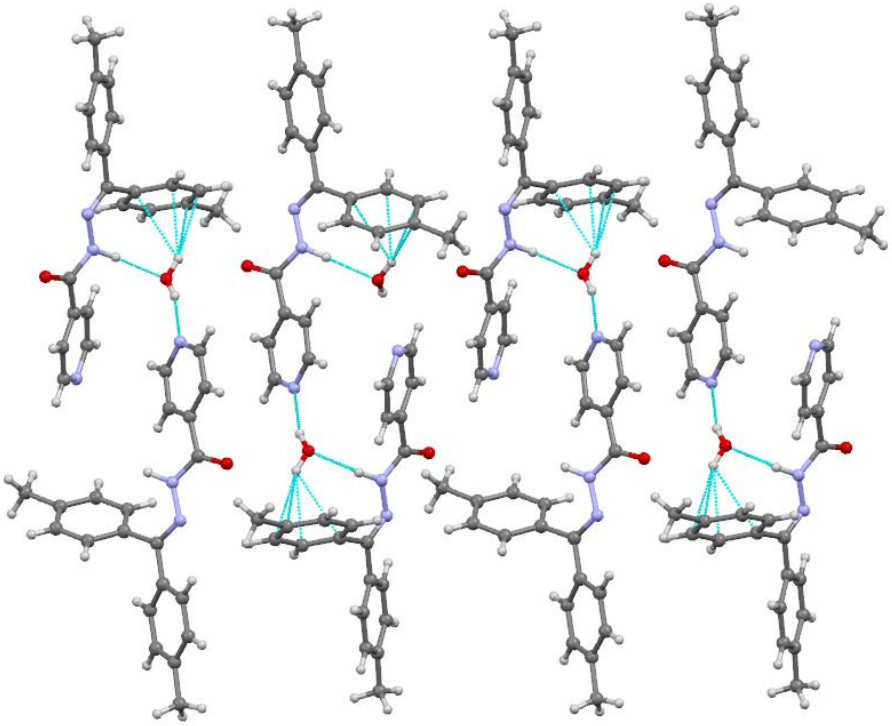

(b)

Figure 5: Packing diagram of **III** showing (a) regular heterosynthons of water with modified isoniazid and (b) the O−H···π interaction between water and the aromatic benzophenone ring.

Compound **IV** crystallizes in the orthorhombic $P2_12_12_1$ space group and the asymmetric unit contains one molecule of (*E*)-*N*'-(phenyl(*p*-hydroxy)methylene)isonicotinohydrazide). Each molecule has three hydrogen bonding sites, resulting in a 3D packing network. The hydrogen bonding of each molecule involves its hydroxyl group, carbonyl oxygen atom and either a pyridyl nitrogen acceptor atom or the amide N−H donor. The hydroxyl donor on each molecule is hydrogen bonded to the carbonyl oxygen atom of an adjacent atom, and the amide hydrogen atom is bonded to the pyridyl nitrogen atom of an adjacent molecule (**Figure 6**). The hydroxyl group on the benzophenone ring is disordered. The position of the hydroxyl group is on either of the two benzophenone rings, with the major disorder component percentage being 89.143(4) %.

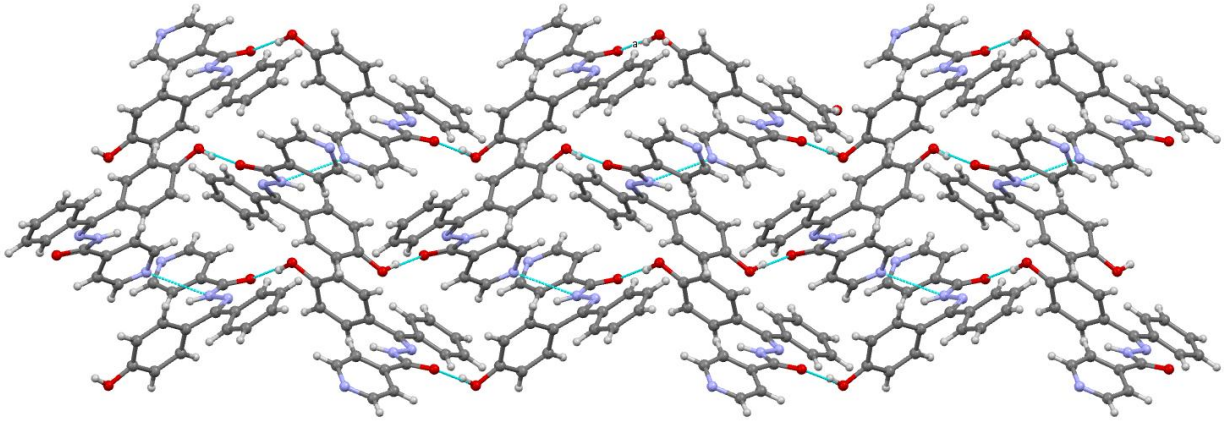

Figure 6: Packing diagram of **IV**.

Compound **V** crystallizes in the orthorhombic *C*2/c space group and the asymmetric unit contains one molecule of *N*'-(bis(2-hydroxyphenyl)methylene)isonicotinohydrazide. There is one hydroxyl group on each of the benzophenone rings. As expected from Etter's rules of hydrogen bonding (Etter *et al*., 1990), one of the hydroxyl groups forms a six-membered intramolecular hydrogen bonded ring with the hydrazide nitrogen atom (N3) and is not involved in any intermolecular interactions (**Figure 2e**). The other hydroxyl group is hydrogen bonded to the pyridyl nitrogen atom of an adjacent molecule via the robust $O{-}H\cdots N_{pyridine}$ heterosynthon. Its oxygen atom acts as an acceptor to the amide hydrogen atom donor (H1). The packing of **V** forms 1D ribbons with a 21 screw axis. This hydrogen bonding pattern forms two rings, namely

an $R_4^4(18)$ ring involving four molecules, and an $R_4^4(14)$ ring involving three molecules as shown in **Figure 7b**.

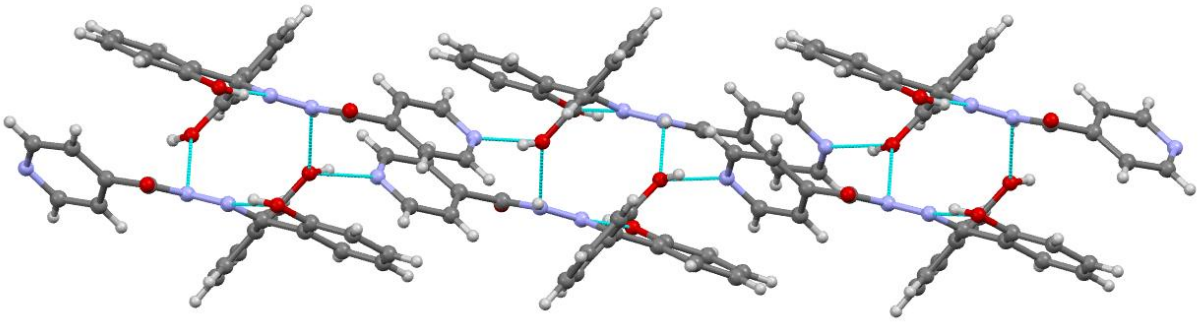

(a)

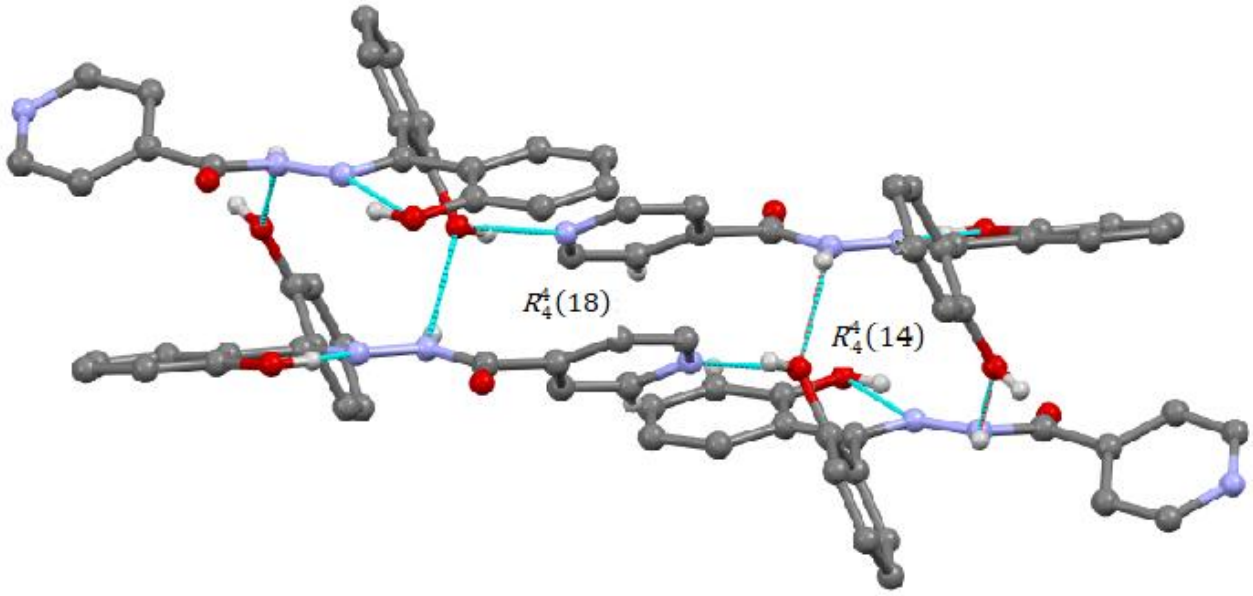

(b)

Figure 7: Packing diagram of **V**, showing (a) the 1D ribbon packing pattern and (b) the two rings formed between the four molecules. As there is a center of inversion, the third ring appearing on the left of the diagram is simply the inverse of the $R_4^4(14)$ ring shown to the right of the diagram.

Structure **VI** is a salt solvate of isoniazid that has been modified with 2,2-dihydroxybenzophenone to yield *N*'-(di-*p*-tolylmethylene)isonicotinohydrazide, chloride salt dihydrate. The source of the chloride ions is via an elimination reaction of the 1,2-dichloroethane

solvent. The salt crystallizes in the $Pca2_1$ space group and the asymmetric unit consists of two molecules of *N*'-(di-*p*-tolylmethylene)isonicotinohydrazide, two water molecules, and two chloride ions. Both modified isoniazid molecules in the asymmetric unit form intramolecular six-membered hydrogen bonded rings involving one of the hydroxyl groups and the hydrazide nitrogen atom (N3). These groups are not involved in intermolecular bonding. The hydrogen atom of the second hydroxyl group of one of the modified isoniazid molecules is hydrogen bonded to a chloride ion. This chloride ion is then hydrogen bonded to a water donor atom, which is in turn bonded to another chloride ion and then another water molecule to form a five molecule long chain (modified isoniazid – chloride – water – chloride – water) (**Figure 2f**). In the packing of structure **VI**, the acidic proton of the pyridyl salt of one molecule is bonded to a chloride ion (one end of the five molecule chain), and the acidic proton of the other modified isoniazid molecule is bonded to a water molecule (the other end of the chain.) The extensive hydrogen bonding of the water molecules and chloride ions result in a 3D packing network. The carbonyl oxygen atom of each modified isoniazid is involved in a C−H···π interaction, stabilizing one of the benzophenone rings. : A packing diagram of **VI**, shown along the *b*-axis, is shown in **Figure 8**.

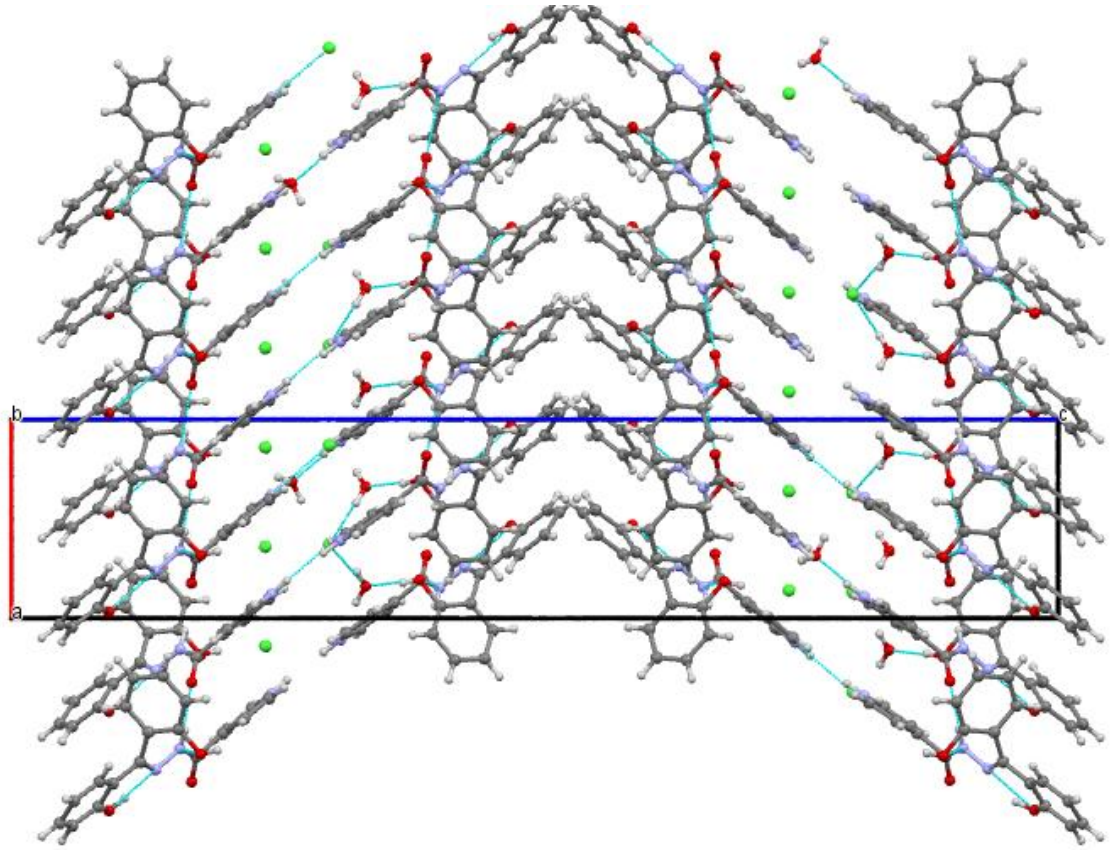

Figure 8: A packing diagram of **VI**, shown along the *b*-axis.

Compound **VII** crystallizes in the $P2_1/c$ space group, and the unit cell contains one molecule of *N*'-(bis(2-hydroxy-4-methoxyphenyl)methylene)isonicotinohydrazide. Each ring of the benzophenone moiety contains one phenol group in the 2-position and one methoxy group in the 4-position. In this compound, the amide :N3 lone pair is masked from the donor and acceptor hydrogen bond functionalities of adjacent molecules by both the steric effect of the benzophenone derivative groups, and by intramolecular hydrogen bonding between the phenol donor group in the 2-position of the 2-hydroxyphenyl ring, O4, and the N3 atom to form a six-membered O4−H4···N3 hydrogen bond. However, one of the phenol groups, O2, has its hydrogen atom free to hydrogen bond further, and forms an O2─H2···N1 heterosynthon to the pyridyl N1. The carbonyl oxygen, O1 bonds to the amide donor atom H1 of an adjacent molecule. These intermolecular bonds result in a 3-dimensional packing network. The methoxy

groups are not involved in any intra- or intermolecular interactions. The packing pattern contains a twofold rotation and a center of inversion about the centre (**Figure 9**).

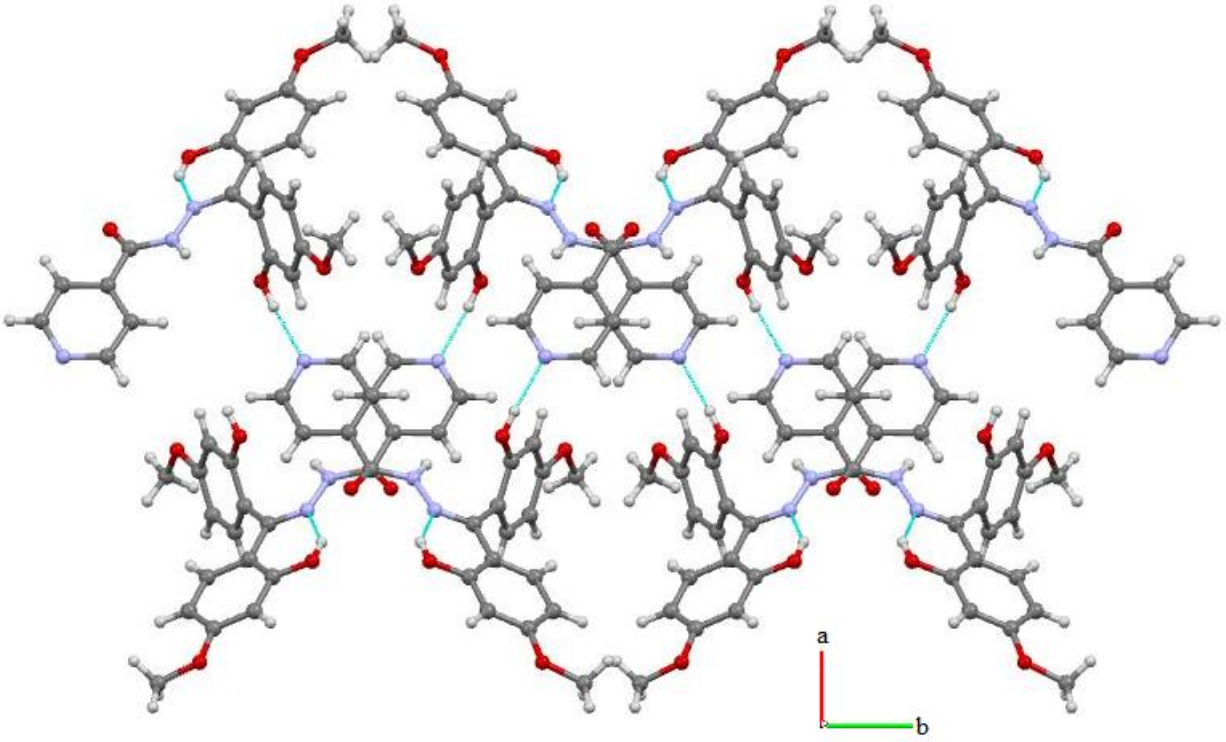

Figure 9: The 3D network formed in the packing of crystal **VII**.

Compound **VIII** crystallizes in the $P2_1/c$ space group, and the unit cell contains one molecule of (*E*)-*N*'-(4-aminophenyl(phenyl)methylene)isonicotinohydrazide). One of the benzophenone rings contains an amino group in the 4-position, although the amino group is disordered over the two rings, with the major disorder component percentage being 57.239(5) %. Each molecule utilizes only two hydrogen bonding sites, namely the carbonyl acceptor, O1 and the amino acceptor, H4D, and the two N1─H4D···O1 heterosynthons form zero-dimensional dimers. This hydrogen bonding pattern forms an $R_2^2(22)$ ring, as shown in **Figure 10**.

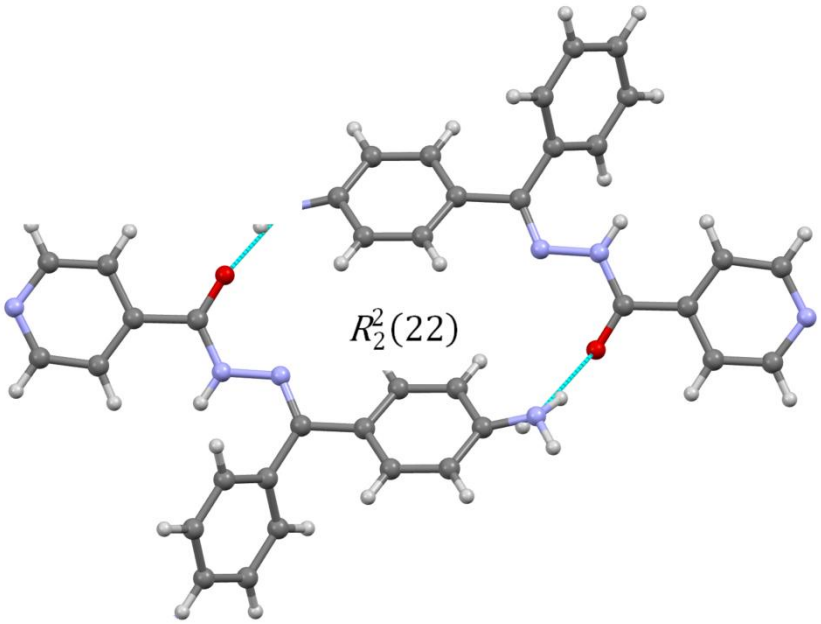

Figure 10: The 0D dimers and $R_2^2(22)$ ring formed by two modified isoniazid molecules in **VIII.**

Compound **IX** crystallizes in the $P2_1/c$ space group, and the unit cell contains one molecule of *N*'-(bis(4-aminophenyl)methylene)isonicotinohydrazide). Each of the benzophenone rings has an amino group in the 4-position. Although crystal **IX** is similar to **VIII**, with only an additional amino group, the intermolecular interactions are much more extensive. The pyridyl nitrogen N2 provides a hydrogen bond acceptor for the amino donor, H4B, of an adjacent molecule via a regular N4─H4B···N2 heterosynthon. The bonding of the carbonyl oxygen atom on each molecule is bifurcated, and bonds to two amino group donors of two different molecules. One hydrogen atom of each amino group bonds to the carbonyl acceptor and the other to the pyridyl nitrogen of neighbouring molecules, thus forming a 3D packing network. The packing is further stabilized by π···π stacking between the benzophenone rings (**Figure 11**). The same $R_2^2(22)$ ring found in crystal **VIII** is also found in **IX**, but the differences in packing between the two crystals are due to the bifurcated bonding of the carbonyl oxygen atom and the involvement of the pyridyl nitrogen atom in intermolecular interactions.

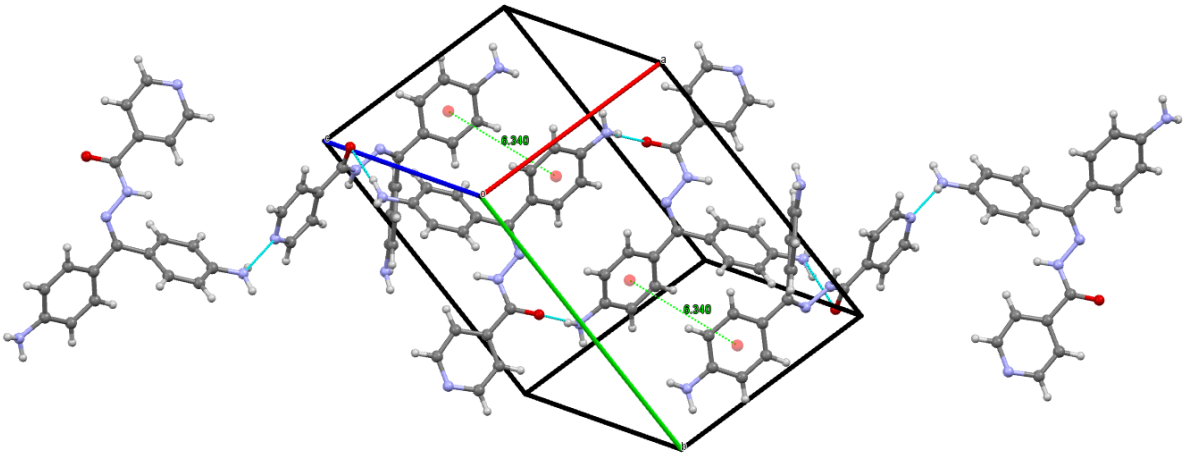

Figure 11: The packing of **IX**, showing the π···π stacking of the benzophenone rings and the carbonyl-amino and pyridyl-amino heterosynthons.

Compound **X** crystallizes in the *Cc* space group and the asymmetric unit contains four molecules of (*E*)-*N*'-((4-(dimethylamino)phenyl)(phenyl)methylene)isonicotinohydrazide), which will be referred to as molecules **A**-**D**. Molecule **A** in the asymmetric unit is hydrogen bonded to molecule **B** via two $N{-}H_{amide}\cdots N_{pyridine}$ heterosynthons which form a $R_2^2(14)$ ring. There is additional π···π stabilization between the pyridyl rings of molecules **A** and **B**, which are stacked on top of each other. There is an additional weak C−H··· π interaction between one of the hydrogen atoms of the pyridyl ring in molecule **A** to the unsubstituted benzophenone ring in molecule **B**. Molecule **B** is hydrogen bonded to molecule **C** solely via three C−H···π interactions. The unsubstituted benzophenone ring of molecule **B** interacts with an *N*-methyl hydrogen atom of the dimethylamino group of molecule **C** via one of the a C−H···π interactions. The second of these interactions is from the *N*-methyl hydrogen atom of the dimethylamino group of molecule **B** to the substituted benzophenone ring of molecule **C**, and the third is a C−H···π interaction of the same substituted benzophenone ring of molecule C to one of the hydrogen atoms on the substituted ring of molecule **B**. Molecule **B** then hydrogen bonds to molecule **D** via a weak C−H···O interaction between the carbonyl oxygen of molecule **B** and one of the hydrogen atoms of the unsubstituted benzophenone rings of molecule **D** (**Figure 12a**). The packing interactions of crystal **X** consists of weak C−H···π and C−H···O interactions. In addition to the C−H···π interactions already described in the asymmetric units, the bonding of the carbonyl oxygen atom acceptor is bifurcated and interacts with two C−H hydrogen donor

atoms on the unsubstituted benzophenone ring of an adjacent molecule (**Figure 12b**). This results in a 1D tape packing arrangement at a 45° angle to the *a*-axis.

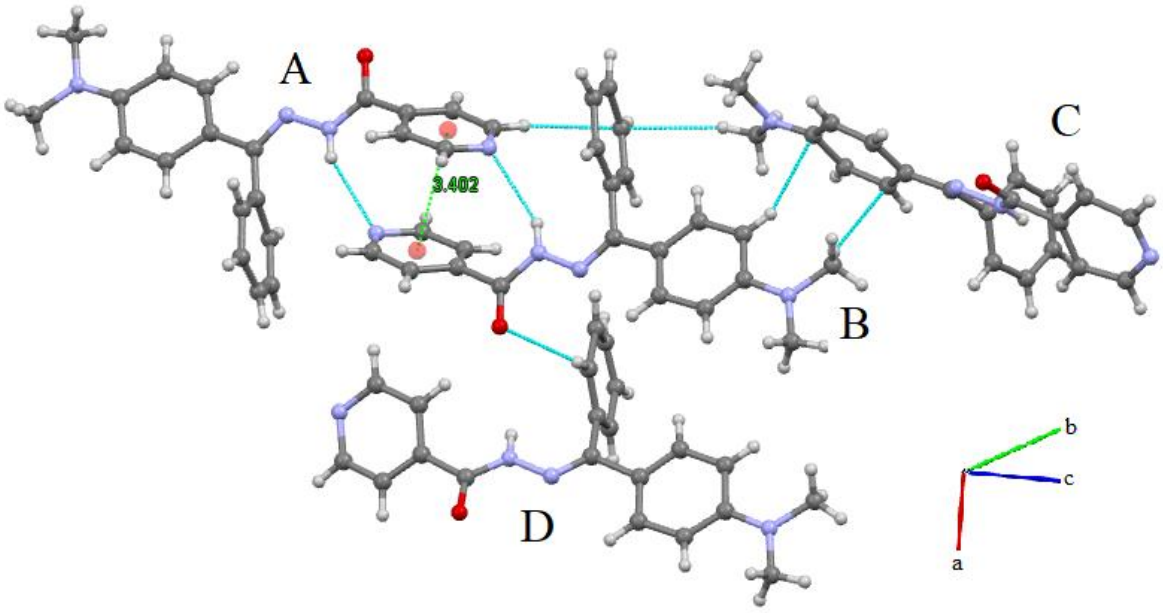

(a)

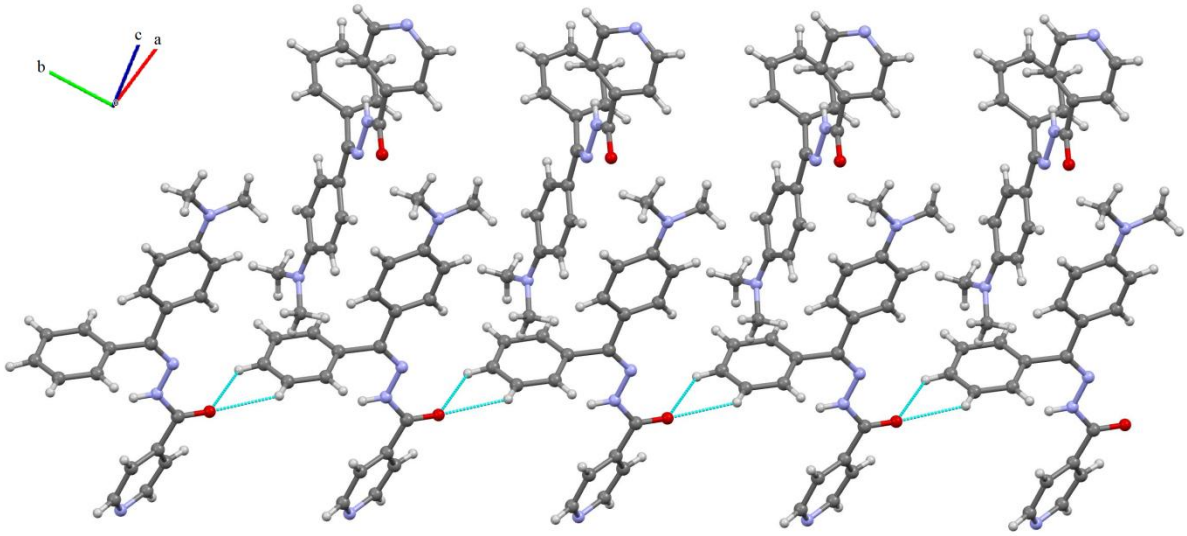

(b)

Figure 12: Heterosynthons and weak C−H···O and C−H···π hydrogen bonding in crystal **X**. Part (a) shows the interactions in the asymmetric unit of **X**, and Part (b) shows the packing.

Conclusion

Ten crystalline derivatives of isoniazid, including one salt solvate were synthesized and structurally characterized. Structure **III** is a hydrate, due to the presence of a water molecule from the dehydration step of the acid-catalyzed condensation reaction. One chloride salt (**VI**) was afforded due to the presence of chloride ions from the elimination reaction of 1,2-dichloroethane. The choice of acid catalyst for the synthesis was dependent on the nature of the electron withdrawing or electron donating properties of the substituents on the benzophenone rings. The synthesized Schiff bases have the desired properties described by Hearn *et al.* as potential agents against multi-drug resistant strains of tuberculosis.

Acknowledgement

The University of the Witwatersrand and the Molecular Sciences Institute are thanked for providing the infrastructure and financial support to do this work. Andreas Lemmerer thanks the Wits Friedel Sellschop award for funding and Mark Smith thanks the Chemistry department of the University of South Africa for the financial support.

Supporting Information Available

Crystallographic data were deposited at the Cambridge Crystallographic Data Center with reference numbers CCDC XXXXXXX-XXXXXXX, which can be requested from The Cambridge Crystallographic Data Centre (http://www.ccdc.cam.ac.uk/data_request/cif). This information is also available free of charge via the internet at http://pubs.acs.org.

References

Aitipamula, S., Wong, A. B. H., Chow, P. S. & Tan, R. B. H. (2013). *CrystEngComm*. **15**, 5877-5887.

Bernstein, J., Davis, R. E., Shimoni, L. & Chang, N.-L. (1995). *Angew. Chem. Int. Ed.* **34**, 1555-1573.

Bruker, SAINT+, . Version 6.02 (Includes XPREP and SADABS) ed. Madison, Wisconsin, USA: Bruker AXS Inc. (2004).

Coelho, T. S., Cantos, J. B., Bispo, M. L. F., Goncalves, R. S. B., Lima, C. H. S., Da Silva, P. E. A. & Souza, M. V. N. (2012). *Infect. Dis. Rep.* **4**, *e*13.

Etter, M. C., Macdonald, J. C. & Bernstein, J. (1990).. *Acta Crystallogr., Sect. B.* **46**, 256-262.

Farrugia, L. (2012). *J. Appl. Crystallogr.* **45**, 849-854.

Hearn, M. J., Cynamon, M. H., Chen, M. F., Coppins, R., Davis, J., Joo-on Kang, H., Noble, A., Tu-Sekine, B., Terrot, M. S., Trombino, D., Thai, M., Webster, E. R. & Wilson, R. (2009). *Eur. J. Med. Chem.* **44**, 4169-4178.

Macrae, C. F., Bruno, I. J., Chisholm, J. A., Edgington, P. R., McCabe, P., Pidcock, E., Rodriguez-Mange, L., Taylor, R., van de Streek, J., & Wood, P. A. (2008). *J. Appl. Cryst.* **41**, 466-470.

Sevukarajan, M., Sodanapalli, R., Thanuja, B. & Nair, R. (2011). *J. Biomed. Sci. and Res.* **3,** 397-402.

Smith, M. G., Forbes, R. P. & Lemmerer, A. (2015). *Cryst. Growth Des.* **15**, 3813-3821.

Sheldrick, G. M. (2015). *Acta Crystallogr., Sect. C.* **71**, 3-8.

Spek, A. (2009). *Acta Crystallogr., Sect. D.* **65**, 148-155.

Xavier, A. & Srividhya, N. (2014). *IOSR-JAC*, **7**, 6-15.

Chapter 6: **Photodimerization of Benzophenone and its Derivatives**

6.1 Introduction

This chapter details a new method of synthesizing benzophenone azines via a photodimerization process and examines the role of the weak C−H···π packing interactions in their supramolecular stucture. The four intermediates of the photodimerization process were also crystallized and their crystal structures are discussed. The crystal structure of di-isoniazid azine, an expected by-product of the photodimerization process, was also described.

NOTE ON CRYSTAL STRUCTURES OF MODIFIED ISONIAZID IN THIS CHAPTER:

Four of the crystals reported in this paper are the same modified isoniazid crystals found in Chapter 5. Their descriptions and crystal structures are repeated in this chapter, but for purposes of publication, depending on which paper is published first, these will paraphrased and fully referenced in the second paper, as the crystal structures of these four crystals are relevant to both studies.

The correlation between the four duplicated structures in the two Chapters is as follows:

Chapter 5	**Chapter 6**
Structure I	Structure I
Structure II	Structure II
Structure III	Structure III
Structure X	Structure IV

Details of the publication status of the paper precede the paper.

6.2 The photodimerization of Schiff bases: synthesis and crystal structures of benzophenone azines and their weak C−H···π interactions

Title of paper:	The photodimerization of Schiff bases: Synthesis and crystal structures of benzophenone azines and their weak C−H···π interactions
Journal:	Will be submitted to *Acta Crystallographica B: Structural Science, Crystal Engineering and Materials*
Reference:	
Status:	Submission Pending. To be submitted by end March 2018.
Date Received:	
Date Revised:	
Date Published:	

Synopsis of Paper

A new method of synthesizing benzophenone azines via a photodimerization process is described. The role of the weak C−H···π packing interactions in their supramolecular stucture is discussed. The four intermediates of the photodimerization process were also crystallized and their crystal structures are discussed. The crystal structure of di-isoniazid azine, an expected by-product of the photodimerization process, was also described.

.

Table 6.1: List of compounds reported in chapter 6.2

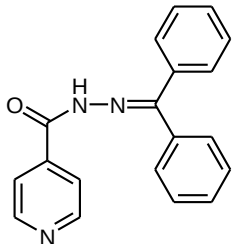	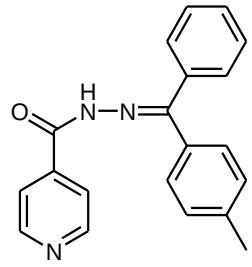
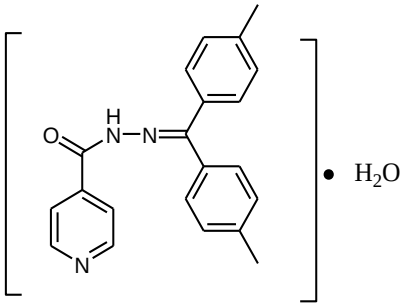	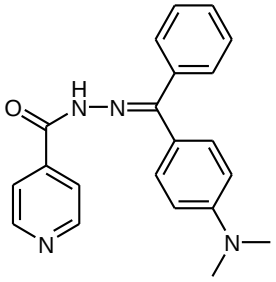
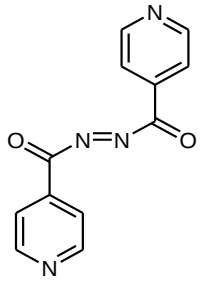	
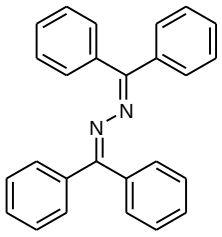	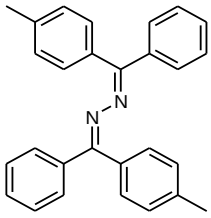
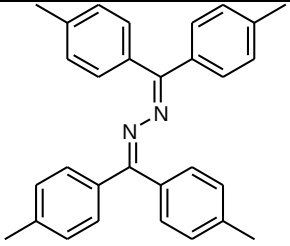	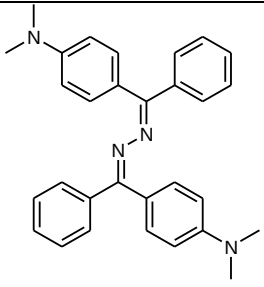

The photodimerization of Schiff bases: Synthesis and crystal structures of benzophenone azines and their weak C−H···π interactions

Mark G. Smith[†] and Andreas Lemmerer*[‡]

†*Department of Chemistry, University of South Africa, Unisa Science Campus, Florida, 1709, Johannesburg, South Africa, and* [‡]*Molecular Sciences Institute, School of Chemistry, University of the Witwatersrand, 2050, Johannesburg, South Africa*

RECEIVED DATE (to be automatically inserted after your manuscript is accepted if required according to the journal that you are submitting your paper to)

To whom correspondence should be addressed:

Dr. Andreas Lemmerer, Molecular Sciences Institute, School of Chemistry, University of the Witwatersrand, Private Bag 3, 2050, Johannesburg, South Africa.
E-mail: andreas.lemmerer@wits.ac.za. Fax: +27-11-717-6749. Tel: +27-11-717-6711.

ABSTRACT:

Four benzophenone azines were synthesized through a photodimerization process. The crystals are constructed purely through weak C–H···π packing interactions, with additional π···π stabilization in two of the crystals. The four intermediates of the photodimerization process were also crystallized and their crystal structures are discussed. The packing of three of these intermediates involves weak C–H···O interactions. The crystal structure of di-isoniazid azine, an expected by-product of the photodimerization process, was also described.

KEYWORDS: Photodimerization, Schiff bases, isoniazid, benzophenone, azines,

Introduction

Ketone azides are frequently used in synthetic chemistry as starting materials for the synthesis of basic aromatic rings (Kost and Grandberg, 1959, Carty, 1972, Wuts and Greene, 2006), as well as for ligands in metal complex catalysis (Verner and Potacek, 2006). The synthesis of benzophenone azine was first proposed by Lauer and Dyer in 1942 (Lauer and Dyer, 1942). They reported benzophenone azine as one of several products of the oxidation of benzophenone oxime (**Figure 1**). Separation of the product from the other reaction products was required. The presence of benzophenone azine was supported by molecular weight determinations. In 1995, Saha *et al*. (Saha *et al*., 1995) synthesized benzophenone azine via the reaction of the iron-containing Lewis acid complex $[\eta^5\text{-}(C_5H_5)Fe(CO)_2(THF)]^+[BF_4]^-$ and provided evidence of an iron carbine intermediate. Inert conditions were required for the synthesis. The crystal and molecular structure was determined and was used to confirm that the azine, rather than the azitine product was afforded.

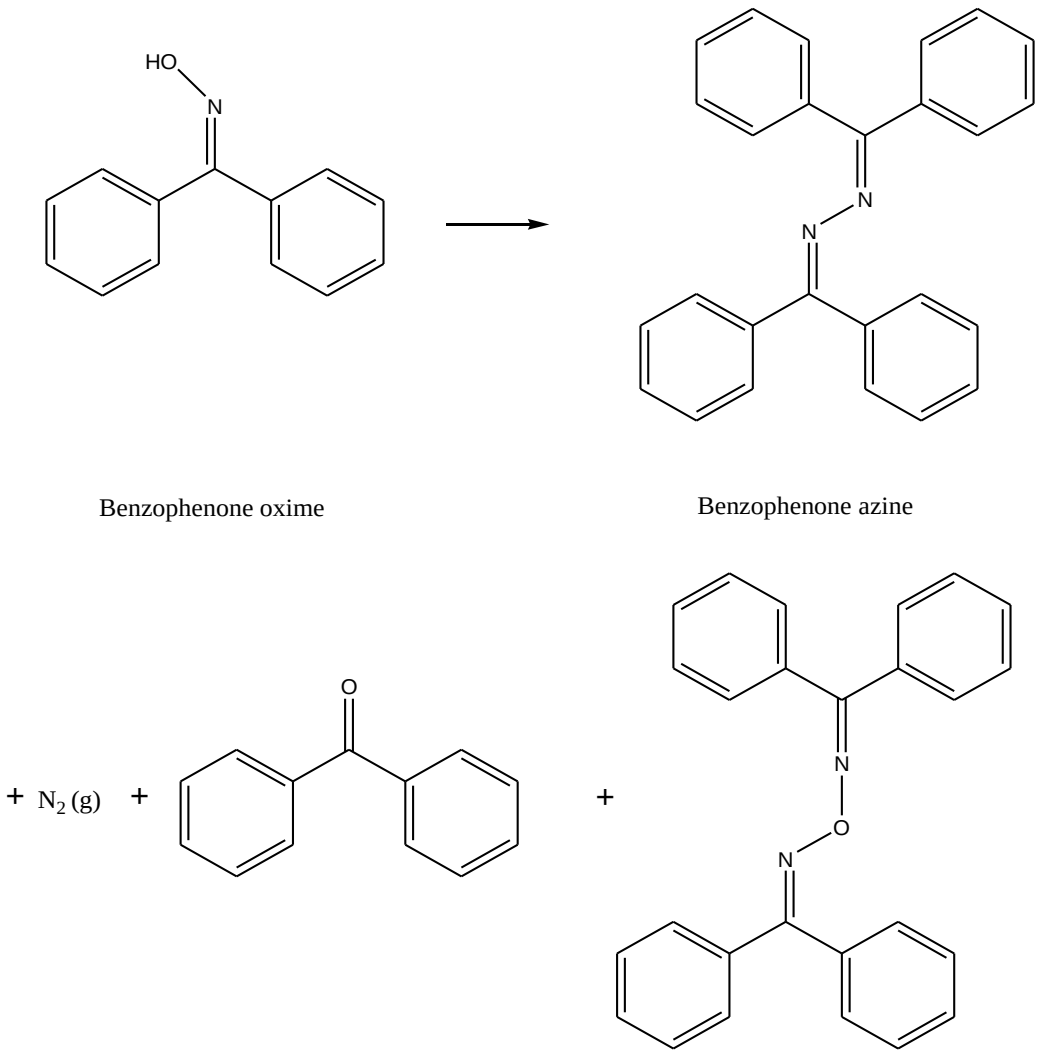

Figure 1: Lauer and Dyer's method of synthesis of benzophenone azine from benzophenone oxime showing also the many side products produced from their method of synthesis

The structures reported in this study describe the synthesis of benzophenone azine and three other benzophenone azine derivatives via a two step synthesis: (1) Step 1 is the covalent modification of isonicotinic acid hydrazide (isoniazid) with benzophenone (or a derivative of benzophenone) via a condensation reaction to form an imine (Schiff base). (2) Step 2 is the photodimerization of this Schiff base intermediate by exposure to sunlight.

As proof of concept, four benzophenone derivatives, namely benzophenone, 4-methylbenzophenone, 4,4-dimethylbenzophenone and 4-(dimethylamino)benzophenone were

reacted with isoniazid in an acid catalyzed condensation reaction to yield the corresponding Schiff base intermediates and then photodimerized in sunlight to yield the corresponding benzophenone azine products (**Scheme 1**).

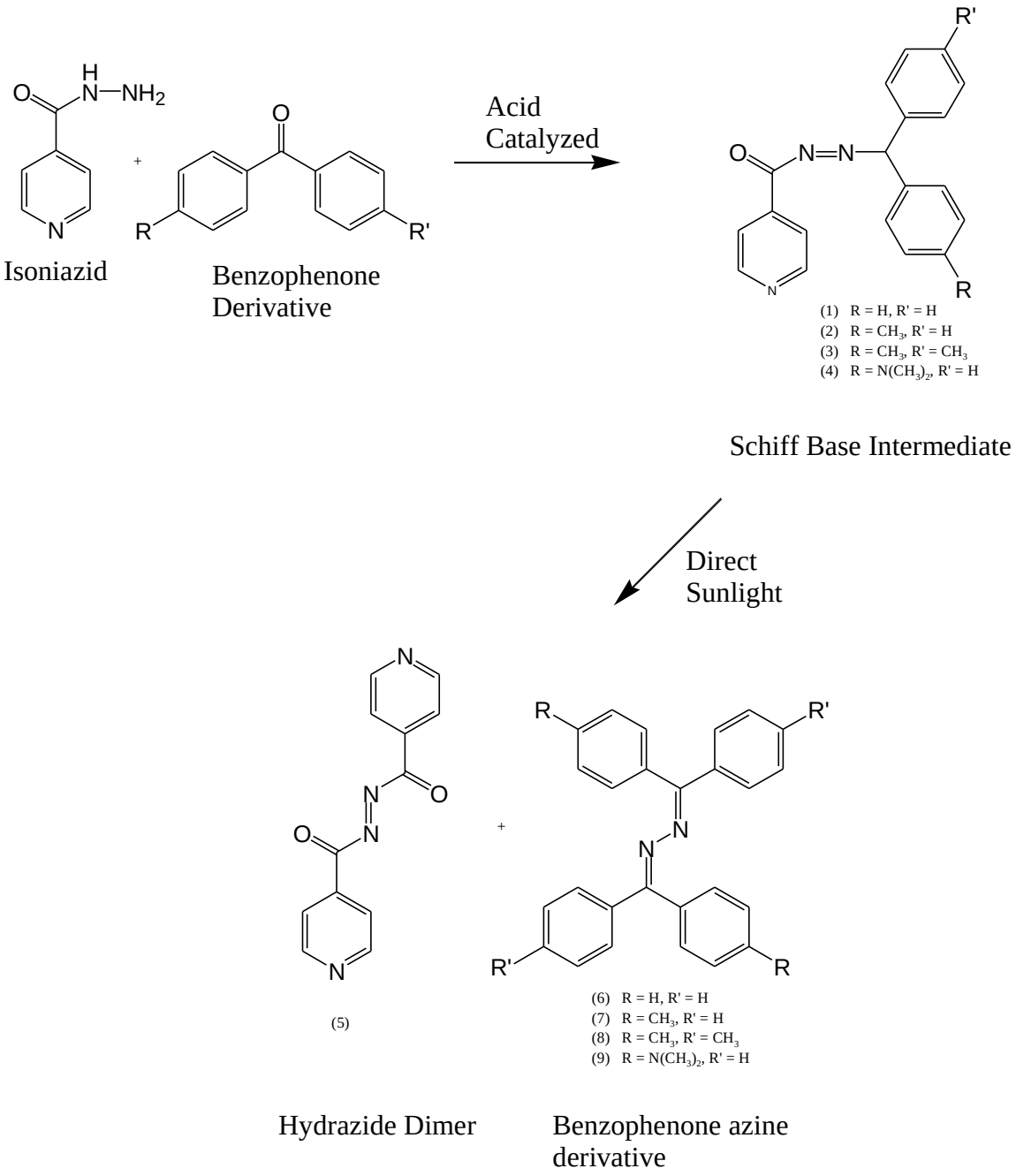

Scheme 1: A schematic diagram detailing the synthesis pathway of benzophenone azines.

The photodimerization process is supported by the fact that, theoretically, photodimerization should result not only in the expected product, the benzophenone azines, but should also yield a hydrazide dimer byproduct (**5** in S**cheme 1**). The hydrazide dimer was indeed observed and confirmed as a byproduct of each reaction. The single-crystal XRD structures of the four Schiff base imine intermediates, the four azine products, as well as the expected hydrazide byproduct are reported here.

In Desiraju's article on weak hydrogen bonds, he describes C−H···π interactions as being "supportive" interactions and mentions that although C−H···π interactions are fairly ubiquitous, they are "*very weak and merely exist in a structure that is wholly determined by other interactions*" (Desiraju, 2005). He also asks the question of whether it is possible to engineer crystal structures consisting of only weak interactions. Two of the benzophenone azines described in this paper are constructed purely of weak C−H···π interactions and two more are constructed of only C−H···π interactions with additional π···π stacking between their aromatic rings. All four benzophenone azines do not have any traditional hydrogen bonds between molecules. In addition to the weak C−H···π interactions described, three of the intermediate products that were crystallized and described in this paper pack together via the much rarer C−H···O and C−H···N interactions discussed by Desiraju in his same publication (Desiraju, 2005).

In this paper, we therefore describe four benzophenone azines synthesized through a photodimerization process. We describe how these azines crystals are constructed purely through weak C−H···π interactions, with additional π···π stabilization in two of the crystals. We also describe the crystallization and crystal structures of the four intermediates of the synthetic process, and the C−H···O interactions in the packing of three of these intermediates. Finally, we describe the crystal structure of the di-isoniazid azine, which is a necessary by-product of the photodimerization process and was crystallized in this study.

Experimental Methods

Synthesis.

Synthesis of Schiff base intermediates:

N'-(diphenylmethylene)isonicotinohydrazide, I

0.0920 g of isonicotinic acid hydrazide (0.6708 mmol) and 0.1202 g of benzophenone (0.6596 mmol) were added into a sample vial. 0.0111 g of *p*-toluenesulphonic acid monohydrate (0.0584 mmol) was added to catalyze the reaction. The solids were dissolved in 3 mL of a 1:1 mixture of AP-grade 1,2-dichloroethane and 1,1,1-trichloroethane and refluxed in a closed sealed screw-top vial for 72 hours at 50°C, and were left to stand at room temperature very slightly opened to the atmosphere. Colourless needles were afforded after 3 days.

(*E*)-*N*'-(phenyl(*p*-tolyl)methylene)isonicotinohydrazide), II

0.0964 g of isonicotinic acid hydrazide (0.703 mmol) and 0.1386 g of 4-methylbenzophenone (0.7062 mmol) were added into a sample vial. 0.0124 g of *p*-toluenesulphonic acid monohydrate (0.0652 mmol) was added to catalyze the reaction. The solids were dissolved in 3 mL of a 2:1 mixture of AP-grade ethanol and acetonitrile and refluxed in a closed sealed screw-top vial for 5 days at 110°C, and were left to stand at room temperature very slightly opened to the atmosphere. Colourless needles were afforded after 3 days.

N'-(di-*p*-tolylmethylene)isonicotinohydrazide, III

0.1197 g of isonicotinic acid hydrazide (0.8728 mmol) and 0.1841 g of 4,4-dimethylbenzophenone (0.8755 mmol) were added into a sample vial. 1 drop of 5M hydrochloric acid was added to catalyze the reaction. The solids were dissolved in 3 mL of methanol and refluxed in a closed sealed screw-top vial for 3 days at room temperature, followed by work-up with sodium bicarbonate: the solution was saturated with sodium bicarbonate, stirred for 5 minutes and then filtered. The filtered solution was then left to stand at room temperature very slightly opened to the atmosphere. Yellow plates were afforded after 3 days.

(*E*)-*N*'-((4-(dimethylamino)phenyl)(phenyl)methylene)isonicotinohydrazide), IV

0.1043 g of isonicotinic acid hydrazide (0.7605 mmol) and 0.1732 g of 4-(dimethylamino)benzophenone (0.7688 mmol) were added into a sample vial. 0.0232 g of *p*-toluenesulphonic acid monohydrate (0.122 mmol) was added to catalyze the reaction. The solids were dissolved in 3 mL of a methanol and refluxed in a closed sealed screw-top vial for 72 hours at 100°C, and were left to stand at room temperature very slightly opened to the atmosphere. Yellow blocks were afforded after 3 days.

Outcome of the photodimerization reactions:

The method of synthesis for crystals **V**, **VI**, **VII**, **VIII** and **IX** is identical and is therefore summarized below the names described here:

(E)-diazene-1,2-diylbis(pyridine-4-ylmethanone), V
1,2-bis(diphenylmethylene)hydrazine, VI
(1*Z*,2*Z*)-1,2-bis(phenyl(*p*-tolyl)methylene)hydrazine, VII
1,2-bis(di-*p*-tolylmethylene)hydrazine, VIII
4,4'-(1*Z*,1'*Z*)-hydrazine-1,2-diylidenebis(phenylmethan-1-yl-1-ylidene)bis(*N*,*N*-dimethylaniline), IX

After crystals **I**, **II**, **III**, **IV** had crystallized, the clear glass vials still containing some of the solvent and the crystals were sealed and placed on the windowsill in direct sunlight for 4 weeks. Crystals **V** and **VI** were afforded from crystal **I**, crystals **V** and **VII** were afforded from crystal **II**, crystals **V** and **VIII** were afforded from crystal **III**, and crystals **V** and **IX** were afforded from crystal **IV**.

Crystal Data and X-ray Structure Analysis.

Intensity data for the nine crystal structures were collected on a Bruker APEX II CCD area detector diffractometer with graphite monochromated Mo-K_α radiation (50 kV, 30 mA) at 173K. The collection method involved ω-scans with a 0.5° width. *SAINT+* version 6.02.6 software was used for data reduction and *SADABS* was used to make empirical absorption corrections (Bruker, 2004). The crystal structures were solved using direct methods on *SHELXS-97* (Sheldrick, 2015). Non-hydrogen atoms were first refined isotropically, followed by anisotropic refinement by full matrix least-squares calculations based on F^2 using *SHELXL-2017* (Sheldrick, 2015). C-bound H atoms were located in the difference electron density map, then positioned geometrically and were allowed to ride on their respective parent atoms, with thermal displacement parameters 1.2 times that of the parent C atom. Where possible, the coordinates and isotropic displacement parameters of the N-bound and O-bound H atoms involved in hydrogen bonding interactions were allowed to refine freely, except for crystals **IV** due to poor refinement stability. The diffraction data and refinement statistics of crystal **IV** was poor even after numerous attempts at recrystallization. Diagrams and publication material were generated using *WinGX* (Farrugia, 2012), *ORTEP-3* (Farrugia, 2012), *PLATON* (Spek, 2009) and *MERCURY (*Macrae, C. F. e*t al.*, 2008). The crystallographic data of each crystal is summarized in Table 1.

Table 1 Crystallographic data for compounds **I-V**

	I	**II**	**III**	**IV**	**V**
Formula	$C_{19}H_{15}N_3O$	$C_{20}H_{17}N_3O$	$C_{21}H_{21}N_3O_2$	$C_{20}H_{20}N_4O_2$	$C_{12}H_{14}N_4O_4$
M_r	301.34	315.36	347.41	348.40	278.27
Temperature/K	173(2)	173(2)	173(2)	173(2)	173(2)
Wavelength/Å	0.71073	0.71073	0.71073	0.71073	0.71073
Crystal size/mm^3	0.226×0.324×0.522	0.066×0.091×0.325	0.084×0.169×0.384	0.093×0.196×0.256	0.124×0.169×0.382
Crystal system	Orthorhombic	Triclinic	Monoclinic	Monoclinic	Orthorhombic
Space group	$P2_12_12_1$	$P\bar{1}$	$P2_1/c$	Cc	$Fdd2$
a/Å	9.7738(4)	7.1641(7)	21.3512(13)	13.200(2)	24.2397(12)
b/Å	9.9605(5)	10.7669(10)	5.9227(4)	13.698(2)	28.1272(13)
c/Å	15.8005(7)	12.0237(10)	14.8729(11)	39.908(7)	3.7546(2)
α/°	90	64.009(4)	90	90	90
β/°	90	82.346(5)	106.040(6)	97.004(5)	90
γ/°	90	82.885(5)	90	90	90
V/Å^3	1538.21(12)	823.99(13)	1807.6(2)	7162(2)	2559.9(2)
Z	4	2	4	16	8
ρ (calcd)/Mg m^{-3}	1.301	1.271	1.277	1.292	1.444
μ/mm^{-1}	0.083	0.081	0.084	0.086	0.111
F(000)	632	332	736	2944	1168
Θ Range for data	2.417 to 27.989	1.892 to 25.495	1.985 to 25.491	2.76 to 26.36	2.218 to 27.997
Reflections collected	27237	9199	10908	17910	5738
No. of unique data	3710 [0.0421]	3066 [0.0755]	3256 [0.1805]	10563 [0.0512]	1439 [0.0503]
No. data with $I \geq 2\sigma(I)$	3496	1430	1139	11901	1306
Final R($I \geq 2\sigma(I)$)	0.0309	0.0627	0.0521	0.1265	0.0394
Final wR_2 (all data)	0.0816	0.1525	0.1103	0.4207	0.0970
CCDC deposition					

	VI	**VII**	**VIII**	**IX**
Formula	$C_{26}H_{20}N_2$	$C_{28}H_{24}N_2$	$C_{30}H_{28}N_2$	$C_{30}H_{30}N_4$
M_r	360.44	388.49	416.54	446.58
Temperature/K	173(2)	173(2)	173(2)	173(2)
Wavelength/Å	0.71073	0.71073	0.71073	0.71073
Crystal size/mm^3	0.260×0.271×0.307	0.088×0.146×0.502	0.403×0.127×0.094	0.085×0.107×0.226
Crystal system	Monoclinic	Orthorhombic	Triclinic	Triclinic
Space group	*C*2/c	*P*ca2$_1$	$P\bar{1}$	$P\bar{1}$
a/Å	21.9428(18)	18.5504(15)	6.4018(2)	6.4693(2)
b/Å	5.4417(4)	5.3952(5)	10.0182(3)	9.3909(3)
c/Å	16.1168(14)	21.3459(16)	10.3622(3)	11.0678(4)
α/°	90	90	116.288(2)	111.711(2)
β/°	94.450(4)	90	92.941(2)	98.257(2)
γ/°	90	90	99.725(2)	100.123(2)
V/Å^3	1918.6(3)	2136.4(3)	581.27(3)	598.76(4)
Z	4	4	1	1
ρ (calcd)/Mg m^{-3}	1.248	1.208	1.190	1.238
μ/mm^{-1}	0.073	0.070	0.069	0.074
F(000)	760	824	222	238
Θ Range for data	1.862 to 27.998	1.908 to 25.496	2.215 to 27.998	2.034 to 27.996
Reflections collected	9256	13097	13248	6110
No. of unique data [R(int)]	2283 [0.0400]	3956 [0.1038]	2805 [0.0662]	2768 [0.0341]
No. data with $I \geq 2\sigma(I)$	2024	2009	1866	1512
Final R($I \geq 2\sigma(I)$)	0.0392	0.0673	0.0528	0.0532
Final wR_2 (all data)	0.1124	0.1645	0.1498	0.1295
CCDC deposition number				

Results and discussion

The photodimerization of the covalently modified isoniazid compound (**I**) to afford the benzophenone azide (**VI**) was discovered after the solution for (**I**) was inadvertently placed on the windowsill in direct sunlight and had been allowed to crystallize. On determining the crystal structure, the structure was found to be that of the isoniazid dimer (**V**). Photodimerization was suspected, and on examining the crystals, it was found that the benzophenone azine (**VI**) was also present in the vial. As proof of concept, isoniazid was then covalently modified with four different benzophenone derivatives (benzophenone, 4-methylbenzophenone, 4,4-dimethylbenzophenone and 4-dimethylaminobenzophenone) and the crystal structures of the corresponding Schiff base products was determined (crystal structures **I**, **II**, **III** and **IV**). These were then placed in direct sunlight for four weeks and the crystal structures of the products were determined (crystal structures **V**, **VI**, **VII**, **VIII**, **IX**). Crystals **V** and **VI** were afforded from crystal **I**, crystals **V** and **VII** were afforded from crystal **II**, crystals **V** and **VIII** were afforded from crystal **III**, and crystals **V** and **IX** were afforded from crystal **IV**. The crystal structures of the products are described here.

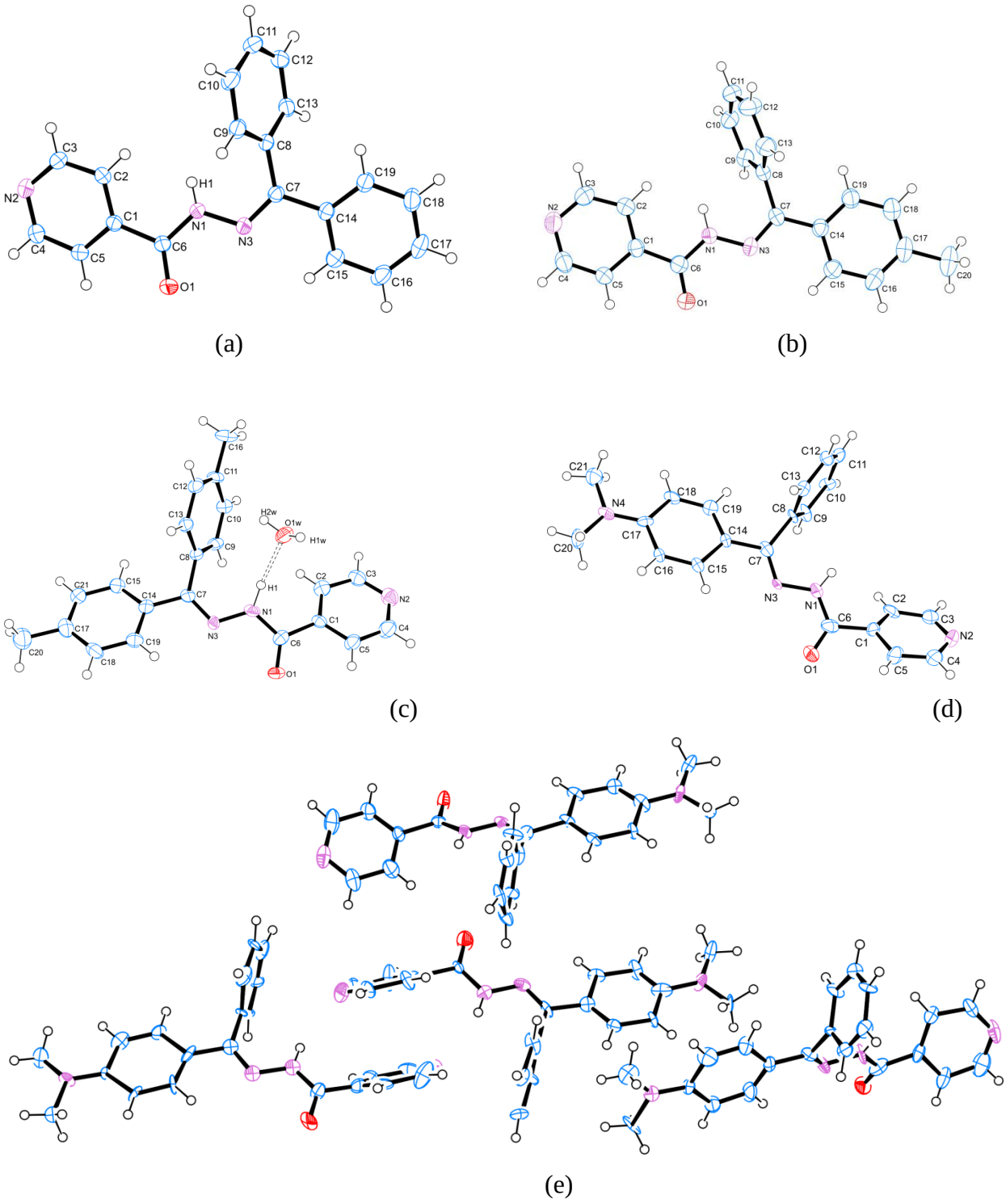

Figure 2: Asymmetric units of (a) crystal **I**, (b) crystal **II**, (c) crystal **III**. Part (d) shows the numbering scheme of a quarter of the asymmetric unit of crystal **IV** (which has four molecules in the asymmetric unit), for clarity. The complete asymmetric unit of **IV** is shown in (e) without atom labels.

Compound **I** crystallizes in the $P2_12_12_1$ space group and the asymmetric unit contains one molecule of *N*'-(diphenylmethylene)isonicotinohydrazide, the product of the covalent modification of isoniazid with benzophenone. The modified isoniazid molecules in **I** hydrogen bond to each other via the $N{-}H_{amide}\cdots N_{pyridine}$ heterosynthon (**Figure 3**) and form one-dimensional (1D) ribbons along the *a*-axis with translational symmetry via a twofold screw axis along the crystallographic *a*-axis, stabilized by π-stacking. The ribbons are formed via chains of seven atoms between hydrogen bonds, with graph-set notation $C_1^1(7)$ (Bernstein *et al*., 1995).

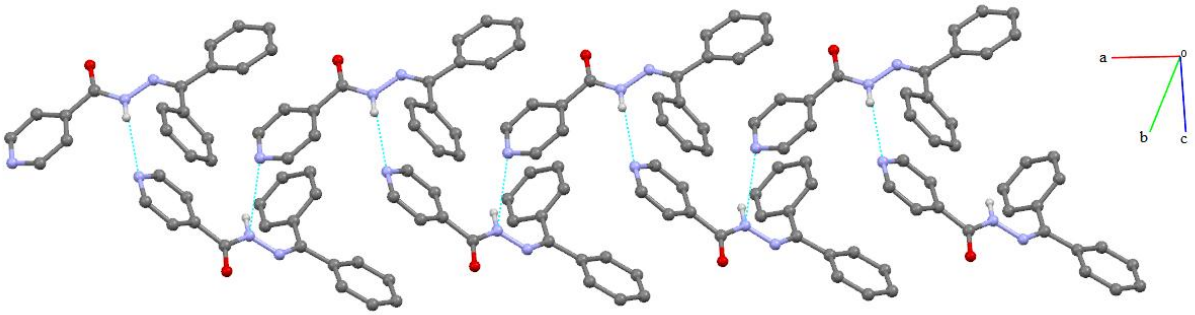

Figure 3: Packing diagram of **I**. One dimensional ribbons extend along the *a*-axis.

Compound **II** crystallizes in the $P\bar{1}$ space group and the asymmetric unit contains one molecule of (*E*)-*N*'-(phenyl(*p*-tolyl)methylene)isonicotinohydrazide). The molecules are aligned in parallel planes, and held together via multiple weak C−H···O and C−H···N interactions and further stabilized via π···π stacking. Each molecule interacts with an adjacent molecule on one side of its plane by a carbonyl oxygen atom (O1) that is hydrogen bonded via a weak C−H···O interaction to a C−H hydrogen atom (H13) of the non-substituted benzophenone ring on an adjacent molecule to form a $R_2^2(16)$ ring. The pyridyl nitrogen atom (N2) also interacts with a hydrogen atom of the methyl group substituent of the other benzophenone ring of the adjacent molecule (H20C) via a weak C−H···N hydrogen bond. On the opposite side of each plane, the hydrazide nitrogen (N3) of each molecule is similarly involved in C−H···N hydrogen bonding, but to a C−H hydrogen atom on the non-substituted benzophenone ring of the adjacent molecule to form a $R_2^2(10)$ ring. The packing is further stabilized by π···π stacking along to form 1D ribbons along the *a*-axis (**Figure 4**).

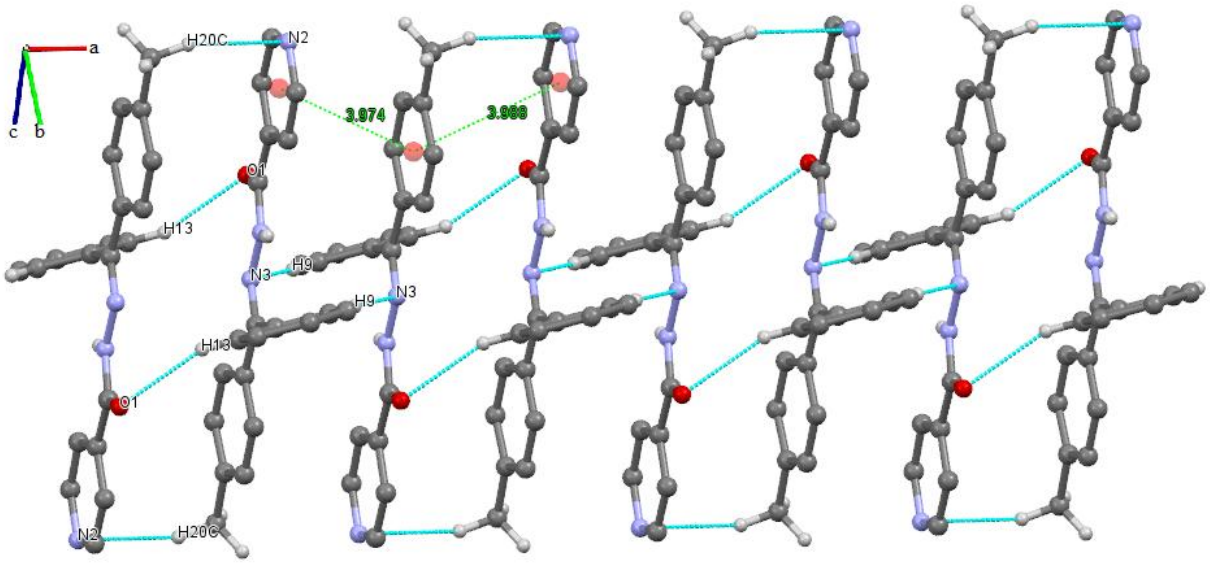

Figure 4: Packing diagram of **II**.

Compound **III** crystallizes in the monoclininc $P2_1/c$ space group and the asymmetric unit contains one molecule of *N*'-(di-*p*-tolylmethylene)isonicotinohydrazide and one water molecule. The hydrate version of isoniazid molecules that have been covalently modified via reaction with ketones are common, as the water molecule is is a byproduct of the acid-catalyzed condensation reaction. This reaction occurs via nucleophilic attack on the carbonyl group by the amine nitrogen to form an unstable carbinolamine moiety, followed by acid catalyzed dehydration to form an imine (Xavier and Srividhya, 2014). In the asymmetric unit the hydrogen bond occurs between the amide nitrogen atom (H1) and the water oxygen atom (O1w). The packing of **III** is a three-dimensional (3D) network with all molecules being hydrogen bonded to water. Each water molecule has three hydrogen bonds and an O−H···π interaction. The bonding of the carbonyl oxygen atom acceptor of the modified isoniazid molecule is bifurcated and hydrogen bonds to both water hydrogen donors. One of the water hydrogen atoms is also hydrogen bonded to the isoniazid pyridine nitrogen acceptor atom (**Figure 5a**). The other water hydrogen atom forms an O−H···π interaction with one of the benzophenone rings on an adjacent modified isoniazid molecule (**Figure 5b**). The oxygen atom of this water molecule acts as a hydrogen bond acceptor to the amide N−H donor atom. The packing is further stabilized by π···π stacking of the pyridyl rings along the *c*-axis.

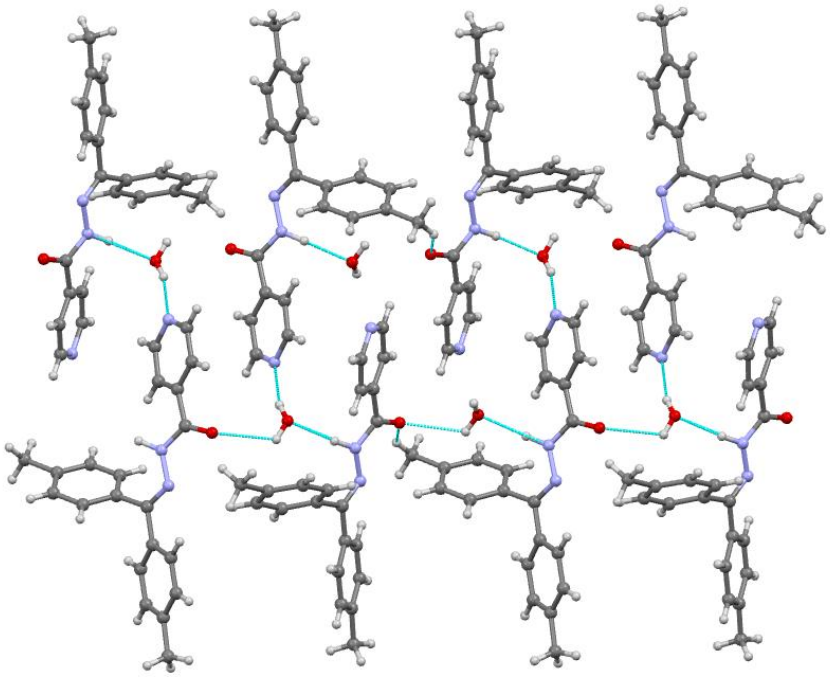

(a)

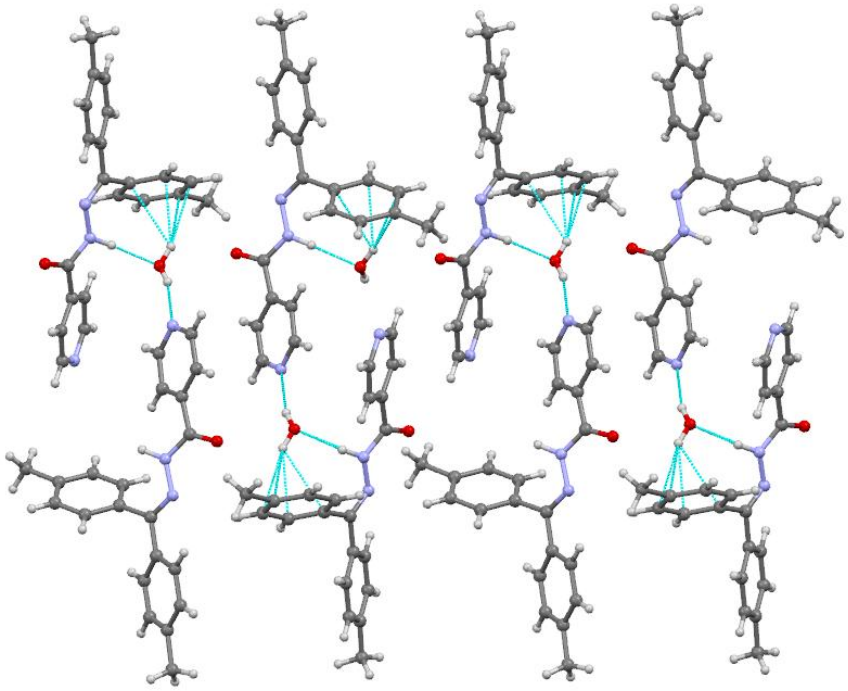

(b)

Figure 5: Packing diagram of **III** showing (a) regular heterosynthons of water with modified isoniazid and (b) the O−H···π interaction between water and the aromatic benzophenone ring.

Compound **IV** crystallizes in the *C*c space group and the asymmetric unit contains four molecules of (*E*)-*N*'-((4-(dimethylamino)phenyl)(phenyl)methylene)isonicotinohydrazide), which will be referred to as molecules **A**-**D**. Molecule **A** in the asymmetric unit is hydrogen bonded to molecule **B** via two $N{-}H_{amide}\cdots N_{pyridine}$ heterosynthons which form a $R_2^2(14)$ ring. There is additional $\pi\cdots\pi$ stabilization between the pyridyl rings of molecules **A** and **B**, which are stacked on top of each other. There is an additional weak C−H··· π interaction between one of the hydrogen atoms of the pyridyl ring in molecule **A** to the unsubstituted benzophenone ring in molecule **B**. Molecule **B** is hydrogen bonded to molecule **C** solely via three C−H···π interactions. The unsubstituted benzophenone ring of molecule **B** interacts with an *N*-methyl hydrogen atom of the dimethylamino group of molecule **C** via one of the a C−H···π interactions. The second of these interactions is from the *N*-methyl hydrogen atom of the dimethylamino group of molecule **B** to the substituted benzphenone ring of molecule **C**, and the third is a C−H···π interaction of the same substituted benzophenone ring of molecule **C** to one of the hydrogen atoms on the substituted ring of molecule **B**. Molecule **B** then hydrogen bonds to molecule **D** via a weak C−H···O interaction between the carbonyl oxygen of molecule **B** and one of the hydrogen atoms of the unsubstituted benzophenone rings of molecule **D** (**Figure 6a**). The packing interactions of crystal **IV** consists of weak C−H···π and C−H···O interactions. In addition to the C−H···π interactions already described in the asymmetric unit, the bonding of the carbonyl oxygen atom acceptor is bifurcated and interacts with two C−H hydrogen donor atoms on the unsubstituted benzophenone ring of an adjacent molecule (**Figure 6b**). This results in a 1D tape packing arrangement at a 45° angle to the *a*-axis.

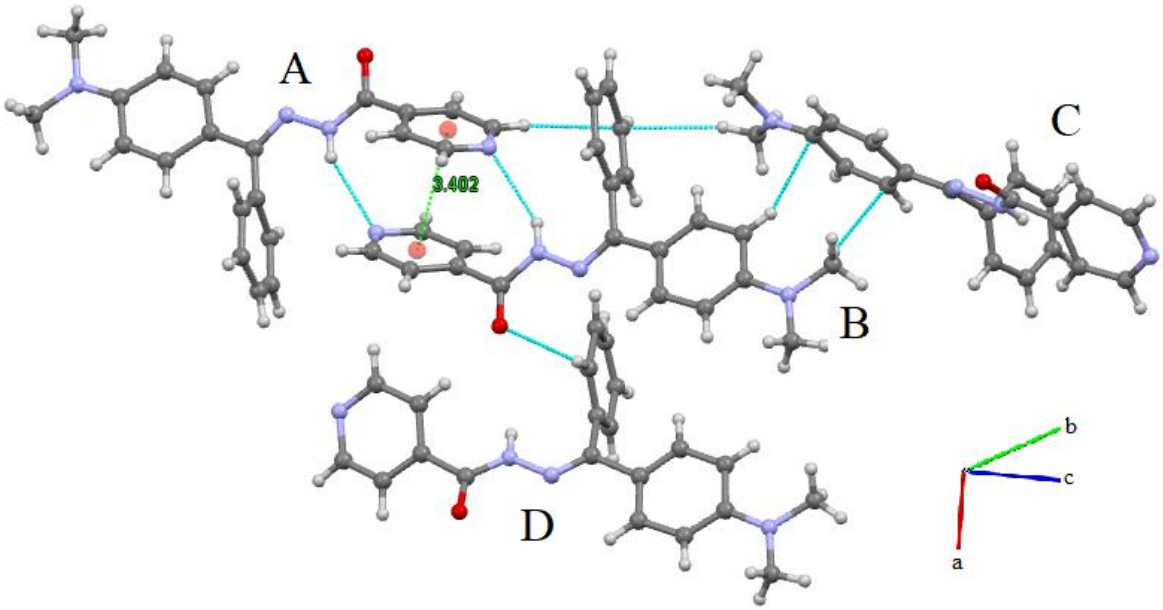

(a)

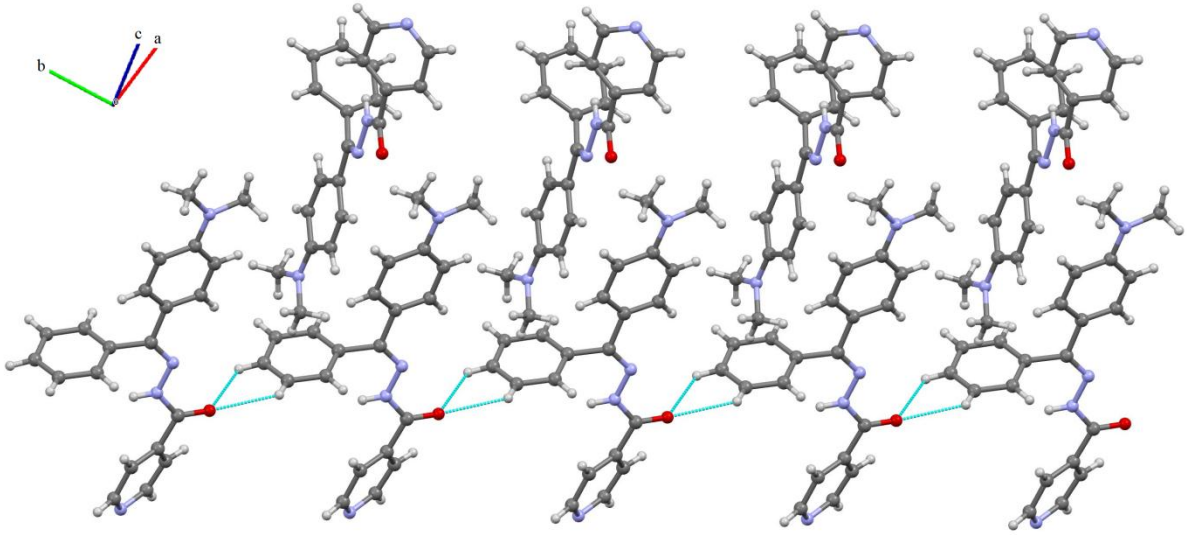

(b)

Figure 6: Heterosynthons and weak C−H···O and C−H···π hydrogen bonding in crystal **IV**. Part (a) shows the interactions in the asymmetric unit of **IV**, and Part (b) shows the packing. Note that the only interactions in the packing are weak C−H···O hydrogen bonds.

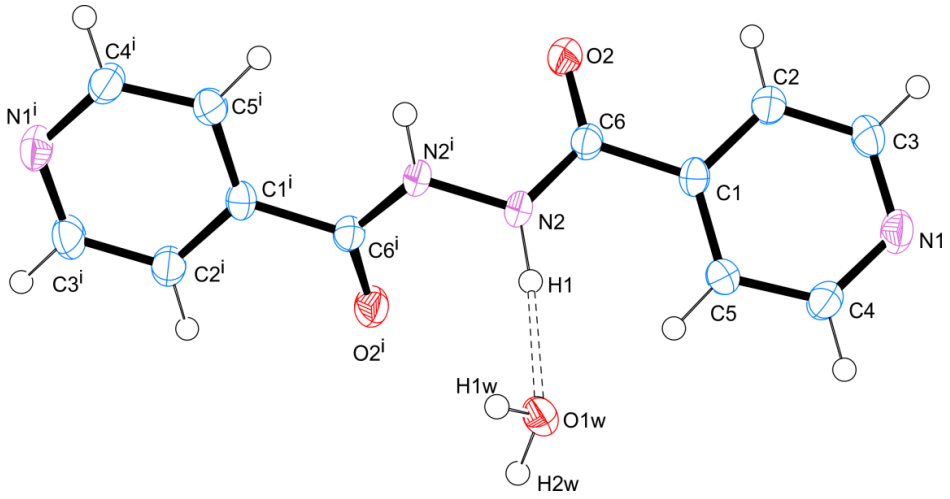

Figure 7: Asymmetric unit of di-isoniazid azine .

Compound **V** is the di-isoniazid azine that was found to form concurrently with crystals **VI**, **VII**, **VIII** and **IX**. It crystallizes in the orthorhombic *F*dd2 space group and the asymmetric unit contains half a molecule of the di-isoniazid azine, (*E*)-diazene-1,2-diylbis(pyridine-4-ylmethanone, and one water molecule (**Figure 7**). The source of the water molecule is the byproduct from the previous step of the synthesis, namely the covalent modification of isoniazid, as previously described for crystal **III**, and the water molecule crystallizes together with the di-isoniazid azine molecule. The hydrogen bonding in the asymmetric unit is via the $N{-}H_{amide}\cdots O_{water}$ heterosynthon with one of the two amide hydrogen atoms (H1) acting as the hydrogen bond donor, and the water oxygen atom as the acceptor. Lemmerer *et al.* has reported a series of five hydrates of modified isoniazid. In all five structures, the hydrazide $N{-}H_{amide}\cdots O_{water}$ and the $O{-}H_{water}\cdots O_{carbonyl}$ synthons were observed. The hydrogen bonding pattern observed in crystal **V** corresponds to the synthons observed in the five reported hydrates (Lemmerer *et al.*, 2011). Crystal **V** packs in a 3D network, with the crystal structure being held together by hydrogen bonding to the water molecule. Each water molecule is bonded to three different isoniazid azine molecules. In addition to the $N{-}H_{amide}\cdots O_{water}$ heterosynthon described in the asymmetric unit, one of the water hydrogen atoms acts as the hydrogen bond donor in the $O{-}H_{water}\cdots N_{pyridine}$ heterosynthon to a second azine molecule, and the carbonyl oxygen atom (O2) of the third azine molecule provides the acceptor for the other hydrogen donor of the water molecule (**Figure 8a**). Each set of four azine molecules and two water molecules form a $R_4^4(14)$ ring (**Figure 8b**).

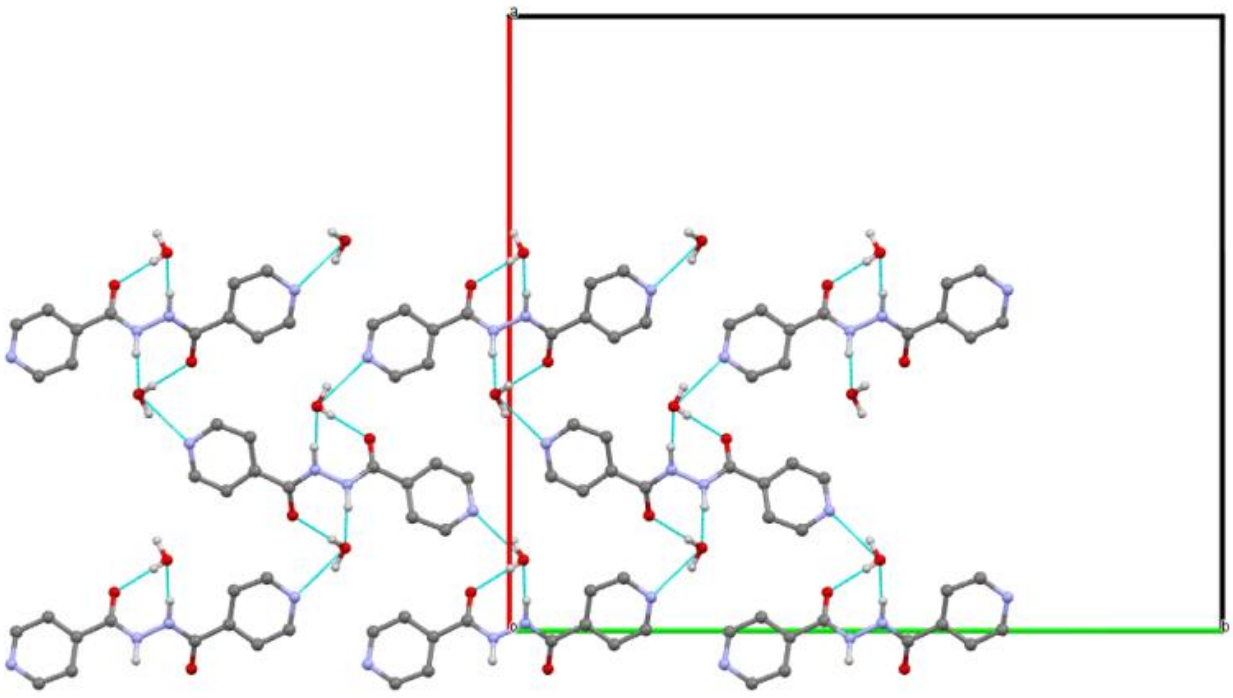

(a)

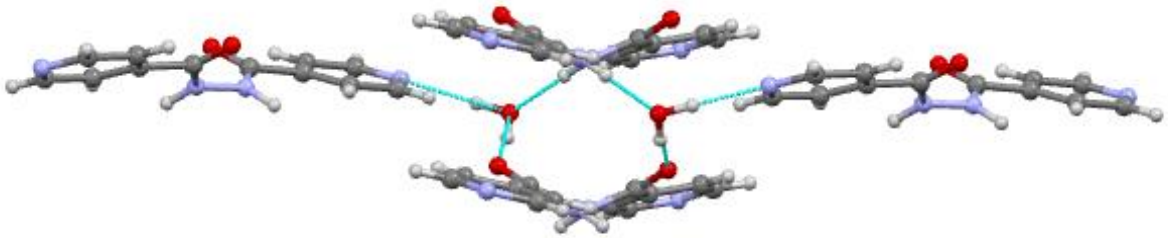

(b)

Figure 8: The heterosynthons found in the packing of crystal **V** are shown in part (a). Note, however, that part (a) is shown down the *c*-axis and does not show the depth of the 3D packing. Each molecule of water is hydrogen bonded to three different azine molecules as shown in Part (b).

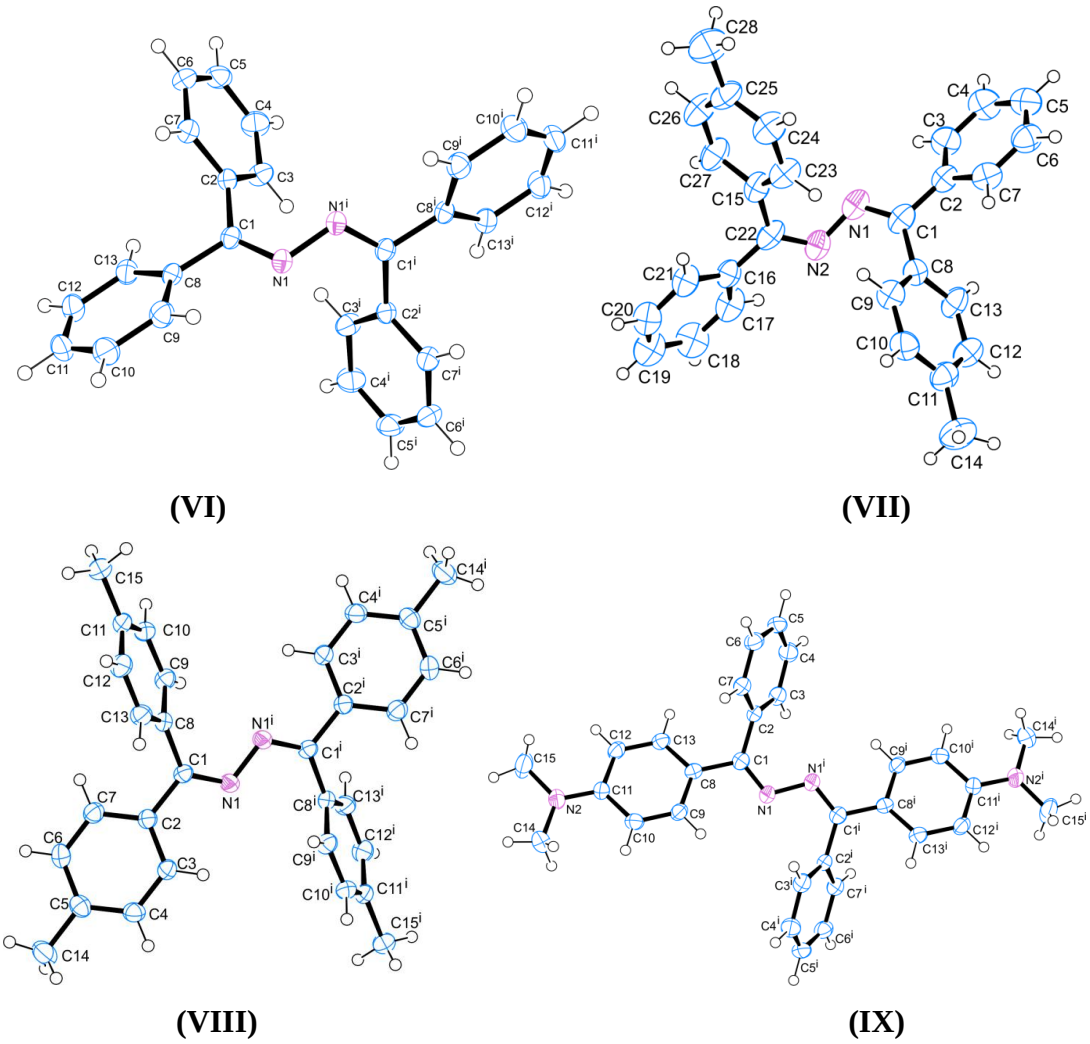

Figure 9: Asymmetric units of benzophenone azines. The asymmetric units of compounds (VI), (VIII) and (IX) each contain half a molecule of the benzophenone azines and the diagrams of the complete dimers are generated by symmetry. The asymmetric unit of (VII) contains one molecule of the benzophenone azine. The different way in which the asymmetric unit diagrams are generated by ORTEP-3 (Farrugia, 2012) accounts for the apparent disproportionally larger thermal ellipsoids for (VII).

Crystals **VI-IX** are the benzophenone azine products formed by the photodimerization of compounds **I-IV** respectively (**Figure 9**). The packing of these benzophenone azines is exclusively via weak C−H···π interactions, with additional π···π stacking in only two of the four azines. No traditional hydrogen bonds or heterosynthons are present in any of their crystal structures.

Compound **VI** crystallizes in the *C*2/c space group and the asymmetric unit contains half a molecule of 1,2-bis(diphenylmethylene)hydrazine. The molecule is centrosymmetric, with the second half of the molecule related to the first by a two-fold rotation giving the molecule a C_2 symmetry. Although the many aromatic rings and lone pairs on the nitrogen allow for resonance structures that might give the N−N bond a double bond character, the bond length between the two nitrogen atoms is 1.400 Å, which is typical of a single N−N bond (Saha *et al*., 1995). The only hydrogen bonding interactions found in the packing of **VI** are weak C−H···π interactions between the terminal hydrogen atom of a benzophenone ring on one azine molecule and the benzophenone ring of an adjacent molecule (**Figure 10**). The packing is further stabilized by π···π stacking between benzophenone rings of adjacent molecules.

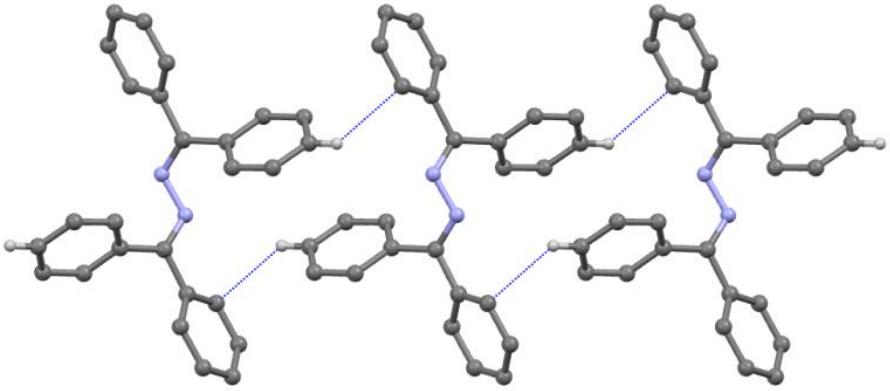

(a)

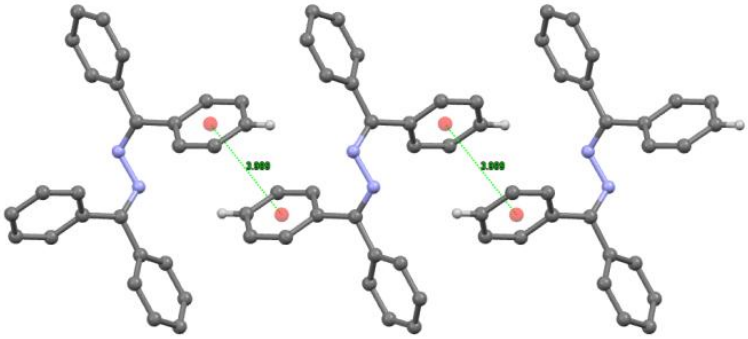

(b)

Figure 10: The packing of **VI** showing (a) the C−H··· π interactions between the terminal hydrogen atom of a benzophenone ring on one azine molecule and the benzophenone ring of an adjacent molecule and (b) the π···π stacking of the benzophenone rings.

Compound **VII** crystallizes in the *P*ca2$_1$ space group and the asymmetric unit contains one molecule of (1*Z*,2*Z*)-1,2-bis(phenyl(*p*-tolyl)methylene)hydrazine. As with crystal **VI**, crystal **VII** is centrosymmetric with C_2 symmetry. The packing involves C−H···π interactions between a methyl hydrogen atom donor and a benzophenone ring π-system acceptor of an adjacent molecule to from 1D ribbons along the *c*-axis. The packing is further stabilized by π···π stacking of the non-substituted benzophenone rings (**Figure 11**). Crystal **VIII** crystallizes in the $P\bar{1}$ space group and the asymmetric unit contains half a molecule of 1,2-bis(di-*p*-tolylmethylene)hydrazine. The second half of the molecule is related to the first by an inversion about the center of the molecule. The packing of **VIII** is purely through weak C−H···π interactions. Unlike in crystal **VII**, the interaction in **VIII** is not via the methyl hydrogen atom donor, but rather through one of the hydrogen atom donors of the substituted benzophenone ring and the unsubstituted ring π–system of an adjacent molecule. Crystal **IX** crystallizes in the $P\bar{1}$ space group and the asymmetric unit contains half a molecule of 4,4'-(1*Z*,1'*Z*)-hydrazine-1,2-diylidenebis(phenylmethan-1-yl-1-ylidene)bis(*N*,*N*-dimethylaniline). The second half of the molecule is related to the first by an inversion about the center of the molecule. As with crystal **VIII**, the packing of **IX** is purely through weak C−H···π interactions. The C−H···π in this case are, similarly to **VII**, between a methyl hydrogen atom donor and the benzophenone ring π-system acceptor of an adjacent molecule. The interactions result in the formation of layers of two-dimensional (2D) sheets.

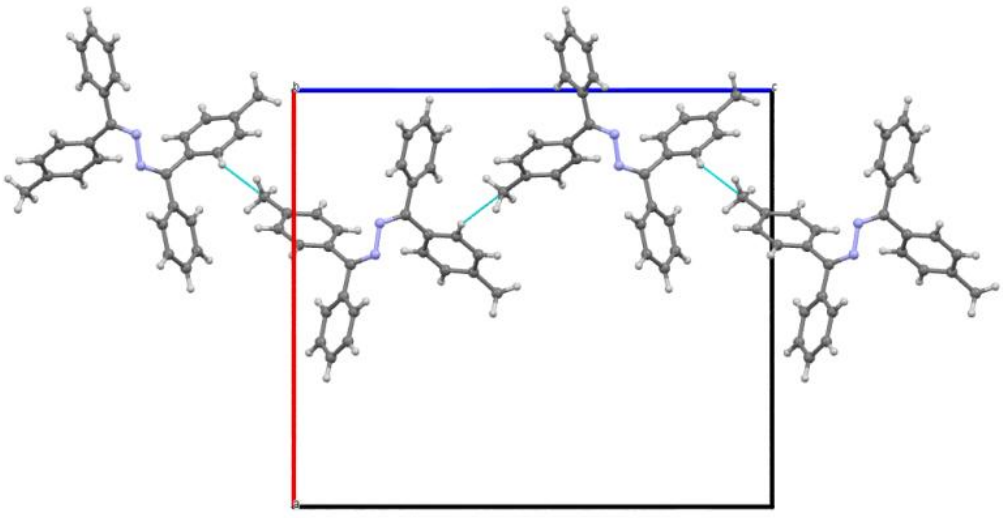

(a)

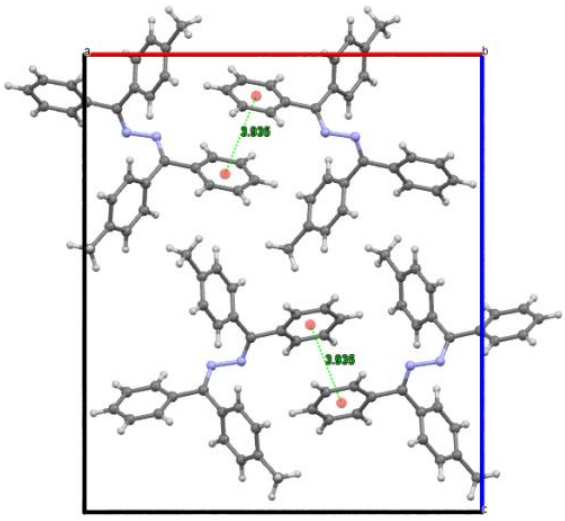

(b)

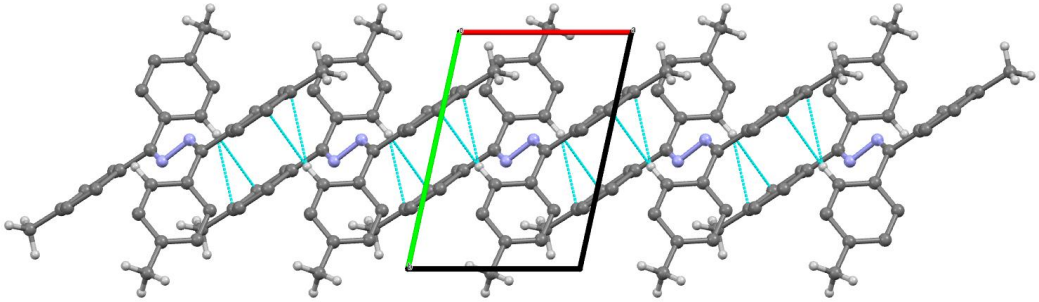

(c)

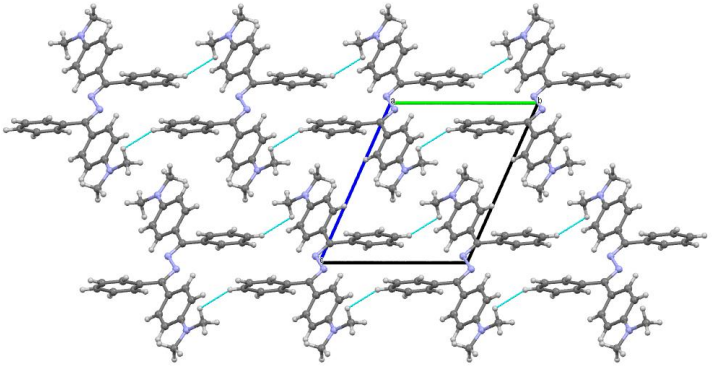

(d)

Figure 11: Part (a) is a diagram of the packing of crystal **VII** showing the C−H···π interactions between the methyl hydrogen atoms and the benzophenone rings of adjacent molecules and (b) the π···π stacking of the benzophenone rings. Part (c) shows the C−H···π interactions of crystal **VIII.** The interaction in **VIII** is not via the methyl hydrogen atom donor as in **VII**, but rather through one of the hydrogen atom donors of the substituted benzophenone ring and the unsubstituted ring π–system of an adjacent molecule. Part (d) shows the packing of crystal **IX**, like **VIII**, is held together purely by C−H··· π interactions.

Conclusion

Isoniazid was covalently modified with four benzophenone derivatives. Crystals of these compounds were harvested and the crystal structures were determined. The packing of three of the four modified isoniazid crystals contain weak C−H···O interactions. The four modified isoniazid crystals were then subjected to direct sunlight, resulting in benzophenone azine and three other benzophenone azine derivatives. The crystal structures were described. Two of the four benzophenone azine crystals were constructed solely through C−H···π packing interactions. The other two azines contained only C−H···π packing interactions, but were further stabilized by π···π stacking. Crystals of di-isoniazid azine, an expected by-product of the photodimerization process were also harvested, and the crystal structure determined.

Acknowledgement

The University of the Witwatersrand and the Molecular Sciences Institute are thanked for providing the infrastructure and financial support to do this work. A Lemmerer thanks the Wits Friedel Sellschop award for funding and M Smith thanks the Chemistry department of the University of South Africa for their financial support.

Supporting Information Available

Crystallographic data were deposited at the Cambridge Crystallographic Data Center with reference numbers CCDC XXXXXXX-XXXXXXX, which can be requested from The Cambridge Crystallographic Data Centre (http://www.ccdc.cam.ac.uk/data_request/cif). This information is also available free of charge via the internet at http://pubs.acs.org.

References

Bernstein, J., Davis, R. E., Shimoni, L. & Chang, N.-L. (1995). *Angew. Chem. Int. Ed.* **34**, 1555-1573.

Bruker, SAINT+, . Version 6.02 (Includes XPREP and SADABS) ed. Madison, Wisconsin, USA: Bruker AXS Inc. (2004).

Carty, A. J. (1972). *Organometallic Chemistry Reviews, Section A: Subject Reviews.* **7**, 191.

Desiraju, G. R. (2005). *Chem. Commun.* ***24***, 2995-3001.

Farrugia, L. (2012). *J. Appl. Crystallogr.* **45**, 849-854.

Kost, A. & Grandberg, I. (1959). *Uspekhi Khimii.* **28**, 921-947.

Lauer, W. M. & Dyer, W. S. (1942). *J. Am. Chem. Soc.* **64**, 1453-1456.

Macrae, C. F., Bruno, I. J., Chisholm, J. A., Edgington, P. R., McCabe, P., Pidcock, E., Rodriguez-Mange, L., Taylor, R., van de Streek, J., & Wood, P. A. (2008). *J. Appl. Cryst.* **41**, 466-470.

Saha, A. K., Hossain, M. M., Grubisha, D. S. & Bennett, D. W. (1995). *J. Chem. Crystallogr.* **25**, 383-387.

Sheldrick, G. M. (2015). *Acta Crystallogr., Sect. C*, **71**, 3-8.

Spek, A. (2009). *Acta Crystallogr., Sect. D.* **65**, 148-155.

Verner, J. & Potacek, M. (2006). *Molecules.* **11**, 34-42.

Wuts, P. G. & Greene, T. W. (2006). *Greene's protective groups in organic synthesis*. John Wiley & Sons.

Xavier, A. & Srividhya, N. (2014). *IOSR-JAC*. **7**, 6-15.

Chapter 7: Co-crystal engineering of 4-aminoantipyrine

7.1 Introduction

This chapter details the systematic implementation of crystal engineering techniques that were employed in order to produce the first reported co-crystal of 4-aminoantipyrine. The synthesis of additional salts of 4AAP and co-crystals of covalently modified 4-AAP are included in the report.

7.2 Novel crystal forms of 4-aminoantipyrine and its derivatives

Title of paper:	Novel crystal forms of 4-aminoantipyrine and its derivatives
Journal:	*Crystal Growth and Design*
Reference:	Pending
Status:	Submitted. Has been reviewed and currently attending to reviewers' comments as per editor's request.
Date Received:	December 2017
Date Revised:	February 2018
Date Published:	

Synopsis of Paper

The first co-crystallization of the pharmaceutical ingredient 4-aminoantipyrine is reported and the method used for its supramolecular synthesis is discussed. Two molecular salts of 4-aminoantipyrine, as well as two co-crystals of a derivative of 4-aminoantipyrine were also synthesized. The complexes discussed show that careful application of synthon theory, choice of solvent and consideration of the pK_a difference between 4-aminoantipyrine and the co-former are required to successfully co-crystallize this molecule.

Table 7.1: List of compounds reported in chapter 7.2

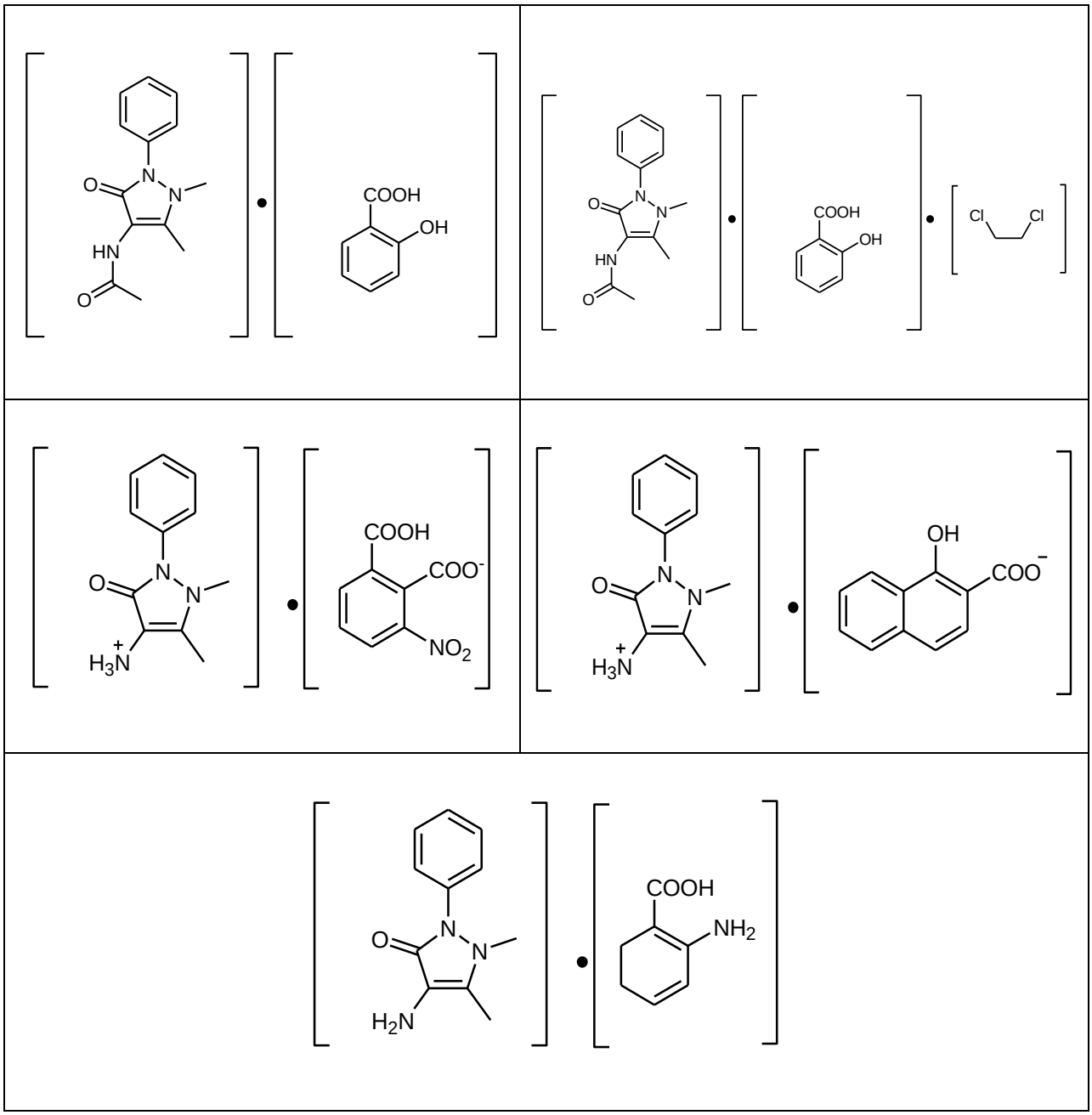

Novel crystal forms of 4-aminoantipyrine and its derivatives

Mark G. Smith[†] and Andreas Lemmerer*[‡]

†*Department of Chemistry, University of South Africa, Unisa Science Campus, Florida, 1709, Johannesburg, South Africa, and* [‡]*Molecular Sciences Institute, School of Chemistry, University of the Witwatersrand, 2050, Johannesburg, South Africa*

RECEIVED DATE (to be automatically inserted after your manuscript is accepted if required according to the journal that you are submitting your paper to)

To whom correspondence should be addressed:

Professor Andreas Lemmerer, Molecular Sciences Institute, School of Chemistry, University of the Witwatersrand, Private Bag 3, 2050, Johannesburg, South Africa.
E-mail: andreas.lemmerer@wits.ac.za. Fax: +27-11-717-6749. Tel: +27-11-717-6711.

ABSTRACT:

The first co-crystallization of the pharmaceutical ingredient 4-aminoantipyrine is reported with 2-aminobenzoic acid as the co-former, and the method used for its supramolecular synthesis is discussed. Two molecular salts of 4-aminoantipyrine, as well as two co-crystals of a derivative of 4-aminoantipyrine were also synthesized. The complexes discussed show that careful application of synthon theory, choice of solvent and consideration of the pK_a difference between 4-aminoantipyrine and the co-former are required to successfully co-crystallize this reactive molecule. In summary, the co-former must be chosen so that its functional group forms a robust heterosynthon with the reactive molecule. The presence of polar solvents or large pK_a differences between 4-aminoantipyrine and its potential co-former favors salt formation, whereas a non-polar solvent and a small pK_a difference is required for the co-crystallization of 4-aminoantipyrine.

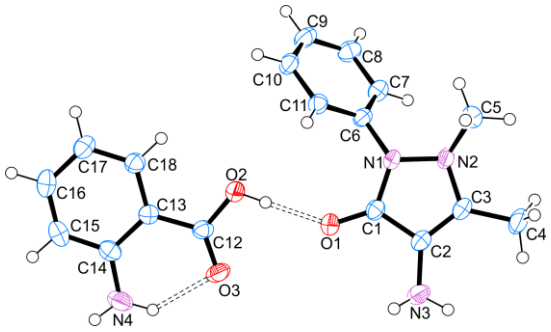

KEYWORDS:

4-Aminoantipyrine, Co-crystal, Supramolecular synthesis, Crystal engineering, Solvent, pK_a, Synthon

Introduction

How does one co-crystallize a highly reactive molecule? 4-Aminoantipyrine (4AAP) is an active pharmaceutical ingredient with powerful anti-inflammatory, antipyretic and analgesic properties. Its amino functional group is highly reactive and it will react readily with ketones and aldehydes at room temperature. Due to its chemical reactivity it has been widely used as a nitrogen scavenger species against hydroxyl radicals.[1] Although 4AAP has many recognized therapeutic benefits, the use of 4AAP has been associated with agranulocytosis.[2] In order to reduce adverse effects in cases of drugs with considerable side effects, a number of derivatives using the 4AAP backbone have been made.[3] In addition, the pharmaceutical industry often turns to the synthesis of salts and co-crystals, where the different physical properties of the co-crystals may enhance the bioavailability of the drug.[4] To date, 251 derivatives of 4AAP have been reported in the Cambridge Structural Database,[5] where the modifying adduct has attached to the amino nitrogen atom. Yet, despite the drive to synthesize salts and co-crystals of pharmaceuticals such as 4AAP, only five molecular salts of 4AAP have been reported,[6-11] of which two are simple salts with halide counter-ions.[6,7] No co-crystal of 4AAP has ever been reported. The scarcity of salts of 4AAP and the complete absence of any co-crystals of the species are presumably due to the fact that it reacts covalently with the potential co-former rather than co-crystallizing on a supramolecular basis.

How then does one go about co-crystallizing 4AAP? Firstly, in "Knowledge-based approaches to co-crystal design",[12] Wood stresses the importance of choosing a suitable synthon. 4AAP possesses amine and carbonyl functional groups which can undergo hydrogen bonding. Both amine and carbonyl functional groups form robust heterosynthons with carboxylic acids, and so carboxylic acids were therefore chosen as the co-formers in all our attempts at co-crystallization. Secondly, solvent choice is critical in determining whether a salt or co-crystal will be formed. A polar solvent stabilizes ionic species through charge-charge or charge-heteroatom interactions, whereas non-polar solvents inhibit the formation of charged species since they cannot interact with the ions.[13] Thirdly, details of the effect of pK_a on co-crystal formation has recently come into the spotlight. Childs *et al*. states that the absolute separation of the pK_a values of a molecule and its potential co-former plays a critical role in determining whether the supramolecular synthesis of two such molecules will result in a salt or in a co-crystal.[14,15] More recently, Lemmerer *et al*. presented empirical evidence to suggest that an absolute ΔpK_a separation of less

than 3 ([ΔpK_a] = [pK_a(protonated base) – pK_a(acid)]) will greatly enhance the formation of a co-crystal rather than a salt (the "Rule of Three").[16] Our strategy therefore was to attempt co-crystallizations of carboxylic acids with 4AAP, and to take into account the calculated pK_a values of the co-formers, as well as considerations of the polarity of the solvent. pK_a values were calculated using ACD/Labs Software V11.02.[17] Co-crystallizations were first attempted with a derivative of 4AAP (namely 4-aminoantipyrine-*N*-acetamide), of which there are several reported co-crystals, in an attempt to find suitable solvents and co-formers, as a proof of concept exercise.

The crystal structure of 4AAP has been reported by Li *et al.*[18] and by Mnguni *et al.*[19] (Figure 1a). 4AAP has a pK_a of 4.07 ± 0.65 (based solely on the calculated pK_a for the species in water solution). Its exocyclic nitrogen atom is readily protonated and forms a chloride salt in the presence of hydrochloric acid and a bromide salt when refluxed in an aqueous dibromomethane solution (Figure 1b & c).[6,7] The crystal structure of these two salts have been reported by Chitradevi and Yang respectively.[6,7] Murtaza *et al*. prepared a three-component salt (Figure 2a) by acidifying the 4AAP with an aqueous solution of hydrochloric acid, and then refluxing with thiourea (pK_a 14.91 ± 0.29) in ethanol ([ΔpK_a] = 10.84).[8] A molecular salt of 4AAP and 2,2'-dithiobenzoic acid was synthesized first by Huo and then Fazil *et al*.[9,10] and was crystallized from ethanol and from a 50% ethanol/water mixture respectively (Figure 2b). Huo commented that the components were selected as building blocks for creating a co-crystal, but proton transfer was observed in the ethanol medium. The calculated pK_a of 2,2'-dithiobenzoic acid is 3.02 ± 0.36 which is much closer to the 4.07 pK_a of 4AAP (with ([ΔpK_a] = 1.05) and therefore more likely to co-crystallize than co- formers with larger pK_a separations. However, the polar solvent (ethanol) lends itself to salt formation as the polar solvent stabilizes the ionic species through charge-charge and charge-heteroatom interactions. Finally, a salt of 4AAP with salicylic acid (pK_a 3.01 ± 0.10) was prepared in aqueous solution by Chitradevi *et al*. ([ΔpK_a] = 1.06)[11] (Figure 2c).

In this report, we describe co-crystals and salts of 4AAP and its derivative 4-aminoantipyrine-*N*-acetamide using salicylic acid, 3-nitrophathalic acid, 1-hydroxy-2-naphthanoic acid and 2-aminobenzoic acid (Figure 3).

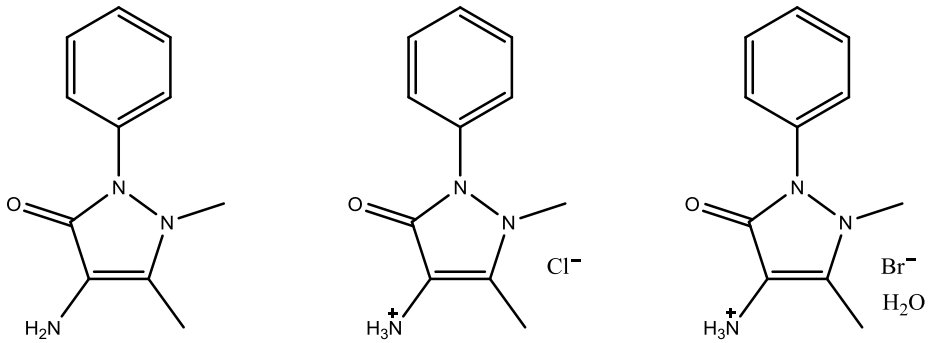

(a) (b) (c)

Figure 1: The structure of 4-aminoantipyrine and its reported simple salts:
(a) 4-aminoantipyrine (SIKBAR), (LOYXEE)
(b) aminoantipyrine-4-aminium chloride (HUKTIS)
(c) aminoantipyrine-4-aminium bromide monohydrate (PAXSOY)

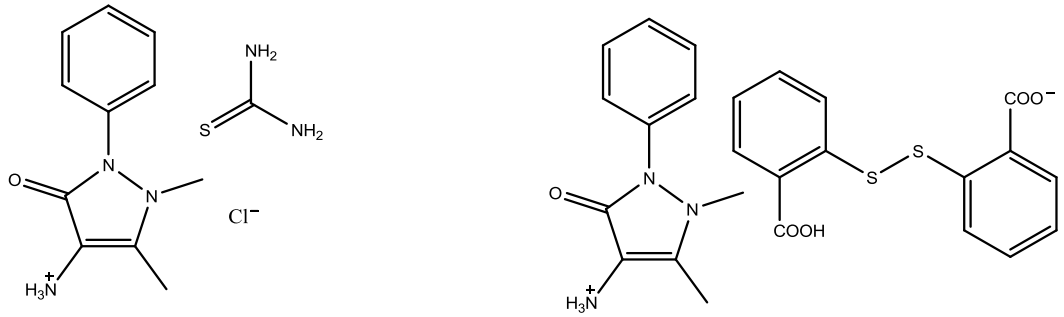

(a) (b)

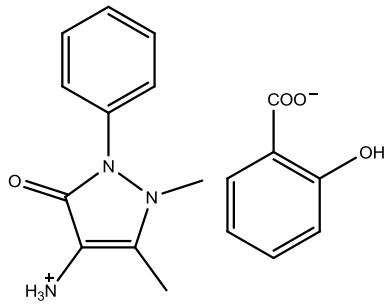

(c)

Figure 2: Previously synthesized salts of 4-aminoantipyrine.
(a) aminoantipyrine-4-aminium thiourea chloride (EVOLIL)
(b) aminoantipyrine-4-aminium 2,2'-dithiodibenzoate (PUGHEF), (PUGHEF01)
(c) aminoantipyrine-4-aminium salicylate (DUHYOV)

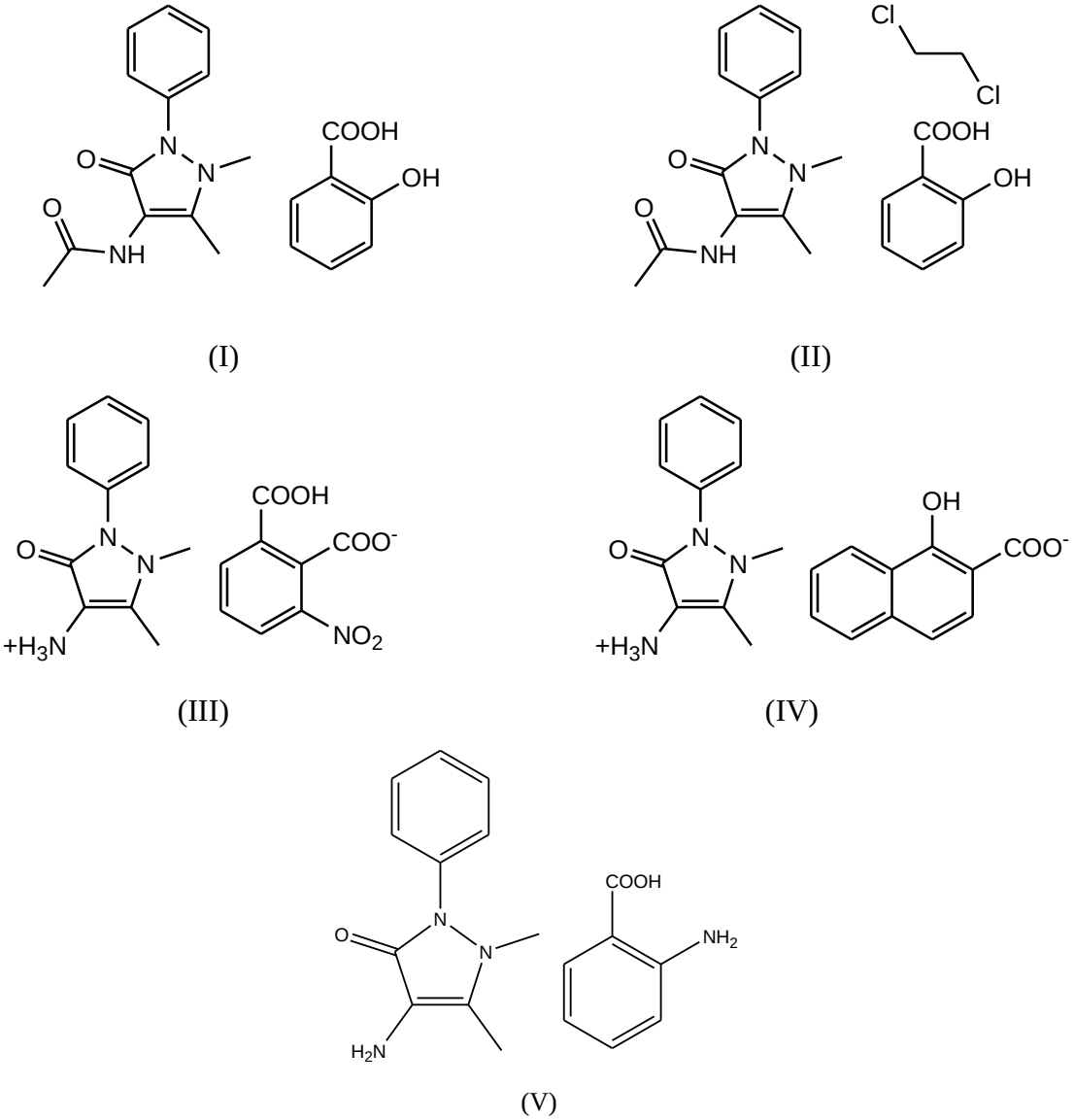

Figure 3: Co-crystals and salts of 4-aminoantipyrine and its derivative 4-aminoantipyrine-*N*-acetamide reported in this paper. Compound **I**, crystallized from methanol, is a two-component co-crystal of 4-aminoantipyrine-*N*-acetamide and salicylic acid. Compound **II**, crystallized from 1,2-dichloroethane, results in a three-component co-crystal consisting of 4-aminoantipyrine-*N*-acetamide, salicylic acid and 1,2-dichloroethane. Salts of aminoantipyrine-4-aminium with 3-nitrophthalate (**III**) and 1-hydroxy-2-naphthoate (**IV**) respectively. Co-crystal of 4-aminoantipyrine and 2-aminobenzoic acid (**V**).

Experimental Methods

Synthesis

(4-aminoantipyrine-*N*-acetamide)·(salicylic acid) (I): 0.1080 g of 4-aminoantipyrine (0.5314 mmol) and 0.0963 g of acetylsalicylic acid (0.535 mmol) were added into a sample vial. The solids were dissolved in AP-grade methanol (3 mL), stirred for 1 hour at 40°C, and were left to stand at room temperature open to the atmosphere. Colorless plates were afforded after 3 days.

(4-aminoantipyrine-*N*-acetamide)·(salicylic acid)·(1,2-dichloroethane) (II): 0.0749 g of 4-aminoantipyrine (0.369 mmol) and 0.0658 g of acetylsalicylic acid (0.365 mmol) were added into a sample vial. The solids were dissolved in 1,2-dichloroethane (3 mL), stirred for 30 minutes at 40°C, and were left to stand at room temperature open to the atmosphere. Colorless needles were afforded after 7 days.

(aminoantipyrine-4-aminium)·(3-nitrophthalate) (III): 0.0753 g of 4-aminoantipyrine (0.371 mmol) and 0.0802 g of 3-nitrophthalic acid (0.380 mmol) were added into a sample vial. The solids were stirred in 1,2-dichloroethane (3 mL) and methanol was added dropwise until all the solids had dissolved. The mixture was stirred for 30 minutes at 40°C, and was left to stand at room temperature open to the atmosphere. The resulting solid was re-dissolved in chloroform, and ethanol was added dropwise until all solid had re-dissolved. The mixture was then stirred for 24 hours and was left to stand at room temperature open to the atmosphere. Colorless plates were afforded after 2 days.

(aminoantipyrine-4-aminium 1-hydroxy-2-naphthoate) (IV): 0.0987 g of 4-aminoantipyrine (0.486 mmol) and 0.0883 g of 1-hydroxy-2-naphthoic acid (0.469 mmol) were added into a sample vial. The solids were dissolved in AP-grade methanol (3 mL), stirred for 1 hour at 40°C, and were left to stand at room temperature open to the atmosphere. Colorless cubes were afforded after 3 days.

(4-aminoantipyrine)·(2-aminobenzoic acid) (V): 0.0996 g of 4-aminoantipyrine (0.490 mmol) and 0.0673 g of 2-aminobenzoic acid (0.491 mmol) were added into a sample vial. The solids were stirred in 1,2-dichloroethane (3 mL) and methanol was added dropwise until all the solids had dissolved. The mixture was stirred for 2 hours at 40°C, and was left to stand at room temperature open to the atmosphere. The resulting solid was re-dissolved in pure chloroform, was stirred for 24 hours, and was left to stand at room temperature open to the atmosphere. Colorless blocks were afforded after 2 days.

Crystal Data and X-ray Structure Analysis.

Intensity data for the five crystal structures were collected on a Bruker APEX II CCD area detector diffractometer with graphite monochromated Mo-K_α radiation (50 kV, 30 mA) at 173K. The collection method involved ω-scans with a 0.5° width. *SAINT+* version 6.02.6 software was used for data reduction and *SADABS* was used to make empirical absorption corrections.[20] The crystal structures were solved using direct methods on *SHELXS-97*.[21] Non-hydrogen atoms were first refined isotropically, followed by anisotropic refinement by full matrix least-squares calculations based on F^2 using *SHELXL-2017*.[21] C-bound H atoms were located in the difference electron density map, then positioned geometrically and were allowed to ride on their respective parent atoms, with thermal displacement parameters 1.2 times that of the parent C atom. Where possible, the coordinates and isotropic displacement parameters of the N-bound and O-bound H atoms involved in hydrogen bonding interactions were allowed to refine freely. Diagrams and publication material were generated using *WinGX*,[22] *ORTEP-3*,[22] *PLATON*[23] and M*ERCURY*[24]. The crystallographic data of each crystal is summarized in Table 1 and the hydrogen bonding geometries in Table 2.

Table 1 Crystallographic data for compounds **1-5**

	I	**II**	**III**	**IV**	**V**
Formula	$(C_{13}H_{15}N_3O_2)\cdot(C_7H_6O_3)$	$(C_{13}H_{15}N_3O_2)\cdot(C_7H_6O_3)\cdot0.5(C_2H_4Cl_2)$	$(C_{11}H_{14}N_3O)\cdot(C_8H_4NO_6)$	$(C_{11}H_{14}N_3O)\cdot(C_{11}H_7O_3)$	$(C_{11}H_{13}N_3O)\cdot(C_7H_7NO_2)$
M_r	383.40	432.87	414.37	391.42	340.38
Temperature/K	173(2)	173(2)	173(2)	173(2)	173(2)
Wavelength/Å	0.71073	0.71073	0.71073	0.71073	0.71073
Crystal size/mm^3	0.52×0.16×0.15	0.60×0.13×0.10	0.24×0.19×0.10	0.64×0.58×0.54	0.38×0.30×0.23
Crystal system	Triclinic	Triclinic	Orthorhombic	Monoclinic	Orthorhombic
Space group	$P\bar{1}$	$P\bar{1}$	$P2_12_12_1$	$P2_1/c$	$Pbca$
a/Å	6.7874(2)	6.5113(5)	7.1537(4)	7.9866(4)	7.5880(10)
b/Å	11.1280(3)	10.9128(7)	7.5193(4)	12.7996(6)	17.448(2)
c/Å	12.8934(3)	15.4411(11)	34.0871(16)	18.8706(8)	25.067(3)
α/°	76.025(1)	89.988(4)	90	90	90
β/°	88.881(1)	83.665(4)	90	98.753(3)	90
γ/°	86.196(1)	75.049(4)	90	90	90
V/Å^3	942.93(4)	1053.12(13)	1833.57(17)	1906.59(15)	3318.7(7)
Z	2	2	4	4	8
ρ (calcd)/Mg m^{-3}	1.350	1.365	1.501	1.364	1.362
μ/mm^{-1}	0.099	0.219	0.117	0.095	0.095
F(000)	404	454	864	824	1440
Θ Range for data collection/°	1.63 to 28.00	1.93 to 25.50	2.39 to 28.00	1.93 to 28.00	1.62 to 27.99
Reflections collected	20961	12450	10125	41500	33204
No. of unique data [R(int)]	4536 [0.0466]	3910 [0.0704]	4379 [0.0862]	4601 [0.1320]	3989 [0.0447]
No. data with $I \geq 2\sigma(I)$	3471	2641	2236	2354	3211
Final R($I \geq 2\sigma(I)$)	0.0402	0.0483	0.0637	0.0587	0.0361
Final wR_2 (all data)	0.1114	0.1316	0.1624	0.1626	0.0995
CCDC deposition number	1586521	1586520	1586519	1586523	1586522

Table 2 Hydrogen bonding details of compounds 1-5

	d(D─H)/Å	*d*(H···A)/Å	*d*(D···A)/Å	∠(D─H···A)/°
I				
N3─H3···O1	0.91(2)	1.90(2)	2.8119(15)	177(2)[a]
O3─H3A···O2	0.95(2)	1.67(2)	2.6144(14)	172(2)
O5─H5···O4	0.94(3)	1.71(3)	2.5799(16)	152(2)
II				
N3─H3···O1	0.95(2)	1.83(2)	2.783(2)	177(2)[b]
O3─H3A···O2	1.04(3)	1.57(4)	2.583(2)	165(3)
O5─H5···O4	0.93(3)	1.73(4)	2.573(3)	148(3)
III				
N3─H3A···O7	0.91	2.03	2.913(5)	162
N3─H3B···O2	0.91	2.22	2.867(6)	128[c]
N3─H3B···O3	0.91	2.16	2.808(5)	127[d]
N3─H3C···O7	0.91	1.98	2.881(5)	168[e]
O2─H2···O6	0.84	1.67	2.507(5)	172[f]
IV				
N3─H3A···O3	0.91	1.89	2.771(3)	163[g]
N3─H3B···O1	0.91	1.88	2.694(2)	148[h]
N3─H3C···O3	0.91	1.78	2.661(3)	162
N3─H3C···O4	0.91	2.65	3.367(3)	136
O2─H2···O4	0.97(4)	1.60(4)	2.502(3)	153(4)
V				
N3─H3A···N4	0.93(2)	2.66(2)	3.349(2)	131(2)[i]
N3─H3B···O3	0.89(2)	2.21(2)	2.9567(16)	141(2)[j]
N4─H4A···O3	0.893(19)	2.004(19)	2.6873(18)	132(2)
N4─H4B···N3	0.88(2)	2.461(19)	3.2747(19)	154(2)[k]
O2─H2···O1	0.94(2)	1.69(2)	2.6303(13)	177(2)

[a]-x + 1, -y + 2, -z + 1. [b]-x + 2,-y + 1, -z. [c]-x + 2, y + 1/2, -z + 3/2. [d]x, y + 1, z. [e]-x + 1, y + 1/2, -z + 3/2. [f]-x + 2,y - 1/2, -z + 3/2. [g]-x + 1, -y, -z + 1. [h]-x + 2, -y, -z + 1. [i]x + 1, y, z. [j]-x + 2, -y + 1, -z + 1. [k]-x + 1, -y + 1, -z + 1.

Results

Compounds **I** and **II** display similar hydrogen bonding patterns with compound **I** being a co-crystal of 4-aminoantipyrine-*N*-acetamide and salicylic acid, and compound **II** containing an additional solvent molecule in the supramolecular structure (Figure 4). Both compounds **I** and **II** crystallize in the $P\bar{1}$ space group. Each 4-aminoantipyrine-*N*-acetamide molecule is hydrogen bonded to a second 4-aminoantipyrine-*N*-acetamide molecule through two N3—H3···O1 hydrogen bonds forming a dimer with 0D packing dimensionality (Figure 5). This packing results in a $R_2^2(10)$ ring between the two 4-aminoantipyrine-*N*-acetamide molecules. There is a centre of inversion in the centre of the $R_2^2(10)$ ring (at unit cell coordinates ½,½,0). In addition to dimerizing, each 4-aminoantipyrine-*N*-acetamide is hydrogen bonded to a salicylic acid acid molecule through a O2—H3A···O3 carboxylic acid/carbonyl heterosynthon. The phenol group on the salicylic acid molecule is not involved in intermolecular hydrogen bonding, but rather, it undergoes intramolecular hydrogen bonding ($S_1^1(6)$ in graph-set notation) through a O5—H5···O4 hydrogen bond which is typical of salicylic acid.[25] Compound **I** was crystallized from methanol and no solvent is present in the supramolecular structure. Compound **II** was crystallized from 1,2-dichloroethane, and this solvent is found between the molecules in a 1 : 1 : 0.5 ratio of 4-aminoantipyrine-*N*-acetamide : salicylic acid : 1,2-dichloroethane. No hydrogen bonds or short contacts are present between the solvent and the co-crystal components.

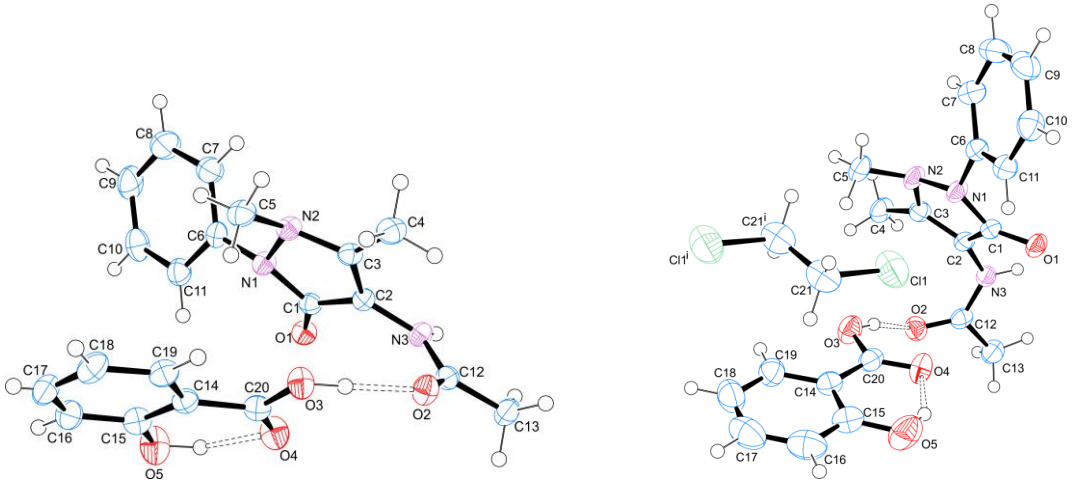

Figure 4: Asymmetric units and numbering scheme of compounds **I** and **II**.

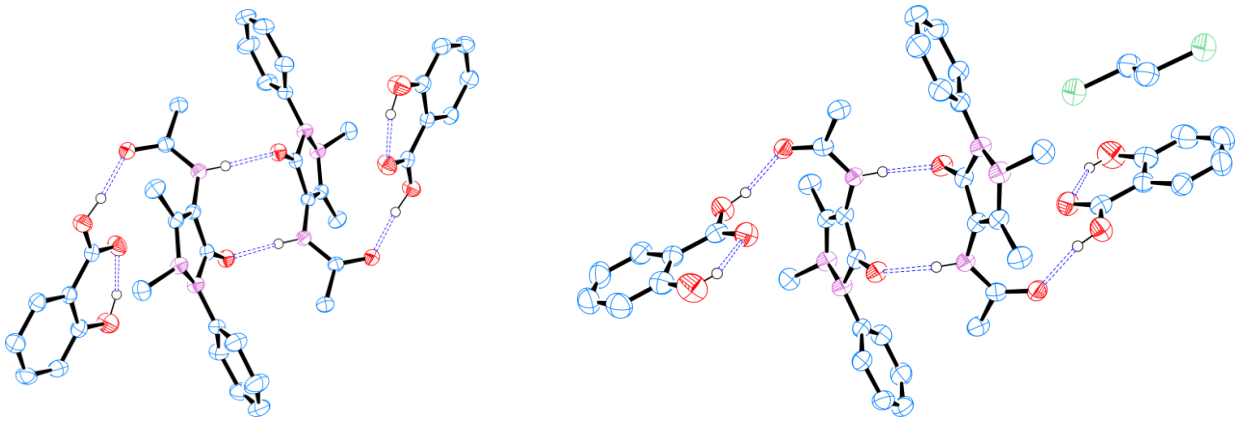

(I) **(II)**

Figure 5: Hydrogen bonding diagrams of compounds **I** and **II**.

Compounds **III** and **IV** are salts formed via charge-assisted hydrogen bonding between the acidic proton (H3A) of the aminium group of a aminoantipyrine-4-aminium cation and an oxygen atom of the carboxylate anion of 3-nitrophthalate (via O7) and 1-hydroxy-2-naphthoate (via O3) respectively (Figure 6). The asymmetric unit of (**III**) consists of the cation and anion in a 1:1 ratio and crystallizes in the $P2_12_12_1$ space group. The packing of structure **III** consists of two-dimensional (2D) ribbons, with translational symmetry via a twofold screw axis along the crystallographic *a*-axis, stabilized by π-stacking. There is an extensive hydrogen bonded network involving one 8-membered, two 11-membered and one 13-membered rings (Figure 7). The 8-membered ring, of type $R_3^3(8)$, involves one aminoantipyrine-4-aminium cation and two 3-nitrophthalate anions. The aminium cation provides two of the H-bond donors, and the third one comes from the carboxylic acid group of one of the 3-nitrophthalate molecules. The 13-membered ring is of the type $R_4^3(13)$ and involves two aminoantipyrine-4-aminium cations and two 3-nitrophthalate anions. There are four H-bond donors, two from each aminium group. An oxygen from each deprotonated carboxylate anion, as well as the carbonyl oxygen of a fully protonated carboxylic acid group of a 3-nitrophthalate molecule, provide the three H-bond acceptors. There are two $R(11)$ rings in the packing of **III.** The $R_2^3(11)$ ring involves three molecules, namely one aminoantipyrine-4-aminium cation and two 3-nitrophthalate anions. H3B

is bifurcated and hydrogen bonds to O2 and O3 of two adjacent 3-nitrophthalate anions. The third hydrogen bond is formed between H2 on the carboxylic acid group of a 3-nitrophthalate molecule to an oxygen of the carboxylate group (O6) of an adjacent 3-nitrophthalate anion. On the other hand, the $R_3^3(11)$ ring involves four molecules, where one of the aminoantipyrine-4-aminium hydrogen atoms (on the aminium functional group) is hydrogen bonded (bifurcated) to an oxygen (O7) of a carboxylate group of one of the 3-nitrophthalate anions and the carbonyl oxygen of a fully protonated carboxylic acid group of the other 3-nitrophthalate molecule. In the second aminoantipyrine-4-aminium, two of the aminium hydrogens are hydrogen bonded, each to a carboxylate oxygen of the two neighbouring 3-nitrophthalate molecules.

Compound **IV** crystallizes in the $P2_1/c$ space group and packs in two-dimensional ribbons along the crystallographic *a*-axis (Figure 8). The hydrogen bonding network along the ribbon consists of alternating $R_2^2(10)$ and $R_4^2(8)$ rings with all three aminium protons of each of the aminoantipyrine-4-aminium cations acting as hydrogen bond donors. There is a centre of inversion in the centre of each of the $R_2^2(10)$ and $R_4^2(8)$ rings. In the $R_2^2(10)$ ring, the carbonyl oxygen (O1) of two aminoantipyrine-4-aminium molecules therefore acts as the acceptor, whereas in the $R_4^2(8)$ring, the acceptors are the oxygen atoms (O3) of two opposite carboxylate groups. In the packing, there is a glide plane perpendicular to [010] with glide component [00½]. For compound **III**, it may be expected that a co-crystal would result rather than a salt because the difference between the pK_a values of the 4-aminoantipyrine and 3-nitrophthalate are quite small (4.07 ± 0.65 and 3.02 ± 0.30 respectively, with [ΔpK_a] = 1.05). However, because a polar solvent (a mixture of ethanol and chloroform) was present, the ethanol stabilized the ionic species through charge-charge interactions, and a salt resulted. Likewise, compound **IV** was expected to be a salt rather than a co-crystal because the polar solvent methanol was used for crystallization.

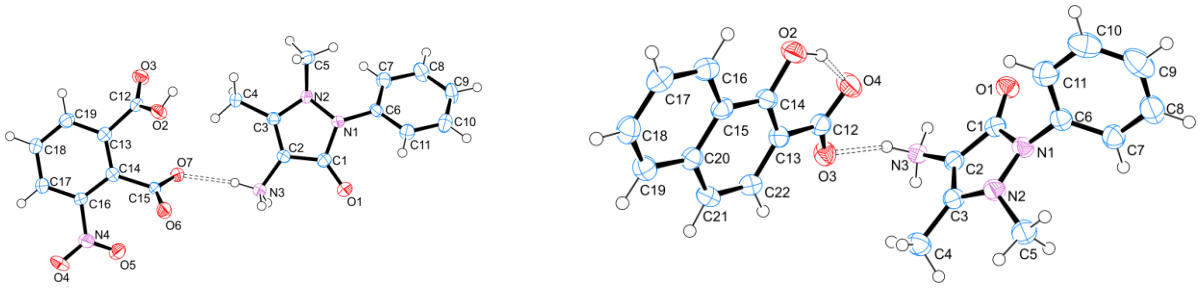

Figure 6: Asymmetric units and numbering scheme of compounds **III** and **IV**.

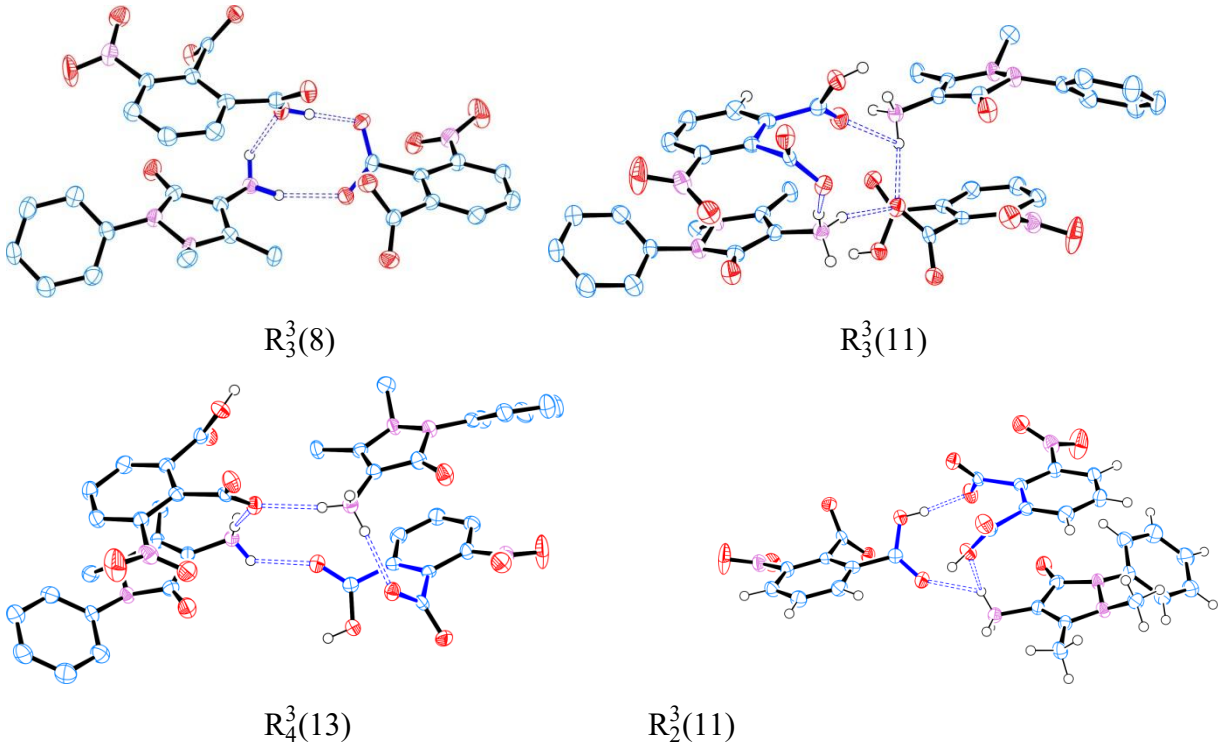

Figure 7: Hydrogen bonding diagrams of compound **III** showing the extensive hydrogen bonding network. The blue lines (solid and dotted) show the outline of the rings.

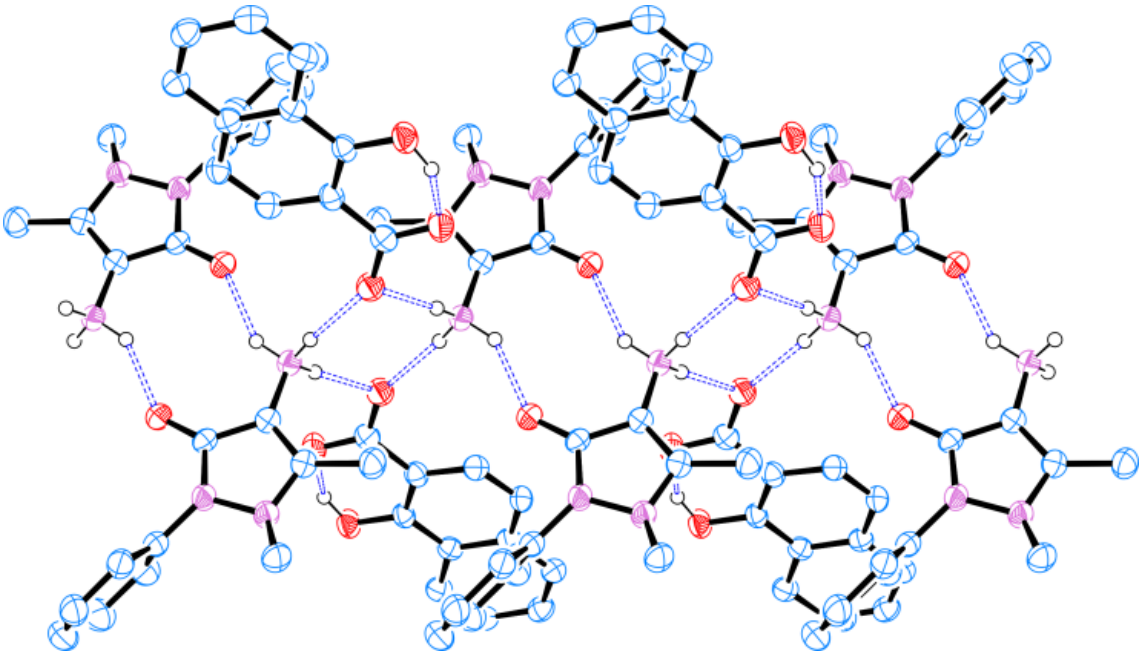

Figure 8: Hydrogen bonding diagram of compound **IV**.

To gain further insight into the usefulness of various solvents for the crystallization of 4AAP and 4-aminoantipyrine-*N*-acetamide, the pure powders of 4AAP and 4-aminoantipyrine-*N*-acetamide were dissolved in eight different solvents and allowed to crystallize out at room temperature using the slow evaporation method and the results were recorded (Table 3). For 4AAP, 1,2-dichloroethane was found to be an ideal solvent as it formed a high yield of large crystals. Crystallization from chloroform was also successful. For 4-aminoantipyrine-*N*-acetamide, 1,2-dichloroethane was likewise found to be the solvent of choice as it also resulted in a high yield of large crystals. Dichloromethane, ethyl acetate and 1-propanol are also suitable solvents for crystallizing 4-aminoantipyrine-*N*-acetamide, should a moderately polar or polar solvent be required.

Table 3 Result at attempts to crystallize 4AAP and acetyl 4AAP from various solvents.

	4-Aminoantipyrine	**4-aminoantipyrine-*N*-acetamide**
Methanol	A gel was formed.	An amorphous mass resulted.
Ethanol	A gel was formed. A few fine crystals formed on the glass above the gel.	Few crystals were formed.
Isopropanol	4AAP was only partially soluble but dissolved on heating. An oil was formed.	Few crystals were formed.
Chloroform	Crystals were formed.	An amorphous mass resulted.
1,2-Dichloroethane	Large crystals were formed.	Large crystals were formed.
Dichloromethane	An amorphous mass resulted.	Crystals were formed.
1-Propanol	An oil was formed. A few very fine crystals formed on the glass above the gel.	Crystals were formed.
Ethyl Acetate	Reacted with the 4AAP to form acetyl-4AAP	Crystals were formed.

In considering the choice of heterosynthon for **V**, the co-former was chosen to be a carboxylic acid with a similar pK_a value to that of 4-aminoantipyrine. Hemamalini *et al*. successfully co-crystallized a series of aminobenzoic acids (including 2-aminobenzoic acid) with aminopyridines.[26] The carboxylic acid functional group on the 2-aminobenzoic acid can form a robust heterosynthon with either the amine or carbonyl functional groups of 4AAP, and has a pK_a of 4.94 ± 0.10, which is reasonably similar to the 4AAP pK_a value of 4.07 ± 0.65, with [ΔpK_a] = 0.87, and was therefore considered a suitable co-former. For solvent choice, the non-polar 1,2-dichloromethane had been successfully used for the synthesis of **II** and **III**, as well as for the crystallization of pure 4AAP (Table 3) and was therefore chosen as the solvent for **V**. However, as the 2-aminobenzoic acid was not completely soluble in the 1,2-dichloromethane,

methanol was slowly added dropwise to the solution until all of the reagents had dissolved. Then, as the presence of methanol was undesirable, all the solvent was evaporated and the resulting solid mass was re-dissolved and recrystallized in pure chloroform, which had also been found to be a good non-polar solvent for the crystallization of 4AAP (Table 3). Compound **V** is finally a 1:1 co-crystal of 4AAP. In the asymmetric unit, the carboxylic acid proton (H2) of 2-aminobenzoic acid is hydrogen bonded to the carbonyl oxygen (O1) of 4AAP (Figure 9). Intramolecular stabilization of the 2-aminobenzoic acid molecule occurs via a six membered $S_1^1(6)$ ring with the amine proton (H4) as the donor and the carbonyl oxygen (O3) of the carboxylic acid group as the acceptor. **V** Packs in a one-dimensional ribbon along the *a*-axis.

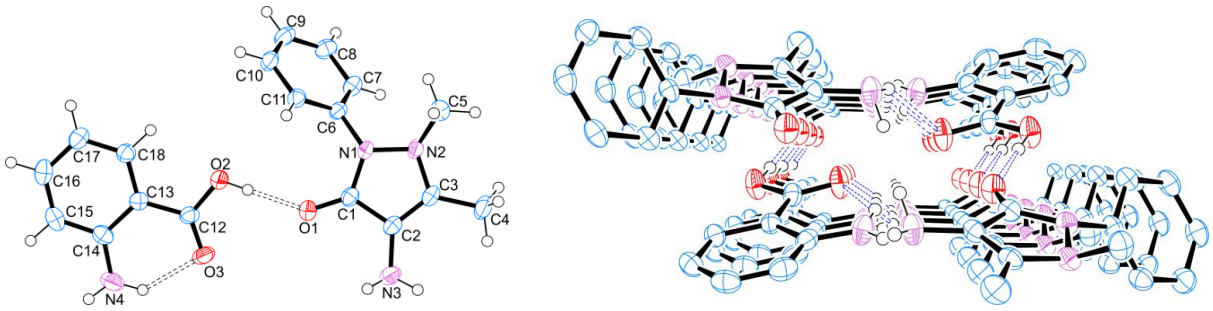

Figure 9: The asymmetric unit of the co-crystal **V** and a view of the packing**.**

Conclusion

Two 4-aminoantipyrine-*N*-acetamide co-crystals, two 4-aminium-4-aminoantipyrine salts and one 4-aminoantipyrine co-crystal were synthesized. The highly reactive 4-aminoantipyrine was co-crystallized with 2-aminobenzoic acid, and is the first reported co-crystal of the active pharmaceutical ingredient, 4-aminoantipyrine. The success of the co-crystallization of the reactive 4-aminoantipyrine is due to the strict application of three criteria: (1) the co-former was chosen so that its functional group formed a known robust heterosynthon with the reactive molecule; (2) the co-former was chosen to have a pK_a value similar to that of the 4-aminoantipyrine and, (3) a non-polar solvent was chosen to inhibit the formation of charged

species. Where polar solvents were used or where the pK_a value was substantially different to 4-aminoantipyrine, the crystallizations resulted in salts.

Acknowledgement

The University of the Witwatersrand and the Molecular Sciences Institute are thanked for providing the infrastructure and financial support to do this work. Andreas Lemmerer thanks the Wits Friedel Sellschop award for funding and Mark Smith thanks the Chemistry department of the University of South Africa for the financial support.

Supporting Information Available

Crystallographic data were deposited at the Cambridge Crystallographic Data Center with reference numbers CCDC 1586519-1586523, which can be requested from The Cambridge Crystallographic Data Centre (http://www.ccdc.cam.ac.uk/data_request/cif). This information is also available free of charge via the internet at http://pubs.acs.org.

References

(1) Santos, P. M. P.; Antunes, A. M. M.; Noronha, J.; Fernandes, E.; Vieira, A. J. S. C., *Eur. J. Med. Chem.* **2010**, *45* (6), 2258-2264.

(2) Bailey, D. N., *J. Anal. Toxicol.* **1983**, *7* (2), 76-8.

(3) Asiri, A. M.; Khan, S. A.; Tan, K. W.; Ng, S. W., *Acta Crystallogr., Sect. E.* **2010**, *66* (7), o1850.

(4) Schultheiss, N.; Newman, A., *Cryst. Growth Des.* **2009**, *9* (6), 2950-2967.

(5) Groom, C. R.; Allen, F. H., *Angew. Chem. Int. Ed.* **2014**, *53* (3), 662-671.

(6) Chitradevi, A.; Suresh Kumar, S.; Athimoolam, S.; Asath Bahadur, S.; Sridhar, B., *J. Mol. Struct.* **2015**, *1099*, 58-67.

(7) Yang, Y.-Y.; Xu, L.; Kang, T.-G.; Chen, T.; Wu, P., *Acta Crystallogr., Sect. E.* **2012**, *68* (6), o1964.

(8) Murtaza, S.; Hamza, M.; Tahir, M. N., *Acta Crystallogr., Sect. E.* **2011**, *67* (8), o2193.

(9) Huo, J.-Z., *Acta Crystallogr., Sect. E.* **2009**, *65* (11), o2691-o2692.

(10) Fazil, S.; Ravindran, R.; Sarau Devi, A.; Bijili, B. K., *J. Mol. Struct.* **2012**, *1021*, 147-152.

(11) Chitradevi, A.; Athimoolam, S.; Sridhar, B.; Bahadur, S. A., *Acta Crystallogr., Sect. E.* **2009**, *65* (12), o3041-o3042.

(12) Wood, P. A.; Feeder, N.; Furlow, M.; Galek, P. T. A.; Groom, C. R.; Pidcock, E., *CrystEngComm.* **2014**, *16* (26), 5839-5848.

(13) Levy, D. E., *Arrow-Pushing in Organic Chemistry: An Easy Approach to Understanding Reaction Mechanisms*. John Wiley & Sons, **2008**.

(14) Childs, S. L.; Stahly, G. P.; Park, A., *Mol. Pharm.* **2007**, *4* (3), 323-338.

(15) Cruz-Cabeza, A. J., *CrystEngComm.* **2012,** *14***,** 6362-6365.

(16) Lemmerer, A.; Govindraju, S.; Johnston, M.; Motloung, X.; Savig, K. L., *CrystEngComm.* **2015**, *17* (19), 3591-3595.

(17) *Calculated using Advanced Chemistry Development (ACD/Labs) Software V11.02 (© 1994-2014 ACD/Labs).*

(18) Li, Y.; Liu, Y.; Wang, H.; Xiong, X.; Wei, P.; Li, F., *Molecules.* **2013**, *18* (1), 877.

(19) Mnguni, M. J.; Lemmerer, A., *Acta Crystallogr., Sect. C.* **2015**, *71* (2), 103-109.

(20) *SAINT+*, , Version 6.02 (Includes XPREP and SADABS); Bruker AXS Inc: Madison, Wisconsin, USA, **2004**.

(21) Sheldrick, G. M., *Acta Crystallogr., Sect. C.* **2015**, *71* (Pt 1), 3-8.

(22) Farrugia, L., *J. Appl. Crystallogr.* **2012**, *45* (4), 849-854.

(23) Spek, A., *Acta Crystallogr., Sect. C.* **2009**, *65* (2), 148-155.

(24) Macrae, C. F., Bruno, I. J., Chisholm, J. A., Edgington, P. R., McCabe, P., Pidcock, E., Rodriguez-Mange, L., Taylor, R., van de Streek, J., & Wood, P. A. (2008). *J. Appl. Cryst.* **41**, 466-470.

(25) Smith, M. G.; Forbes, R. P.; Lemmerer, A., *Cryst. Growth Des.* **2015**, *15* (8), 3813-3821.

(26) Hemamalini, M.; Loh, W.-S.; Quah, C. K.; Fun, H.-K., *Chemistry Central Journal* **2014**, *8* (1), 31.

Chapter 8: Crystal Engineering of 4-aminoantipyrine

8.1 Introduction

4-Aminoantipyrine was covalently modified to form a series of Schiff bases. This chapter details the synthesis of the crystals and a structural study a series of 4-aminoantipyrine derivatives.

Details of the publication status of the paper precede the paper.

8.2 A structural study of nine 4-aminoantipyrine derivatives

Title of paper: A structural study of nine 4-aminoantipyrine derivatives

Journal: Will be submitted to *Acta Crystallographica C: Structural Chemistry*

Reference:

Status: Submission pending. To be submitted by end March 2018.

Date Received:

Date Revised:

Date Published:

Synopsis of Paper

In this paper, nine crystalline derivatives of 4-aminoantipyrine that have been covalently modified are synthesized and structurally characterized.

Table 8.1: List of compounds reported in chapter 8.2

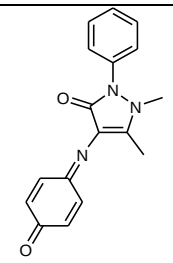	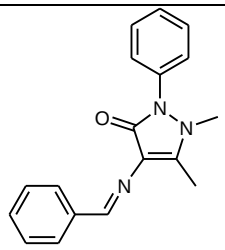
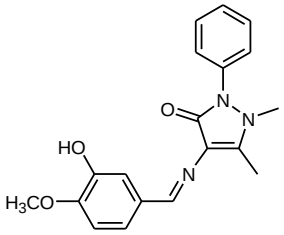	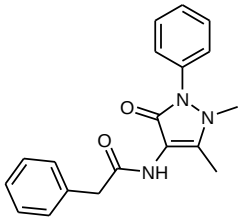
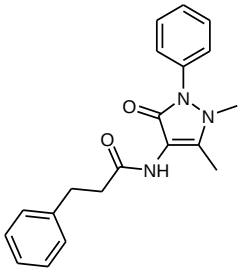	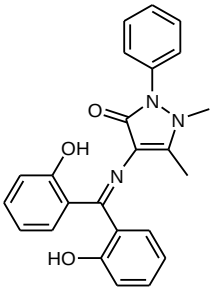
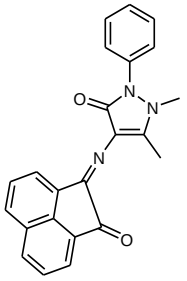	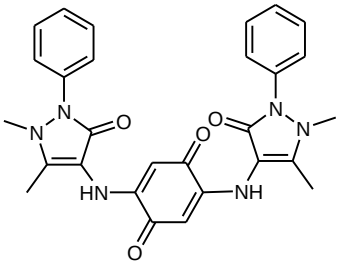
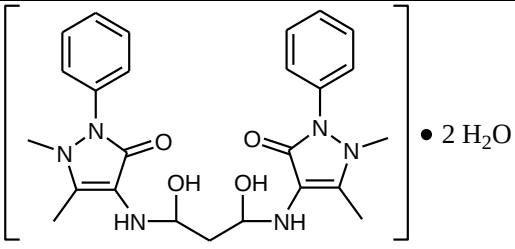	

A structural study of nine 4-aminoantipyrine derivatives

Mark G. Smith[†] and Andreas Lemmerer*[‡]

†*Department of Chemistry, University of South Africa, Unisa Science Campus, Florida, 1709, Johannesburg, South Africa, and* [‡]*Molecular Sciences Institute, School of Chemistry, University of the Witwatersrand, 2050, Johannesburg, South Africa*

RECEIVED DATE (to be automatically inserted after your manuscript is accepted if required according to the journal that you are submitting your paper to)

To whom correspondence should be addressed:

Professor Andreas Lemmerer, Molecular Sciences Institute, School of Chemistry, University of the Witwatersrand, Private Bag 3, 2050, Johannesburg, South Africa.
E-mail: andreas.lemmerer@wits.ac.za. Fax: +27-11-717-6749. Tel: +27-11-717-6711.

ABSTRACT:

Nine derivatives of 4-amino-1,5-dimethyl-2-phenyl-2,3-dihydro-1*H*-pyrazol-3-one (4-aminoantipyrine), $C_{11}H_{13}N_3O$, have been synthesized and structurally characterized. The derivatives were synthesized from the reactions of various ketones, aldehydes, alcohols and carboxylic acids, producing: 1,5-dimethyl-4-(4-oxocyclohexa-2,5-dienylideneamino)-2-phenyl-1*H*-pyrazol-3(2*H*)-one, $C_{17}H_{15}N_3O$, (**I**), 4-(benzylideneamino)-1,5-dimethyl-2-phenyl-1*H*-pyrazol-3(2*H*)-one, $C_{18}H_{17}N_3O$, (**II**), 4-(3-hydroxy-4-methoxybenzylideneamino)-1,5-dimethyl-2-phenyl-1*H*-pyrazol-3(2*H*)-one, $C_{19}H_{19}N_3O_3$, (**III**), *N*-(1,5-dimethyl-3-oxo-2-phenyl-2,3-dihydro-1*H*-pyrazol-4-yl)-2-phenylacetamide, $C_{19}H_{19}N_3O_2$, (**IV**), *N*-(1,5-dimethyl-3-oxo-2-phenyl-2,3-dihydro-1*H*-pyrazol-4-yl)-3-phenylpropanamide, $C_{20}H_{21}N_3O_2$, (**V**), 4-(bis(2-hydroxyphenyl)methyleneamino)-1,5-dimethyl-2-phenyl-1*H*-pyrazol-3(2*H*)-one, $C_{24}H_{21}N_3O_3$, (**VI**), 1,5-dimethyl-4-(2-oxoacenaphthylen-1(2*H*)-ylideneamino)-2-phenyl-1*H*-pyrazol-3(2*H*)-one, $C_{23}H_{17}N_3O_2$, (**VII**), 2,5-bis(1,5-dimethyl-3-oxo-2-phenyl-2,3-dihydro-1*H*-pyrazol-4-ylamino)cyclohexa-2,5-diene-1,4-dione, $C_{28}H_{26}N_6O_4$, (**VIII**), and 4,4'-(1,3-dihydroxypropane-1,3-diyl)bis(azanediyl)bis(1,5-dimethyl-2-phenyl-1*H*-pyrazol-3(2*H*)-one) dihydrate, $C_{25}H_{29}N_6O_6$, (**IX**). The reaction of 4-aminoantipyrine with ketones and aldehydes yielded imines, whereas its reaction with an alcohol yielded an enamine. The reaction of 4-aminoantipyrine with carboxylic acids yielded two amides and one enamine. These reactions of the amine functional group of 4-aminoantipyrine with carboxylic acid functional groups is unusual, as two of them occurred at room temperature and one at 40°C, whereas these reactions are usually only expected to take place at over 100°C.

KEYWORDS:

4-Aminoantipyrine, crystal engineering, imines, enamines, amides

Introduction

4-Aminoantipyrine (4AAP) is an API with powerful antipyretic (fever reducing) properties (Acheson, 1960), and is considered a prophylactic against oxidative stress (Teng *et al*., 2011a). The crystal structure of 4AAP has been reported by Li *et al.* (Li *et al*., 2013) and by Mnguni *et al (*Mnguni and Lemmerer, 2015). Two of its derivatives, aminoantipyrine and 4-(*N*,*N*-dimethyl)-aminoantipyrine, have been used as analgesic and anti-inflammatory drugs since the late 19th century. Their concurrent use with aspirin is particularly beneficial as they have been shown to prevent or attenuate the anti-platelet effects of aspirin (Hohlfeld *et al*., 2008). However, despite the many documented therapeutic benefits, these pyrazolones have been associated with agranulocytosis and their use has been largely discontinued (Teng *et al*., 2011b). This has sparked a drive to produce covalently modified derivatives of 4AAP (Deshmukh *et al*., 2015). Deshmukh commented that due to the significant benefits of 4AAP derivatives, and their interactions with DNA, the precise nature and structures of these Schiff bases is of "*remarkable importance*". The desired modification of 4AAP to prepare pharmaceutically significant derivatives is by the covalent addition of adducts to the 4-amino functional group shown in **Figure 1**. Mnguni *et al.* recently reported that in 4AAP that has been covalently modified to form Schiff bases to form enamines, six-membered intermolecular N−H···O hydrogen bonding is favoured, with imines having C−H···O bonds. Mnguni notes that of 146 structures in the Cambridge Structural Database (CSD, Version 5.34) (Groom and Allen, 2014) of modified isoniazid that crystallize with an imine backbone, all 136 non-solvated or hydrated structures have an intramolecular C−H···O bond. All structures having an enamine backbone contain intramolecular N−H···O hydrogen bonding (Mnguni and Lemmerer, 2015). This report contains a structural study of 4-aminoantipyrine molecules that have been covalently modified to form Schiff bases.

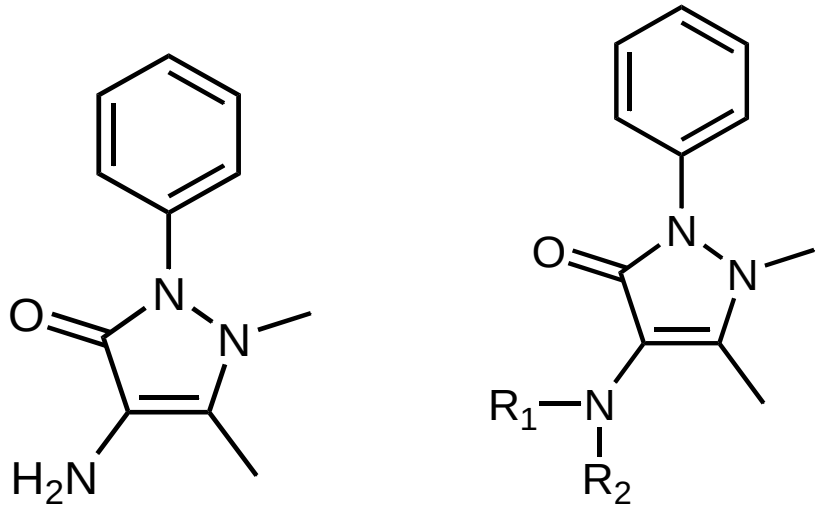

Figure 1: Structure of 4AAP and its derivatives. The desired modification of 4AAP is by the covalent addition of adducts (R_1 and/or R_2) to the 4-amino functional group.

Experimental Methods

1,5-dimethyl-4-(4-oxocyclohexa-2,5-dienylideneamino)-2-phenyl-1*H*-pyrazol-3(2*H*)-one, I

0.0631 g of 4-aminoantipyrine (0.311 mmol) and 0.0343 g of 1,4-benzoquinone (0.317 mmol) were added into a sample vial. The solids were dissolved in 3 mL of 1,2-dichloroethane, stirred for 30 minutes at room temperature, and were left to stand very slightly opened to the atmosphere. Red plates were afforded after 2 days.

4-(benzylideneamino)-1,5-dimethyl-2-phenyl-1*H*-pyrazol-3(2*H*)-one, II

0.0998 g of 4-aminoantipyrine (0.491 mmol) and 1.0 mL of benzaldehyde were added into a sample vial. 3 mL of 1,2-dichloroethane was added, the solution stirred for 30 minutes at room temperature, and left to stand very slightly opened to the atmosphere. White needles were afforded after 3 days.

4-(3-hydroxy-4-methoxybenzylideneamino)-1,5-dimethyl-2-phenyl-1*H*-pyrazol-3(2*H*)-one, III

0.1025g of 4-aminoantipyrine (0.5043 mmol) and 0.0805 g of 3-hydroxy-4-methoxybenzaldehyde (0.529 mmol) were added into a sample vial. The solids were dissolved in 10 mL of a 1:1 1,2-dichloroethane : acetonitrile mixture, and stirred for 60 minutes at room temperature. Dimethylformamide (DMF) was added dropwise until all the solids had dissolved. The solution was then left to stand opened to the atmosphere. Colourless blocks were afforded after 60 days.

***N*-(1,5-dimethyl-3-oxo-2-phenyl-2,3-dihydro-1*H*-pyrazol-4-yl)-2-phenylacetamide, IV**

0.0821 g of 4-aminoantipyrine (0.404 mmol) and 0.0577 g of phenylethanoic acid (0.424 mmol) were added into a sample vial. The solids were dissolved in 3 mL of 1,2-dichloroethane, stirred for 30 minutes at room temperature, and were left to stand very slightly opened to the atmosphere. The resultant solid mass was re-dissolved in chloroform and again left to stand very slightly opened to the atmosphere. Yellow blocks were afforded after 24 hours.

***N*-(1,5-dimethyl-3-oxo-2-phenyl-2,3-dihydro-1*H*-pyrazol-4-yl)-3-phenylpropanamide, V**

0.0978 g of 4-aminoantipyrine (0.481 mmol) and 0.0727 g of phenylpropanoic acid (0.484 mmol) were added into a sample vial. The solids were dissolved in 3 mL of methanol, stirred for 30 minutes at 40°C, and were left to stand very slightly opened to the atmosphere. Colourless plates were afforded after 3 days.

4-(bis(2-hydroxyphenyl)methyleneamino)-1,5-dimethyl-2-phenyl-1*H*-pyrazol-3(2*H*)-one, VI

0.0733 g of 4-aminoantipyrine (0.361 mmol) and 0.0782 g of 2,2'-dihydroxybenzophenone (0.365 mmol) were added into a sample vial. The solids were dissolved in 5 mL of a 1:1 mixture of 1,2-dichloroethane : methanol, stirred for 30 minutes was left to stand opened to the atmosphere. 3 mL of chloroform and 3mL of ethanol was added to re-dissolve the resultant solid mass after all the solvent had evaporated, and the solution was again left to stand very slightly opened to the atmosphere. Yellow blocks were afforded after 2 days.

1,5-dimethyl-4-(2-oxoacenaphthylen-1(2*H*)-ylideneamino)-2-phenyl-1*H*-pyrazol-3(2*H*)-one, VII

0.0672 g of 4-aminoantipyrine (0.331 mmol) and 0.0611 g of acenaphthylene-1,2-dione (0.335 mmol) were added into a sample vial. The solids were dissolved in 5 mL of a 1:1 mixture of 1,2-dichloroethane : methanol, and stirred for 60 minutes. 6 drops of dimethylformamide (DMF) were added to ensure that the solid was fully dissolved. The solution was then left to stand very slightly opened to the atmosphere. Orange blocks were afforded after 14 days.

2,5-bis(1,5-dimethyl-3-oxo-2-phenyl-2,3-dihydro-1*H*-pyrazol-4-ylamino)cyclohexa-2,5-diene-1,4-dione, VIII

0.0832 g of 4-aminoantipyrine (0.409 mmol) and 0.0611 g of 2,5-dihydroxy-1,4-benzoquinone (0.408 mmol) were added into a sample vial. The solids were dissolved in 20 mL of a mixture of equal parts of 1,2-dichloroethane, methanol, chloroform, and toluene, and stirred for 120 minutes. 6 drops of dimethylformamide (DMF) were added to ensure that the solid was fully dissolved. The solution was then left to stand very slightly opened to the atmosphere. Red plates were afforded after 14 days. (The unusual mixture of solvents is due to the fact that initially the reagents would not dissolve in 5 mL of 1,2-dichloroethane. Therefore, 5 mL of each of the other solvents were added one by one until the reagents started dissolving.)

4,4'-(1,3-dihydroxypropane-1,3-diyl)bis(azanediyl)bis(1,5-dimethyl-2-phenyl-1*H*-pyrazol-3(2*H*)-one) dihydrate, IX

0.0742 g of 4-aminoantipyrine (0.365 mmol) and 0.0391 g of malonic acid (0.376 mmol) were added into a sample vial. The solids were dissolved in 3 mL of a 1:1 mixture of 1,2-dichloroethane : methanol, stirred for 30 minutes at room temperature, and were left to stand very slightly opened to the atmosphere. The resultant solid mass was re-dissolved in chloroform and again left to stand very slightly opened to the atmosphere. Colourless blocks were afforded after 3 days.

Crystal Data and X-ray Structure Analysis.

Intensity data for the nine crystal structures were collected on a Bruker APEX II CCD area detector diffractometer with graphite monochromated Mo-K_α radiation (50 kV, 30 mA) at 173K. The collection method involved ω-scans with a 0.5° width. *SAINT+* version 6.02.6 software was used for data reduction and *SADABS* was used to make empirical absorption corrections (Bruker, 2004). The crystal structures were solved using direct methods on *SHELXS-97* (Sheldrick, 2015). Non-hydrogen atoms were first refined isotropically, followed by anisotropic refinement by full matrix least-squares calculations based on F^2 using *SHELXL-2017* (Sheldrick, 2015). C-bound H atoms were located in the difference electron density map, then positioned geometrically and were allowed to ride on their respective parent atoms, with thermal displacement parameters 1.2 times that of the parent C atom. Diagrams and publication material were generated using *WinGX* (Farrugia, 2012), *ORTEP-3* (Farrugia, 2012), *PLATON (Spek, 2009)* and *MERCURY (*Macrae, C. F. e*t al.*, 2008). The crystallographic data of each crystal is summarized in **Table 1,** the hydrogen bonding geometries in **Table 2**, and a table of bond lengths for bonds involving N1 in **Table 3**.

Table 1 Crystallographic data for compounds **1-9**

	I	**II**	**III**	**IV**	**V**
Formula	$C_{17}H_{15}N_3O$	$C_{18}H_{17}N_3O$	$C_{19}H_{19}N_3O_3$	$C_{19}H_{19}N_3O_2$	$C_{20}H_{21}N_3O_2$
M_r	293.32	291.34	337.37	321.37	335.40
Temperature/K	173(2)	173(2)	173(2)	173(2)	173(2)
Wavelength/Å	0.71073	0.71073	0.71073	0.71073	0.71073
Crystal size/mm^3	0.078×0.151×0.282	0.134×0.198×0.387	0.122×0.302×0.529	0.032×0.291×0.393	0.116×0.190×0.668
Crystal system	Monoclinic	Monoclinic	Monoclinic	Triclinic	Orthorhombic
Space group	$P2_1/c$	$P2_1/c$	$P2_1/c$	$P\bar{1}$	$Pca2_1$
a/Å	8.2850(5)	12.9148(4)	7.0345(2)	10.1188(9)	15.6407(5)
b/Å	23.9870(14)	6.8245(2)	26.0987(6)	10.4488(9)	6.8754(2)
c/Å	7.2890(4)	17.0268(5)	9.0665(2)	17.8713(15)	32.4198(13)
α/°	90	90	90	100.768(4)	90
β/°	98.162(4)	90.112(2)	98.3950(10)	92.597(4)	90
γ/°	90	90	90	116.833(4)	90
V/Å^3	1433.89(14)	1500.69(8)	1646.70(7)	1638.2(3)	3486.3(2)
Z	4	4	4	4	8
ρ (calcd)/Mg m^{-3}	1.359	1.290	1.361	1.303	1.278
μ/mm^{-1}	0.092	0.082	0.094	0.086	0.084
F(000)	616	616	712	680	1424
Θ Range for data	1.698 to 25.475	1.577 to 25.498	1.560 to 27.993	2.846 to 27.999	2.513 to 26.320
Reflections collected	15414	9987	26500	77304	14726
No. of unique data	2661 [0.0742]	2223 [0.0637]	3964 [0.0471]	7908 [0.0583]	7908 [0.0583]
No. data with $I \geq 2\sigma(I)$	1577	1565	3234	6188	4236
Final R($I \geq 2\sigma(I)$)	0.0504	0.0650	0.0451	0.0456	0.0545
Final wR_2 (all data)	0.1287	0.1975	0.1153	0.1063	0.1529
CCDC deposition					

	VI	**VII**	**VIII**	**IX**
Formula	$C_{24}H_{21}N_3O_3$	$C_{23}H_{17}N_3O_2$	$C_{28}H_{26}N_6O_4$	$C_{25}H_{29}N_6O_6$
M_r	399.44	367.39	510.55	509.54
Temperature/K	173(2)	173(2)	173(2)	173(2)
Wavelength/Å	0.71073	0.71073	0.71073	0.71073
Crystal size/mm^3	0.203×0.214×0.264	0.095×0.100×0.249	0.046×0.222×0.266	0.140×0.204×0.292
Crystal system	Monoclinic	Triclinic	Monoclinic	Triclinic
Space group	$P2_1$	$P\bar{1}$	$P2_1/n$	$P\bar{1}$
a/Å	7.8217(4)	7.1299(2)	13.0398(4)	9.8423(6)
b/Å	15.7139(8)	9.2954(3)	7.1786(2)	11.2923(7)
c/Å	8.7602(4)	13.9034(4)	14.9824(5)	13.3810(8)
α/°	90	75.985(2)	90	69.053(3)
β/°	108.278(3)	84.244(2)	112.642(2)	73.926(4)
γ/°	90	83.840(2)	90	68.979(3)
V/Å^3	1022.39(9)	886.22(5)	1294.37(7)	1277.49(14)
Z	2	2	2	2
ρ (calcd)/Mg m^{-3}	1.298	1.377	1.310	1.325
μ/mm^{-1}	0.087	0.090	0.091	0.097
F(000)	420	384	536	538
Θ Range for data	2.448 to 27.997	2.267 to 25.500	1.764 to 27.993	1.654 to 27.999
Reflections collected	8444	13937	13992	22991
No. of unique data [R(int)]	4210 [0.0238]	3222 [0.0443]	3129 [0.0553]	6140 [0.0632]
No. data with $I \geq 2\sigma(I)$	3888	2479	2084	3310
Final R($I \geq 2\sigma(I)$)	0.0364	0.0378	0.0458	0.0757
Final wR_2 (all data)	0.0957	0.1094	0.1133	0.2364
CCDC deposition number				

Table 2 Hydrogen bonding details of compounds **I-IX**

	d(D─H)/Å	*d*(H···A)/Å	*d*(D···A)/Å	∠(D─H···A)/°
I				
C4-H4C···O1[a]	0.98	2.33	3.282(3)	164
C11-H11···N1[b]	0.95	2.63	3.576(3)	175
C14-H14···O2[c]	0.95	2.41	3.348(3)	170
C16-H16···O1[d]	0.95	2.51	3.384(3)	152
C17-H17···O1	0.95	2.11	2.961(3)	148
I				
C4-H4C···O1[e]	0.98	2.53	3.497(4)	168
C5-H5A···O1[e]	0.98	2.59	3.476(4)	151
C12-H12···O1	0.95	2.41	3.072(4)	127
III				
C4-H4C···O1[f]	0.98	2.34	3.3111(19)	172
C7-H7···O2[g]	0.95	2.53	3.2721(18)	135
C11-H11···N1[h]	0.95	2.69	3.6306(19)	172
C12-H12···O1	0.95	2.35	3.0401(18)	129
O2-H2···O1[g]	0.84	1.83	2.6570(15)	167
IV				
C4-H4A···O2	0.98	2.51	3.1241(19)	120
C23-H23C···O4	0.98	2.58	3.0803(19)	112
C32-H32A···O4[i]	0.99	2.53	3.4177(17)	150
N1-H1···O3	0.88	1.95	2.8250(14)	173
N4-H4···O1	0.88	1.96	2.8093(14)	162
V				
C4-H4A···O1[j]	0.98	2.58	3.435(7)	146
C4-H4B···O2	0.98	2.40	3.066(7)	125
C5-H5A···O4	0.98	2.56	3.248(7)	127
C5-H5C···O1[j]	0.98	2.48	3.260(7)	137
N1-H1···O3[k]	0.88	2.00	2.833(7)	158
C24-H24A···O3[j]	0.98	2.55	3.396(7)	145
C24-H24B···O4	0.98	2.41	3.079(7)	125
C25-H25A···O2[j]	0.98	2.58	3.253(7)	126
C25-H25C···O3[j]	0.98	2.47	3.274(7)	139
N4-H4···O1[l]	0.88	2.01	2.850(7)	159

VI				
O2-H2···N1	0.84	1.83	2.567(2)	146
O3-H3···O1[m]	0.84	1.89	2.727(2)	172
VII				
C4-H4C···O1[n]	0.98	2.41	3.378(2)	168
C5-H5C···O2[o]	0.98	2.43	3.397(2)	167
VIII				
C4-H4C···O1[p]	0.98	2.41	3.387(2)	172
C5-H5C···O2[q]	0.98	2.25	3.213(2)	168
C7-H7···O2[r]	0.95	2.59	3.262(2)	128
N1-H1···O1[s]	0.88	2.09	2.8645(18)	147
IX				
C5-H5C···O1W[t]	0.98	2.50	3.475(5)	173
C17-H17A···O2[u]	0.98	2.55	3.502(5)	165
C23-H23···O2W	0.95	2.52	3.434(5)	161
C25-H25A···O3[v]	0.99	2.32	3.210(5)	149
C25-H25B···O1[w]	0.99	2.65	3.448(4)	138
N1-H1···O1$_w$	0.90(3)	1.86(3)	2.764(3)	177(3)
N4-H4···O3[v]	0.99(5)	1.99(5)	2.938(4)	160(4)
O1W-H1W···O2	0.89	1.91	2.770(4)	162
O1W-H2W···O3	0.91	1.81	2.709(4)	170
O2W-H3W···O4[x]	0.85	2.13	2.914(6)	153

[a] x,y,z+1. [b] -x,-y+1,-z+2. [c] x,-y+3/2,z+1/2. [d] -x+1,-y+1,-z+1. [e] x,y+1,z. [f] x-1,y,z. [g] -x+1,-y+1,-z+1. [h] -x,-y+1,-z+2 [i] -x+2,-y+2,-z+1. [j] x,y-1,z. [k] x-1/2,-y+2,z. [l] x+1/2,-y+2,z. [m] x,y,z-1. [n] x+1,y,z. [o] -x+1,-y+1,-z+1. [p] x,y+1,z. [q] x+1/2,-y+1/2,z+1/2. [r] x+1/2,-y-1/2,z+1/2. [s] -x+3/2,y+1/2,-z+1/2. [t] -x+1,-y+1,-z+1. [u] x-1,y,z. [v] -x,-y+2,-z+1. [w] -x+1,-y+2,-z. [x] -x,-y+1,-z+1.

Table 3 Bond lengths for bonds involving N1	Bond lengths [Å]
I	
C2-N1	1.375(3)
C12-N1	1.312(3)
II	
C2-N1	1.381(4)
C12-N1	1.290(4)
III	
C2-N1	1.3937(18)
C12-N1	1.2844(19)
IV	
C2-N1	1.4070(16)
C12-N1	1.3572(17)
N1-H1	0.8800
V	
C2-N1	1.407(8)
C12-N1	1.363(8)
N1-H1	0.8800
VI	
C2-N1	1.421(3)
C12-N1	1.290(3)
VII	
C2-N1	1.386(2)
C12-N1	1.2881(19)
VIII	
C2-N1	1.4139(19)
C12-N1	1.339(2)
N1-H1	0.8800
IX	
C2-N1	1.411(4)
C12-N1	1.335(4)
N1-H1	0.90(3)

Results

The asymmetric units of structures **I** to **IX** are shown in Figure 2.

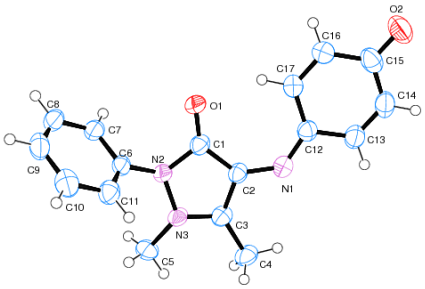

(I)

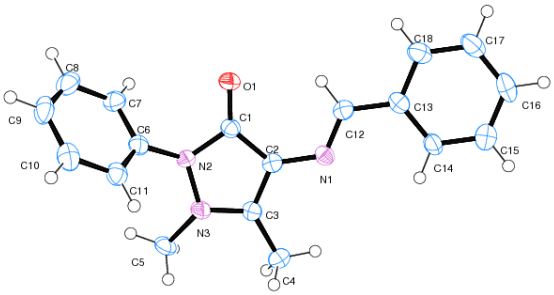

(II)

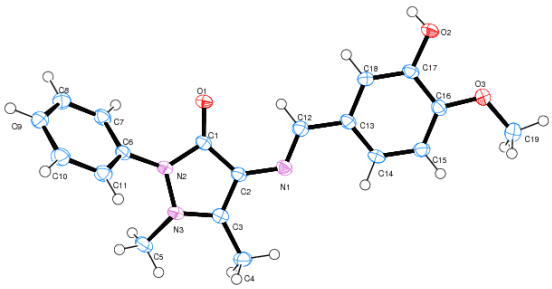

(III)

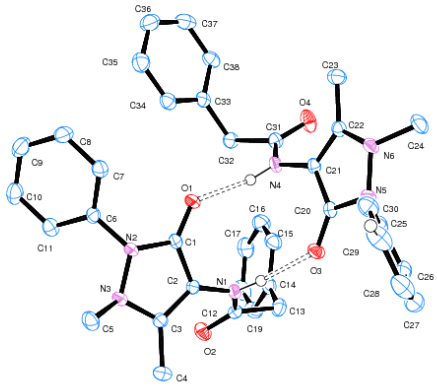

(IV)

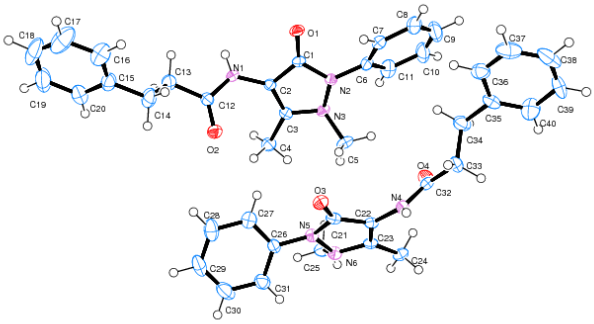

(V)

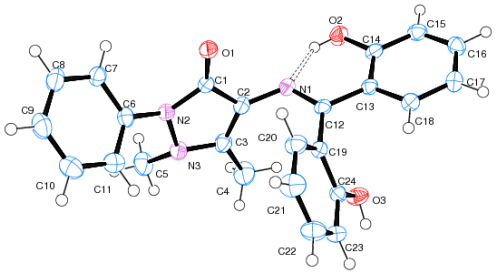

(VI)

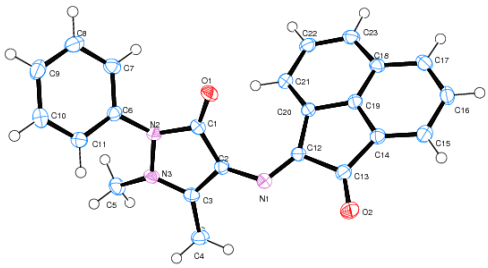

(VII)

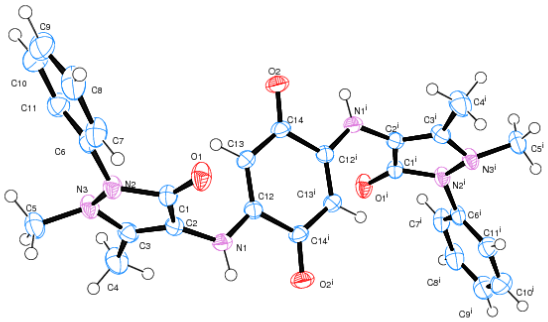

(VIII)

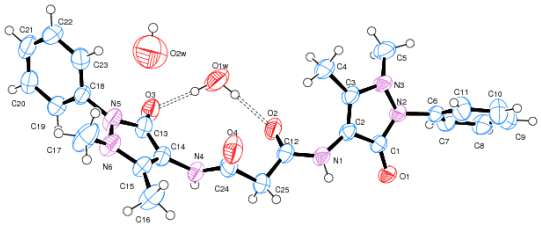

(IX)

Figure 2: Asymmetric units of structures **I**-**IX**.

The reaction of the ketone group of 1,4-benzoquinone with the amine group of 4AAP produced the imine **I**. Structure **I** crystallizes in the $P2_1/c$ space group and contains one molecule of 1,5-dimethyl-4-(4-oxocyclohexa-2,5-dienylideneamino)-2-phenyl-1*H*-pyrazol-3(2*H*)-one. The molecules in crystal **I** form discreet zero-dimensional (0D) entities that are not hydrogen bonded to any other molecules. The crystal structure is held together entirely through multiple weak C−H···O and C−H···N interactions. The C−H···O interactions occur between both the carbonyl oxygen on the benzoquinine moiety and the antipyrine carbonyl oxygen with hydrogen atoms on the benzoquinone ring of neighbouring molecules as shown in **Figure 3**. The C−H···N interaction is between the amine nitrogen atom and the benzene ring of the antipyrine moiety.

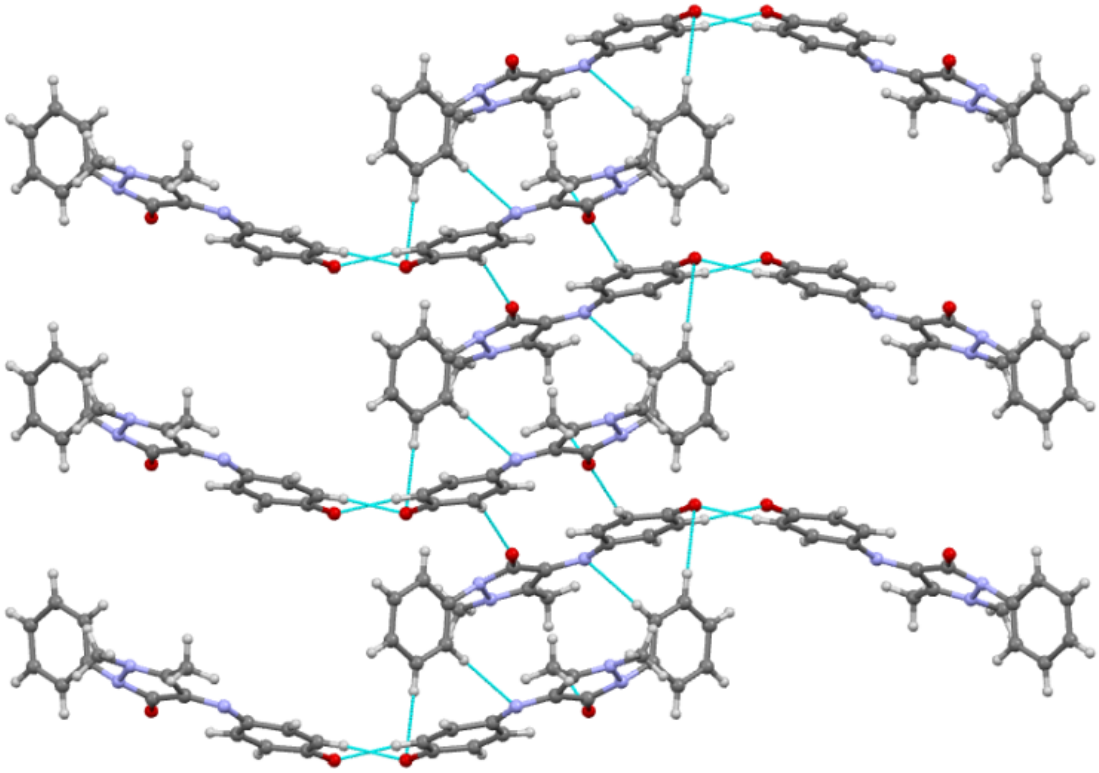

Figure 3: Packing diagram of **I** showing the multiple weak C−H···O and C−H···N interactions.

The reaction of the aldehyde group of benzaldehyde with the amine group of 4AAP produced the imine **II**. Structure **II** crystallizes in the $P2_1/c$ space group and contains one molecule of 4-(benzylideneamino)-1,5-dimethyl-2-phenyl-1*H*-pyrazol-3(2*H*)-one. As with crystal **I**, crystal **II** does not have regular hydrogen bonding, but packs via weak C−H···O and C−H···π interactions. The carbonyl oxygen atom of the antipyrine ring interacts with the H18 atom of the benzaldehyde aromatic ring via a C−H···O interaction and the methyl hydrogen atom H4B undergoes a C−H···π interaction with the π-system on the antipryring ring shown in **Figure 4a**. This results in a visually pleasing 1D tape along the *b*-axis with the aromatic rings directed towards the edges of the tape as shown in **Figure 4b**.

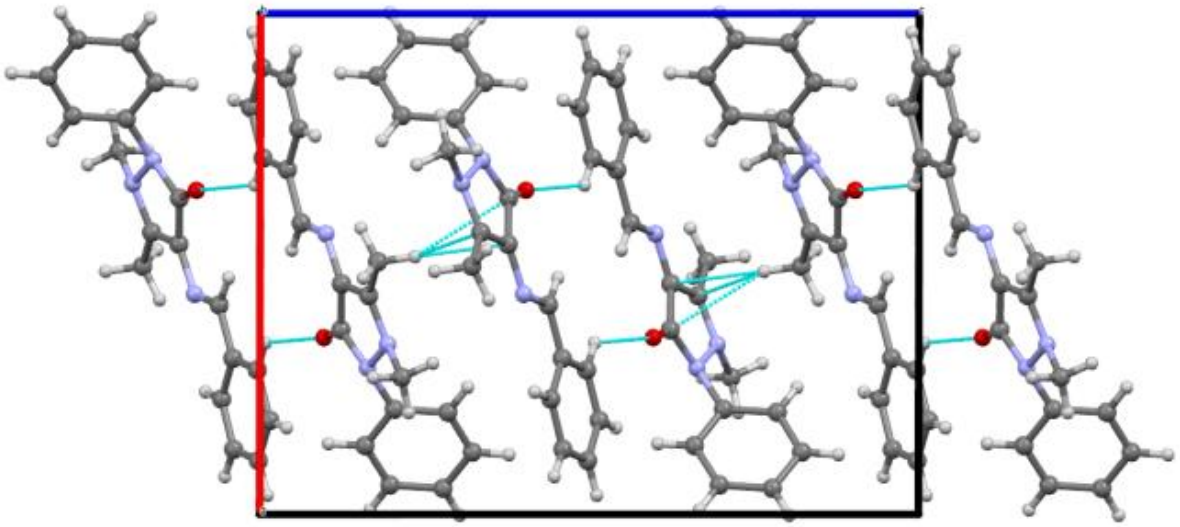

(a)

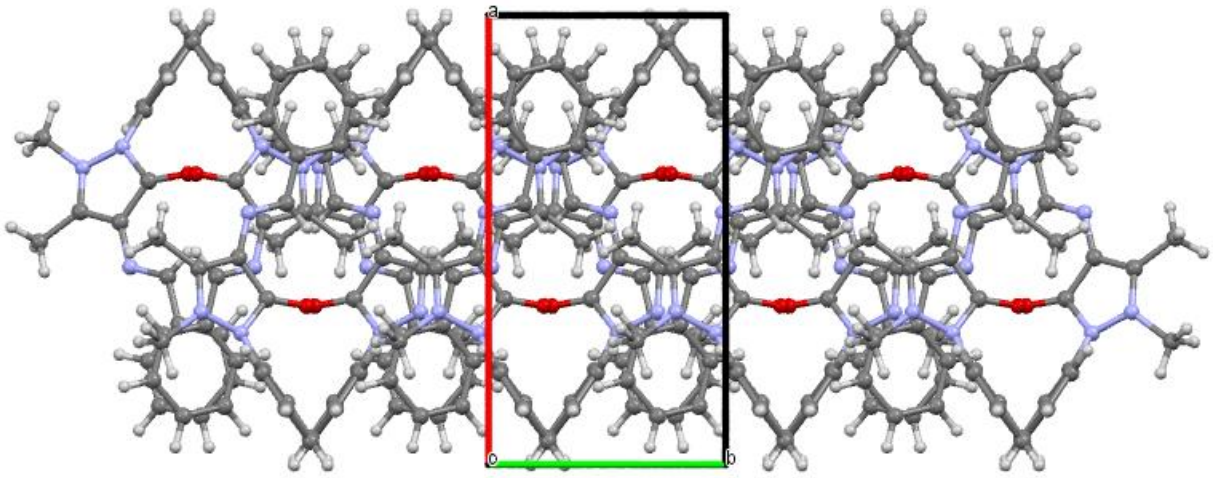

(b)

Figure 4: Packing diagram of **II** showing (a) C−H···O and C−H··· π interactions and (b) the 1D ribbon formed along the *b*-axis.

The reaction of the aldehyde group of 3-hydroxy-4-methoxybenzaldehyde with the amine group of 4AAP produced the imine **III**. Structure **III** crystallizes in the $P2_1/c$ space group and contains one molecule of 4-(3-hydroxy-4-methoxybenzylideneamino)-1,5-dimethyl-2-phenyl-1*H*-pyrazol-3(2*H*)-one. The 3-hydroxy group on the benzaldehyde adduct provides a hydrogen bond donor (H2) to the carbonyl acceptor (O1) of a neighbouring molecule to form a dimer via two sets of

C−H···O heterosynthons with graph set notation $R_2^2(20)$ (Bernstein *et al*., 1995)) This results in a packing pattern consisting of 0D entities as shown in **Figure 5**.

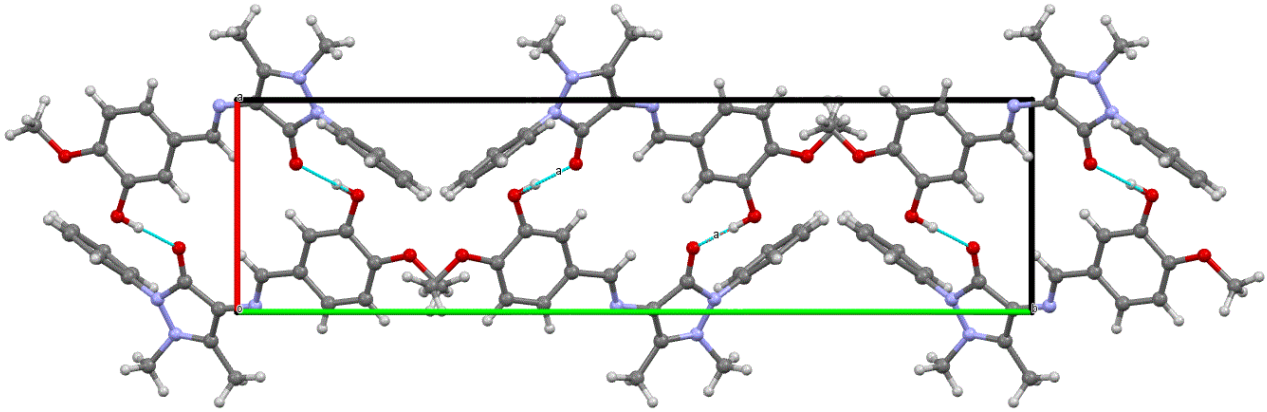

Figure 5: Packing diagram of **III** showing the dimers and the $R_2^2(20)$ ring formed by two C−H···O heterosynthons.

The reaction of the carboxylic acid group of phenylethanoic acid with the amine group of 4AAP produced the amide **IV**. Structure **IV** crystallizes in the $P\bar{1}$ space group and contains two molecules of *N*-(1,5-dimethyl-3-oxo-2-phenyl-2,3-dihydro-1*H*-pyrazol-4-yl)-2-phenylacetamide. The two molecules in the asymmetric unit form a dimer via two N−H···O heterosynthons formed between the carbonyl oxygen aceptor atoms and the amine hydrogen donor atoms, resulting in 10 membered ring, with graph-set notation $R_2^2(10)$. The reaction of the amine group with a carboxylic acid group at room temperature is unusual, because at room temperature one would expect the basic amine to deprotonate the carboxylic acid to form an unreactive carboxylate. However, at high temperatures (above 100°C), dehydration can occur with the loss of a water molecule, and the nitrogen lone pair attacks the resulting carbocation forming an amide. However, in the case of **IV**, the dehydration reaction occurred at room temperature. This unusual dehydration reaction was also observed at room temperature in crystal **IX** described below, and at 40°C in crystal **V**. The hydrogen bonded dimers form a 0D packing pattern as shown in **Figure 6**.

The reaction of the carboxylic acid group of phenylpropanoic acid with the amine group of 4AAP produced the amide **V**. Structure **V** crystallizes in the $Pca2_1$ space group and contains two molecules of *N*-(1,5-dimethyl-3-oxo-2-phenyl-2,3-dihydro-1*H*-pyrazol-4-yl)-3-phenylpropanamide. Structure **V** packs in one dimensional (1D) tubes along the *b*-axis (**Figure**

6b) which are held together by a $R_2^2(10)$ ring formed via two N−H···O heterosynthons, where the amine hydrogen atom of each molecule in the asymmetric unit provides the hydrogen bond donor to the carbonyl acceptor atom of the other molecule in the asymmetric unit.

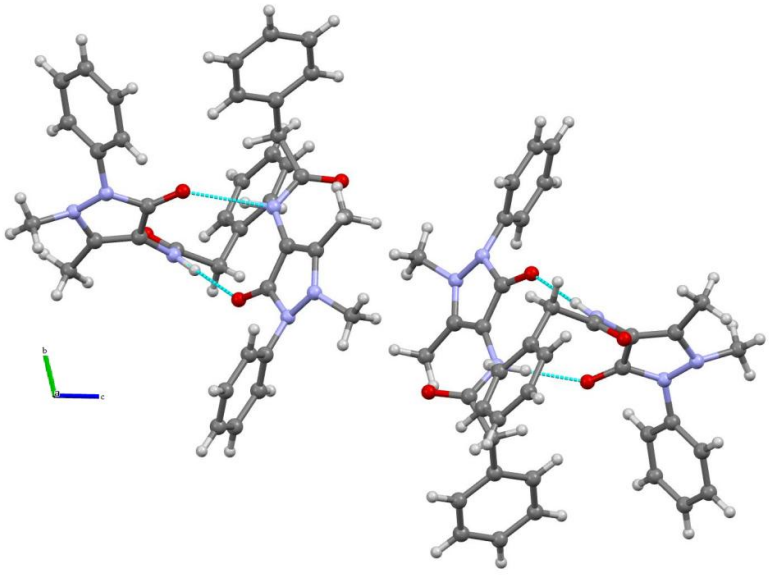

(a)

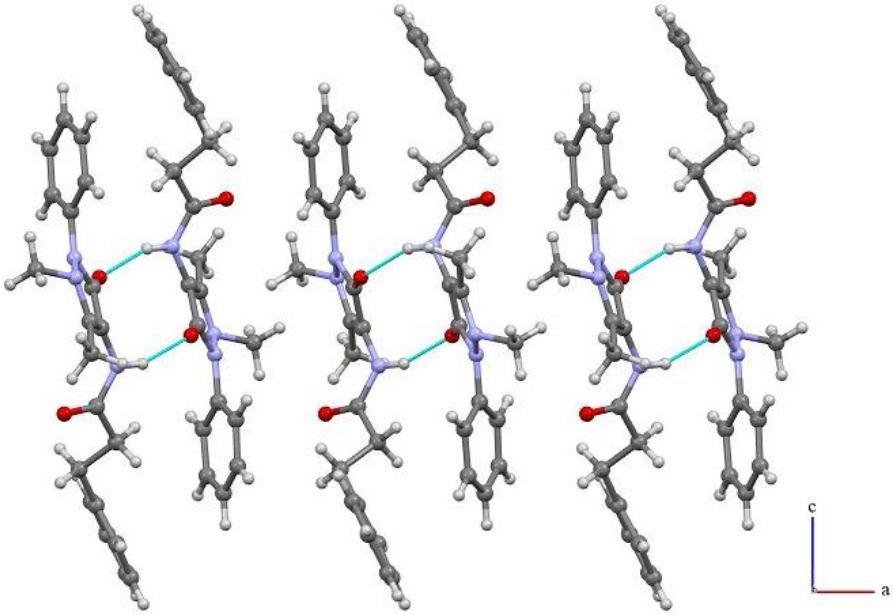

(b)

Figure 6: Packing diagram of (a) **IV** showing the dimers and the $R_2^2(20)$ ring formed by two C−H···O heterosynthons (b) Crystal **V** showing the "square tubing" packing pattern along the *b*-axis.

The reaction of the ketone group of 2,2'-dihydroxybenzophenone with the amine group of 4AAP produced the imine **VI**. Structure **VI** crystallizes in the $P2_1$ space group and contains one molecule of 4-(bis(2-hydroxyphenyl)methyleneamino)-1,5-dimethyl-2-phenyl-1*H*-pyrazol-3(2*H*)-one. As expected from Etter's rules of hydrogen bonding (Etter *et al.*, 1990), one of the hydroxyl group donors (H2) forms a six-membered intramolecular hydrogen bonded ring (graph set notation *S*(6)) with the imine nitrogen atom (N1). The other hydroxyl group forms a regular C−H···O heterosynthon with the carbonyl oxygen acceptor atom of an adjacent molecule to form a $C_1^1(9)$ chain or ribbon along the *c*-axis (**Figure 7a**). The structure is further stabilized by π ···π stacking of the aromatic antipyrine ring of one molecule and one of the benzophenone rings of another molecule in a slightly tilted fashion, 4.063 Å apart along the *a*-axis with a distance of 4.063 Å between the rings (**Figure 7b**).

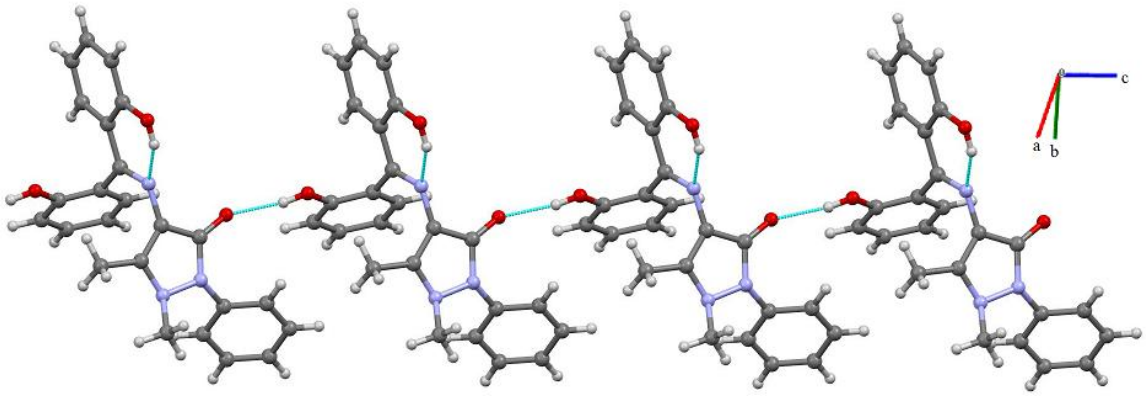

(a)

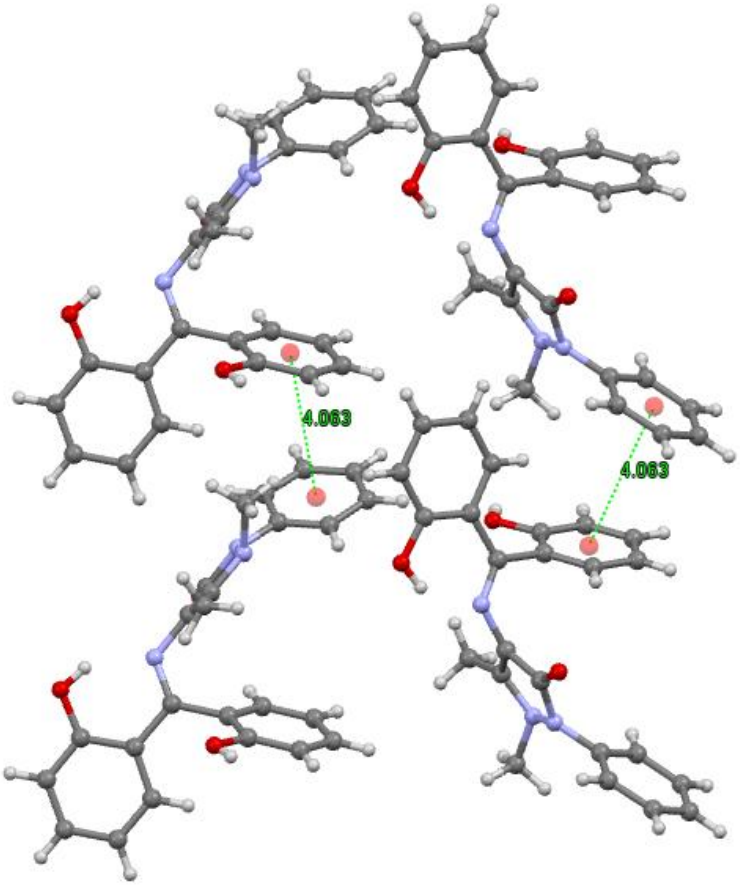

(b)

Figure 7: Packing diagram of **VI** showing (a) the 1D chain or ribbon formed along the *c*-axis and (b) the π···π stacking of the aromatic antipyrine ring and one of the benzophenone rings along the *a*-axis.

The reaction of the ketone group of acenaphthylene-1,2-dione with the amine group of 4AAP produced the imine **VII**. Structure **VII** crystallizes in the $P\bar{1}$ space group and contains one molecule of 1,5-dimethyl-4-(2-oxoacenaphthylen-1(2*H*)-ylideneamino)-2-phenyl-1*H*-pyrazol-3(2*H*)-one. The extensive π system of the acenaphthylene lends itself to π···π nteractions in the asymmetric unit, and indeed, the molecules of this crystal stack together with the acenaphthylene groups stacked on top of each other as shown in **Figure 8a** with the aromatic ring involved in π···π interactions having a distance of 3.269 Å apart . The packing is supported by C−H···O ands C−H··· π interactions. The carbonyl oxygen (O1) of the antipyrine moiety has a weak C−H···O interaction with the H8 hydrogen atom of the antipyrine aromatic ring and the acenaphthylene carbonyl oxygen (O2) has a weak C−H···O interaction with the H22 atom of the acenaphthylene group of an adjacent molecule. Lastly a C−H···π interaction is found between the H9 hydrogen atom of the antipyrine aromatic ring and the acenaphthylene π system as shown in **Figure 8b**.

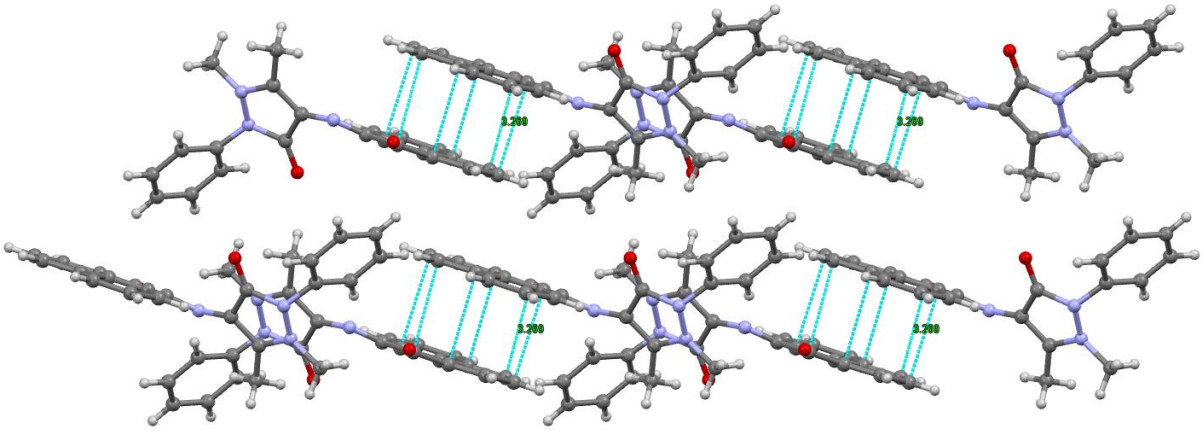

(a)

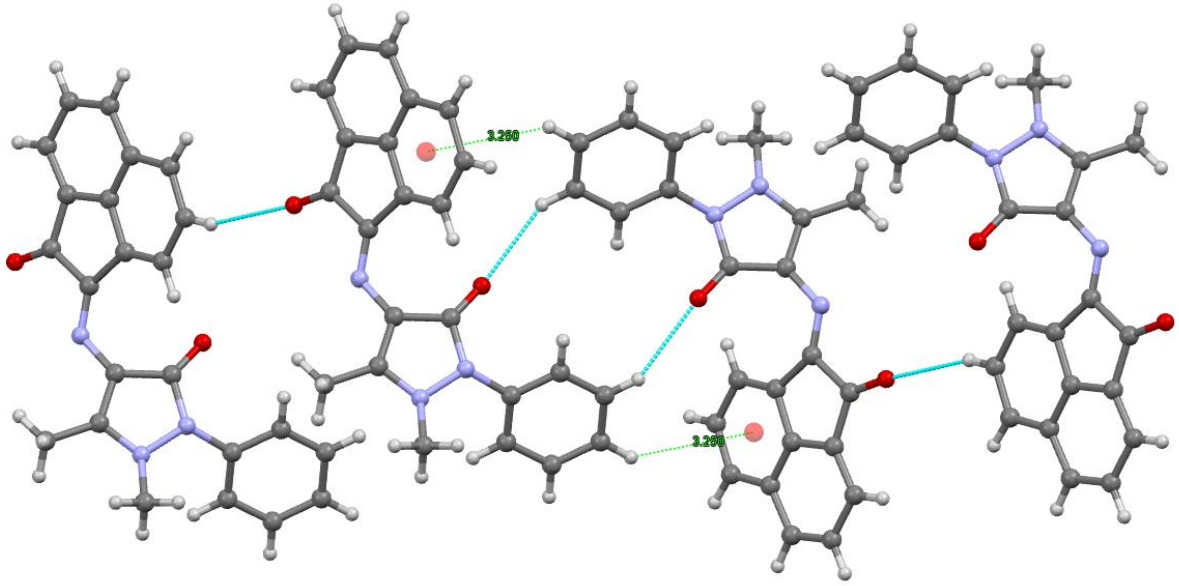

(b)

Figure 8: Packing diagram of **VII** showing (a) the extensive π ···π stacking of the acenaphthylene groups and (b) the weak supporting C−H···O and C−H··· π interactions.

The reaction of the two hydroxy groups of 2,5-dihydroxy-1,4-benzoquinone with the amine groups of two 4AAP molecules produced the enamine **VIII**. Structure **VIII** crystallizes in the $P2_1/n$ space group and contains one molecule of 2,5-bis(1,5-dimethyl-3-oxo-2-phenyl-2,3-dihydro-1*H*-pyrazol-4-ylamino)cyclohexa-2,5-diene-1,4-dione. The two amine groups provide hydrogen bond donors to the antipyrine carbonyl acceptor of two different molecules to form

two N−H···O heterosynthons. These hydrogen bonds form a $C_1^1(10)$ chain which zig-zags down the *b*-axis, resulting in 1D ribbons along that axis.

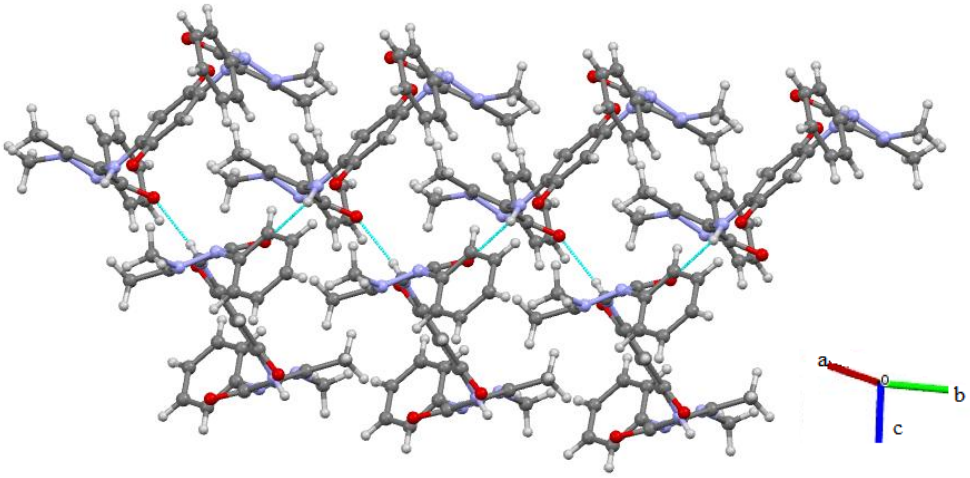

(a)

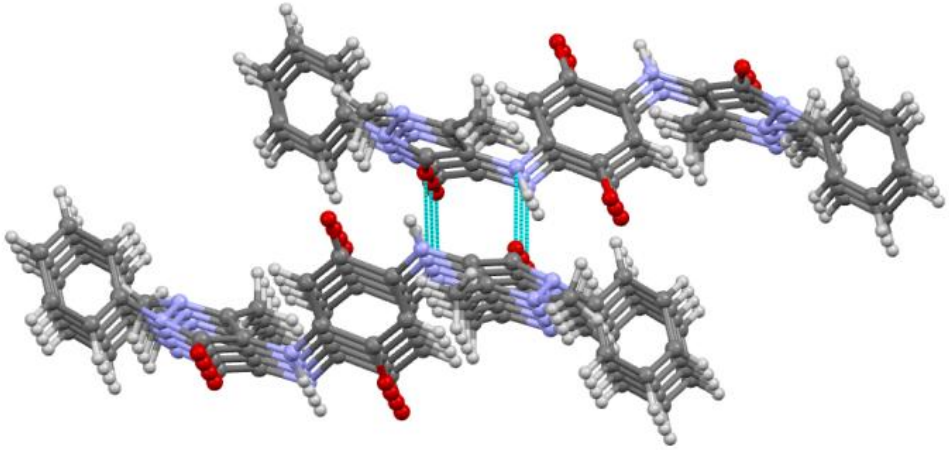

(b)

Figure 9: (a) and (b): Two different views of the chain formed down the b-axis by the two N−H···O heterosynthons in crystal **VIII.**

The reaction of the two carboxylic acid groups of malonic acid with the amine groups of two 4AAP molecules produced the enamine **IX**, which is a dihydrate crystal. Structure **IX** crystallizes in the $P\bar{1}$ space group and contains one molecule of 4,4'-(1,3-dihydroxypropane-1,3-diyl)bis(azanediyl)bis(1,5-dimethyl-2-phenyl-1*H*-pyrazol-3(2*H*)-one) dihydrate and two water

molecules. Although the stoichiometry of the reactants was 1:1, both carboxylic acid groups of the malonic acid reacted with the amine groups of two separate 4AAP molecules. One of the water molecules forms a bridge by hydrogen bonding through its two H-atoms to the carbonyl oxygen atoms of O2 and O3 respectively. This bridge creates a $R_2^2(11)$ hydrogen bonded ring. There is a second water molecule in the asymmetric unit shown in **Figure 2**, but it was not possible to determine the position of the second hydrogen atom, and hence it is shown in the diagram as having only one hydrogen atom, which also explains the reason for the larger ellipsoid. On the opposite side of the molecule to the water molecules, two 4,4'-(1,3-dihydroxypropane-1,3-diyl)bis(azanediyl)bis(1,5-dimethyl-2-phenyl-1*H*-pyrazol-3(2*H*)-one) molecules are joined to each other via two N−H···O heterosynthons, formed between the amine hydrogen atoms and the antipyrine carbonyl oxygen atoms. This reults in a $R_2^2(10)$ hydrogen bonded ring between the two molecules. The extensive hydrogen bonding results in a 3D packing network (**Figure 10**).

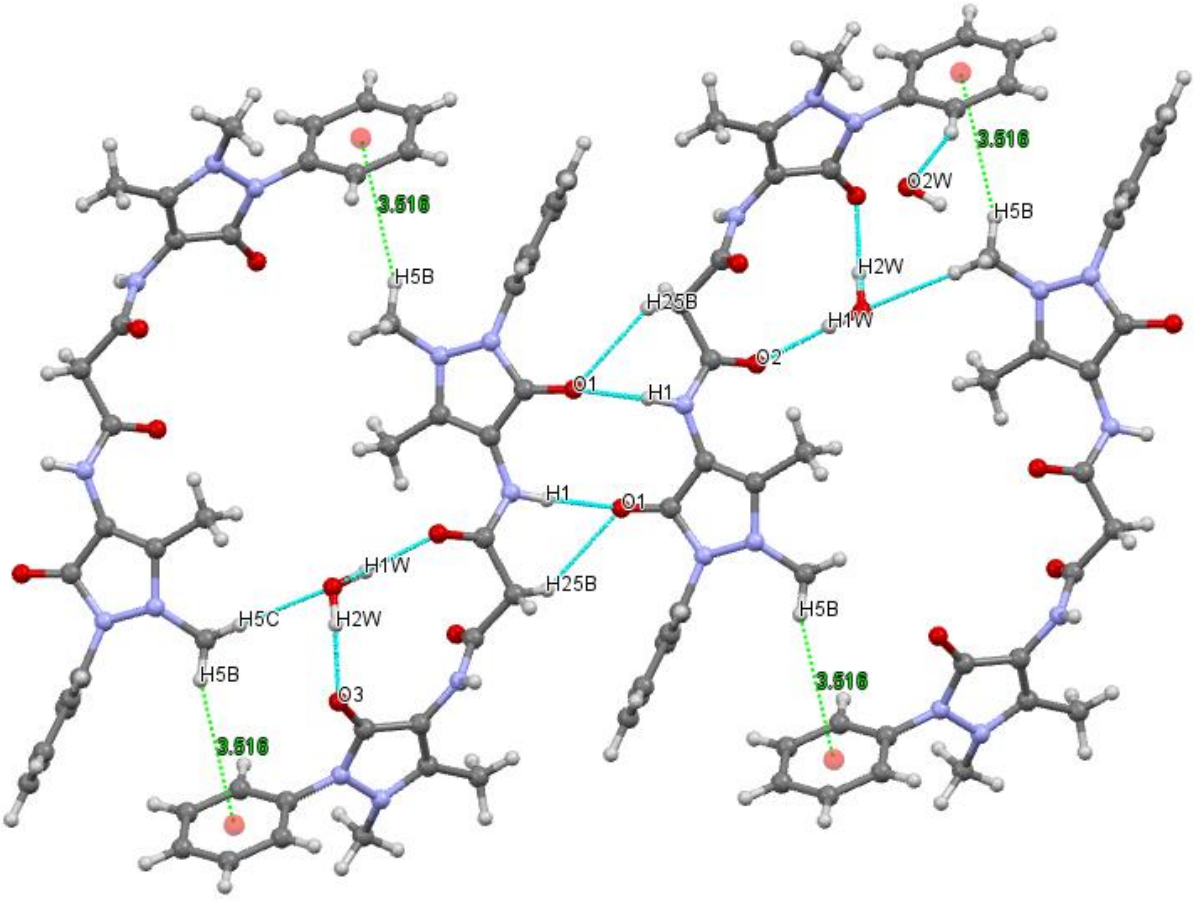

Figure 10: The 3D network formed by the extensive hydrogen bonding of structure **IX**.

Conclusion

Three reactions of 4-aminoantipyrine with ketones (Structures **I**, **VI** and **VII**) and two with aldehydes (**II**, **III**) yielded imines, whereas the reaction of 4AAP with an alcohol (**VIII**) resulted in an enamine. Two amides (**IV**, **V**) and one enamine (**IX**) resulted from the reaction of 4AAP with carboxylic acids. The reactions of the amine functional group of 4AAP with carboxylic acid functional groups is unusual, as two of them occurred at room temperature and one at 40°C, whereas these reactions are usually only expected to take place at over 100°C. Regular hydrogen bonding is absent in structures **I** and **II**, and the packing of these structures is solely via weak C−H···O, C−H···N, C−H···π interactions. The extensive π system of **VII** leads to packing that is primarily via π···π stacking interactions with supporting weak C−H···O interactions.

Acknowledgement

The University of the Witwatersrand and the Molecular Sciences Institute are thanked for providing the infrastructure and financial support to do this work. Andreas Lemmerer thanks the Wits Friedel Sellschop award for funding and Mark Smith thanks the Chemistry department of the University of South Africa for the financial support.

Supporting Information Available

Crystallographic data were deposited at the Cambridge Crystallographic Data Center with reference numbers CCDC XXXXXXX-XXXXXXX, which can be requested from The Cambridge Crystallographic Data Centre (http://www.ccdc.cam.ac.uk/data_request/cif). This information is also available free of charge via the internet at http://pubs.acs.org.

References

Acheson, R. M. (1960). *J. Pharm. Sci.* **49**, 739.

Bernstein, J., Davis, R. E., Shimoni, L. & Chang, N.-L. (1995). *Angew. Chem. Int. Ed.* **34**, 1555-1573.

Bruker, SAINT+, . Version 6.02 (Includes XPREP and SADABS) ed. Madison, Wisconsin, USA: Bruker AXS Inc. (2004).

Deshmukh, P., Soni, P. K., Kankoriya, A., Halve, A. K. & Dixit, R. (2015). *IJPSRR.* **34**, 162-170.

Etter, M. C., Macdonald, J. C. & Bernstein, J. (1990). *Acta Crystallogr., Sect. C.* **46**, 256-262.

Farrugia, L. (2012). *J. Appl. Crystallogr.* **45**, 849-854.

Groom, C. R. & Allen, F. H. (2014). *Angew. Chem. Int. Ed.* **53**, 662-671.

Hohlfeld, T., Zimmerman, N., Weber, A. A., Jessen, G., Weber, H., Schror, K., Holtje, H. D. & Ebel, R. (2008). *J. Thromb. Haemost.* **6**, 166-73.

Macrae, C. F., Bruno, I. J., Chisholm, J. A., Edgington, P. R., McCabe, P., Pidcock, E., Rodriguez-Mange, L., Taylor, R., van de Streek, J., & Wood, P. A. (2008). *J. Appl. Cryst.* **41**, 466-470.

Mnguni, M. J. & Lemmerer, A. (2015). *Acta Crystallogr., Sect. C.* **71**, 103-109.

Sheldrick, G. M. (2015). *Acta Crystallogr., Sect. C.* **71**, 3-8.

Spek, A. (2009). *Acta Crystallogr., Sect. D.* **65**, 148-155.

Teng, Y., Liu, R., LI, C. & Zhang, H. (2011a). *J. Hazard. Mater.* **192**, 1766-71.

Teng, Y., Zhang, H. & Jliu, R. (2011b). *Mol. BioSyst.* **7**, 3157-3163.

Chapter 9: Conclusion

9.1 Concluding remarks

In this study, crystal and co-crystal engineering was applied to synthesize 49 novel crystals and co-crystals of covalently modified isoniazid and 4-aminoantipyrine. Isoniazid was modified by bulky modifiers, namely benzophenone and benzophenone derivatives, and crystallized in the absence and presence of co-formers. The effects of reaction and crystallization conditions on the supramolecular structure of isoniazid was studied and reported. Co-crystal design strategies were developed to synthesize the first reported co-crystal of 4-aminoantipyrine, and the supramolecular synthesis of covalently modified 4-aminoantipyrine was studied. Side reactions of benzophenone were observed and this study was expanded to determine the origin and crystallization processes of these benzophenone azines observed during crystallization. The work reported in this thesis contributes to the development of co-crystal design strategies and to the understanding of co-crystal and crystal structures of isoniazid, 4-aminoantipyrine, benzophenone and their derivatives as detailed below.

A series of co-crystals of isoniazid that had been modified with benzophenone and benzophenone derivatives were synthesized and their supramolecular structures were studied. All co-crystals were synthesized with 2-hydroxybenzoic acid (salicylic acid) and control of dimensionality was achieved. As expected, the salicylic acid co-formers formed intramolecular rings, leaving only the carboxylic acid available for intermolecular hydrogen bonding with the pyridine group of the modified isoniazid molecule. It was found that the benzophenone modifiers sterically masked the amide functional groups from participating in any intermolecular interactions. This steric masking is predictable and consistent and provides a general method whereby an amide functional group can be sterically blocked from intermolecular interactions. Only one structure of isoniazid which has been modified with a benzophenone modifier has been reported where the amide hydrogen is not masked, due to the the small size and planar geometry of the *m*-hydroxybenzoic acid co-former.

Carrying on the theme of the covalent assisted supramolecular synthesis of isoniazid with bulky ligands, another series of co-crystals was synthesized to study the effect of reaction and crystallization conditions on their supramolecular synthesis. A change in reflux time of the reagents resulted in stoichiometric variation in the resulting co-crystals. The addition of excess reagents as an additive resulted in polymorphism. Addition or absence of an acid catalyst either promoted or prevented solvate formation. It was also reported that the addition of either one or two methyl groups to the benzophenone aromatic rings did not substantially alter the packing patterns of the crystal structures.

As the formation of co-crystals may either enhance or inhibit bioavailability and solubility of the drugs, the covalent modification of isoniazid was repeated in the absence of co-formers. The absence of the carboxylic acid co-former provided synthetic challenges as the co-former previously acted as a catalyst and enhanced the covalent modification of the isoniazid. The covalent modification without the co-former was difficult and harsh reaction conditions were often required. The use of new catalysts and the development of new synthetic strategies such as refluxing under pressure at higher temperatures than regular reflux setups allow, through the use of high-pressure screw-top vials, was therefore incorporated into the synthetic methods. A full structural study was done and reported on the covalently modified isoniazid crystals.

Benzophenone azines were observed as side products during the studies mentioned above, and the study was therefore expanded to determine the origin and mechanism of the formation of these benzophenone azines to provide a comprehensive and complete picture of all processes involved in the study. Covalently modified isoniazid intermediates were isolated and the crystal structures determined. These, when placed in direct sunlight, resulted in the formation of an isoniazid dimer and benzophenone azine in each case, confirming the presence of a photodimerization process. The benzophenone azines crystals were found to be held together through weak interactions and a structural study of the packing of these crystals was reported.

This thesis also contains an extensive literature review of all the relevant work done on the covalent modification, crystallization and co-crystallization to date. The work done on isoniazid as detailed above provides a potentially effective method of synthesizing effective drugs against multi-drug-resistant strains of *Mycobacterium tuberculosis.* This thesis therefore provides a comprehensive picture for a researcher who might be interested in synthesizing crystalline drugs

against multi-drug resistant strains of *Mycobacterium tuberculosis*, as well as providing methods by which the supramolecular synthesis may be achieved, as well as an understanding of the structures of such crystals and co-crystals.

The formation of a co-crystal of 4-aminoantipyrine has long evaded researchers. Co-crystal design strategies were developed to synthesize the first reported co-crystal of 4-aminoantipyrine. The relevant chapter in this thesis details several reported literature attempts at synthesizing this co-crystal and provides details of the successes and failures on the path to synthesizing this co-crystal. Two novel salts of 4-aminoantipyrine and two co-crystals of covalently modified 4-aminoantipyrine were also reported.

As it has been reported in literature that the covalent modification of 4-aminoantipyrine is of significant pharmaceutical importance, a series of crystals of covalently modified 4-aminoantipyrine were synthesized and a full structural study of these crystals was presented.

9.2 Future work

The work done on isoniazid as detailed above provides a potentially effective method of synthesizing effective drugs against multi-drug-resistant strains of *Mycobacterium tuberculosis.* However, biological assays should be performed to determine the effectiveness of the crystals and co-crystals presented in this thesis against multi-drug-resistant strains of TB. Methods should be developed to test the efficacy of co-crystals as compared with crystals of covalently modified isoniazid.

With regard to future co-crystal engineering, this study was largely confined to the use of mono-carboxylic acid co-formers such as 2-, 3- and 4-hydroxybenzoic acids. However it would be of interest to prepare series of modified isoniazid with dicarboxylic acids, where 2D planes and 3D networks would be favoured, and to study the structures generated with these co-formers. Liquid assisted grinding (LAG) was also reported in the literature review to have produced several polymorphs of isoniazid co-crystals, a phenomenon not often seen with solvent dissolution in

isoniazid co-crystals. It would therefore be instructive to determine how effective covalent assisted supramolecular synthesis would be using LAG.

With regards to 4-aminoantipyrine, the reaction of the amine group with a carboxylic acid at ambient temperature is unusual, because at room temperature one would expect the basic amine to deprotonate the carboxylic acid to form an unreactive carboxylate, whereas at high temperatures (above 100°C), dehydration can occur with the loss of a water molecule, and the nitrogen lone pair attacks the resulting carbocation forming an amide. However, this unusual dehydration reaction was observed at room temperature in two crystals and at 40°C in a third crystal, and it would be of interest to determine whether 4AAP will react with other carboxylic acids at room temperature. The methods of supramolecular synthesis of 4AAP co-crystals should also be applied to develop series of 4AAP co-crystals, as such co-crystals have the potential to mitigate some of the harmful side effects of treatment with this drug.

"The beauty of crystals lies in the planeness of their faces."

~ Alfred Edwin Howard Tutton in "The Natural History of Crystals"

Chapter 10: References

Aakeröy, C. (1997). *Acta Cryst. B***53**, 569-586.

Aakeröy, C. B. & Beatty, A. M. (2001). *Aust. J. Chem.* **54**, 409-421.

Aakeröy, C. B., Beatty,, A. M. & Leinen, D. S. (2001). *Cryst. Growth Des.* **1**, 47-52.

Aakeröy, C. B., Hussain, I., Forbes, S. & Desper, J. (2007). *CrystEngComm.* **9**, 46-54.

Aakeröy, C. B. & Salmon, D. J. (2005). *CrystEngComm.* **7**, 439-448.

Acheson, R. M. (1960). *J. Pharm. Sci.* **49**, 739.

Addadi, L., Van Mil, J., Gati, E. & Lahav, M. (1981). *Orig. Life.* **11**, 107-18.

Afonin, A. V., Ushakov, I. A., Pavlov, D. V., Levanova, E. P. & Levkovskaya, G. G. (2012). *Russ. Chem. Bull.* **61**, 1117-1120.

Aitipamula, S., Banerjee, R., Bansal, A. K., Biradha, K., Cheney, M. L., Choudhury, A. R., Desiraju, G. R., Dikundwar, A. G., Dubey, R., Duggirala, N., Ghogale, P. P., Ghosh, S., Goswami, P. K., Goud, N. R., Jetti, R. R. K. R., Karpinski, P., Kaushik, P., Kumar, D., Kumar, V., Moulton, B., Mukherjee, A., Mukherjee,, G., Myerson, A. S., Puri, V., Ramanan, A., Rajamannar, T., Reddy, C. M., Rodriguez-Hornedo, N., Rogers, R. D., Row, T. N. G., Sanphui, P., Shan, N., Shete, G., Singh, A., Sun, C. C., Swift, J. A., Thaimattam, R., Thakur, T. S., Kumar Thaper, R., Thomas, S. P., Tothadi, S., Vangala, V. R., Variankaval, N., Vishweshwar, P., Weyna, D. R. & Zawarotko, M. J. (2012). *Cryst. Growth Des.* **12**, 2147-2152.

Aitipamula,, S., Wong, A. B. H., Chow, P. S. & Tan, R. B. H. (2013). *CrystEngComm.* **15**, 5877-5887.

Akalin, E. & Akyuz, S. (2007). *J. Mol. Struct.* **834**, 492-497.

Almarsson, O. & Zawarotko, M. J. (2004). *Chem. Commun. (Camb)*. **35** (17) 1889-96.

André V., Shemchuk, O., Grepioni, F., Braga, D. & Duarte, M. T. (2017). *Cryst. Growth Des.* (Accepted)

Asiri, A. M., Khan, S. A., Tan, K. W. & Ng, S. W. (2010). *Acta Crystallogr., Sect. E.* **66**, o1850.

Bailey, D. N. (1983). *J. Anal. Toxicol.* **7**, 76-8.

Bernstein, J., Davis, R. E., Shimoni, L. & Chang, N.-L. (1995). *Angew. Chem. Int. Ed.* **34**, 1555-1573.

Bhatt, P. M., Azim, Y., Thakur, T. S. & Desiraju, G. R. (2009). *Cryst. Growth Des.* **9**, 951-957.

Bhogala, B. R., Basavoju, S. & Nangia, A. (2005). *CrystEngComm.* **7**, 551-562.

Boldyreva, E. V. (2003). *J. Mol. Struct.* **647**, 159-179.

Bruker, SAINT+, . Version 6.02 (Includes XPREP and SADABS) ed. Madison, Wisconsin, USA: Bruker AXS Inc. (2004).

Burdock, G. A., Pence, D. H. & Ford, R. A. (1991). *Food Chem. Toxicol.* **29**, 741-750.

Burrows, A. D. (2004). Crystal Engineering Using Multiple Hydrogen Bonds. *In:* Mingos, D. M. P. (ed.) *Supramolecular Assembly via Hydrogen Bonds I.* Berlin, Heidelberg: Springer Berlin Heidelberg.

Carty, A. J. (1972). *Organometalic Chemistry Reviews, Section A: Subject Reviews.* **7**, 191.

Cheney, M. L., Weyna, D. R., Shan, N., Hanna, M., Wojtas, L. & Zaworotko, M. J. (2011). *J. Pharm. Sci.* **100**, 2172-81.

Cherukuvada, S. & Nangia, A. (2012). *CrystEngComm.* **14**, 2579-2588.

Childs, S. L., Stahly, G. P. & Park, A. (2007). *Mol. Pharm.* **4**, 323-338.

Chitradevi, A., Athimoolam, S., Sridhar, B. & Bahadur, S. A. (2009). *Acta Crystallogr., Sect. E.* **65**, o3041-o3042.

Chitradevi, A., Suresh Kumar, S., Athimoolam, S., Asath Bahadur, S. & Sridhar, B. (2015). *J. Mol. Struct.* **1099**, 58-67.

Chiya, T. J. & Lemmerer, A. (2012). *CrystEngComm.* **14**, 5124-5127.

Coelho, T. S., Cantos, J. B., Bispo, M. L. F., Goncalves, R. S. B., Lima, C. H. S., Da Silva, P. E. A. & Souza, M. V. N. (2012). *Infect. Dis. Rep.* **4**, e13.

Cunha, M. S., Ribeiro, C. E. P., Corrêa, C. C., Diniz, R., (2017).. *J. Mol. Struct.* **1150**, 586-594.

Cruz-Cabeza, A. J. (2012). *CrystEngComm*. **14**, 6362-6365.

Deshmukh, P., Soni, P. K., Kankoriya, A., Halve, A. K. & Dixit, R. (2015). *IJPSRR.* **34**, 162-170.

Desiraju, G. R. (1995). *Angew. Chem. Int. Ed.* **34**, 2311-2327.

Desiraju, G. R. (2003). *CrystEngComm.* **5**, 466-467.

Desiraju, G. R. (2005). *Chem. Commun.* **24**, 2995-3001.

Desiraju, G. R. (2013). *J. Am. Chem. Soc.* **135** (27), 9952-9967.

Diniz, L. F., Souza, M. S., Carvalho, P. S., Da Silva, C. C. P., D'vries, R. F., Ellena, J., (2018). *J. Mol. Struct.* **1153**, 58-68.

Elder, R. L. (1983). *J. Am. Coll. Toxicol.* **2**, 35-77.

Etter, M. C. (1990). Acc. Chem. Res. **23**, 120–126.

Etter, M. C., MacDonald, J. C. & Bernstein, J. (1990). *Acta Crystallogr., Sect. B.* **46**, 256-262.

Farrugia, L. (2012). *J. Appl. Crystallogr.* **45**, 849-854.

Fazil, S., Ravindran, R., Sarau Devi, A. & Bijili, B. K. (2012). *J. Mol. Struct.* **1021**, 147-152.

Feltz, A. (1985). A. I. Kitaigorodsky. *Cryst. Res. Technol.* **20**, 498-498.

Ferraresi-Curotto, V., Echeverría, G. A., Piro, O. E., Pis-Diez, R. & González-BARÓ, A. C. (2017). *J. Mol. Struct.* **1133**, 436-447.

Grobelny, P., Mukherjee, A. & Desiraju, G. R. (2011). *CrystEngComm.* **13**, 4358-4364.

Groom, C. R. & Allen, F. H. (2014). *Angew. Chem. Int. Ed.* **53**, 662-671.

Grothe, E., Meekes, H., Vlieg, E., Ter Horst, J. H. & De Gelder, R. (2016). *Cryst. Growth Des.* **16**, 3237-3243.

Guillory, J. K. (2003). *J. Med. Chem.* **46**, 1277-1277.

Hearn, M. J., Cynamon, M. H., Chen, M. F., Coppins, R., Davis, J., Joo-On Kang, H., Noble, A., Tu-Sekine, B., Terrot, M. S., Trombino, D., Thai, M., Webster, E. R. & Wilson, R. (2009). *Eur. J. Med. Chem.* **44**, 4169-4178.

Hemamalini, M., Loh, W.-S., Quah, C. K. & Fun, H.-K. (2014). *Chemistry Central Journal.* **8**, 31.

Hohlfeld, T., Zimmermann, N., Weber, A. A., Jessen, G., Weber, H., Schror, K., Holtje, H. D. & Ebel, R. (2008). *J. Thromb. Haemost.* **6**, 166-73.

Huo, J.-Z. (2009). *Acta Crystallogr., Sect. E.* **65**, o2691-o2692.

Jensen, L. H. (1954). *J. Am. Chem. Soc.* **76**, 4663-4667.

Kaur, R., Perumal, S. S. R.R., Bhattacharyya, A. J., Yashonath, S., Guru Row, T. N., (2014). *Cryst. Growth Des.* **14**, 423-426.

Kitaigorodskii, A. I. (1984). Mixed crystals. New York: Springer-Verlag.

Kost, A. & Grandberg, I. (1959). *Uspekhi Khimii.* **28**, 921-947.

Kuduva, S. S., Blaser, D., Boese, R. & Desiraju, G. R. (2001). *J. Org. Chem.* **66**, 1621-6.

Lauer, W. M. & Dyer, W. S. (1942). *J. Am. Chem. Soc.* 64, 1453-1456.

Leiserowitz, L. (1976). *Acta Cryst. B.* **32**. 775-802.

Lemmerer, A. (2012). *CrystEngComm.* **14**, 2465-2478.

Lemmerer, A., Bernstein, J. & Kahlenberg, V. (2010). *CrystEngComm.* **12**, 2856-2864.

Lemmerer, A., Bernstein, J. & Kahlenberg, V. (2011). *CrystEngComm.* **13**, 5692-5708.

Lemmerer, A., Govindraju, S., Johnston, M., Motloung, X. & Savig, K. L. (2015). *CrystEngComm*. **17**, 3591-3595.

Li, Y., Liu, Y., Wang, H., Xiong, X., Wei, P. & Li, F. (2013). *Molecules.* **18**, 877.

Macrae, C. F., Bruno, I. J., Chisholm, J. A., Edgington, P. R., McCabe, P., Pidcock, E., Rodriguez-Mange, L., Taylor, R., van de Streek, J., & Wood, P. A. (2008). *J. Appl. Cryst.* **41**, 466-470.

Mashhadi, S. M. A., Yunus, U., Bhatti, M. H., Ahmed, I. & Tahir, M. N. (2014). *J. Mol. Struct.* **1076**, 446-452.

Mashhadi, S. M. A., Yunus, U., Bhatti, M. H. & Tahir, M. N. (2016). *J. Mol. Struct.* **1076**, 17-21.

Meir, L. & Leslie, L. (2015). *Phys. Scr.* **90**, 118003.

Meng, X.-G., Xiao, Y.-L., Zhang, H. & Zhou, C.-S. (2008). *Acta Crystallogr., Sect. C.* **64**, o261-o263.

Mnguni, M. J. & Lemmerer, A. (2015). *Acta Crystallogr., Sect. C.* **71**, 103-109.

Murtaza, S., Hamza, M. & Tahir, M. N. (2011). *Acta Crystallogr., Sect. E.* **67**, o2193.

Nangia, A. (2009). Supramolecular chemistry and crystal engineering. *In:* Mukunda, N. (ed.) *Current Trends in Science,*. Bangalore: Indian Academy of Sciences.

Oruganti, M., Khade, P., Das, U. K. & Trivedi, D. R. (2016). *RSC Advances*, **6**, 15868-15876.

Palovics, E., Faigl, F. & Fogassy, E. (2012). Separation of the Mixtures of Chiral Compounds by Crystallization. *In:* Mastai, Y. (ed.) *Advances in Crystallization Processes.* Hungary: Hungarian Academy of Sciences.

Price, S. L. (2014). *Chem. Soc. Rev.* 2014, **43**, 2098-2111

Qiao, N., LI, M., Schlindwein, W., Malek, N., Davies, A. & Trappitt, G. (2011). *Int. J. Pharm.* **419**, 1-11.

Ravikumar, N., Gaddamanugu, G., Anand, S. K. (2013). *J. Mol. Struct.* ***1033***, 272-279

Saha, A. K., Hossain, M. M., Grubisha, D. S. & Bennett, D. W. (1995). *J. Chem. Crystallogr.* **25**, 383-387.

Sander, J. R. G., Bucar, D.-K., Henry, R. F., Giangiorgi, B. N., Zhang, G. G. Z. & MacGillivray, L. R. (2013). *CrystEngComm.* **15**, 4816-4822.

Sanphui, P. & Nangia, A. (2014). *J. Chem. Sci.* **126**, 1249-1264.

Santos, P. M. P., Antunes, A. M. M., Noronha, J., Fernandes, E. & Vieira, A. J. S. C. (2010). *Eur. J. Med. Chem.* **45**, 2258-2264.

Sarcevica, I., Kons, A., Orola, L. (2016). *CrystEngComm.* **18**, 1625-1635.

Sarcevica, I., Orola, L., Veidis, M. V. & Belyakov, S. (2014). *Acta Crystallogr., Sect. C.* **70**, 392-395.

Sarcevica, I., Orola, L., Veidis, M. V., Podjava, A. & Belyakov, S. (2013). *Cryst. Growth Des.* **13**, 1082-1090.

Schultheiss, N. & Newman, A. (2009). *Cryst. Growth Des.* **9**, 2950-2967.

Sevukarajan, M., Sodanapalli, R., Thanuja, B. & Nair, R. (2011). *J. Biomed. Sci. and Res.* **3**, 397-402.

Shan, N. & Zaworotko, M. J. (2008). *Drug Discov. Today.* **13**, 440-6.

Sheldrick, G. M. (2015). *Acta Crystallogr., Sect. C.* **71**, 3-8.

Silva, F. P., Ellena, J., Ferreira, M. D. L., Mascarenhas, Y. P., De Souza, M. V. N., Vasconcelos, T. R. A., Wardell, J. L. & Wardell, S. M. S. V. (2006). *J. Mol. Struct.* **788**, 63-71.

Smith, M. G., Forbes, R. P. & Lemmerer, A. (2015). *Cryst. Growth Des.* 15, 3813-3821.

Spek, A. (2009). *Acta Crystallogr., Sect. D.* **65**, 148-155.

Stilinović V. & Kaitner, B. (2012). *Cryst. Growth Des.* **12**, 5763-5772.

Suarez, J., Ranguelova, K., Jarzecki, A. A., Manzerova, J., Krymov, V., Zhao, X., Yu, S., Metlitsky, L., Gerfen, G. J. & Magliozzo, R. S. (2009). *J. Biol. Chem.* **284**, 7017-7029.

Swapna, B., Maddileti, D. & Nangia, A. (2014). *Cryst. Growth Des.* **14**, 5991-6005.

Teng, Y., Liu, R., Li, C. & Zhang, H. (2011a). *J. Hazard. Mater.* **192**, 1766-71.

Teng, Y., Zhang, H. & JLiu, R. (2011b). *Mol. BioSyst.,* **7**, 3157-3163.

Verner, J. & Potacek, M. (2006). *Molecules.* **11**, 34-42.

Vishweshwar, P., McMahon, J. A., BIS, J. A. & Zaworotko, M. J. (2006). *J. Pharm. Sci.* **95**, 499-516.

Vishweshwar, P., McMahon, J. A., Peterson, M. L., Hickey, M. B., Shattock, T. R. & Zaworotko, M. J. (2005). *Chem. Commun.* **0**, 4601-4603.

Weissbuch, I., Leiserowitz, L. & Lahav, M. 2001. "Tailor-Made" Additives and Impurities. *In:* MERSMANN, A. (ed.) *Crystallization Technology Handbook.* 2nd ed. New York: Marcel Dekker.

Wood, P. A., Feeder, N., Furlow, M., Galek, P. T. A., Groom, C. R. & Pidcock, E. (2014). *CrystEngComm.* **16**, 5839-5848.

Wuts, P. G. & Greene, T. W. (2006). *Greene's protective groups in organic synthesis*, John Wiley & Sons.

Xavier, A. & Srividhya, N. (2014). *IOSR-JAC.* **7**, 6-15.

Yang, Y.-Y., Xu, L., Kang, T.-G., Chen, T. & Wu, P. (2012). *Acta Crystallogr., Sect. E.,* **68**, o1964.

APPENDIX 1

Note that the DSC traces in this Appendix were produced and analyzed by Prof. Lemmerer and the Pawley refinements in this Appendix were done by Dr. Roy Forbes as required by the referees for the publication "Covalent Assisted Supramolecular Synthesis: Masking of Amides in Co-Crystal Synthesis using Benzophenone Derivatives".

The powder diffraction patterns were originally collected and analyzed by myself, but I did not contribute to the Pawley refinements in this Appendix and these therefore do not form part of this thesis. The supplementary material for this published paper is placed here for completeness.

Supporting Information

Covalent Assisted Supramolecular Synthesis: Masking of Amides in Co-Crystal Synthesis using Benzophenone Derivatives

Mark G. Smith, Roy P. Forbes and A. Lemmerer

Table of Contents

SI1. Melting Points for Co-Crystals 1-6b

Table S1. Melting points for Co-Crystals as determined by a Mettler Toledo MP50 melting point system. Melting points for polymorphs 3a and 3b, and 6a and 6b were determind by DSC (below).

Co-Crystal	**Melting Point (°C)**
Co-Crystal **1**	145.8
Co-Crystal **2**	128.2
Co-Crystal **3a**	134.3 (See text)
Co-Crystal **3b**	151.7 (See text)
Co-Crystal **4**	128.2
Co-Crystal **5**	204.9
Co-Crystal **6a**	136.6 (See text)
Co-Crystal **6b**	163.2

SI2. Representative DSC traces for Co-Crystals 3a, 3b, 6a, 6b

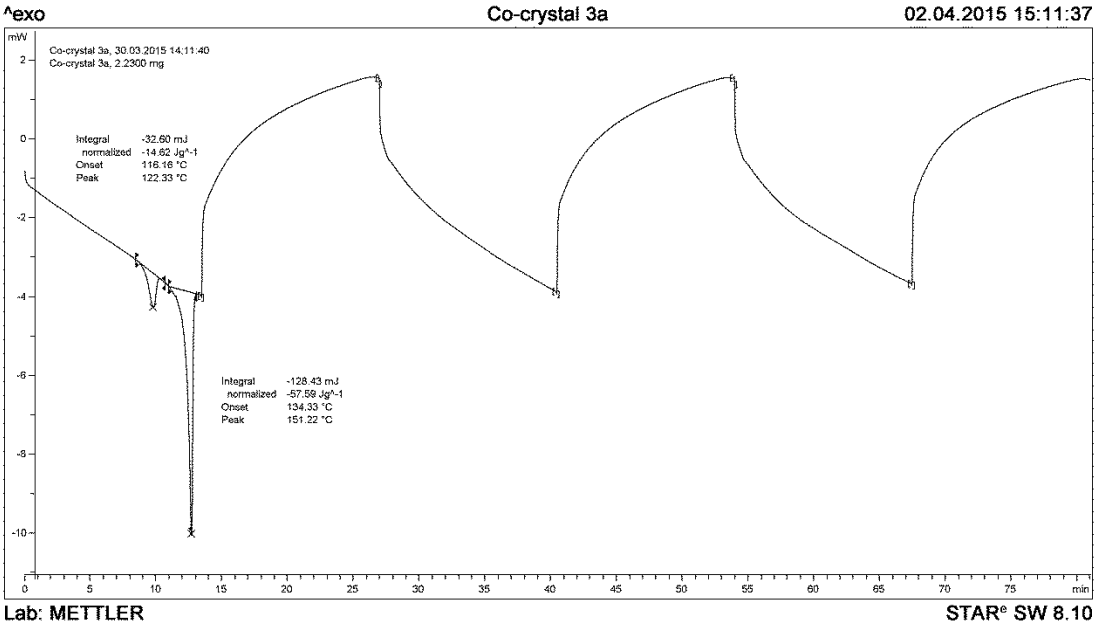

3a

Figure S1: Representative DSC trace (exothermic is up) for Co-Crystal **3a**.

3b

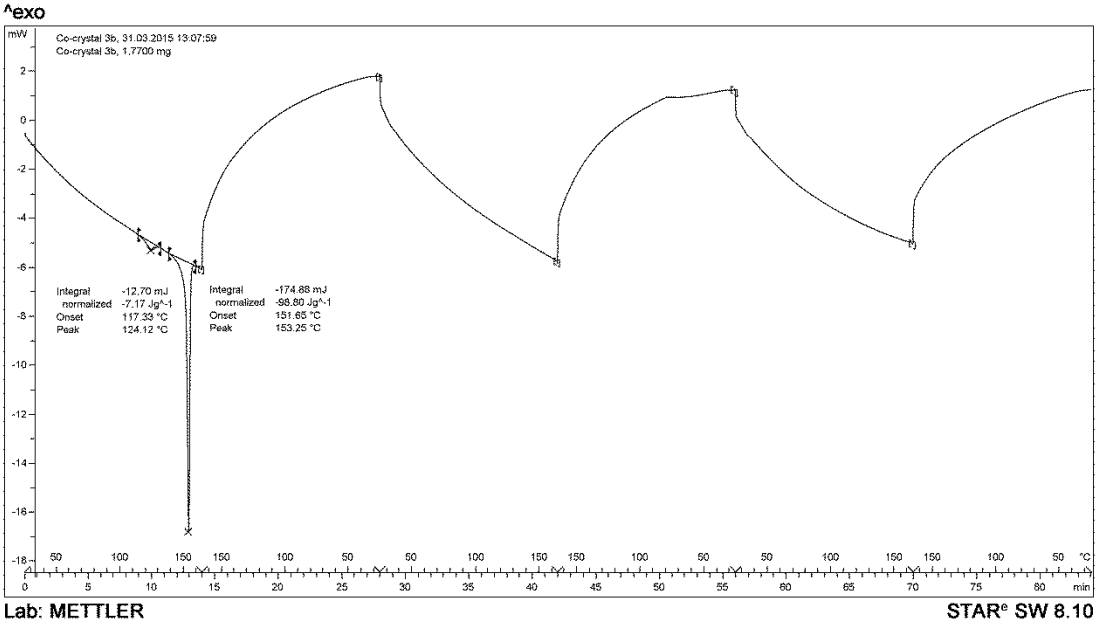

Figure S2: Representative DSC trace (exothermic is up) for Co-Crystal **3b**.

6a

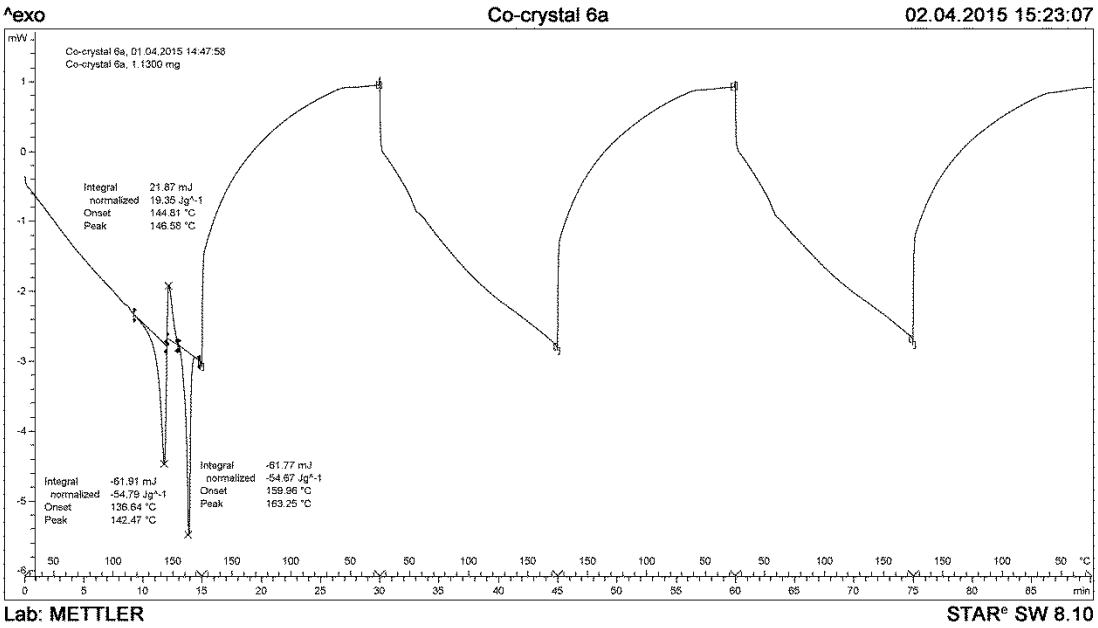

Figure S3: Representative DSC trace (exothermic is up) for Co-Crystal **6b**.

6b

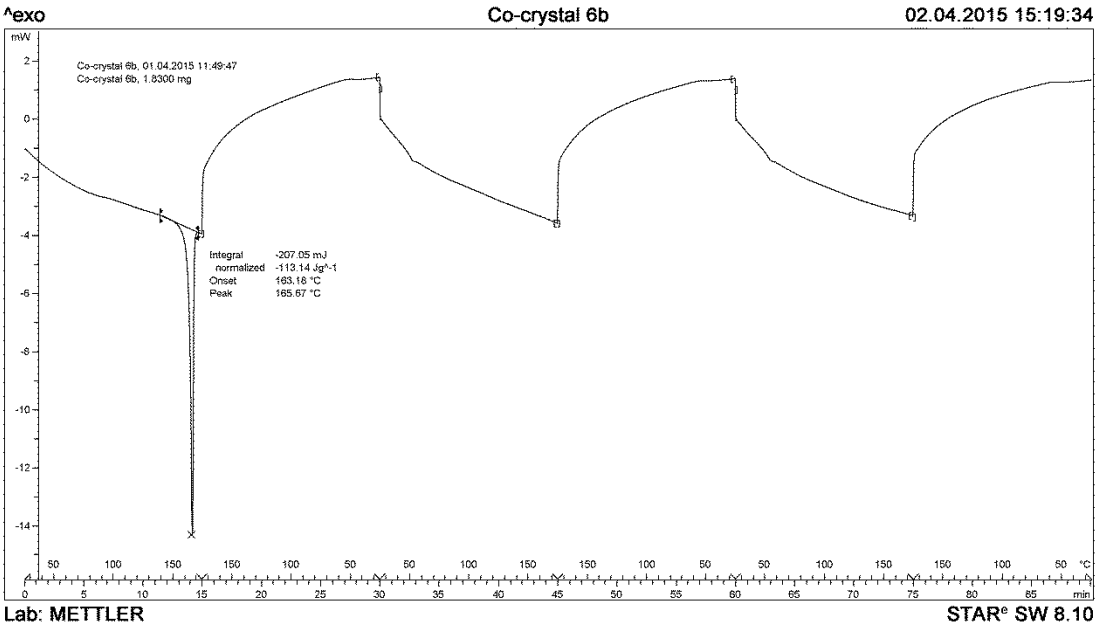

Figure S4: Representative DSC trace (exothermic is up) for Co-Crystal **6b**.

SI3. Powder X-ray diffraction patterns for Co-Crystals 1 - 6b

Experimental diffraction patterns of Co-crystals **1** – **6b** were collected on a Bruker D2 Phaser using Co $K\alpha_{1/2}$ radiation ($K_{\alpha1}$ =1.788960 and $K_{\alpha2}$ = 1.789879 Å) and a Lynxeye PSD detector. Pawley refinements were carried out on all data using Bruker AXS TOPAS version 4.2.

1: (N'-(diphenylmethylene)isonicotinohydrazide)·(salicylic acid)

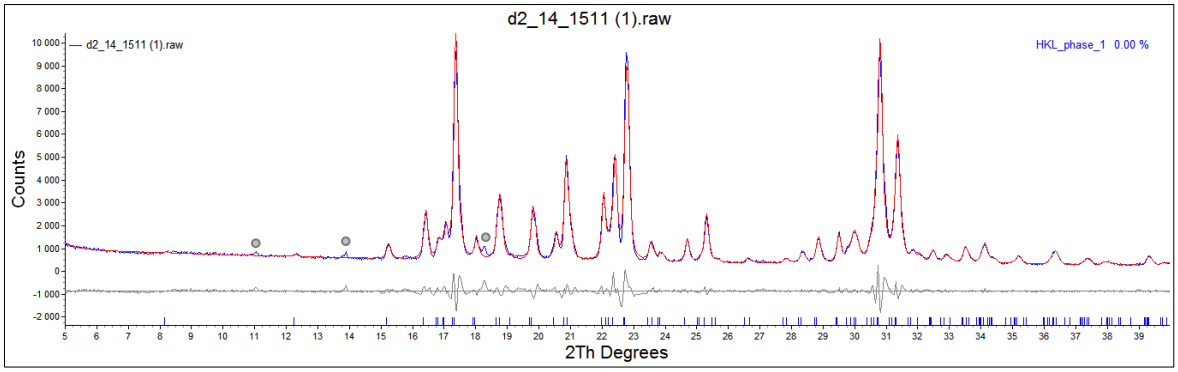

Figure S5: Pawley refinement of **1**, recorded at room temperature; the red line represents the diffraction pattern calculated from the unit cell of **1**, the blue line represents the experimental diffraction pattern of **1**, the grey line represents the difference curve between the calculated and experimental diffraction patterns while the HKL reflections (blue lines) predicted for the crystal structure of **1** are shown above the X-axis. The grey spheres highlight the positions of unidentified reflections.

The result of the Pawley refinement shown in Figure S5 suggests that the crystal structure of **1** is representative of the bulk sample. Minor unidentified reflections, most likely due to the presence of impurity phases were also observed. The difference between the lattice parameters calculated at room temperature and that of the crystal structure data collected at 173K are shown below in Table S2.

Table S2: A comparison of the lattice parameters of the input crystal structure and that obtained from the Pawley refinement

	Lattice Parameters			
	a (Å)	**b (Å)**	**c (Å)**	**β (º)**
Crystal structure	25.8071(6)	6.924(2)	12.2426(3)	103.501(10)
Pawley refinement	25.8856(53)	7.041(14)	12.2471(27)	103.358(11)

2: (N'-(bis(2-hydroxyphenyl)methylene)isonicotinohydrazide)·(salicylic acid)

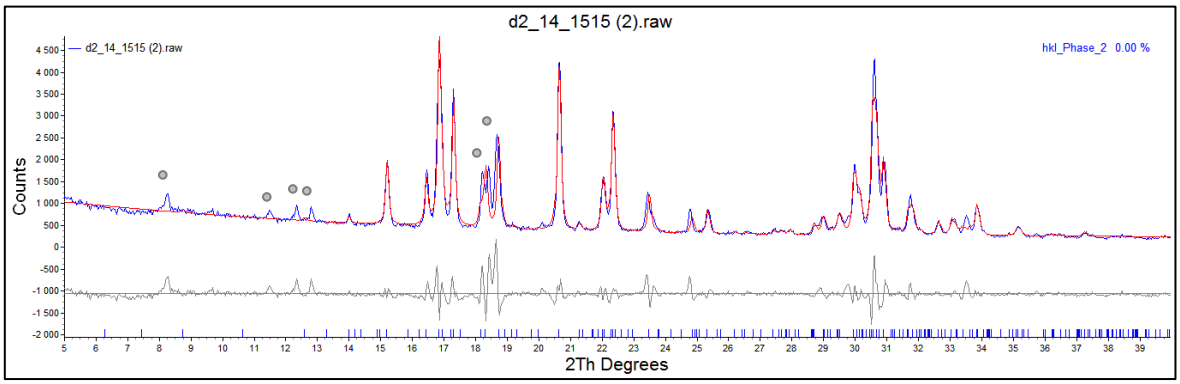

Figure S6: Pawley refinement of **2**, recorded at room temperature; the red line represents the diffraction pattern calculated from the unit cell of **2**, the blue line represents the experimental diffraction pattern of **2**, the grey line represents the difference curve between the calculated and experimental diffraction patterns while the HKL reflections (blue lines) predicted for the crystal structure of **2** are shown above the X-axis. The grey spheres highlight the positions of unidentified reflections.

The result of the Pawley refinement shown in Figure S6 suggests that the crystal structure of **2** is representative of the bulk of the sample though several unidentified reflections are observed. These reflections may be present as a result of impurities in the sample. Alternatively, the unidentified reflections may also be as a result of structural changes that occur on heating the sample from 173K to ambient temperature. The difference between the lattice parameters calculated at room temperature and that of the crystal structure data obtained collected at 173K are shown below in Table S3.

Table S3: A comparison of the lattice parameters of the input crystal structure and that obtained from the Pawley refinement

	Lattice Parameters					
	a (Å)	**b (Å)**	**c (Å)**	**α (°)**	**β (°)**	**γ (°)**
Crystal structure	6.6193(2)	12.3234(3)	14.418(3)	98.727(2)	98.596(2)	100.665(2)
Pawley refinement	6.5544(11)	12.3372(28)	14.523(31)	99.355(20)	99.111(12)	100.543(17)

3a: (N'-(di-p-tolylmethylene)isonicotinohydrazide)·(salicylic acid), Form I

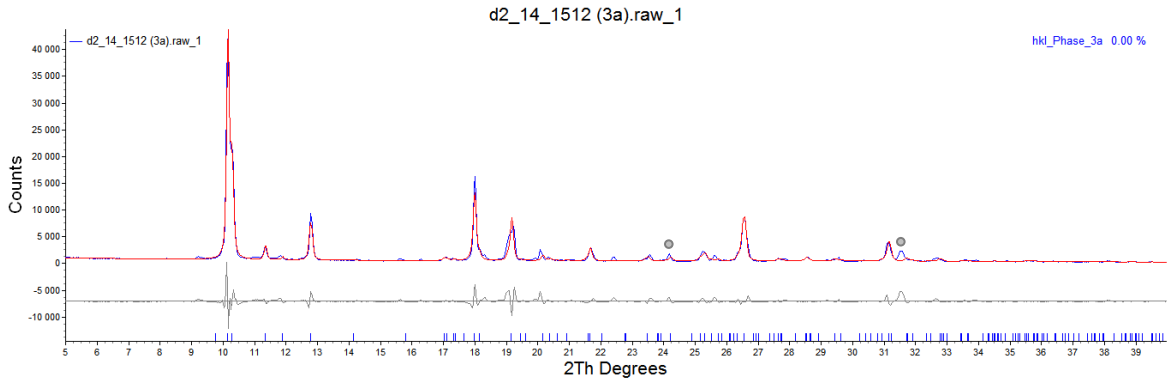

Figure S7: Pawley refinement of **3a**, recorded at room temperature; the red line represents the diffraction pattern calculated from the unit cell of **3a**, the blue line represents the experimental diffraction pattern of **3a**, the grey line represents the difference curve between the calculated and experimental diffraction patterns while the HKL reflections (blue lines) predicted for the crystal structure of **3a** are shown above the X-axis. The grey spheres highlight the positions of unidentified reflections.

The result of the Pawley refinement shown in Figure S7 suggests that the crystal structure of **3a** is representative of the bulk sample. Minor unidentified reflections were also observed. These reflections may be the result of the presence of impurity phases. The difference between the lattice parameters calculated at room temperature and that of the crystal structure data obtained collected at 173K are shown below in Table S4.

Table S4: A comparison of the lattice parameters of the input crystal structure and that obtained from the Pawley refinement

	Lattice Parameters					
	a (Å)	**b (Å)**	**c (Å)**	**α (º)**	**β (º)**	**γ (º)**
Crystal structure	9.9062(2)	12.0906(3)	12.4633(3)	113.5360(10)	113.0770(10)	96.2970(10)
Pawley refinement	9.8931(43)	12.1068(28)	12.4539(42)	113.648(17)	113.229(26)	96.387(27)

3b: (N'-(di-p-tolylmethylene)isonicotinohydrazide)·(salicylic acid), Form II

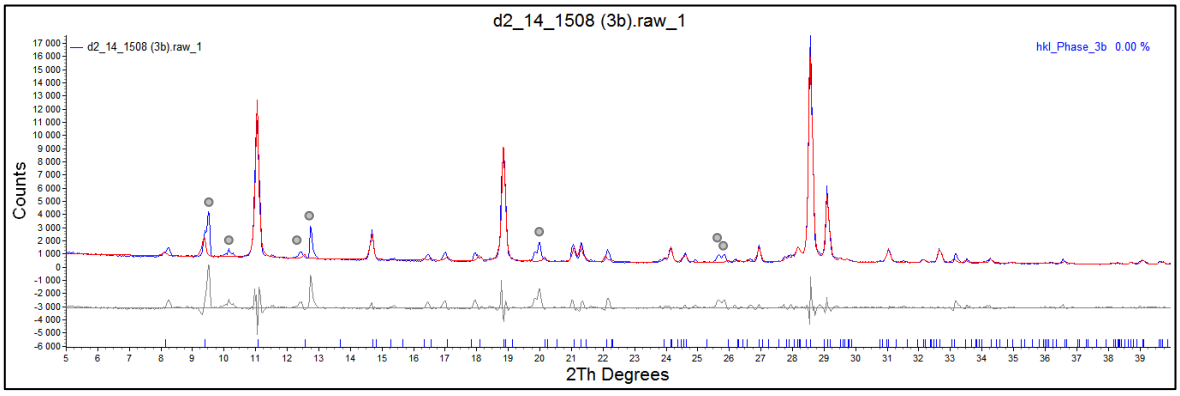

Figure S8: Pawley refinement of **3b**, recorded at room temperature; the red line represents the diffraction pattern calculated from the unit cell of **3b**, the blue line represents the experimental diffraction pattern of **3b**, the grey line represents the difference curve between the calculated and experimental diffraction patterns while the HKL reflections (blue lines) predicted for the crystal structure of **3b** are shown above the X-axis. The grey spheres highlight the positions of unidentified reflections.

The result of the Pawley refinement shown in Figure S8 suggests that the crystal structure of **3b** is representative of the bulk sample. Minor unidentified reflections were also observed. These reflections may be due to the presence of impurity phases or maybe the result of structural changes that occur on heating the sample from 173K to ambient temperature. The difference between the lattice parameters calculated at room temperature and that of the crystal structure data obtained collected at 173K are shown below in Table S5.

Table S5: A comparison of the lattice parameters of the input crystal structure and that obtained from the Pawley refinement

	Lattice Parameters					
	a (Å)	**b (Å)**	**c (Å)**	**α (°)**	**β (°)**	**γ (°)**
Crystal structure	8.2520(3)	11.2852(4)	12.9411(5)	77.516(2)	85.880(2)	82.910(2)
Pawley refinement	8.2499(24)	11.2635(33)	12.8957(42)	77.543(22)	86.084(24)	82.672(31)

4: ((E)-N'-(phenyl(p-tolyl)methylene)isonicotinohydrazide)·(salicylic acid)

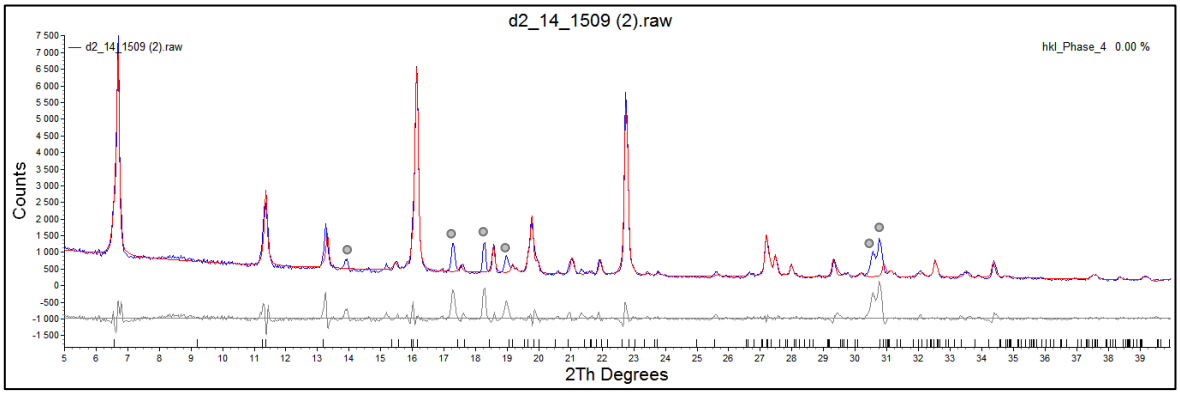

Figure S9: Pawley refinement of **4**, recorded at room temperature; the red line represents the diffraction pattern calculated from the unit cell of **4**, the blue line represents the experimental diffraction pattern of **4**, the grey line represents the difference curve between the calculated and experimental diffraction patterns while the HKL reflections (blue lines) predicted for the crystal structure of **4** are shown above the X-axis. The grey spheres highlight the positions of unidentified reflections.

The result of the Pawley refinement shown in Figure S9 suggests that the crystal structure of **4** is representative of the bulk sample. As described previously for co-crystals **3a** and **3b**, unidentified reflections were also observed. The difference between the lattice parameters calculated at room temperature and that of the crystal structure data obtained collected at 173K are shown below in Table S6.

Table S6: A comparison of the lattice parameters of the input crystal structure and that obtained from the Pawley refinement

	Lattice Parameters					
	a (Å)	**b (Å)**	**c (Å)**	**α (°)**	**β (°)**	**γ (°)**
Crystal structure	7.0057(4)	11.5495(7)	15.6046(9)	87.598(4)	82.792(4)	72.850(3)
Pawley refinement	7.0266(34)	11.6277(29)	15.7048(55)	87.460(18)	82.774(44)	73.806(38)

5: ((E)-N'-((4-(dimethylamino)phenyl)(phenyl)methylene)isonicotinohydrazide)·(salicylic acid)

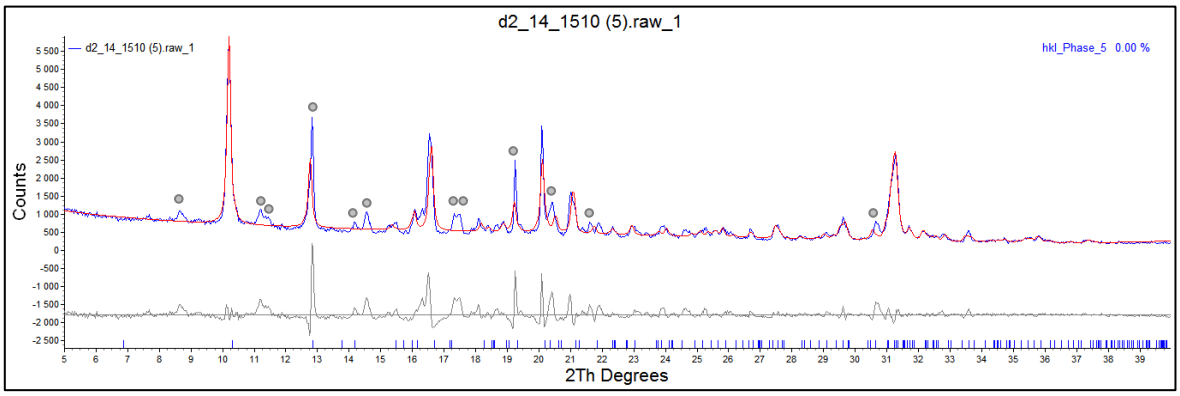

Figure S10: Pawley refinement of **5**, recorded at room temperature; the red line represents the diffraction pattern calculated from the unit cell of **5**, the blue line represents the experimental diffraction pattern of **5**, the grey line represents the difference curve between the calculated and experimental diffraction patterns while the HKL reflections (blue lines) predicted for the crystal structure of **5** are shown above the X-axis. The grey spheres highlight the positions of unidentified reflections.

The result of the Pawley refinement shown in Figure S10 suggests that the unit cell of the crystal structure of **5** may be dissimilar to that obtained from the input crystal structure. The fit was improved by means of a lattice parameter search during the Pawley refinement. The difference between the lattice parameters calculated at room temperature and that of the crystal structure data obtained collected at 173K are shown below in Table S7. Furthermore, several minor unidentified reflections are observed. These reflections may be due to the presence of impurity phases or may be indicative of a structural change that occurs on heating the sample to ambient temperature.

Table S7: A comparison of the lattice parameters of the input crystal structure and that obtained from the Pawley refinement

	Lattice Parameters			
	a (Å)	**b (Å)**	**c (Å)**	**β (º)**
Crystal structure	25.010(2)	6.9708(7)	12.4779(11)	90.949(6)
Pawley refinement	29.918(20)	8.2867(44)	11.1485(45)	86.185(27)

6a: (E)-N'-((4-aminophenyl)(phenyl)methylene)isonicotinohydrazide)_(salicylic acid), Form I

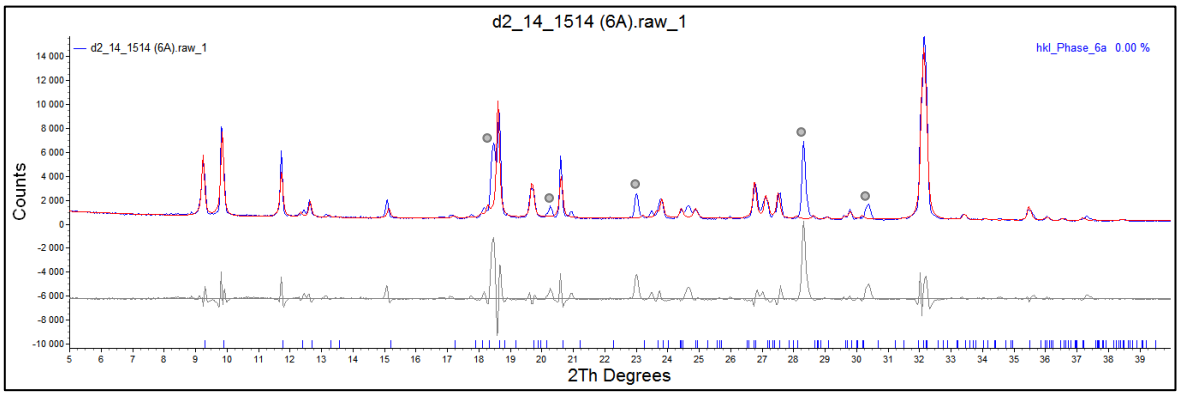

Figure S11: Pawley refinement of **6a**, recorded at room temperature; the red line represents the diffraction pattern calculated from the unit cell of **6a**, the blue line represents the experimental diffraction pattern of **6a**, the grey line represents the difference curve between the calculated and experimental diffraction patterns while the HKL reflections (blue lines) predicted for the crystal structure of **6a** are shown above the X-axis. The grey spheres highlight the positions of unidentified reflections.

The result of the Pawley refinement shown in Figure S11 suggests that the unit cell of the crystal structure of **6a** accounts for the majority of the reflections observed in the experimental powder diffraction data. Again, unidentified reflections are observed and these may be due to the presence of impurity phases or may be indicative of a structural change that may have occurred on heating the sample to ambient temperature. The difference between the lattice parameters calculated at room temperature and that of the crystal structure data obtained collected at 173K are shown below in Table S8.

Table S8: A comparison of the lattice parameters of the input crystal structure and that obtained from the Pawley refinement

	Lattice Parameters					
	a (Å)	**b (Å)**	**c (Å)**	**α (°)**	**β (°)**	**γ (°)**
Crystal structure	9.2815(3)	11.7198(3)	12.2187(3)	94.4050(10)	110.971(2)	113.076(2)
Pawley refinement	9.2724(50)	11.7070(57)	12.1547(56)	94.175(39)	110.291(38)	113.908(34)

6b: (E)-N'-((4-aminophenyl)(phenyl)methylene)isonicotinohydrazide)_(salicylic acid), Form II

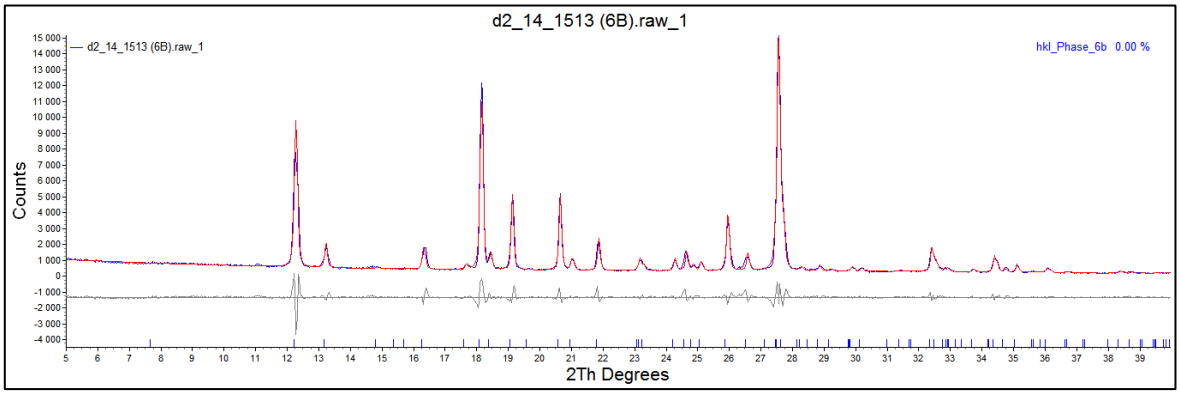

Figure S12: Pawley refinement of **6b**, recorded at room temperature; the red line represents the diffraction pattern calculated from the unit cell of **6b**, the blue line represents the experimental diffraction pattern of **6b**, the grey line represents the difference curve between the calculated and experimental diffraction patterns while the HKL reflections (blue lines) predicted for the crystal structure of **6b** are shown above the X-axis.

The result of the Pawley refinement shown in Figure S12 suggests that the crystal structure of **6b** is representative of the bulk sample. The difference between the lattice parameters calculated at room temperature and that of the crystal structure data obtained collected at 173K are shown below in Table S6.

Table S9: A comparison of the lattice parameters of the input crystal structure and that obtained from the Pawley refinement

	Lattice Parameters			
	a (Å)	**b (Å)**	**c (Å)**	**β (°)**
Crystal structure	7.8452(3)	10.7034(4)	13.1775(5)	93.234(3)
Pawley refinement	7.8222(10)	10.8071(13)	13.4288(15)	93.9322(62)